AUTHOR: JOHN ARIS SLANKIS

TITLE: TELLURIC AND MAGNETOTELLURIC SURVEYS AT 8 HZ

DEPARTMENT: MINING ENGINEERING AND APPLIED GEOPHYSICS

DEGREE: DOCTOR OF PHILOSOPHY

ABSTRACT

The use of natural electro-magnetic fields at 8 Hz for mineral exploration and geological mapping has been investigated and optimum measurement techniques have been developed.

Both telluric and magnetotelluric surveys have detected resistivity variations associated with some metallic sulphide deposits and geological contacts. Such conductivity discontinuities are characterized by variations in the apparent resistivity, the spatial anisotropy of the telluric field and, in some instances, the presence of a strong vertical magnetic field component. Also, the correlation and phase relationship between the telluric field near a conductivity discontinuity and the background field is variable.

For the case where the telluric field is measured normal to the strike of a conductivity discontinuity theoretical results for two-dimensional models of the actual geology agree well with the observed and offer an explanation for the variable phase and correlation.

SHORT TITLE:

TELLURIC AND MAGNETOTELLURIC SURVEYS AT 8 HZ

AUTHOR: JOHN ARIS SLANKIS

TITLE: TELLURIC AND MAGNETOTELLURIC SURVEYS AT 8 HZ

DEPARTMENT: MINING ENGINEERING AND APPLIED GEOPHYSICS

DEGREE: DOCTOR OF PHILOSOPHY

ABSTRACT

The use of natural electro-magnetic fields at 8 Hz for mineral exploration and geological mapping has been investigated and optimum measurement techniques have been developed.

Both telluric and magnetotelluric surveys have detected resistivity variations associated with some metallic sulphide deposits and geological contacts. Such conductivity discontinuities are characterized by variations in the apparent resistivity, the spatial anisotropy of the telluric field and, in some instances, the presence of a strong vertical magnetic field component. Also, the correlation and phase relationship between the telluric field near a conductivity discontinuity and the background field is variable.

For the case where the telluric field is measured normal to the strike of a conductivity discontinuity theoretical results for two-dimensional models of the actual geology agree well with the observed and offer an explanation for the variable phase and correlation.

TELLURIC AND MAGNETOTELLURIC
SURVEYS AT 8 HZ

by

John Aris Slankis

A thesis submitted to the Faculty of Graduate Studies and Research of McGill University in partial fulfilment of the requirements for the degree of Doctor of Philosophy.

Department of Mining Engineering
and Applied Geophysics,
McGill University,
Montreal.

July, 1970.

ACKNOWLEDGEMENTS

The writer would like to thank his thesis advisor, Dr. W.M. Telford, for his encouragement and guidance throughout this investigation.

The support of the Geological Survey of Canada is gratefully acknowledged. Particular gratitude is expressed to Dr. A. Becker who supervised the field work and to Mr. L.S. Collett, Head of the Electrical Methods Section, who showed continued interest in this work.

The help of Messrs. R.A. Fisher and G.A. Bojars in the field work is appreciated.

The writer's colleagues, in particular Messrs. W.J. Scott and C.R.S. Haslam, are thanked for their interest and assistance.

The following companies are thanked for providing both access to their properties and a great deal of geological and geophysical information:

Atlantic Nickel Mines Ltd.

East Sullivan Mines Ltd.

Kennco Explorations (Canada) Ltd.

Opemisca Explorers Ltd.

Rio Tinto Canadian Exploration Ltd.

St Lawrence Columbium and Metals Corporation

Tache Lake Mines Ltd.

Teck Corporation Ltd.

Texas Gulf Sulphur Company

Vendome Mines Ltd.

TABLE OF CONTENTS

CHAPTER I

INTRODUCTION

1.1 Natural Electromagnetic Field Methods

Standard geophysical electrical and electromagnetic methods, used to determine the electrical properties of the ground or to search for electrical conductors, use a transmitter and receiver which are coupled galvanically or inductively through the ground. Where deep penetration is desired these methods require powerful transmitters whose weight and size increase the cost and reduce the speed of operation.

It is possible, however, to resort to another class of electrical prospecting methods which employs ambient natural electromagnetic fields. The attractive features of these methods are that no transmitter is required and a complete spectrum of frequencies is available.

The practical use of naturally occurring electric fields to investigate the electrical characteristics of the ground was first discussed by Leonardon (1928). Subsequent attempts to utilize telluric currents for geological mapping (Schlumberger, 1939; Neunschwander and Metcalf, 1942; Dahlberg, 1945) achieved some success but were generally hampered by low equipment sensitivity. Also, there was no theoretical basis for interpretation at that time.

The electromagnetic nature of magnetotelluric fields was discovered in the early 1950's and Tikhonov (1950) suggested that additional information could be obtained by measuring both the magnetic and telluric fields. However, it was not until Cagniard (1953) published his classic paper on magnetotelluric theory that the potential of natural field measurements became apparent. He showed that the resistivity of uniform ground can be determined by measuring the ratio of telluric and magnetic fields at one frequency or, if the ground consists of horizontal layers of different resistivities, the variations in resistivity with depth can be found by measuring the field ratio over a range of frequencies.

Consequently, considerable effort has been devoted to both the theoretical and practical development of natural field methods. Magnetotelluric theory has been extended to two-dimensional resistivity geometries and the inverse problem of interpreting field data has been attempted. The field techniques that have been developed include the magnetotelluric, telluric and Afmag methods. Strangway and Vozoff (1970) have summarized the main features of each method.

The magnetotelluric method measures both the telluric and magnetic fields. It is the only one which can be used to detect resistivity changes with depth. Utilizing natural fields in the frequency range of 10^{-5} Hz to 50 Hz, magnetotellurics have been used for depth sounding in the search for petroleum and for studies of the earth's interior. This technique is slower and more expensive than the other methods.

The Afmag method measures the ratio between the vertical and horizontal magnetic fields at frequencies from 100 Hz to 1000 Hz. The measurements may be made either on the ground or in an airplane. This technique will detect only lateral changes in the resistivity of the ground. It has been successfully employed in mineral prospecting and to outline geological features such as faults and contacts. In high latitudes the use of the Afmag method is somewhat restricted by diurnal and seasonal variations in the source signals.

The telluric method measures directional and spatial variations in the telluric current intensity and, like Afmag, can only detect lateral changes in resistivity. This technique has been used less than the other natural field methods and only a few papers, describing its application to geological mapping (Boissonas and Leonardon, 1948; Berdichevskii, 1960; Srivastava et al., 1963), have been published. The telluric method does not appear to have been applied to mineral exploration to any extent.

1.2 Purpose and Development of Present Work

This thesis describes a joint project of McGill University and the Geological Survey of Canada to evaluate the use of sub-audio frequency telluric and magnetotelluric measurements for mineral exploration and, to a lesser extent, for geological mapping. The author was employed by the G.S.C. during the summers from 1966 to 1968 to carry out the field measurements. Also, most of the field equipment was designed and constructed at the G.S.C.. The processing of field results and the theoretical analyses were carried out at McGill.

In order to keep the equipment simple and portable, measurements were made at a single frequency using the 8 Hz thunderstorm signal propagated in the first Schumann resonance mode. The choice of this frequency was dictated by the strength and relatively steady level of the 8 Hz signal (Galejs, 1964; Shand, 1966) and the desire to obtain a considerable depth of penetration.

Initial field tests were made over near-surface massive sulphide zones. The basic criteria for selecting test locations were easy road access and the availability of sufficient diamond drill data to outline mineralized zones. When positive results were obtained in these cases, subsequent locations were chosen to examine the penetration and resolution of the methods. Several test sites were visited more than once either to check the repeatability of results or to test equipment modifications and new measurement techniques.

Theoretical studies were subsequently carried out to explain the observed field results and to determine the parameters that limit the effectiveness of natural field methods. Because analytic solutions are possible only for very simple resistivity geometries, numerical methods were used to derive theoretical anomalies over two-dimensional models of the actual field geology.

CHAPTER II

THEORETICAL ANALYSIS

2.1 Magnetotelluric Theory

Natural electromagnetic fields originate from two sources (Bleil, 1964). At frequencies below 1-5 Hz the sources are considered to be ionospheric current sheets. Higher frequency fields are of atmospheric origin; in particular, the Schumann resonance fields originate from lightning discharges in the lower atmosphere and the energy propagates in the earth-ionosphere resonant cavity. In either case the electromagnetic field travels through the atmosphere and is reflected and refracted at the air-earth interface.

The equations that describe the behaviour of the electromagnetic fields have been derived by many authors (Cagniard, 1953; Neves, 1957; Price, 1962; Rankin, 1962; Weaver, 1963; Blake and Swift, 1967; Swift, 1967; Madden and Swift, 1969).

In the following derivation all media are assumed to be homogeneous and isotropic, to have the permeability (μ_o) and permittivity (ε_o) of free space and to contain no sources. The rationalized MKS system of units and Cartesian coordinates (Fig. 2.1) are used.

The electric field E and the magnetic field H satisfy Maxwell's equations:

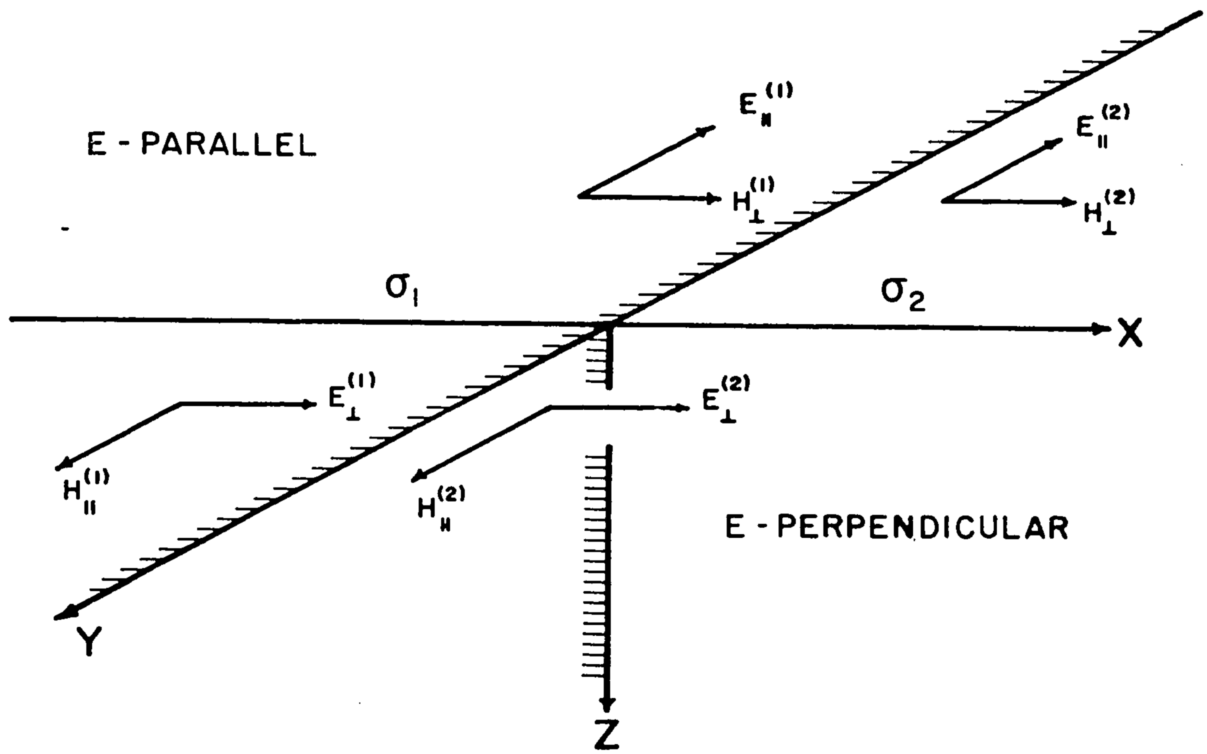

Fig. 2.1 Coordinate system and electromagnetic field components for E-parallel and E-perpendicular polarizations.

$$\nabla \times E = -\frac{\partial B}{\partial t}$$

$$\nabla \times H = J + \frac{\partial D}{\partial t}$$

where $B = \mu_o H$, $J = \sigma E$ and $D = \varepsilon_o E$.

If a periodic signal with $e^{i\omega t}$ time dependence is assumed, the equations become

$$\nabla \times E = -i\omega\mu_o H \qquad 2.1 - 1a$$

$$\nabla \times H = \sigma E + i\omega\varepsilon_o E \qquad 2.1 - 1b$$

These can be combined into the vector Helmholtz equations

$$\nabla^2 \begin{pmatrix} E \\ H \end{pmatrix} + k^2 \begin{pmatrix} E \\ H \end{pmatrix} = 0 \qquad 2.1 - 2$$

where $k^2 = -i\omega\mu_o\sigma + \varepsilon_o\mu_o\omega^2$.

At magnetotelluric frequencies the propagation constant k in the earth is dominated by the conduction term. Therefore $k^2_{earth} = -i\omega\mu_o\sigma$ and the Helmholtz equations become complex diffusion equations. Because the air has zero conductivity $k^2_{air} = \varepsilon_o\mu_o\omega^2$.

Furthermore, the propagation constant is much larger in the ground than in the air so that, regardless of the angle of incidence of the source field, the refracted electromagnetic field will travel straight down as a plane wave. The amplitude of the field decreases with depth according to the skin effect.

This assumption of plane waves within the earth has been criticized by Wait (1954) and Price (1962). They have shown that the assumption is not valid unless the incident field is uniform over horizontal distances much larger than its skin depth in the ground. This restriction becomes severe at low frequencies. However, Madden and Nelson (1964) have concluded that for realistic models of earth conductivities the plane wave assumption is valid for the frequency range from 10^{-4} to 10^{4} Hz. Certainly it should be true for the frequency and distances involved in this work.

One-Dimensional Problem

The solution of the Helmholtz equations for either a homogeneous or horizontally layered earth is straightforward. Because of the one-dimensional nature of the problem all fields are laterally invariant ($\frac{\partial}{\partial x} = \frac{\partial}{\partial y} = 0$) and we may consider any two orthogonal field components E_x and H_y. In this case, for homogeneous ground, the vector equations (Eq. 2.1 - 2) become scalar equations

$$\partial^2 E_x/\partial z^2 - i\eta^2 E_x = 0 \qquad 2.1 - 3a$$

$$\partial^2 H_y/\partial z^2 - i\eta^2 H_y = 0 \qquad 2.1 - 3b$$

where $\eta^2 = \omega\mu_o\sigma$.

A solution for 2.1 - 3b that satisfies the condition $\lim_{z\to\infty} H_y = 0$ is $H_y = H_y^o\, e^{-\sqrt{i}\eta z}$ where H_y^o is the magnetic field at the surface ($z = 0$).

In the one-dimensional case equation 2.1 - 1b becomes

$$- \partial H_y/\partial z = \sigma E_x$$

Therefore $$E_x = \sqrt{i}\sqrt{\frac{\omega\mu_o}{\sigma}}\, H_y^o\, e^{-\sqrt{i}\eta z}$$

and, at the surface of the ground

$$E_x^o \,/\, H_y^o = \sqrt{\frac{\omega\mu_o}{\sigma}}\sqrt{i} = \sqrt{\frac{\omega\mu_o}{\sigma}}\underline{/45^o} \qquad 2.1 - 4$$

The ratio $E_x^o \,/\, H_y^o$ is the electromagnetic impedance of the medium - in this case the ground. If it is homogeneous, the electric field leads the space-orthogonal magnetic field by 45^o. Equation 2.1 - 4 may be rewritten as

$$\rho = \frac{1}{\omega\mu_o} \left|E_x^o \,/\, H_y^o\right|^2 \qquad 2.1 - 5$$

where $\rho = 1/\sigma$. This is the magnetotelluric equation in MKS units. The more familiar form of this expression, in suitable units, is

$$\rho = 0.2T \left|E_x^o \,/\, H_y^o\right|^2$$

where ρ = resistivity in ohm-meters

T = period in seconds

E_x^o = electric field in mV/km

H_y^o = magnetic field in gammas

From equation 2.1 - 5 it can be seen that, if the electric and magnetic fields are measured simultaneously at one location, the resistivity of the ground can be determined. If the ground is homogeneous the measured value will be the true resistivity. If this is not the case, we will obtain an apparent resistivity that is a function of the resistivity and the thickness of the horizontal layers. Also, since the phase angle and the measured resistivity are functions of frequency, by measuring both over a range of frequencies it is possible to determine approximately the resistivity variations with depth. This is the basis of the magnetotelluric method.

Two-Dimensional Problem

The homogeneous cr layered-media solutions are inappropriate in areas where lateral conductivity variations exist. Ideally the problem should be considered in three dimensions but at present analytic and numerical methods are restricted to two-dimensional situations. In this discussion all resistivity features will be assumed to have infinite strike length in the y direction (Fig. 2.1) and the electromagnetic field to be invariant along strike ($\frac{\partial}{\partial y} = 0$). The errors introduced by modelling a three-dimensional field situation by a two-dimensional model are discussed in Section 2.2.

We will consider the vertical contact between two homogeneous media shown in Figure 2.1. Regardless of the orientation of the source field the electric and magnetic fields can be resolved into components normal and parallel to the strike of the discontinuity. Therefore, there are two pairs of orthogonal fields, $E_{\perp}$ and $H_{\parallel}$, and, $E_{\parallel}$ and $H_{\perp}$. Various authors have referred to these as either the E-perpendicular, TM (Transverse Magnetic) or H-polarization and E-parallel, TE (Transverse Electric) or E-polarization cases. This work uses the terms E-parallel and E-perpendicular because they are descriptive of the direction in which the telluric field was measured in the field work.

At large distances from the contact any disturbances introduced in the magnetotelluric fields by the contact will have disappeared. The resistivity value will be that appropriate to each medium whether $E_\perp$ and $H_\parallel$ or $E_\parallel$ and $H_\perp$ are measured. The anomaly observed over the contact will depend on the boundary conditions that govern the behaviour of the electromagnetic field components at the conductivity interface.

For the E-perpendicular case the two-dimensional form ($\frac{\partial}{\partial y} = 0$) of Maxwell's equations (Eqs. 2.1 - 1a and - 1b) is

$$\partial E_z/\partial x - \partial E_x/\partial z = i\omega\mu_o H_y \qquad 2.1 - 6a$$

$$-\partial H_y/\partial z = \sigma E_x \qquad 2.1 - 6b$$

$$\partial H_y/\partial x = \sigma E_z \qquad 2.1 - 6c$$

These can be combined to give a scalar Helmholtz equation in H_y

$$\partial^2 H_y/\partial x^2 + \partial^2 H_y/\partial z^2 - i\eta^2 H_y = 0 \qquad 2.1 - 7$$

where $\eta^2 = \omega\mu_o\sigma$.

H_y is a convenient variable in two-dimensional problems: since it is parallel to all interfaces, boundary conditions are relatively simple and the other field components E_x and E_z can be easily derived from it. Also, the air has zero conductivity and at magnetotelluric frequencies displacement currents can be neglected, so that $J_z\big|_{z=o} = 0$. Therefore, $E_z\big|_{z=o} = 0$, $\partial H_y/\partial x\big|_{z=o} = 0$ (Eq. 2.1 - 6c), and H_y does not vary along the surface of the ground. Thus, for the E-perpendicular polarization, any lateral changes in the resistivity of the ground will be reflected only in variations in the electric field. These simplifying conditions are important for both the theoretical solution and practical use of this polarization.

For theoretical solutions we need only consider the behaviour of the electromagnetic fields in the ground and can neglect the air layer. For this reason it has been possible to obtain explicit analytic solutions for a vertical fault (d'Erceville and Kunetz, 1962; Weaver, 1963; Blake and Swift, 1967) and a vertical dike (Rankin, 1962; Blake and Swift, 1967).

In the field, if $E_\perp$ and $H_\parallel$ are simultaneously measured at two points, then from equation 2.1 - 5

$$E_x^{(1)}/E_x^{(2)} = \sqrt{\rho_1/\rho_2}\ \left|H_y^{(1)}/H_y^{(2)}\right| \qquad 2.1 - 8$$

Since $H_y^{(1)} = H_y^{(2)}$, the ratio of telluric field strengths is proportional to the square roots of the apparent resistivities at the two locations.

For the E-parallel polarization the two-dimensional form $\left(\frac{\partial}{\partial y} = 0 \right)$ of Maxwell's equations is

$$\partial E_y/\partial x = - i\omega\mu_o H_z \qquad 2.1 - 9a$$

$$\partial E_y/\partial z = i\omega\mu_o H_x \qquad 2.1 - 9b$$

$$\partial H_x/\partial z - \partial H_z/\partial x = \sigma E_y \qquad 2.1 - 9c$$

From these can be derived a scalar Helmholtz equation for E_y

$$\partial^2 E_y/\partial x^2 + \partial^2 E_y/\partial z^2 - i\eta^2 E_y = 0 \qquad 2.1 - 10$$

E_y is used here for the same reasons that H_y was chosen for the other polarization. In this case, however, all the field components E_y , H_x and H_z are continuous across the air-ground interface and the effect of the air layer has to be included in the solution. Published analytic solutions for this polarization (d'Erceville and Kunetz, 1962; Weaver, 1963; Blake and Swift, 1967) have incorrectly assumed that the horizontal electric field is constant at the surface of the ground. It appears that solutions for this polarization can only be obtained by numerical methods. In the field both $E_{\parallel}$ and $H_{\perp}$ have to be measured to determine the ratio of apparent resistivities at two locations.

2.2 Solution of Magnetotelluric Problem by Numerical Methods

Finite Difference Method

The first numerical calculations of magnetotelluric anomalies were made by Neves (1957). He used finite differences to compute apparent resistivities over vertical and dipping interfaces between media of different conductivities. Finite difference methods have also been used by Patrick and Bostick (1969) to map apparent resistivity data into one- and two-dimensional structures.

Since the advent of digital computers considerable information has been published on the formulation of finite difference equations and methods of solution (Sheldon, 1958; Forsythe and Wasow, 1960; Vitkovitch, 1966; Wachspress, 1966; Westlake, 1968). Figure 2.2 summarizes the basic features of the method.

The geologic section is divided into a non-uniform mesh, whose spacing is small in the area of conductivity discontinuities, where complex shapes need to be mapped and the magnetotelluric fields undergo rapid changes. Away from the interfaces the mesh spacing increases according to a geometric progression. Thus the boundaries of the mesh can be located sufficiently far from the conductivity anomaly to assume that the magnetotelluric fields are undisturbed and Dirichlet boundary conditions can be applied.

The finite difference form of the Helmholtz equation for H_y or E_y (Eqs. 2.1 - 7 and 2.1 - 10) at a mesh point is obtained by

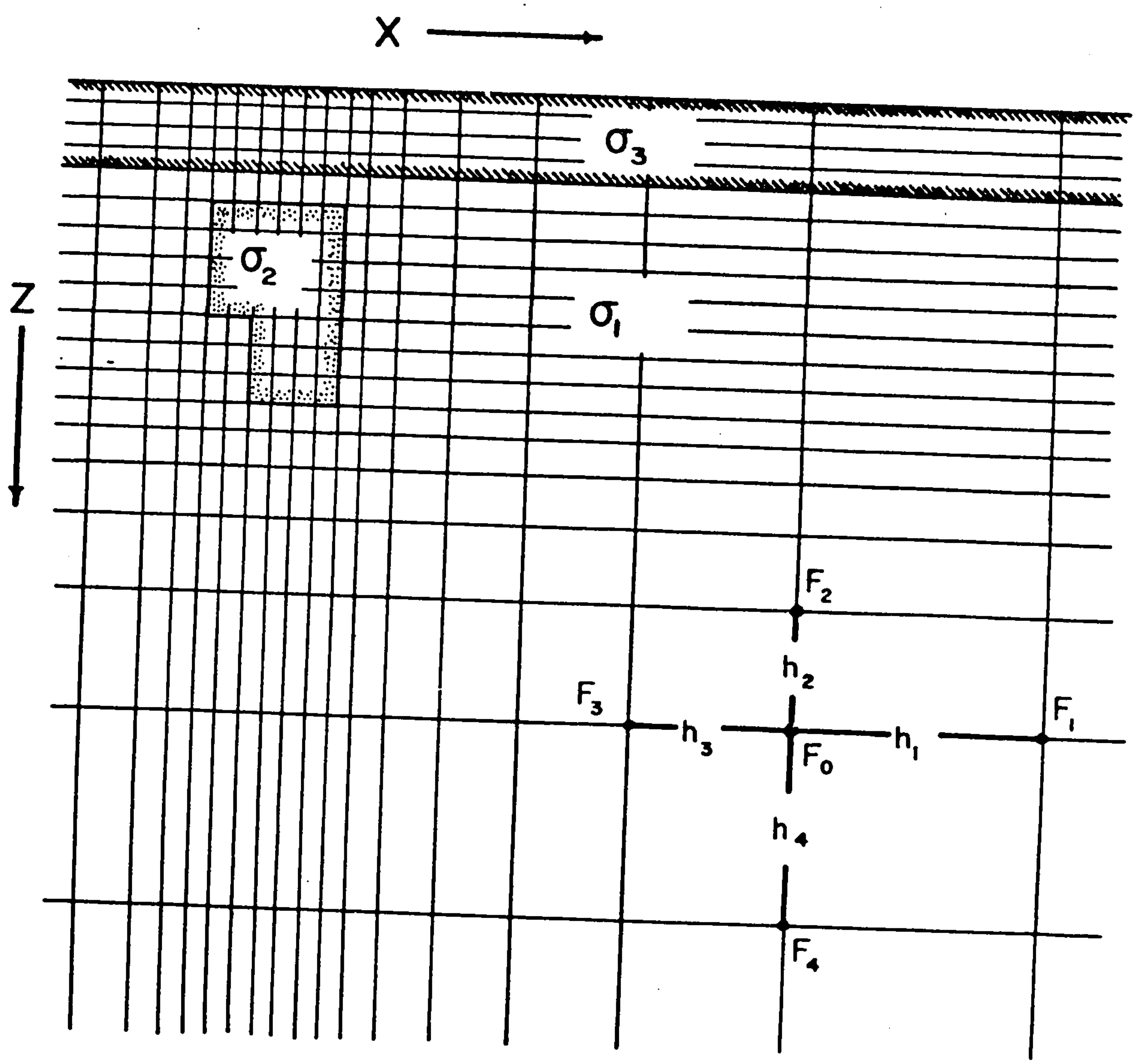

Fig. 2.2 Finite difference mesh.

replacing the partial derivatives by approximate expressions of central differences involving the field-function values at adjacent mesh points. The Helmholtz equations may be written

$$\nabla^2 F - i\eta^2 F = 0 \qquad 2.2 - 1$$

where $F = H_y$ or E_y and $\nabla^2 = \frac{\partial^2}{\partial x^2} + \frac{\partial^2}{\partial z^2}$. By expanding F in a Taylor's series about the central point (Fig. 2.2) we obtain

$$\nabla^2 F_0 = 2\left[\frac{F_1}{h_1(h_1+h_3)} + \frac{F_2}{h_2(h_2+h_4)} + \frac{F_3}{h_3(h_1+h_3)} + \frac{F_4}{h_4(h_2+h_4)} - F_0\left[\frac{1}{h_1 h_3} + \frac{1}{h_2 h_4}\right]\right] \qquad 2.2 - 2$$

The method of solution requires that the real and imaginary components of F be considered separately. If $F = R + iI$, where R and I are the real and imaginary components, we obtain from equation 2.2 - 1 the following coupled equations

$$\nabla^2 R + \eta^2 I = 0$$

$$\nabla^2 I - \eta^2 R = 0$$

Then, from equation 2.2 - 2

$$R_0 = R_1 G_1 + R_2 G_2 + R_3 G_3 + R_4 G_4 + I_0 G_5 \qquad 2.2 - 3a$$

$$I_0 = I_1 G_1 + I_2 G_2 + I_3 G_3 + I_4 G_4 - R_0 G_5 \qquad 2.2 - 3b$$

where

$$p = 1/h_1h_3 + 1/h_2h_4$$

$$G_1 = 1/(ph_1(h_1+h_3))$$

$$G_2 = 1/(ph_2(h_2+h_4))$$

$$G_3 = 1/(ph_3(h_1+h_3))$$

$$G_4 = 1/(ph_4(h_2+h_4))$$

$$G_5 = \eta^2/2p$$

For mesh points located on the boundary between media of different conductivities the finite difference equations are modified to conform to the appropriate electric and magnetic field continuity conditions.

For the E-perpendicular polarization Dirichlet boundary conditions are used at the mesh boundaries. The magnetic field H_y is constant at $z = 0$ and has values consistent with laterally homogeneous media at the edges of the mesh. In problems involving finite conductivity anomalies the bottom of the mesh is deep enough to assume a uniform field. For conductivity geometries involving infinite depth extent the mesh is extended sufficiently deep to approximate $H_y = 0$ at the bottom.

In the E-parallel case the boundary values for E_y on the sides and at the bottom of the mesh are determined in the same way as for the E-perpendicular polarization. However, in this instance, the top of the mesh corresponds to the air-ionosphere interface. At low frequencies, where ionospheric currents are the source of magnetotelluric fields, the magnetic field (H_x) is assumed to be constant at the top of the air layer (Swift, 1967; Patrick and Bostick, 1969). Hence, Neumann boundary conditions based on equation 2.1 - 9b ($\partial E_y/\partial z = i\omega\mu_o H_x$) are used for E_y. The 8 Hz fields are of atmospheric origin but, because the ionosphere is much more conductive than the atmosphere and its conductivity is laterally constant, $H_z = 0$ at the air-ionosphere interface. Since $\partial E_y/\partial x = - i\omega\mu_o H_z$ (Eq. 2.1 - 9a), E_y must be constant at the top of the air layer. In practice, excepting theoretical cases involving frequencies below 1000 Hz and non-horizontal contacts between semi-infinite media, identical results are obtained whether E_y or $\partial E_y/\partial z$ are assumed to be constant at the top of the air layer.

The values of the fields at interior mesh points were computed iteratively using point successive overrelaxation (Wachspress, 1966). The real and imaginary parts of the field function (Eqs. 2.2 - 3a and 2.2 - 3b) were calculated in alternating sweeps through the mesh. For the E-perpendicular case an overrelaxation factor of 1.5 was used whereas, for E-parallel, the factors were 1.3 and 1.7 in the ground and in the air layer respectively. These optimum factors were determined empirically.

Good agreement was obtained between analytic and numerical results for simple conductivity geometries (Fig. 2.4). However, an excessive amount of programming is required to set up the complex conductivity geometries encountered in modelling actual geologic structures. In particular, because special finite difference equations are required at mesh points located on conductivity interfaces, it is necessary to define all such boundary points and insert the appropriate forms of the equations.

Impedance Network Method

This method uses the voltages and currents in an impedance network as analogues to the actual fields involved in a problem. The variety of possible network elements gives this method great versatility. Vine (1966) has presented a comprehensive study of the application of this method to obtain numerical solutions for many types of partial differential equations. A number of authors (Madden and Thompson, 1965; Swift, 1967; Madden and Swift, 1969) have used impedance networks to obtain numerical solutions of the magnetotelluric equations in one and two dimensions.

Slater (1942) gives the following voltage-current relationships for the two-dimensional impedance network shown in Figure 2.3 :

$$\text{grad } V = - ZI \qquad 2.2 - 4a$$

$$\text{div } I = - YV \qquad 2.2 - 4b$$

where V = volts

I = amperes/m

Y = mhos/m^2 (admittance)

Z = ohms (impedance)

Therefore, if $\frac{\partial}{\partial y} = 0$,

$$\partial I_x/\partial x + \partial I_z/\partial z = - YV \qquad 2.2 - 5a$$

$$\partial V/\partial z = - ZI_z \qquad 2.2 - 5b$$

$$\partial V/\partial x = - ZI_x \qquad 2.2 - 5c$$

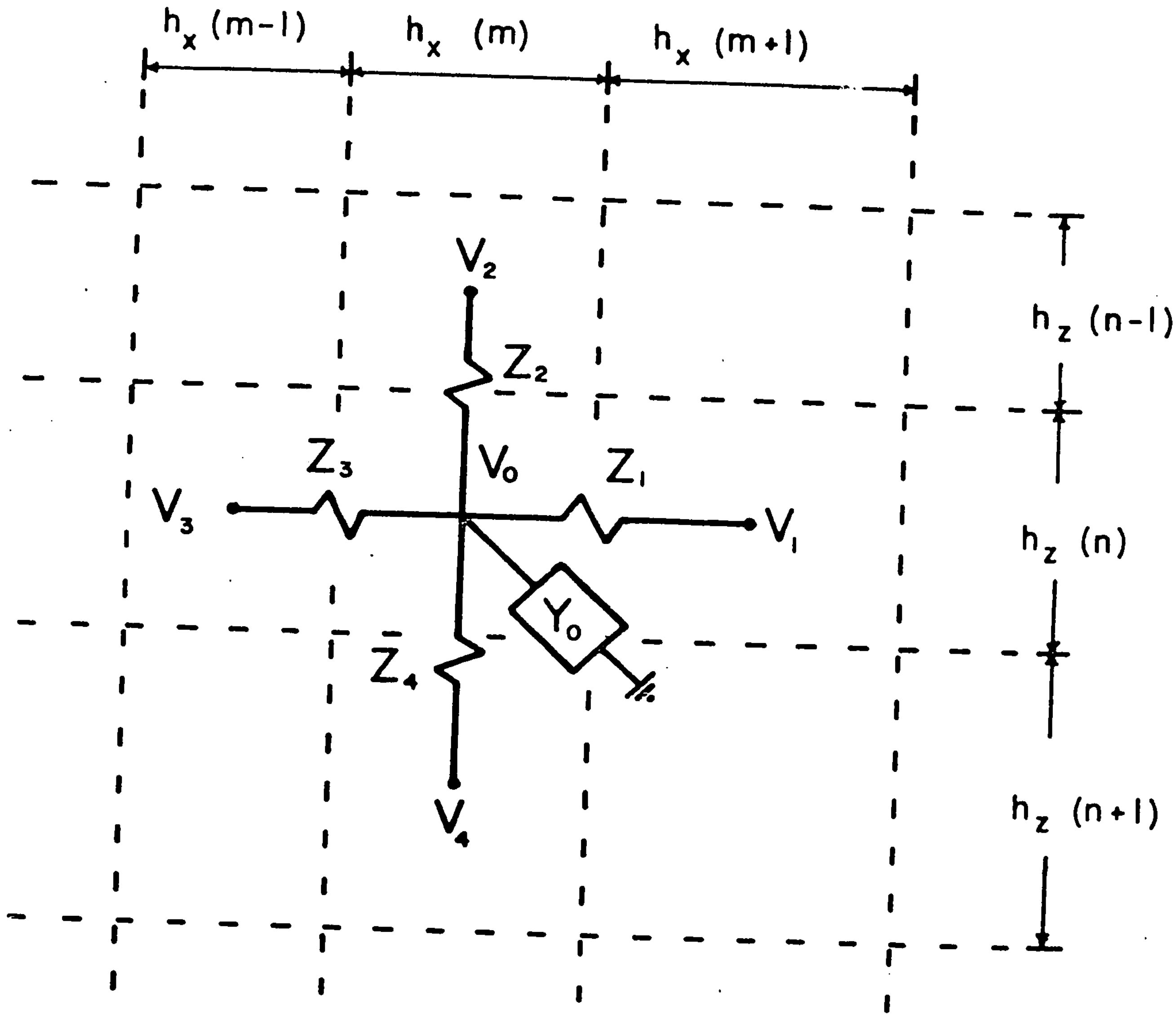

Fig. 2.3 Impedance mesh.

Comparison of equations 2.1 - 6 and 2.2 - 5 gives the following associations between field and network quantities for the E-perpendicular polarization

$$
\begin{aligned}
H_y &\longleftrightarrow V \\
E_x &\longleftrightarrow I_z \\
E_z &\longleftrightarrow - I_x \\
\sigma &\longleftrightarrow Z \\
i\omega\mu_o &\longleftrightarrow Y
\end{aligned}
\qquad 2.2 - 6
$$

For the E-parallel polarization the corresponding associations can be obtained from equations 2.1 - 9 and 2.2 - 5

$$
\begin{aligned}
E_y &\longleftrightarrow V \\
H_x &\longleftrightarrow - I_z \\
H_z &\longleftrightarrow I_x \\
\sigma &\longleftrightarrow Y \\
i\omega\mu_o &\longleftrightarrow Z
\end{aligned}
\qquad 2.2 - 7
$$

The lumped circuit elements Y and Z depend on the mesh geometry. The admittance is proportional to the area of the cell and the impedance is proportional to the distance between nodes and inversely proportional to the width of the associated surface.

The lumped network elements for the E-perpendicular polarization are

$$Y_0 = i\omega\mu_o(h_x[m]\ h_z[n])$$
$$Z_1 = (\sigma[m,n]\ h_x[m]/2 + \sigma[m+1,n]\ h_x[m+1]/2)/h_z[n]$$
$$Z_2 = (\sigma[m,n]\ h_z[n]/2 + \sigma[m,n-1]\ h_z[n-1]/2)/h_x[m] \qquad 2.2-8$$
$$Z_3 = (\sigma[m,n]\ h_x[m]/2 + \sigma[m-1,n]\ h_x[m-1]/2)/h_z[n]$$
$$Z_4 = (\sigma[m,n]\ h_z[n]/2 + \sigma[m,n+1]\ h_z[n+1]/2)/h_x[m]$$

Similarly, for the E-parallel case

$$Y_0 = \sigma[m,n]\ h_x[m]\ h_z[n]$$
$$Z_1 = i\omega\mu_o(h_x[m]/2 + h_x[m+1]/2)/h_z[n]$$
$$Z_2 = i\omega\mu_o(h_z[n]/2 + h_z[n-1]/2)/h_x[m] \qquad 2.2-9$$
$$Z_3 = i\omega\mu_o(h_x[m]/2 + h_x[m-1]/2)/h_z[n]$$
$$Z_4 = i\omega\mu_o(h_z[n]/2 + h_z[n+1]/2)/h_x[m]$$

Kirchoff's law of current continuity is used to derive the relationship between the voltage at the central node and the voltages at adjacent mesh points

$$\sum_{k=1}^{4} \frac{V_k - V_o}{Z_k} - Y_o V_o = 0 \qquad 2.2-10$$

For iterative solutions, V is separated into real and imaginary components $V = R + iI$ to obtain the following coupled equations

$$R_0 = Z_5(R_1/Z_1 + R_2/Z_2 + R_3/Z_3 + R_4/Z_4 + I_0Y_0)$$

$$I_0 = Z_5(I_1/Z_1 + I_2/Z_2 + I_3/Z_3 + I_4/Z_4 - R_0Y_0)$$

where $Z_5 = 1/(1/Z_1 + 1/Z_2 + 1/Z_3 + 1/Z_4)$.

The form of these equations is identical to the finite difference equations (Eqs. 2.2 - 3a and 2.2 - 3b). However, because conductivity changes are included in calculating the network parameters (Eqs. 2.2 - 8 and 2.2 - 9), the impedance network approach does not require special equations at points located on conductivity interfaces.

The treatment of mesh boundaries for the impedance mesh approach is very similar to that used in the finite difference method. For the E-perpendicular case a constant V at $z = 0$ corresponds to a uniform surface magnetic field. For E-parallel, a constant electric field at the top of the air layer is modelled by V = constant or, alternatively, I_z = constant is equivalent to a uniform magnetic field. In the air layer $\sigma = 0$ so that there are no admittances to ground.

The bottom of the mesh is sufficiently deep so that diffraction effects from near-surface conductivity discontinuities are negligible. The network is terminated by the characteristic impedances

$$Z_c = \sqrt{Z/Y}\,/h_x[m]$$

appropriate to the media.

Boundary values at the edges of the mesh are obtained by numerically solving a one-dimensional transmission line problem.

The iterative solutions converged satisfactorily for the same overrelaxation factors as were used for finite differences. Good agreement was obtained between analytic and numerical solutions for the E-perpendicular polarization (Fig. 2.4). The time required to solve a 1000 mesh point problem ranged from 30 to 180 seconds on an IBM 360-75 computer. This was deemed excessive and solutions by direct matrix methods were investigated.

Minor alterations converted the existing iterative impedance mesh programs to a form suitable for matrix solution. A highly optimized routine for solving band matrices by Gaussian elimination (Chari, 1970) was adapted to handle complex matrices.

Figure 2.4 illustrates the results obtained by matrix solution over a vertical contact between two media for the E-perpendicular polarization. The accuracy of the E-parallel calculations was checked against the analytic solution for an infinitely long conductive cylinder in a non-conducting medium (Ward, 1967). The results are shown in Figure 2.5 .

In most instances the direct matrix solutions proved to be superior to the iterative. A problem involving 1000 (50x20) mesh points can be solved in less than 14 seconds and a 525 (35x15) point mesh in less than 6 seconds. However, exclusive of the program compilation, the core required for a 50x20 mesh is 135000 bytes for

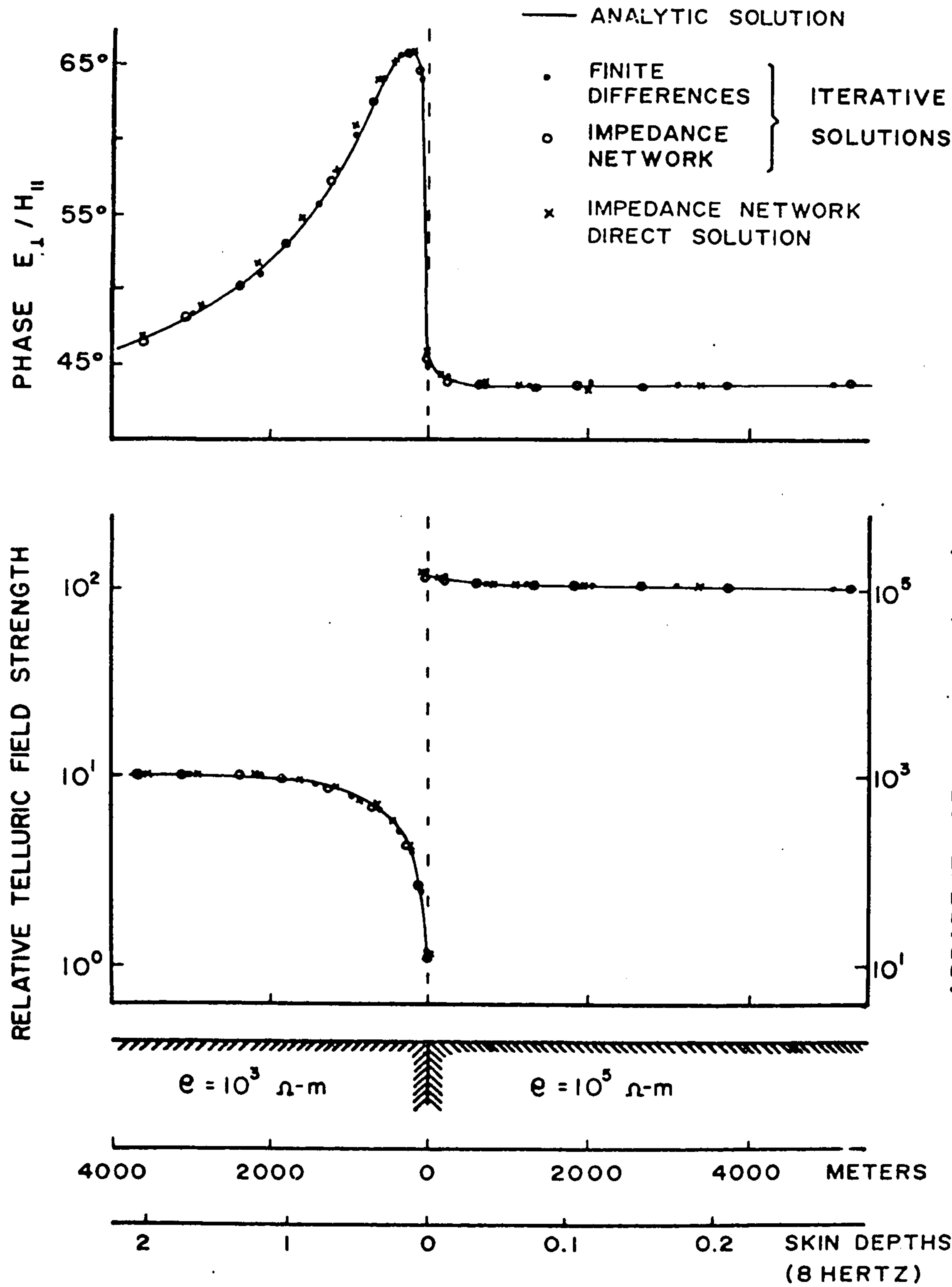

Fig. 2.4 Comparison of analytic (d'Erceville and Kunetz, 1962) and numerical solutions over vertical contact between semi-infinite media for E-perpendicular polarization.

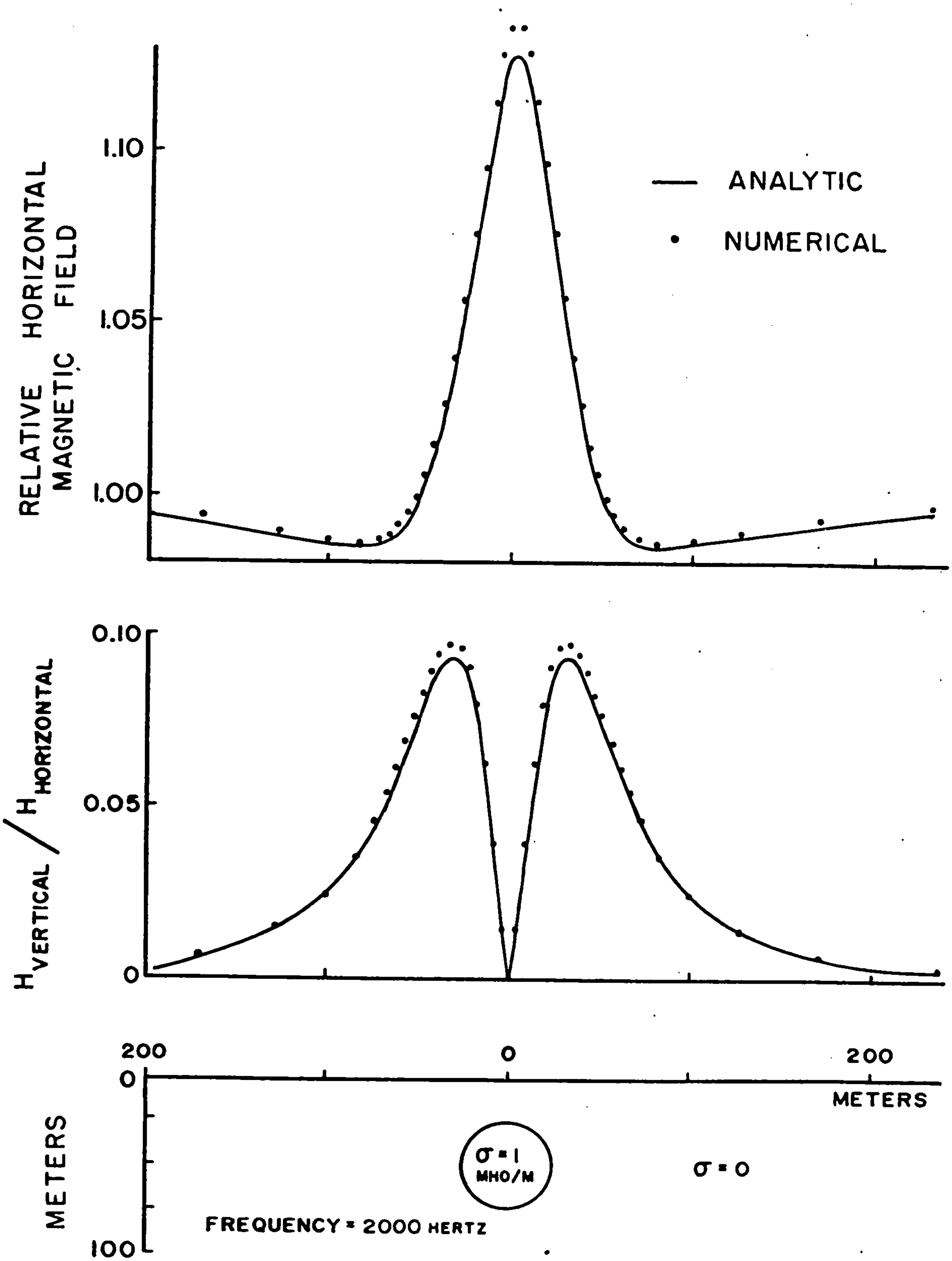

Fig. 2.5 Comparison of analytic (Ward, 1967) and numerical results over conductive cylinder in non-conducting medium for E-parallel polarization.

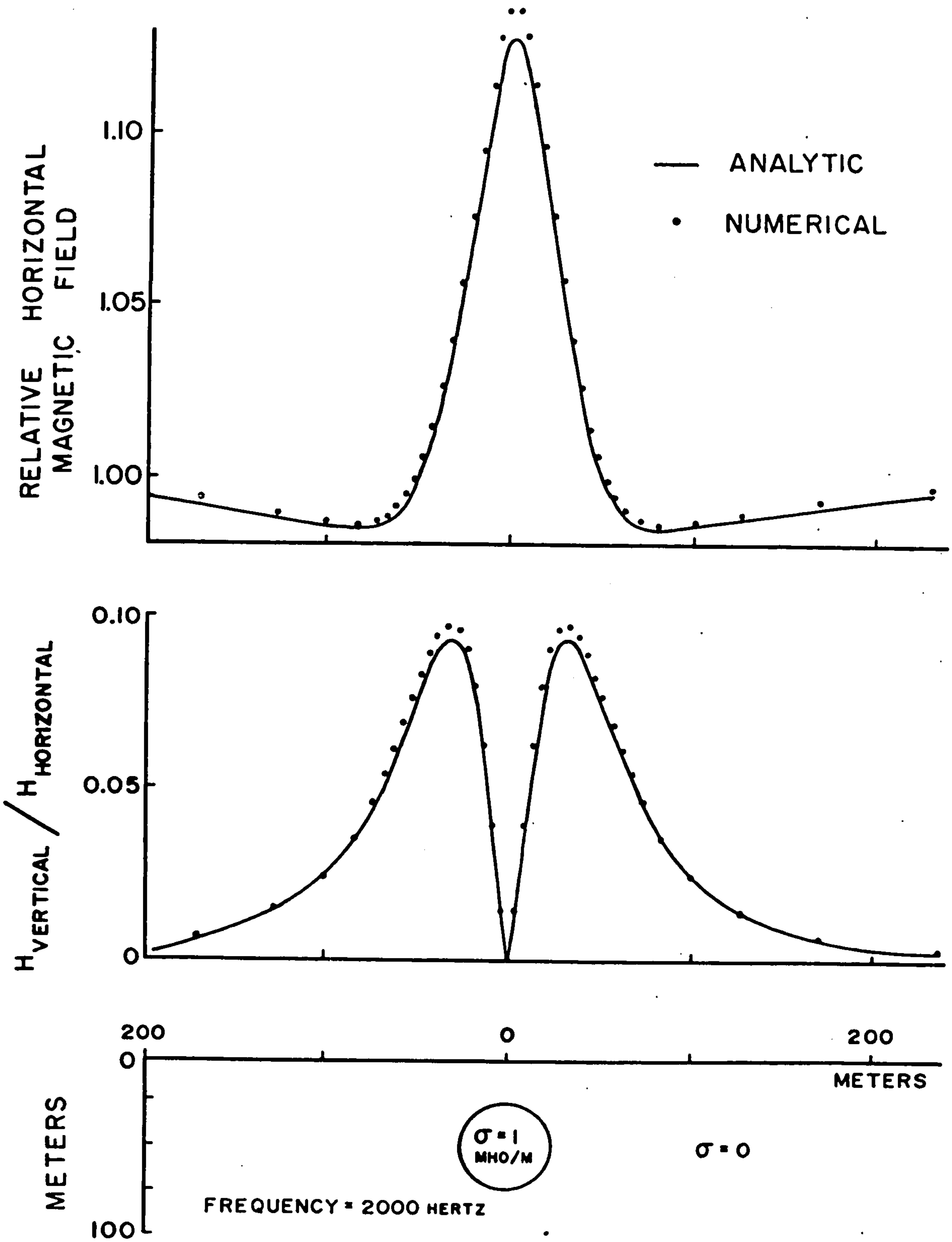

Fig. 2.5 Comparison of analytic (Ward, 1967) and numerical results over conductive cylinder in non-conducting medium for E-parallel polarization.

the matrix solution and 28000 bytes for the iterative. For a 50x40 mesh the corresponding values are 590000 and 56000 bytes. Also, the time required to obtain a solution by direct methods increases approximately as n^3 where n is the number of interior mesh points. Consequently, for problems involving a large number of mesh points, iterative solutions can be more economical.

Limitations of Two-Dimensional Solutions

Numerical solutions of the magnetotelluric equations are possible only for two-dimensional conductivity geometries with infinite strike extent. The geologic structures encountered in the field usually have limited strike length. Therefore the use of numerical methods to compute theoretical anomalies over actual geologic structures depends on the applicability of two-dimensional models to three-dimensional shapes. In particular, it is necessary to examine the effect of limited strike length on observed magnetotelluric anomalies. This can be illustrated very qualitatively by considering the behaviour of either the electric or magnetic field around a conductive slab buried in a resistive medium (Fig. 2.6). This discussion considers the behaviour of the electric field.

Magnetotelluric anomalies are disturbances in the electromagnetic field components caused by conductivity discontinuities. In this instance, the greater the difference between the electric fields inside and outside the slab, the greater will be the resultant anomaly. Hence a qualitative assessment of the effect of limited

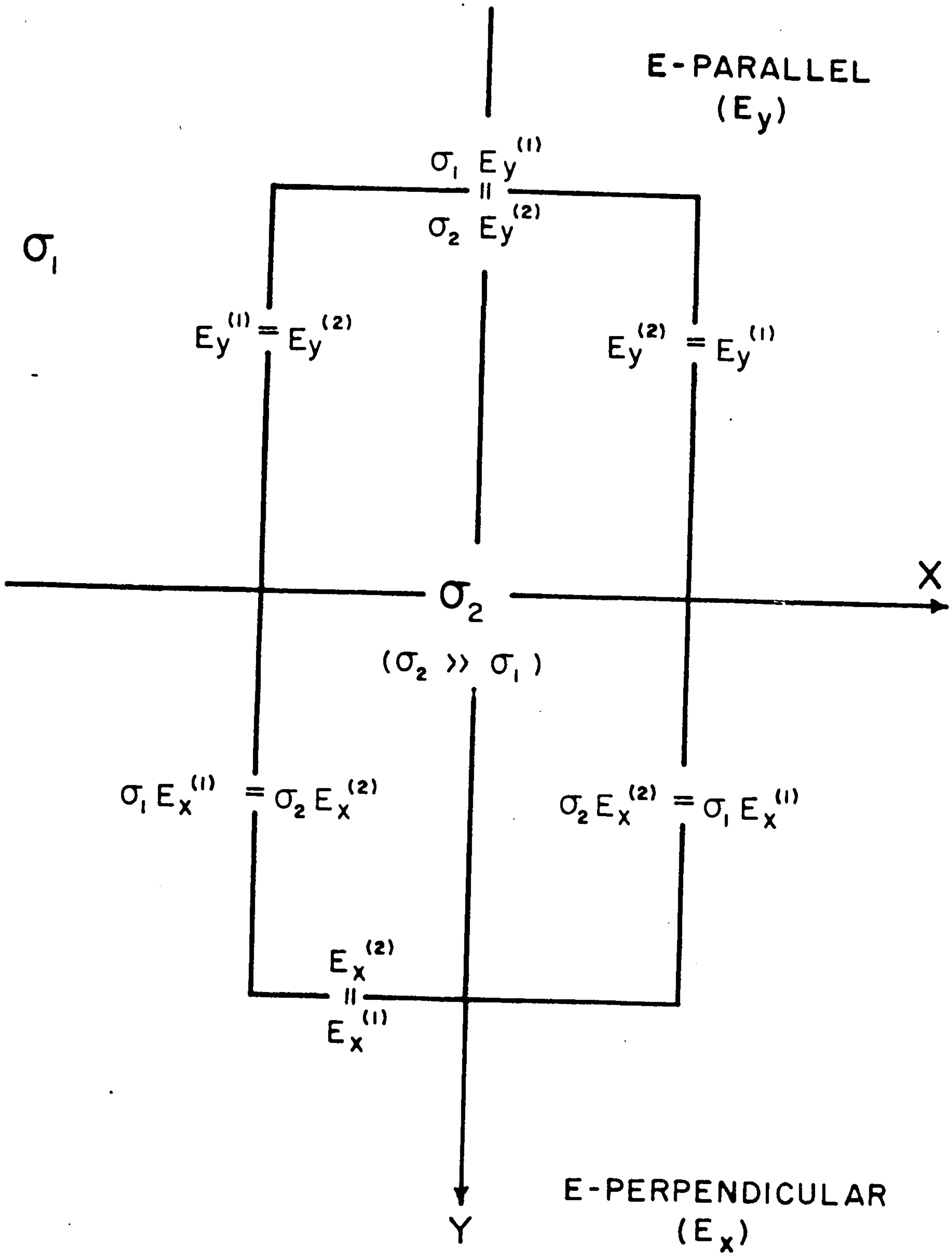

Fig. 2.6 Plan view of conductive slab in resistive medium showing boundary conditions for parallel and perpendicular electric fields at conductivity interfaces.

strike length can be made by considering the decrease in the magnitude of the interior electric field as a result of end effects.

The strike of the conductive slab is in the y direction. E_x and E_y are the electric fields perpendicular and parallel to the strike. The relationships between internal and external electric fields on the boundaries are derived from the electromagnetic field continuity conditions at conductivity interfaces. The depth of burial and depth extent of the slab are arbitrary. E_x and E_y are continuous across the top and bottom surfaces and do not affect the discussion.

In the E-perpendicular case, the electric field (E_x) inside the conductor is governed by the boundary conditions on the sides of the zone. Here the field is discontinuous and the interior field is much smaller than the exterior. The ends of the conductor have a relatively small effect because the condition that the electric field be continuous exerts virtually no constraint on the magnitude of the internal field. However, an anomalously low external field will extend beyond the ends of the slab. Thus, for the E-perpendicular polarization, the two-dimensional model should give reasonable results.

For the E-parallel polarization the magnitude of the internal electric field is affected by the ends of the slab. Here E_y is discontinuous and the field inside the conductor is again much smaller strike length can be made by considering the decrease in the magnitude of the interior electric field as a result of end effects.

The strike of the conductive slab is in the y direction. E_x and E_y are the electric fields perpendicular and parallel to the strike. The relationships between internal and external electric fields on the boundaries are derived from the electromagnetic field continuity conditions at conductivity interfaces. The depth of burial and depth extent of the slab are arbitrary. E_x and E_y are continuous across the top and bottom surfaces and do not affect the discussion.

In the E-perpendicular case, the electric field (E_x) inside the conductor is governed by the boundary conditions on the sides of the zone. Here the field is discontinuous and the interior field is much smaller than the exterior. The ends of the conductor have a relatively small effect because the condition that the electric field be continuous exerts virtually no constraint on the magnitude of the internal field. However, an anomalously low external field will extend beyond the ends of the slab. Thus, for the E-perpendicular polarization, the two-dimensional model should give reasonable results.

For the E-parallel polarization the magnitude of the internal electric field is affected by the ends of the slab. Here E_y is discontinuous and the field inside the conductor is again much smaller than the external field but the end effects control this situation more than the boundary conditions on the sides of the zone. Therefore, in the E-parallel case, the field anomaly is dependent on the strike length. Theoretical solutions for this polarization appear to be applicable only in cases where the strike length of the actual body is much larger than its magnetotelluric skin depth.

In view of the above conclusions, the theoretical examples presented are limited to the E-perpendicular polarization.

Theoretical Examples

The basic theoretical model considered here is a body of rectangular cross-section and 50 ohm-meter resistivity buried in a 5000 ohm-meter medium. The body has a width of 100 feet, a depth of burial of 50 feet and a depth extent of 200 feet. The theoretical anomalies are for an 8 Hz source field frequency. Changes in the anomaly caused by varying the parameters of the conductive zone are illustrated by Figures 2.7 to 2.11 . Figure 2.12 shows the effect of a conductive overburden.

Increasing the resistivity contrast (Fig. 2.7) intensifies but does not widen the anomaly. In this particular model a limit is reached at a resistivity contrast of 50; greater contrasts have essentially no effect on the profile. The limiting value depends on the geometry of the model.

Decreasing the depth of burial intensifies and narrows the anomaly (Fig. 2.8). For shallow depths the width of the anomaly

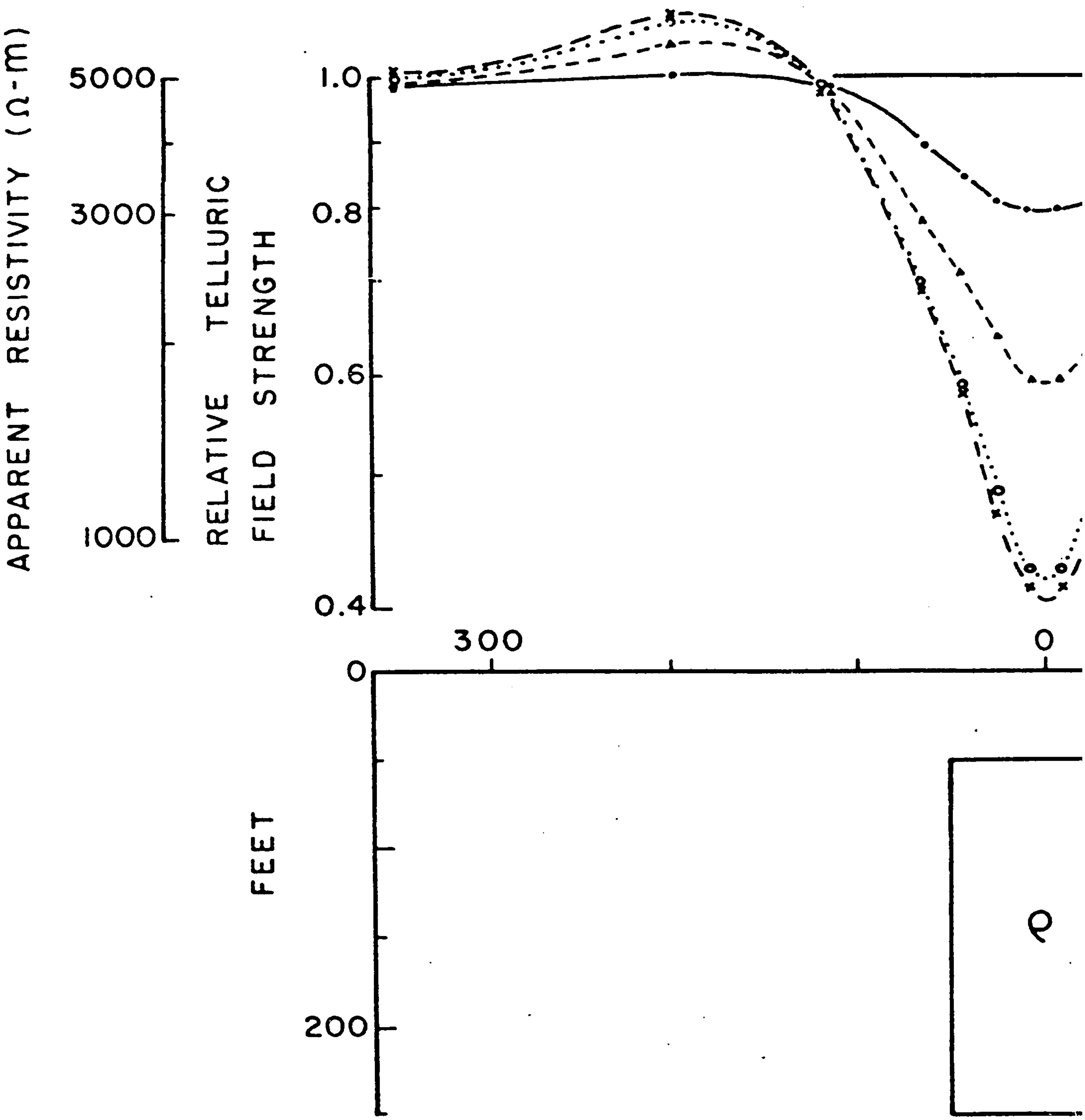

Fig. 2.7 Theoretical profiles for va

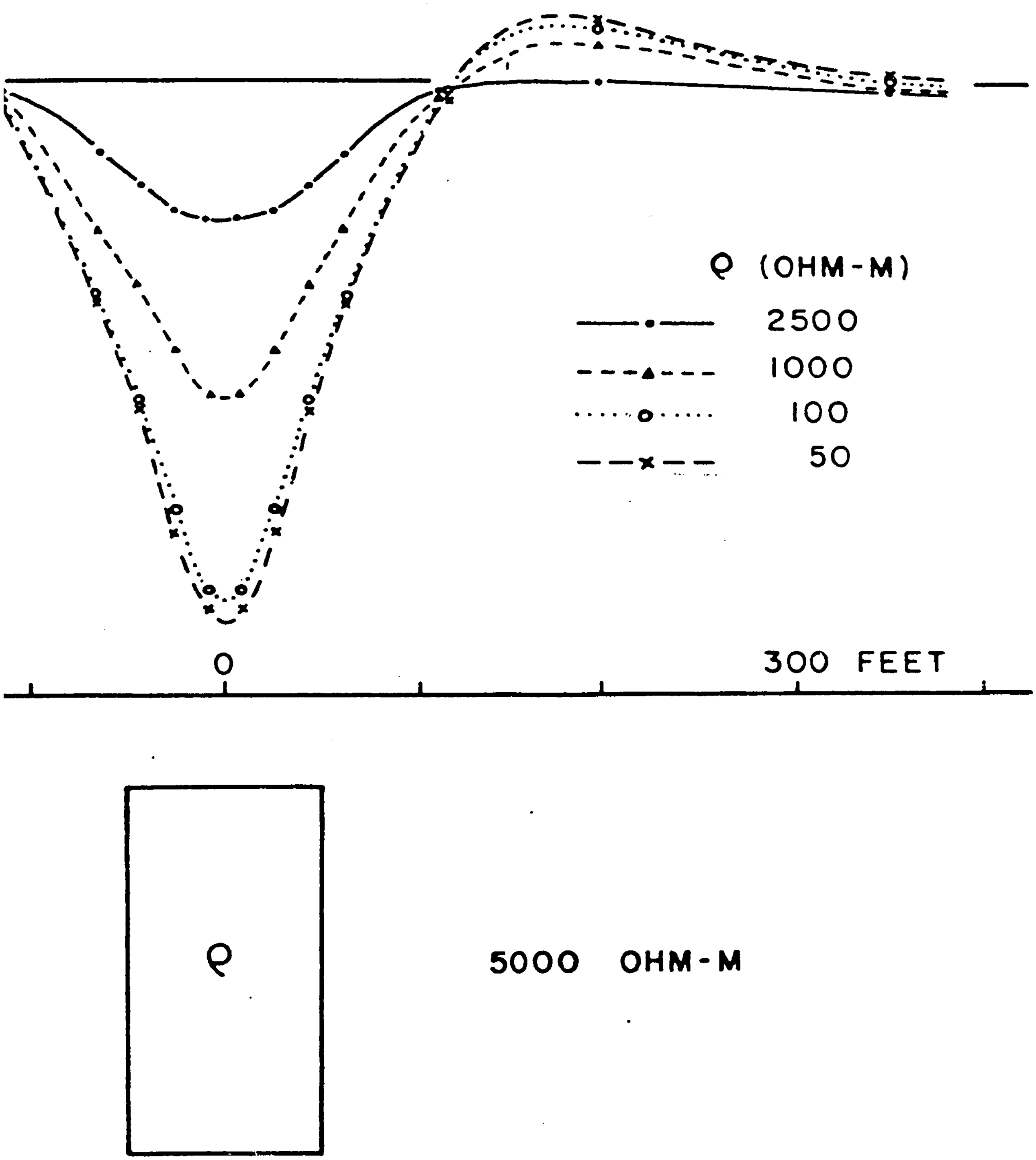

profiles for variable conductor resistivity.

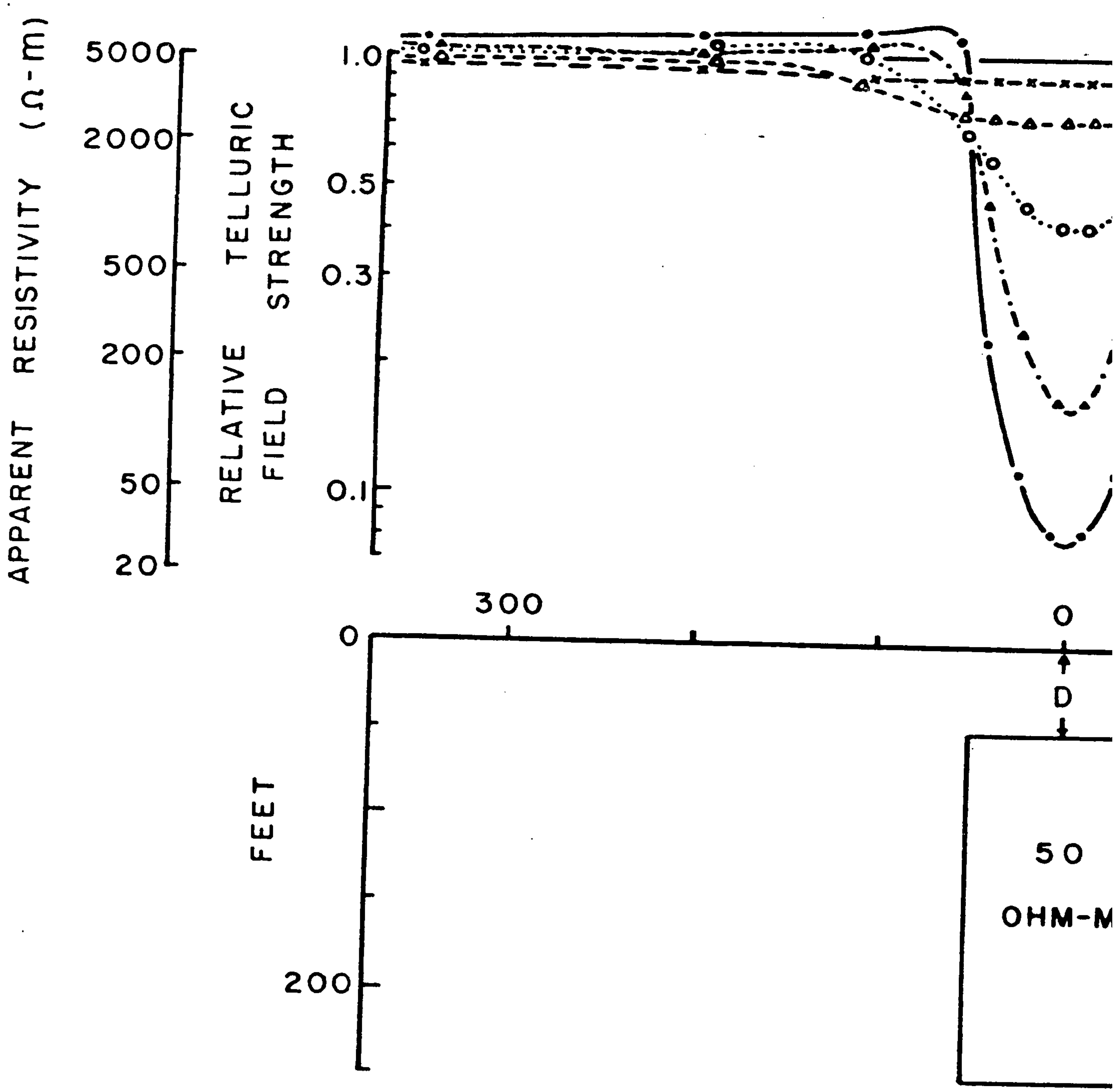

Fig. 2.8 Theoretical profiles for variable

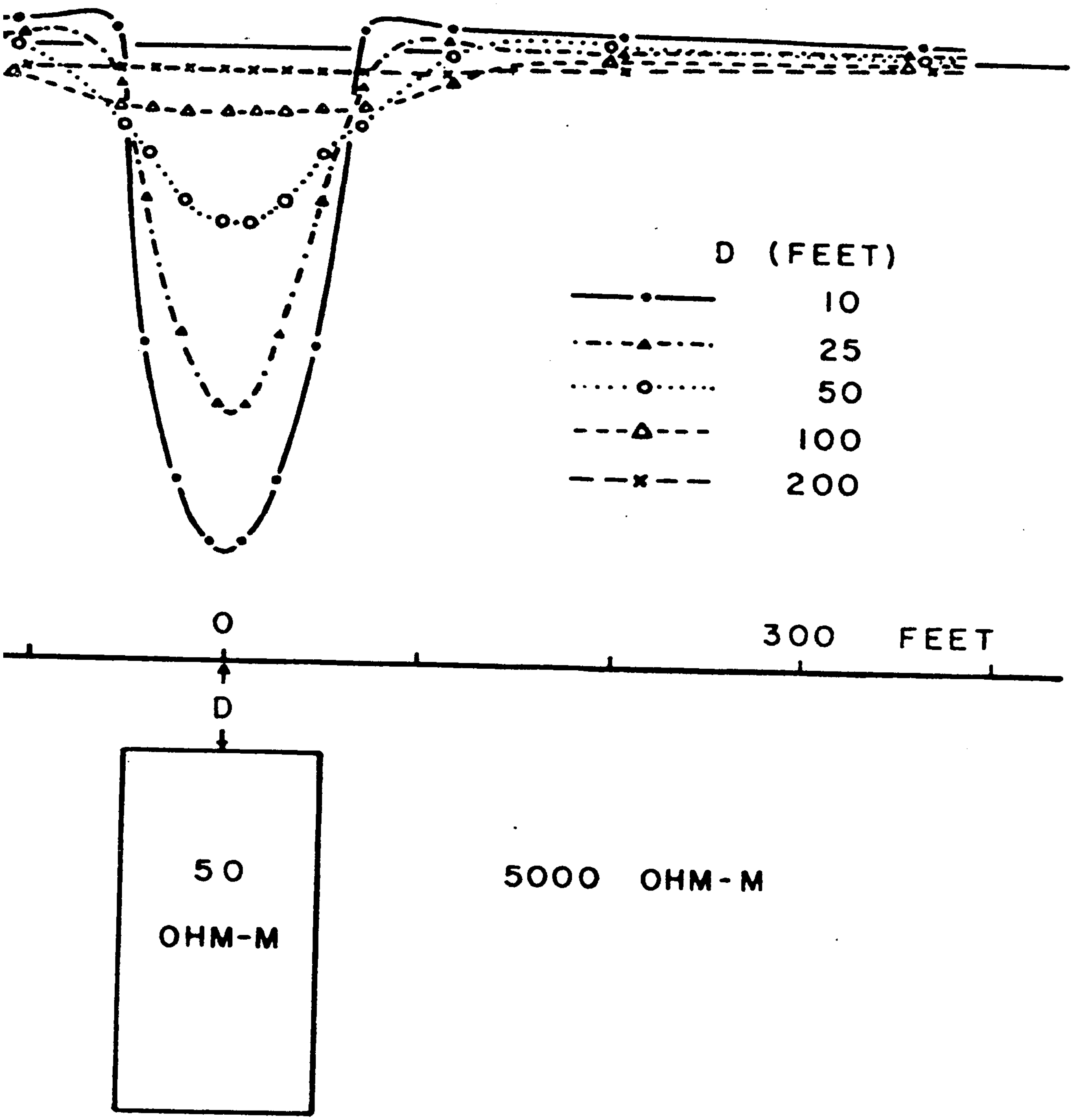

s for variable conductor depth.

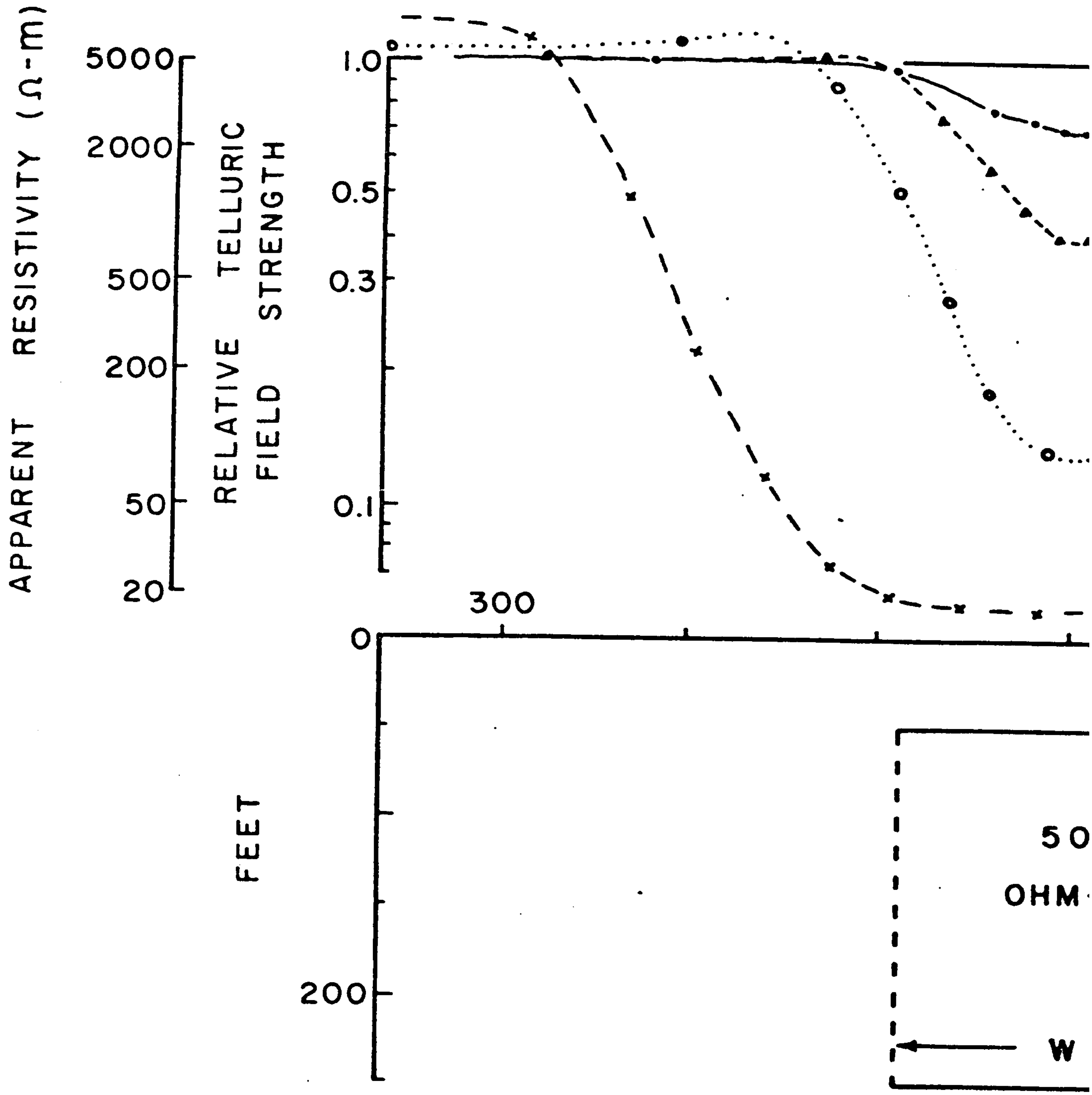

Fig. 2.9 Theoretical profiles for varia

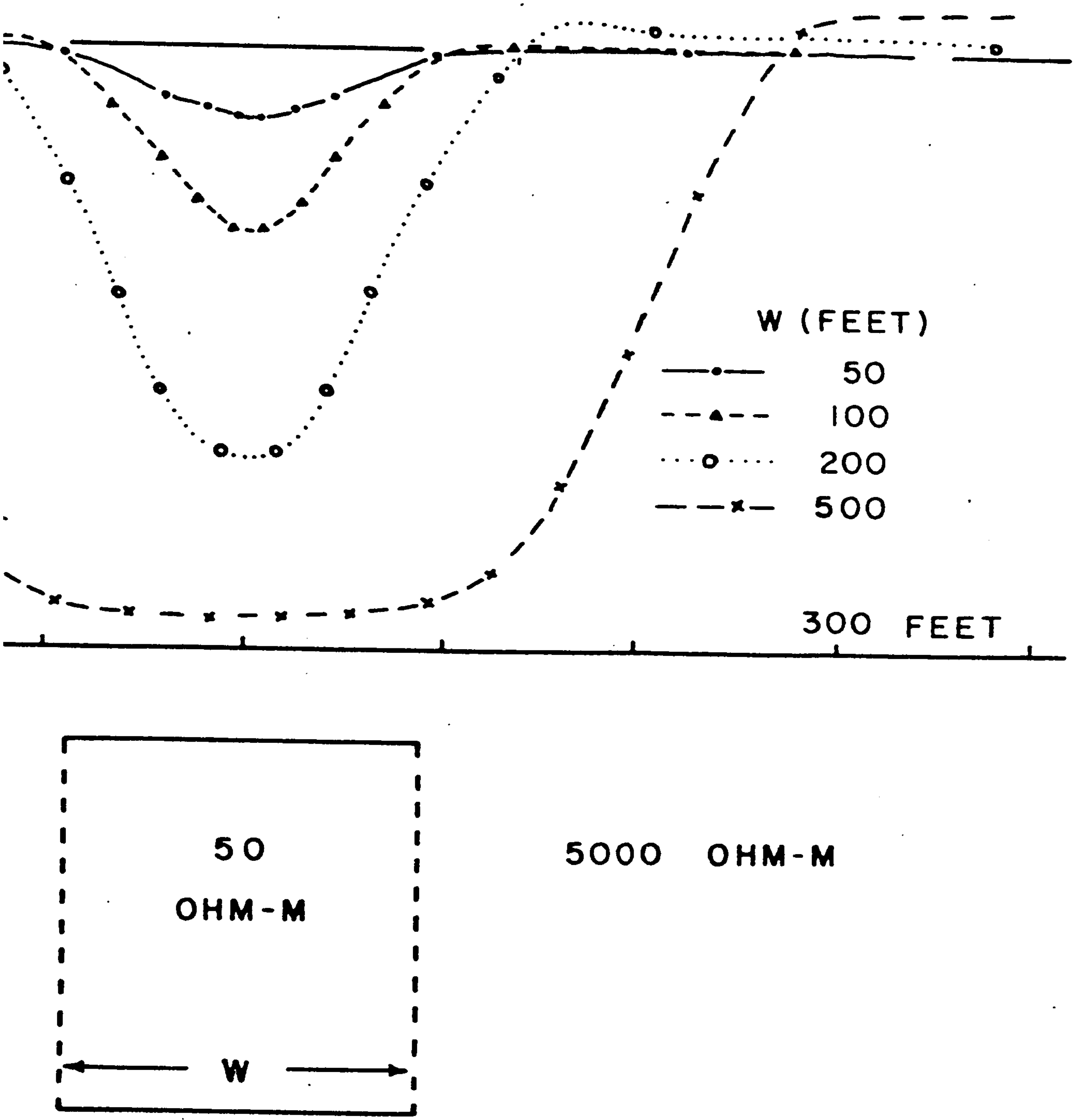

iles for variable conductor width.

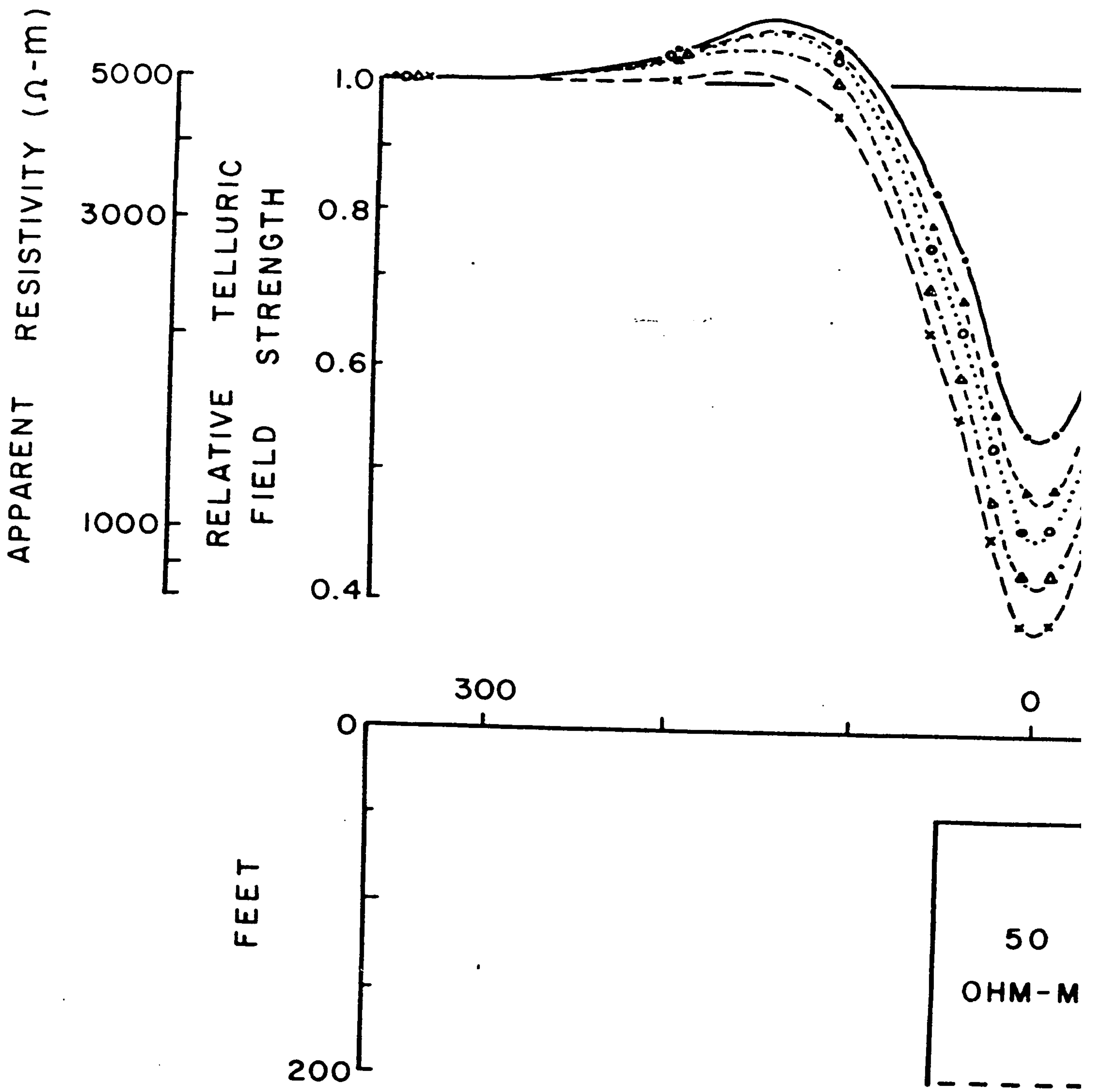

Fig. 2.10 Theoretical profiles for variable

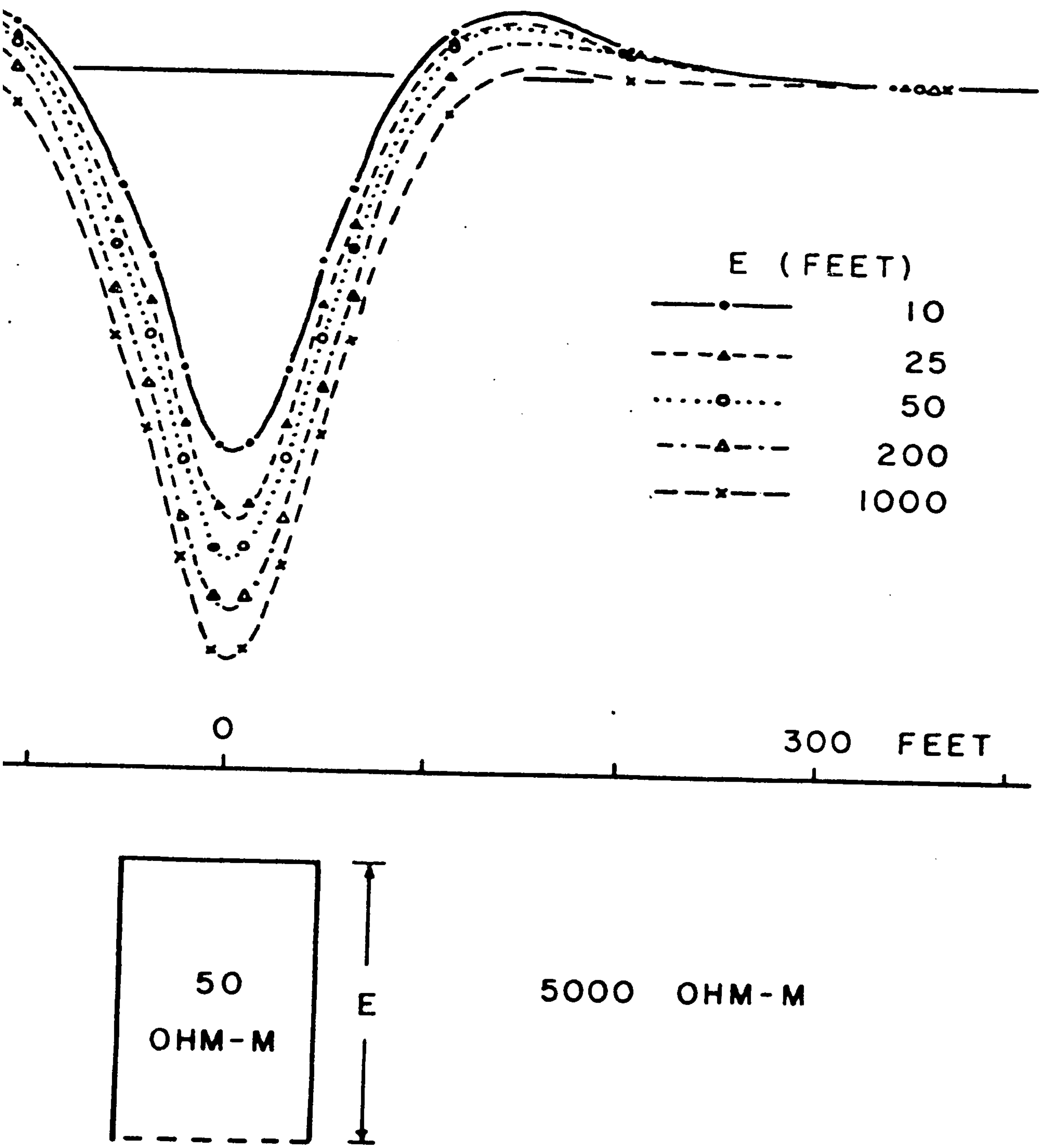

les for variable conductor extent.

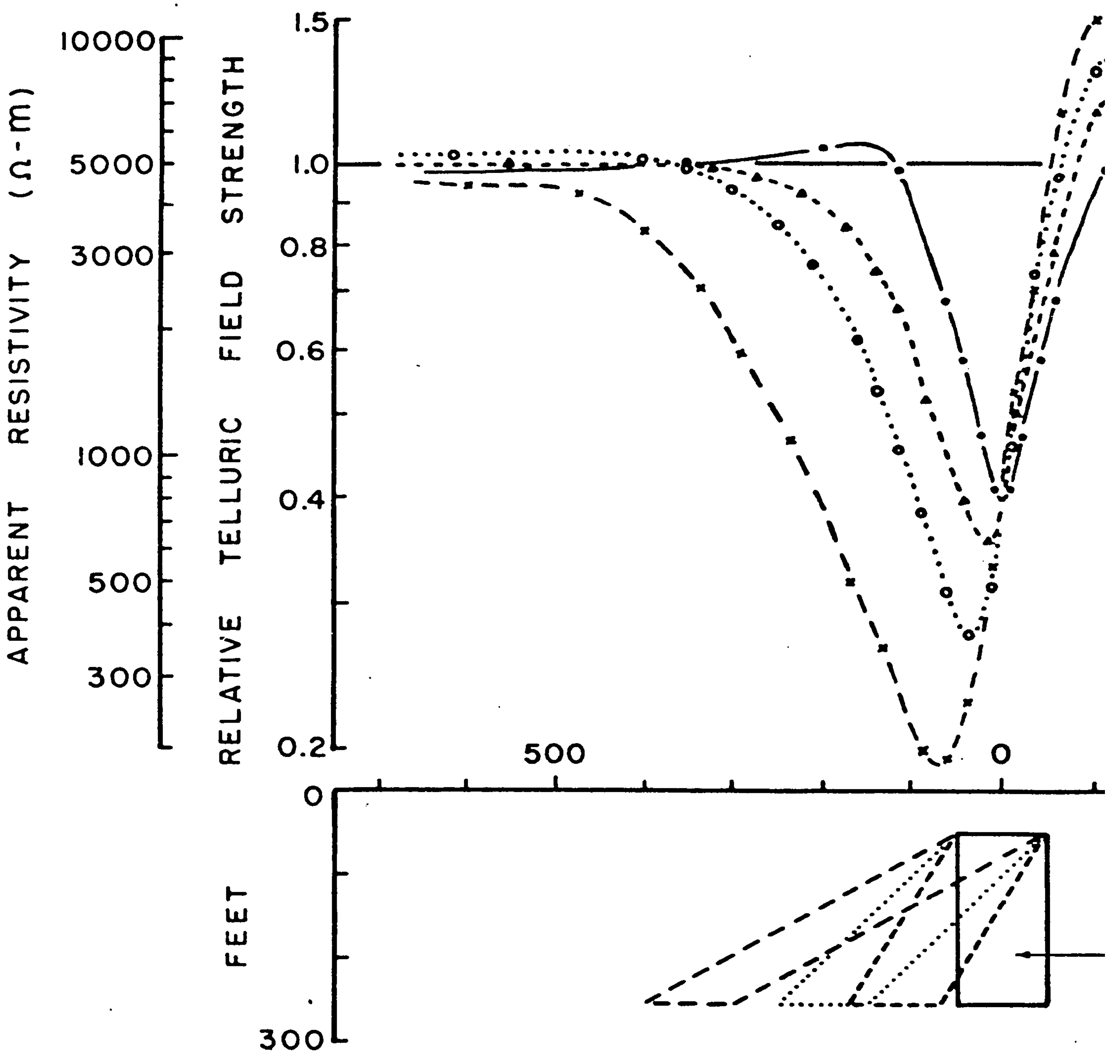

Fig. 2.11 Theoretical profiles for variabl

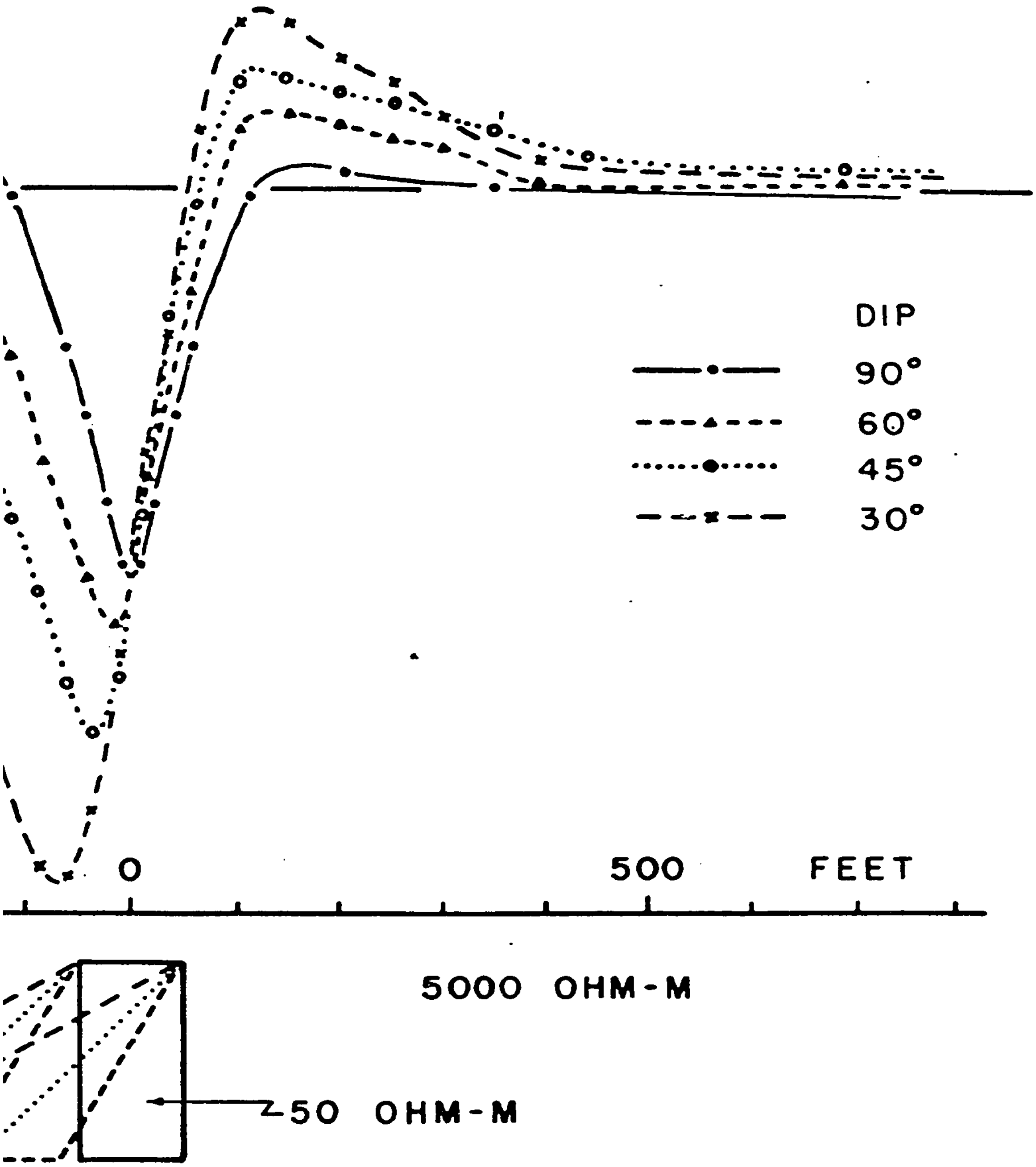

; for variable conductor dip.

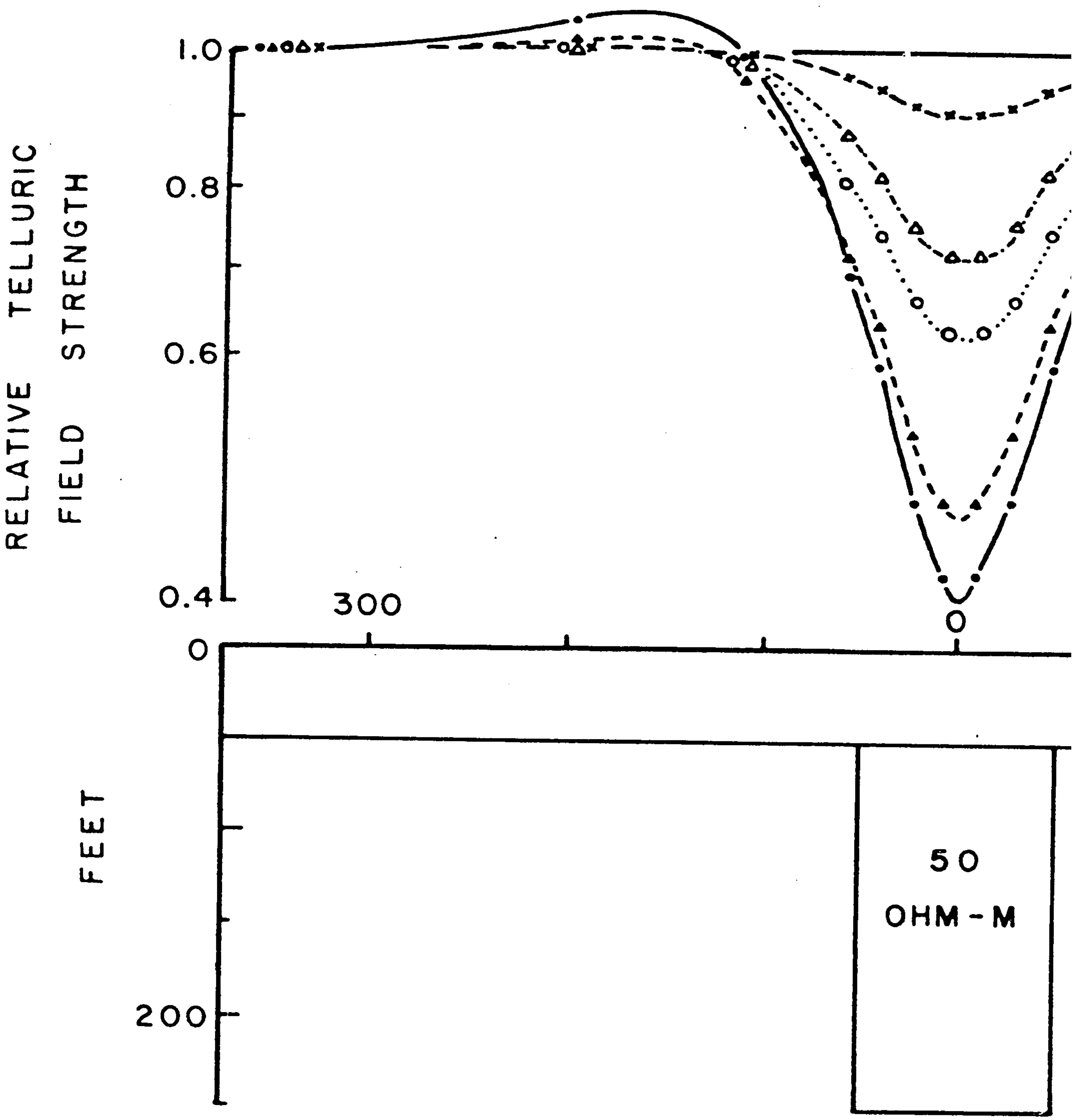

Fig. 2.12 Theoretical profiles for variable over

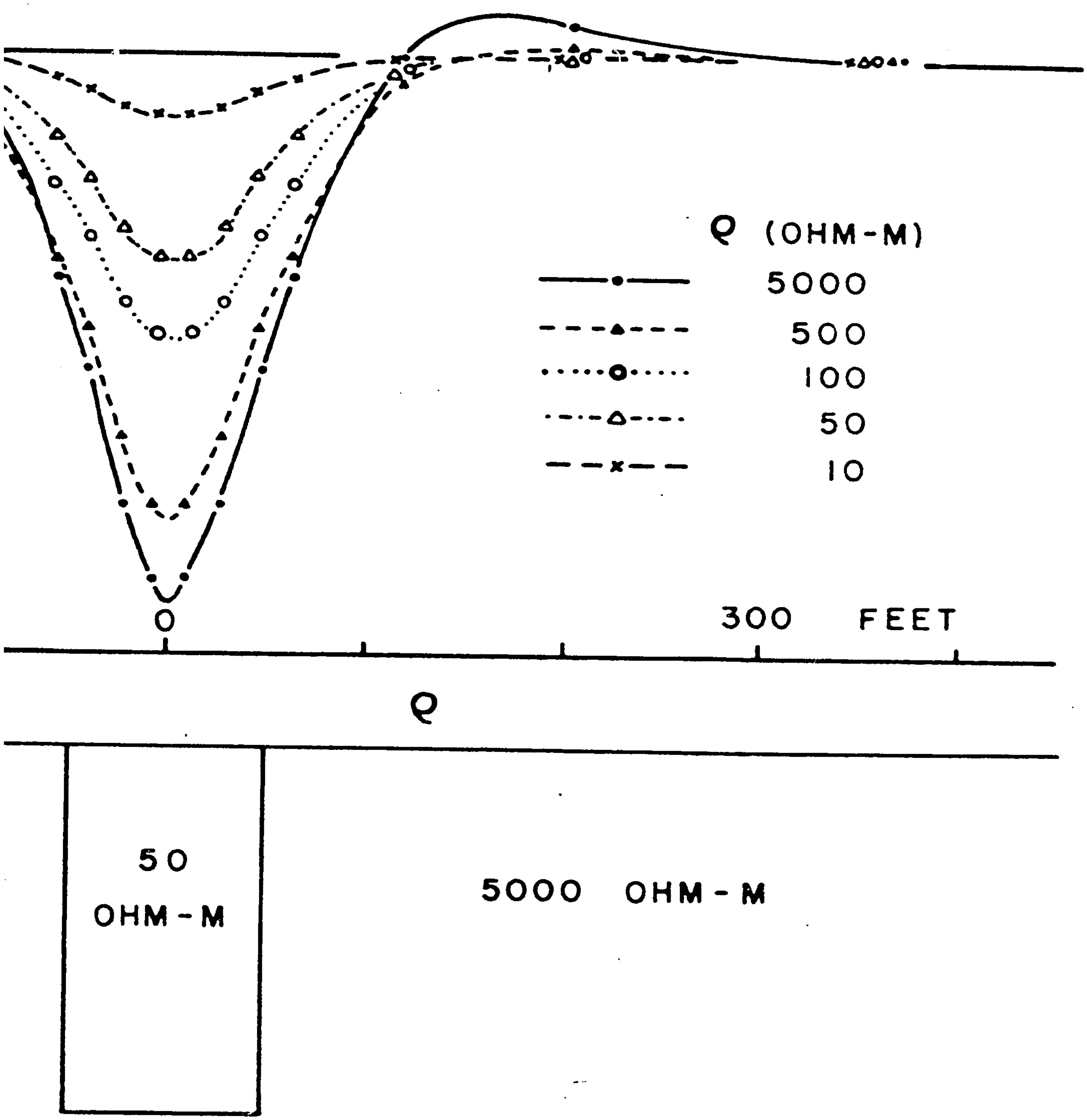

or variable overburden resistivity.

corresponds closely to the width of the conductor.

The width and intensity of the anomaly increase with the width of the conductive zone (Fig. 2.9). For this model the minimum telluric field strength over the 500 feet wide body is a limiting value. Little change from this minimum is observed for larger widths.

Changes in the depth extent (Fig. 2.10) alter the profiles much less than variations in any other parameter.

The cross-sectional area of the conductive zone has been maintained constant for the dipping slabs shown in Figure 2.11 . As the dip decreases the profile becomes increasingly asymmetric while the apparent resistivity on the updip side becomes progressively greater than the background value. On the downdip side the profile remains smooth. The increase in anomaly intensity and width with decreasing dip can be partly attributed to the larger lateral extent of the body.

At 8 Hz the presence of 50 feet of conductive overburden can have a pronounced effect (Fig. 2.12). However, for realistic overburden resistivities ($\rho \geq 100$ ohm-meters), the telluric field anomaly is still 60-70% of that observed with no overburden (i.e. $\rho_{overburden} = 5000$ ohm-meters).

In this diagram the apparent resistivity is not shown in order to permit stacking of the profiles. The background apparent resistivity varies from 5000 ohm-meters with no overburden to 1700 ohm-meters for an overburden resistivity of 10 ohm-meters.

CHAPTER III

EQUIPMENT AND FIELD OPERATIONS

3.1 Amplifiers

A prototype 8 Hz amplifier was built and tested in 1965 by the personnel of the Geological Survey of Canada. The following year the telluric amplifiers used throughout this project were constructed (Becker and Flint, 1967). These were basically two identical microvoltmeters which measured the telluric field as a voltage integrated over a time interval of 3 minutes. The amplifiers were tuned to have a flat pass band between 7 and 9 Hz with 3 dB points at 4 and 15 Hz.

Field trials during the summer of 1966 showed that the pass band of the filters was much too wide and that the gain of the amplifiers was temperature sensitive. The tests also indicated that a record of the telluric signals would be an advantage over the integrated signal on the meters.

For the 1967 field season the existing filters were replaced by temperature compensated commercial twin-T units with a much narrower pass band. The integrators were replaced by a galvanometer recorder. Power for the recorder was supplied by a Honda E-300 generator.

For the 1968 field season, integrators were again incorporated in the amplifiers so that the field signals could be both recorded and integrated. The improved equipment permitted a reduction of the integration period to 30 seconds.

Figure 3.1 is a block diagram of the amplifiers. Only one unit includes a bandpass compensator having the same frequency characteristics as the magnetic sensing system. Thus, with switch SW1 in the position shown, the two amplifiers could be used for telluric surveys. For magnetotelluric measurements the set with the extra filter section was used to measure the telluric field.

Figure 3.2 shows the frequency responses of the amplifiers in the telluric and magnetotelluric modes. These have been superimposed on a typical power spectrum of the Schumann resonance magnetic field (Shand, 1966).

The specifications of the amplifiers are as follows:

Sensitivity	1 μV
Average noise	0.1 μV for 10K source
Dynamic range	30 dB
Maximum gain	535
Band pass	Center frequency at 8 Hz, 3 dB points at 7 and 9 Hz, 20 dB per octave roll-off.
60 Hz rejection	Better than 80 dB.
Power source	Two 6 V lantern batteries.
Power consumption	Approximately 2 watts when integrating signal, 1.5 watts when recording.
Weight	8 lbs

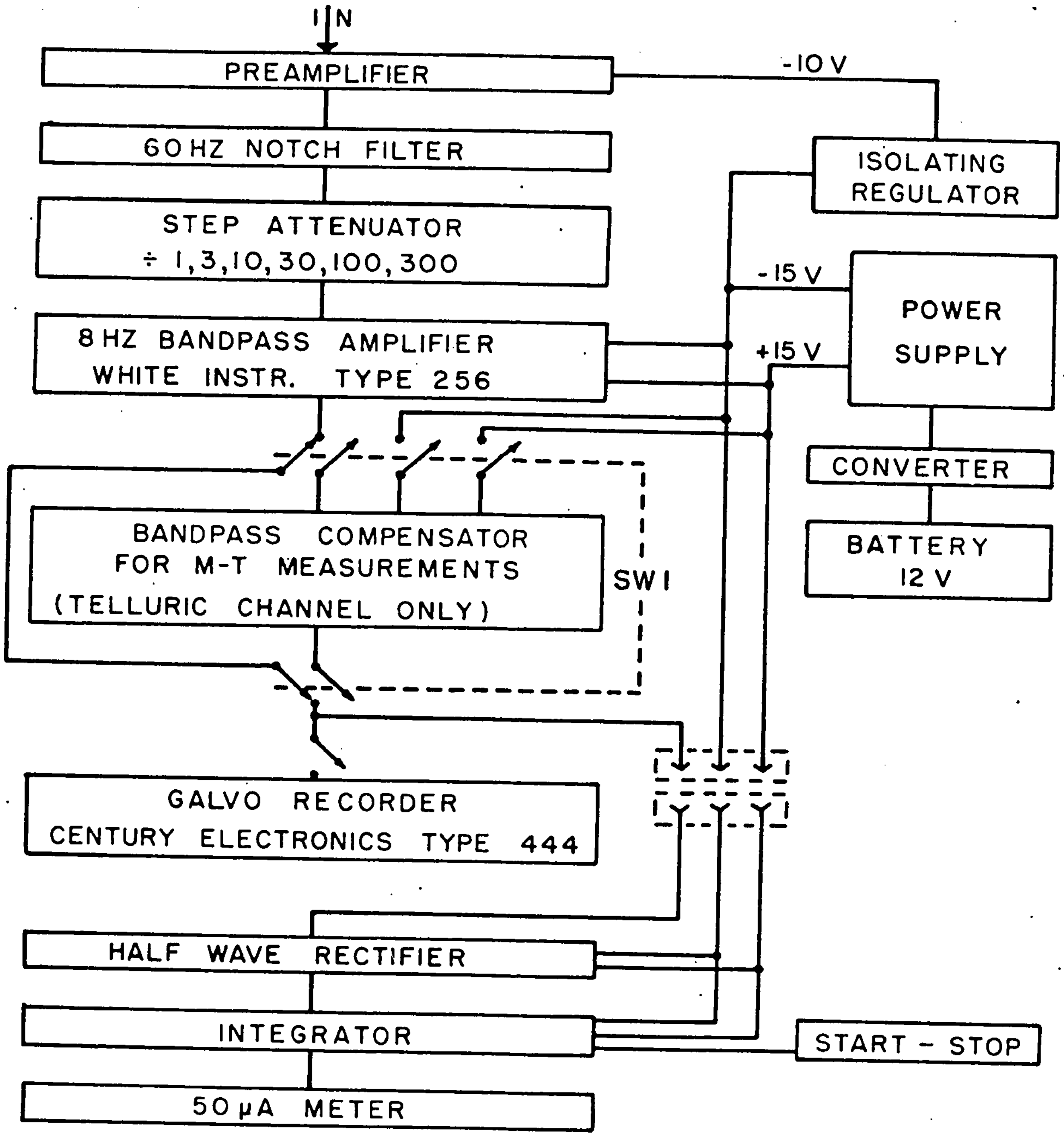

Fig. 3.1 Block diagram of 8 Hz amplifiers.

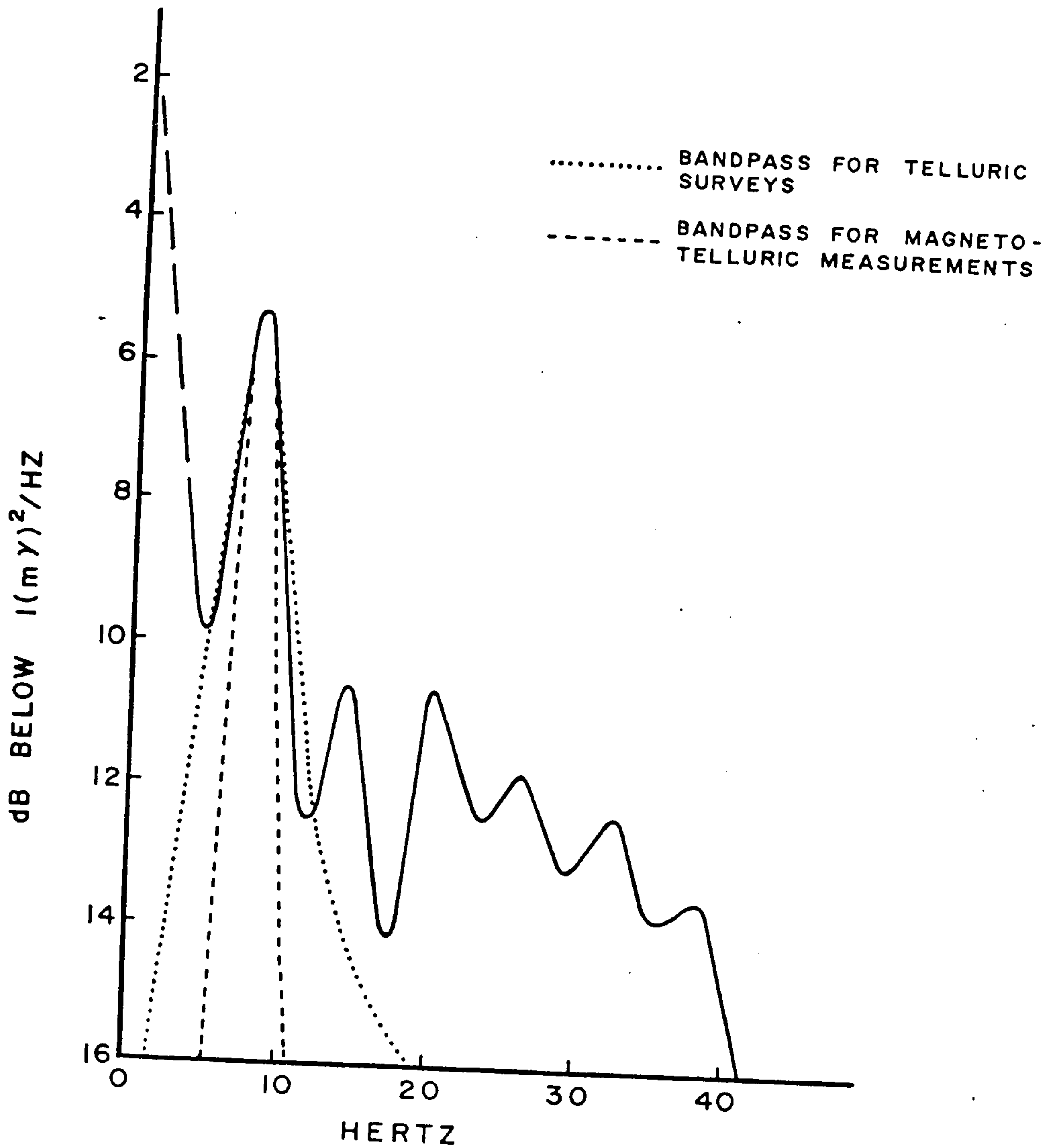

Fig. 3.2 Power spectrum of sub-audio frequency natural magnetic field and bandpass of telluric and magnetotelluric amplifiers.

3.2 Magnetic Sensing System

An air-cored induction coil, capacitively tuned to 8 Hz, was used to detect the magnetic field. A Princeton Applied Research CR-4 low-noise amplifier provided an additional gain stage before the 8 Hz amplifier.

The design of the induction coil was based on formulas published by Becker (1967). The factors controlling the design were the noise characteristics of the CR-4, and a required sensitivity of 1 mγ for a signal to noise ratio of 5.

The specifications of the induction coil are as follows:

Wire	#16 aluminum magnet wire
Number of turns	2392 (52 layers of 46 turns each)
Outside diameter	38.6 inches
Winding cross-section	2.5 inches wide x 2.9 inches deep
Weight	71 lbs
Inductance	9.3 Hy
D.C. Resistance	143 ohms
Stray capacitance	80 pF
Tuning (shunt) capacitance	42.9 μF
Output	0.26 μV/mγ
Noise of coil and CR-4	0.05 μV

Figure 3.3 shows the assembled field equipment. The box contains the two amplifiers and the recorder. The telluric field is measured between the two electrodes along the road. The magnetic sensing coil and the box containing the tuning capacitors and the CR-4 preamplifier are in the background.

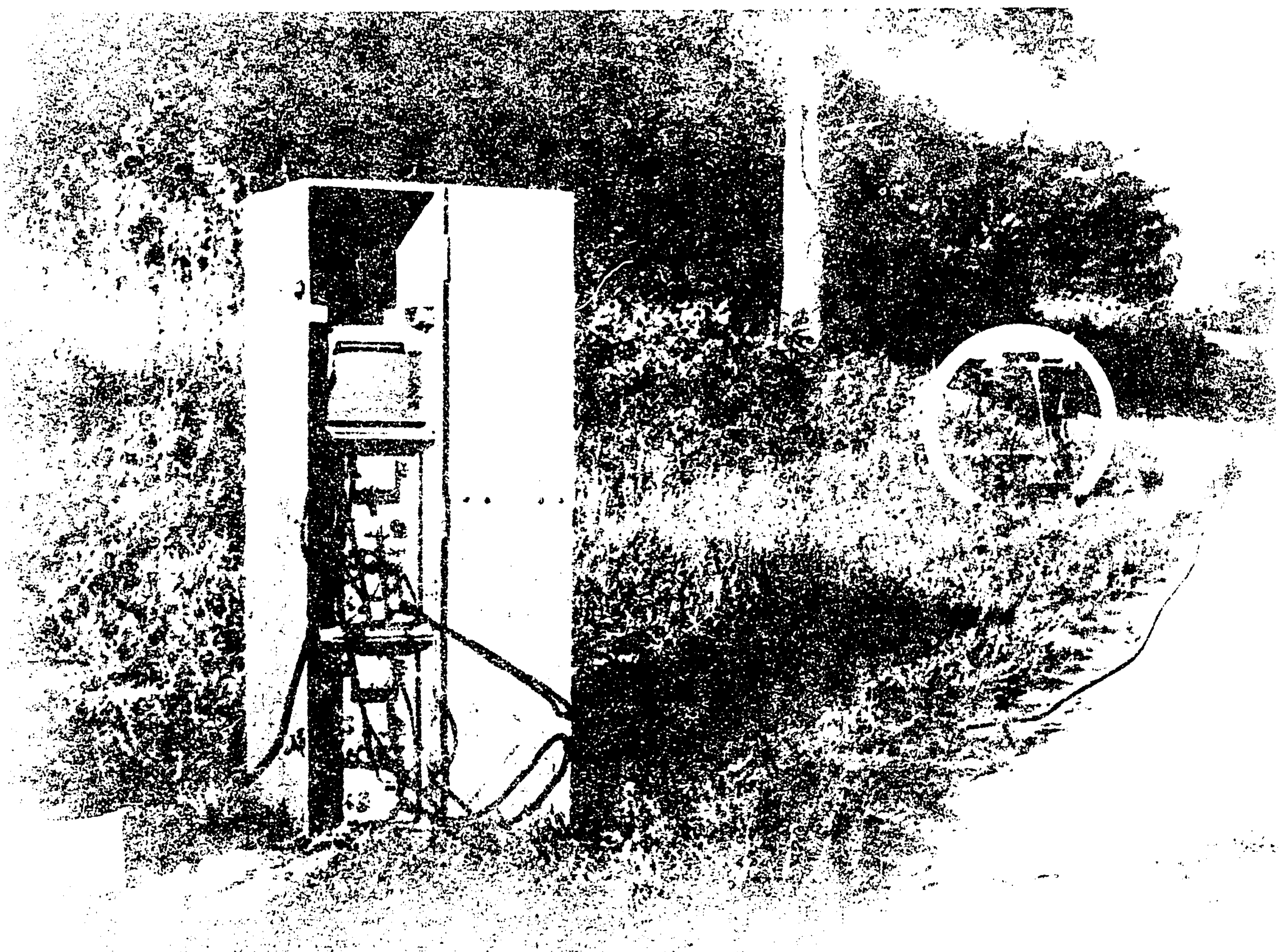

3.3 Telluric Surveys

Telluric surveys were carried out by establishing a fixed base station, moving the field station along a traverse line, and either recording or integrating the two signals simultaneously. For recording purposes the output of the field amplifier was transmitted through a 2-wire cable to the recorder located at the base station where both signals were recorded for 30-60 seconds at a chart speed of 1 ips. When the signals were integrated, the connecting cable was not necessary. Using Walkie-Talkie, the base station operator gave the signal to start integration and both operators used stop watches to time the 30 second integration period. At each field station location the integrations were repeated a sufficient number of times to obtain a good average value for the relative telluric field strength. Figures 3.4(a) and 3.4(b) show the equipment layout for measuring the telluric field perpendicular and parallel to the strike of a conductive zone.

The usual orientation of traverse lines in mineral prospecting is normal to the strike of the target zone. As a result, the telluric field perpendicular to strike was usually measured: occasionally, in relatively open bush, it was possible to measure the parallel telluric field as well.

Another technique that was evaluated involved measuring the telluric field gradient by leapfrogging the two stations along the traverse line. This method was found to be unsatisfactory, partly

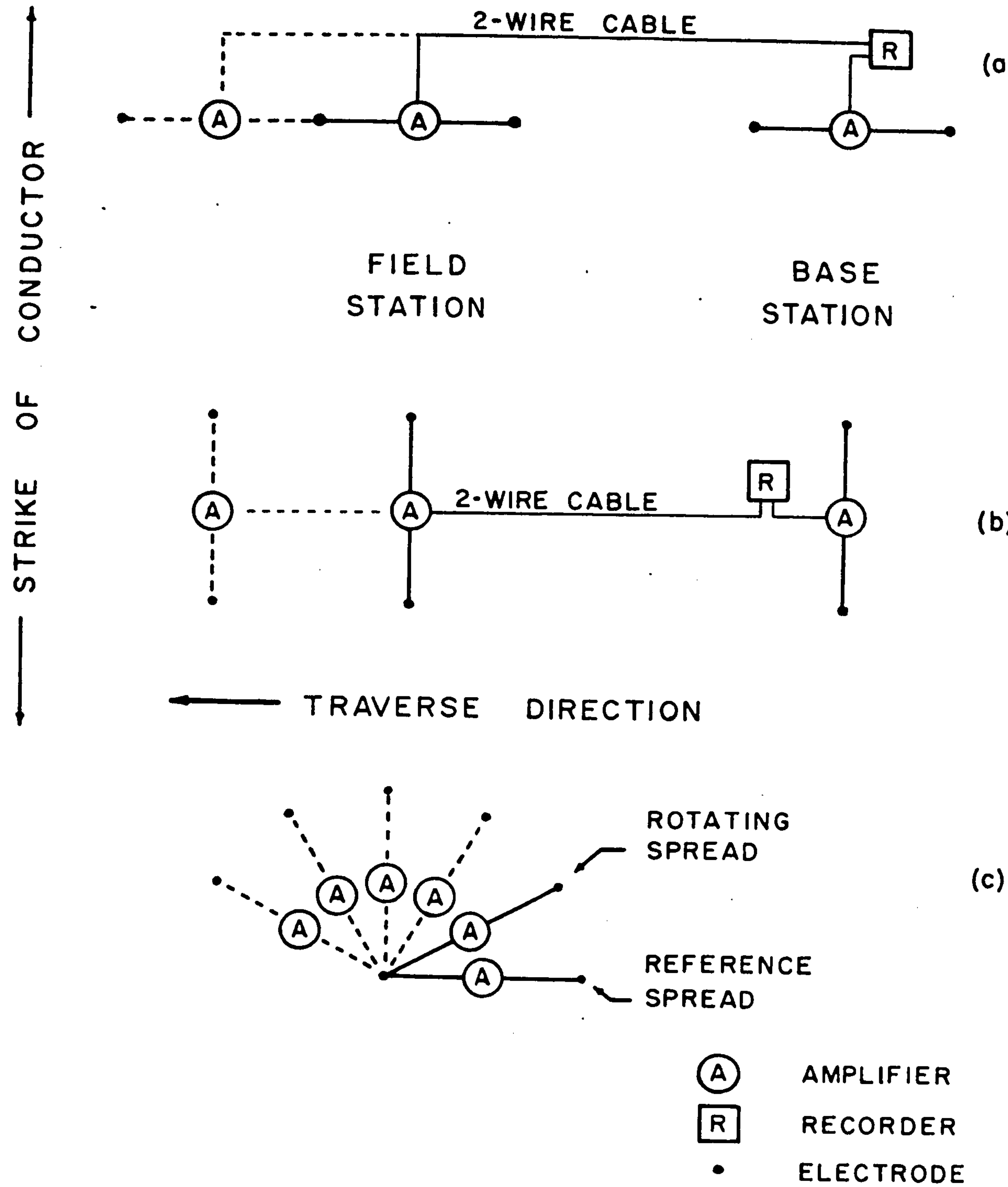

Fig. 3.4 Equipment layout for telluric measurements.

(a) Telluric field perpendicular to strike ($E_{\perp}$).

(b) Telluric field parallel to strike ($E_{\parallel}$).

(c) Directional variation in field strength.

because it was comparatively slow, partly because the observed anomalies were in the form of crossovers which appeared to be less diagnostic of the subsurface structure than relative telluric field strength profiles.

Figure 3.4(c) shows the method used to measure directional variations in the telluric field strength. The reference electrode spread remains fixed while the other is rotated through 180° in 30° increments.

The standard electrode spacing used in telluric surveys was 100 feet; 50 and 25 foot separations were occasionally employed for detailing anomalies if the signal level was sufficiently high. The electrodes were 3/8 x 3/8 inch brass rods approximately two feet long. Since results obtained with porous pots and metal electrodes proved to be identical, it was not necessary to use the former. At the beginning of this work, shielded cable was used to connect the amplifiers to the electrodes in order to avoid capacitive pick-up. This precaution was found to be unnecessary and light, flexible laboratory test wire was substituted.

When 100 foot electrode spreads were used and the signals were integrated about 600 feet of continuous profiling could be done in an hour. With 25 foot spreads, production was 200 feet an hour. If the signals were recorded, production was about 75% higher but the lengthy record processing greatly increased the overall time required to obtain usable field data.

3.4 Magnetotelluric Measurements

Magnetotelluric surveys were initially carried out by measuring the telluric field along the traverse line and the horizontal magnetic field component perpendicular to the line. At each station the fields were recorded for 40-60 seconds at a chart speed of 1 ips and for 10 seconds at 5 ips. The higher chart speed provided a means of estimating the phase relationship between the telluric and magnetic fields. The primary purpose of these early surveys was to determine whether equivalent results could be obtained by the telluric and magnetotelluric methods.

Subsequently, magnetotelluric measurements were used only occasionally to investigate the behaviour of the magnetic field and to determine the background apparent resistivity at the field test locations. The apparent resistivity proved to be highly anisotropic so that it was necessary to measure the orthogonal telluric and magnetic fields in 30° increments through 180° (Fig. 3.5). The vertical magnetic field was measured by maintaining the magnetic coil horizontal.

A major problem encountered in magnetic field measurements was that the induction coil proved to be highly susceptible to wind and ground motion. Because of the tight tuning, any movement of the coil through the earth's magnetic field produced a large transient 8 Hz output signal. Good magnetic field measurements could only be obtained in very calm weather, usually at night.

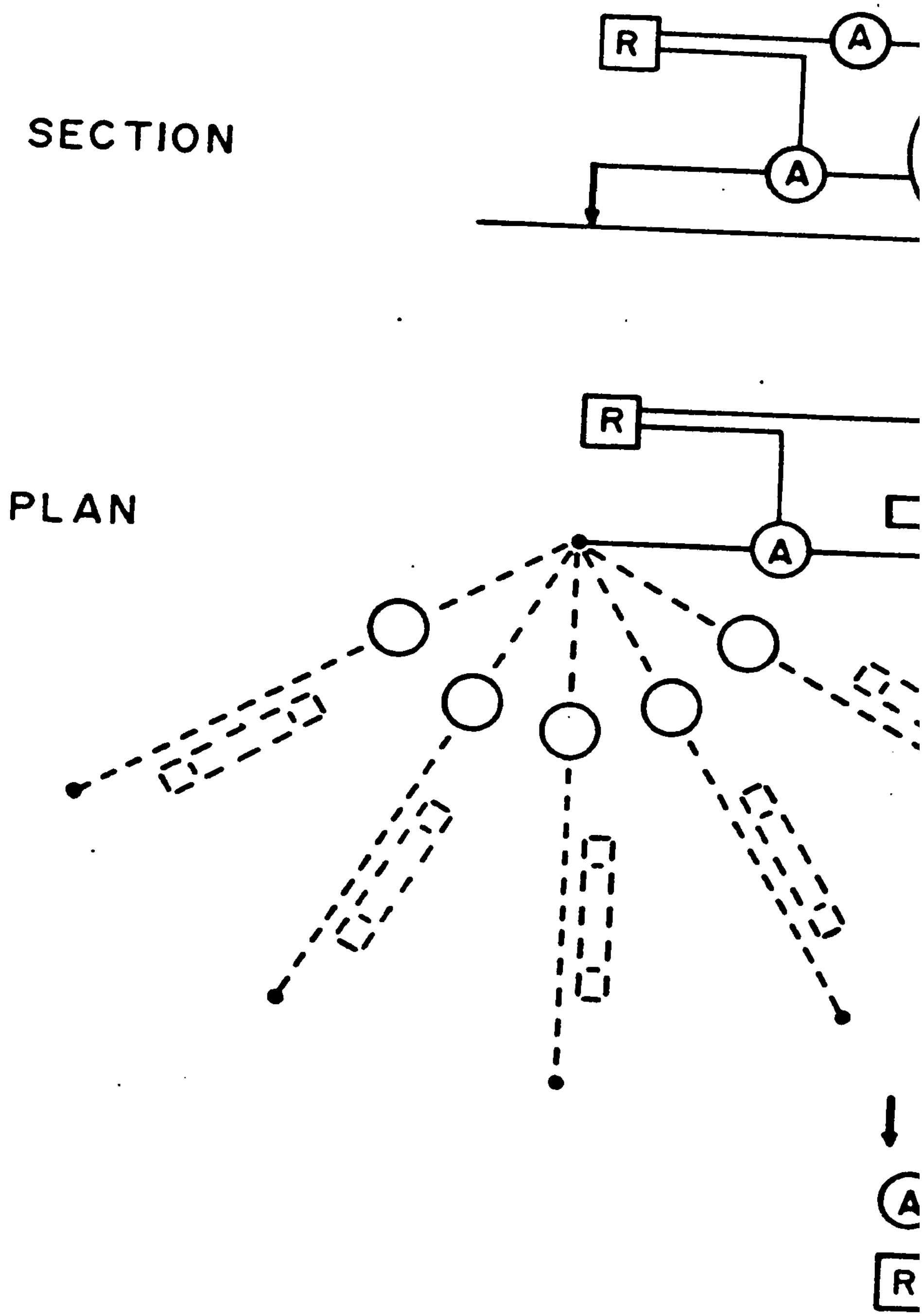

Fig. 3.5 Equipment layout for magnetotell

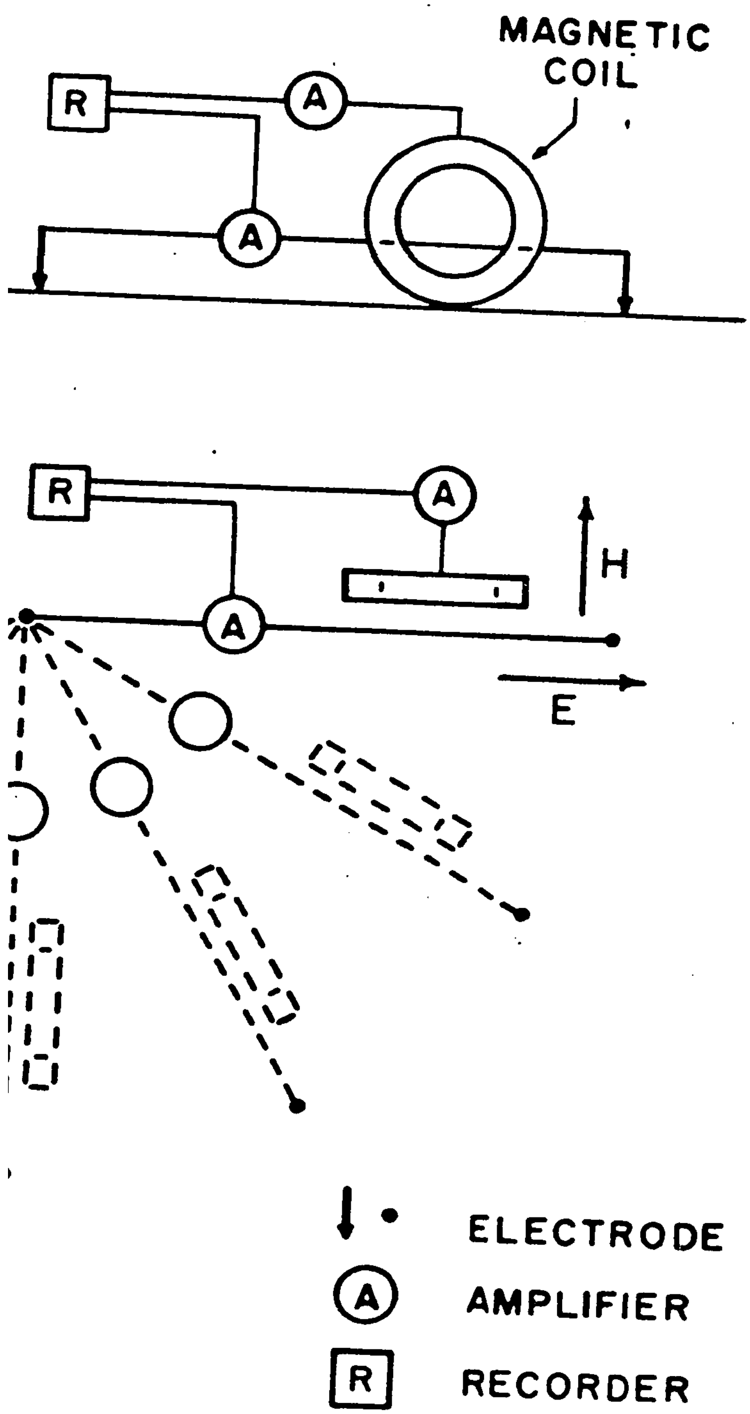

for magnetotelluric measurements.

3.5 Nature of 8 Hz Fields

Signal Strength

The 8 Hz Schumann resonance signal consists of repeated pearl-like bursts (Fig. 3.6). Each burst corresponds to one or more lightning discharges somewhere in the world (Shand, 1966).

Figure 3.7 illustrates the diurnal and short-term variations in the telluric field strength. These measurements were made at different field test locations where a base station was occupied for a lengthy period. The short-term changes in the signal level are indicated by the range of base station readings. The ranges show the maximum and minimum readings obtained during the 30 second integration times. The diurnal variation appears as a gradual change in the base station readings.

The short-term variations in the average signal intensity can occasionally exceed 50% but generally are less than 20%. Diurnally the signal level changes by less than a factor of 3. This agrees with previous results (Slankis and Becker, 1969) based on continuous 3 minute integrations extended over periods of several days.

The average signal level increases when there are nearby thunderstorms. The frequency of signal bursts does not change but there are occasional large amplitude bursts due to the local lightning.

In general, the signal level was always sufficient for field surveys. The only limitation was that over relatively conductive ground

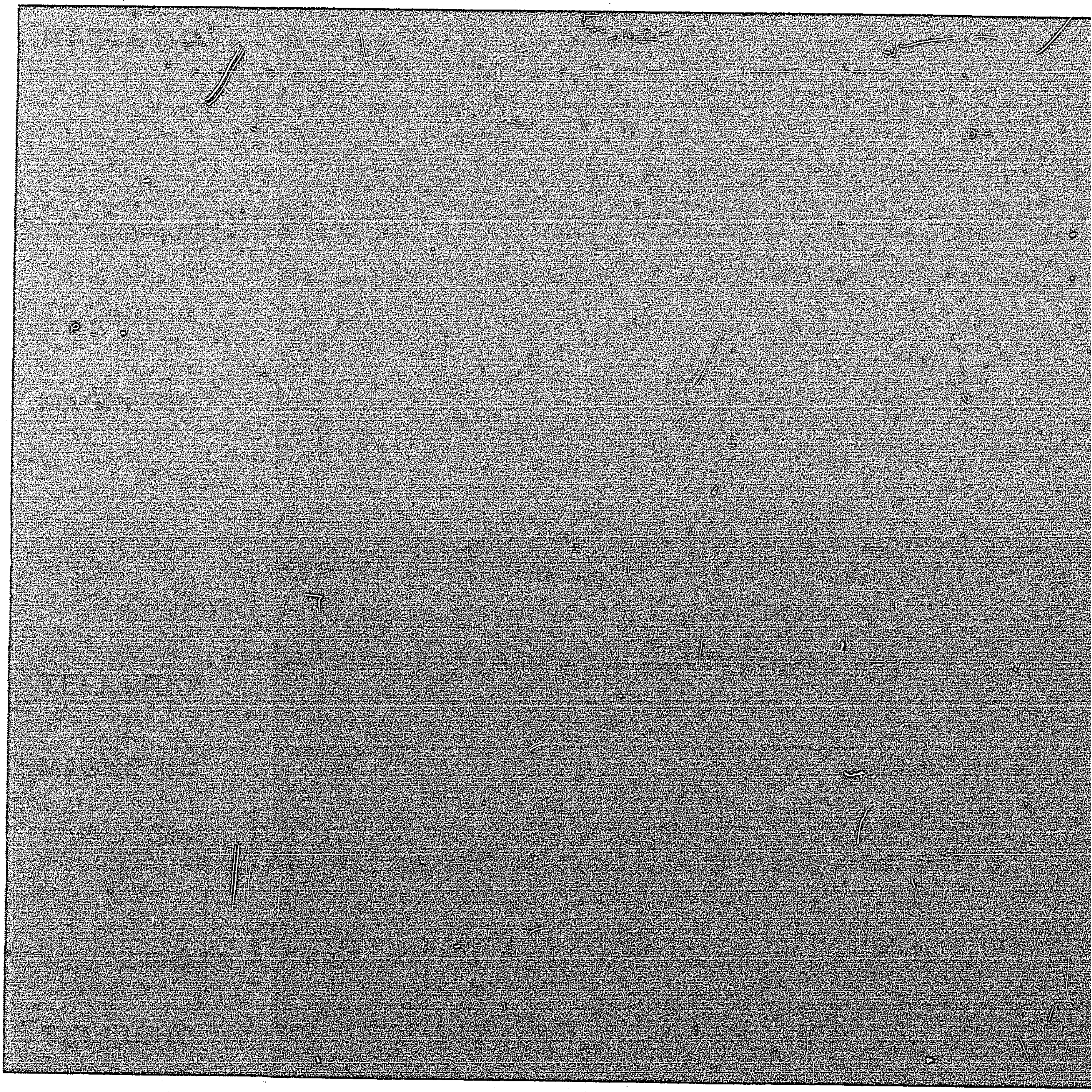

Fig. 3.6   8 Hz magnetotelluric signals (Test Site 6 (Se

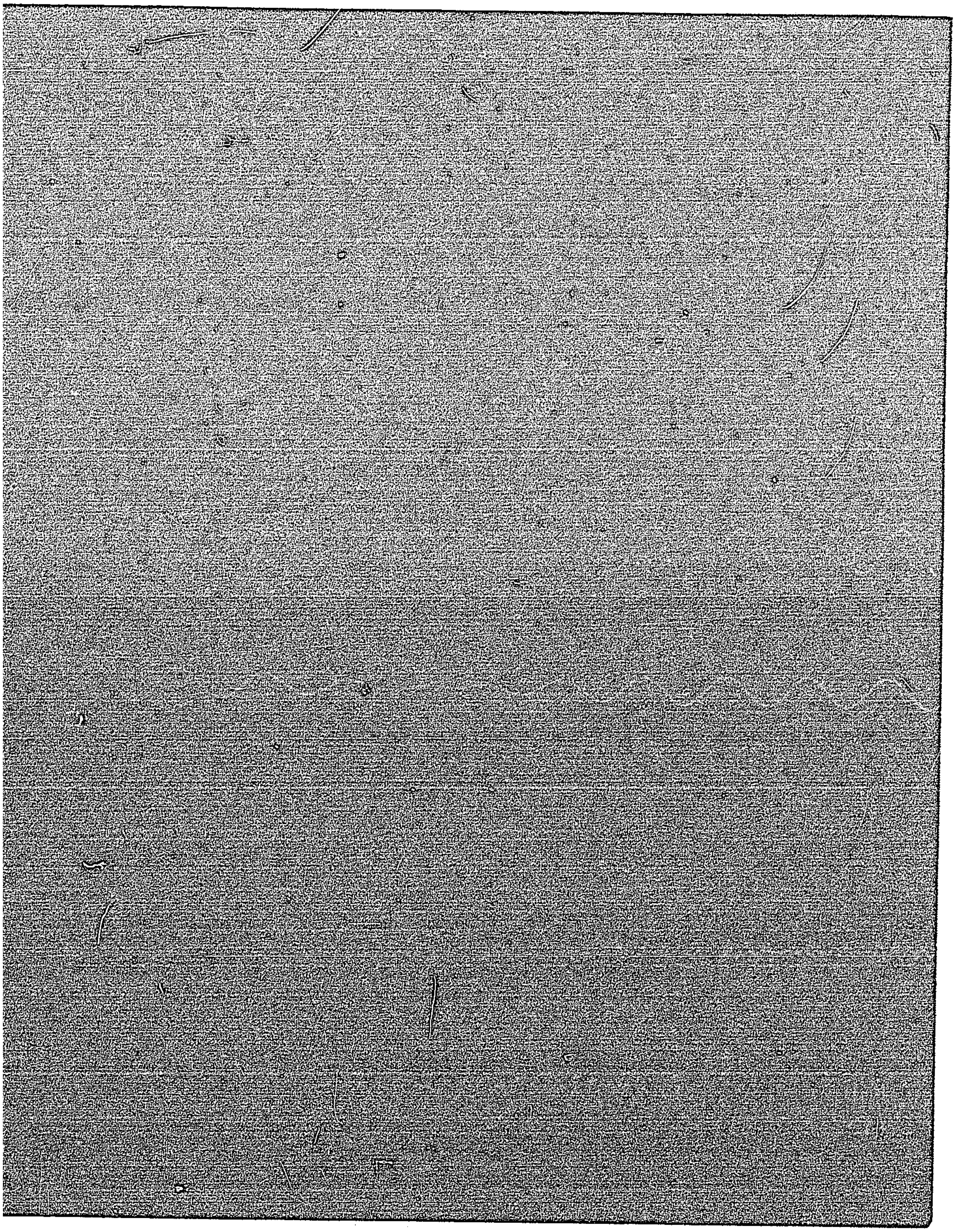

(a)

(b)

(c)

ıals (Test Site 6 (Section 4.6)).

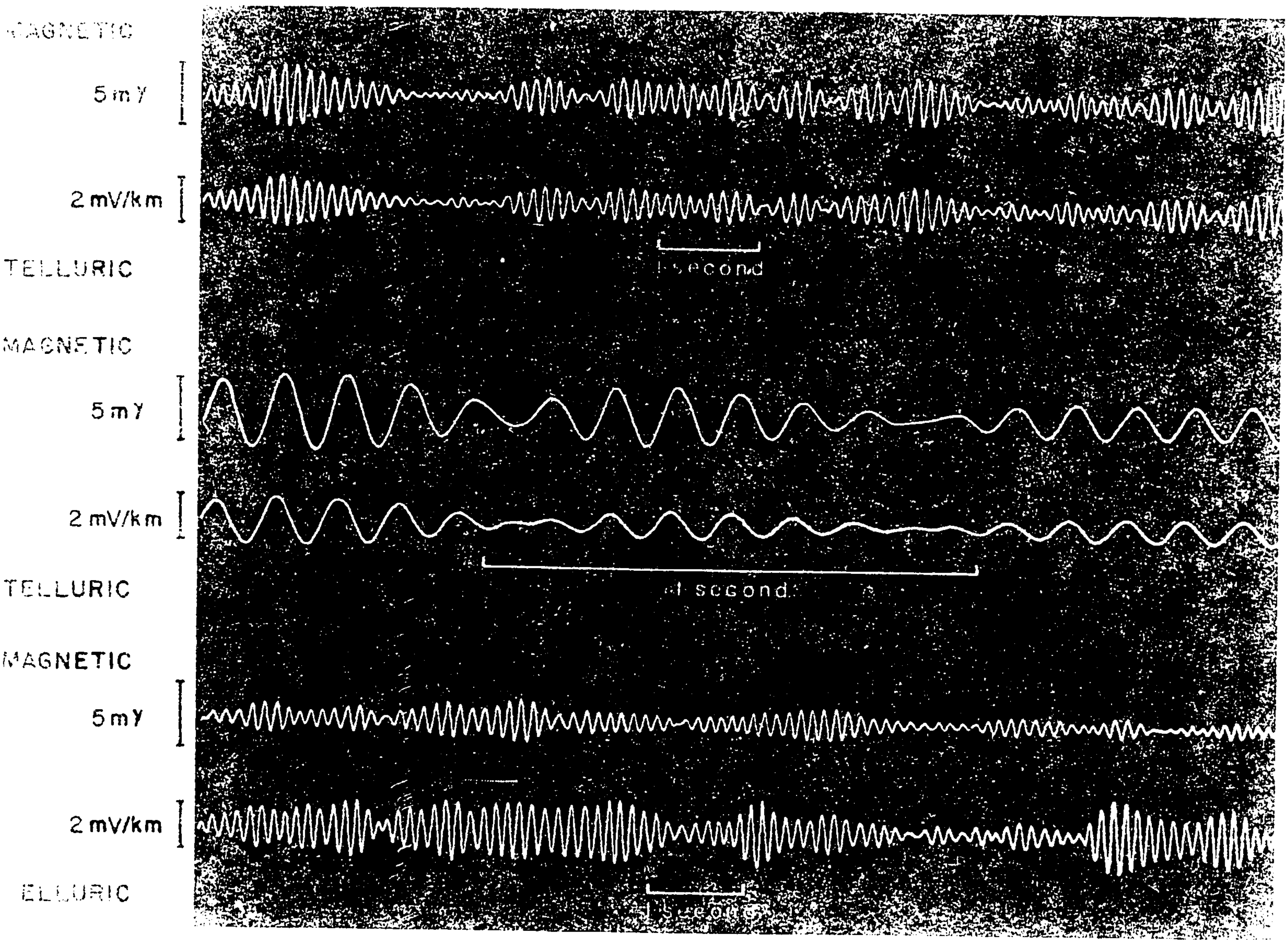

MAGNETIC
5 mγ
2 mV/km
TELLURIC
1 second
MAGNETIC
5 mγ
2 mV/km
TELLURIC
1 second
MAGNETIC
5 mγ
2 mV/km

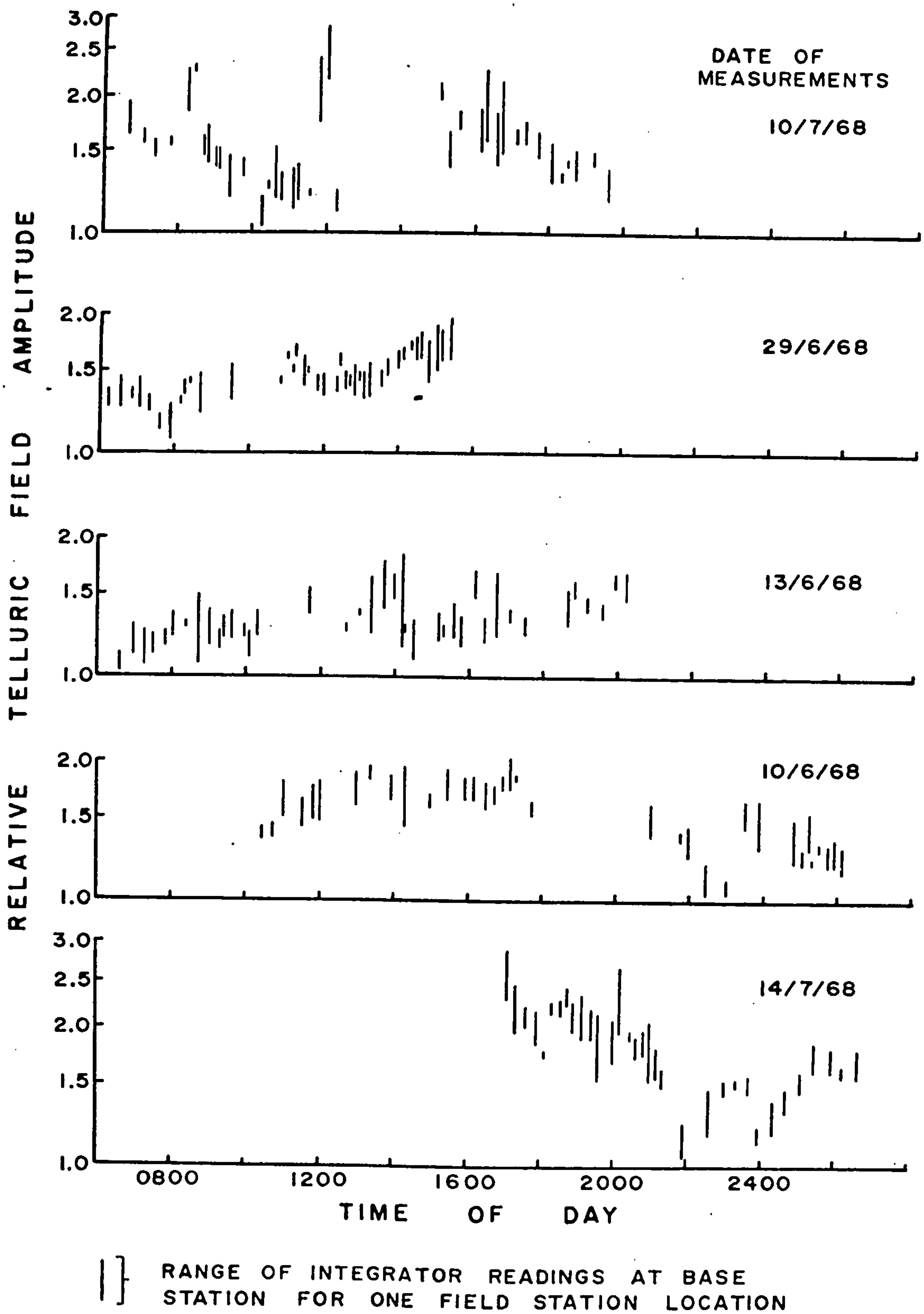

Fig. 3.7 Diurnal and short-term variations in the 8 Hz telluric field strength.

(ρ_{app} < 3000 ohm-m) the intensity was always too low to use electrode separations smaller than 100 feet. Local lightning did not affect survey results but, because of the danger of overloading the amplifiers, work was stopped when thunderstorms were closer than approximately 10 miles.

Telluric Signals

In the course of a telluric survey across a conductivity discontinuity the relation between the telluric signals at the base and field stations proved to be highly variable. Figures 3.8 and 3.9 illustrate fairly typical changes in the amplitude ratio, phase and correlation of the two signals. The results shown in Figure 3.9 were obtained during a part of the field work when four telluric amplifiers were available.

When the base and field stations are on the same side of the conductive zone (Figs. 3.8(a) and 3.9(a)) the signals are in phase and correlate very well. This was generally true in the absence of conductivity discontinuities. The presence of the conductor is indicated by a decrease in the amplitude of the field station signal. Also, the base and field signals do not correlate and the phase relationship is erratic (Fig. 3.9(b)). When the two stations are on opposite sides of the conductor, in one case (Fig. 3.8(c)) the signals do not correlate and are approximately 180° out of phase. In the other example (Fig. 3.9(c)) they are in phase and correlate fairly well.

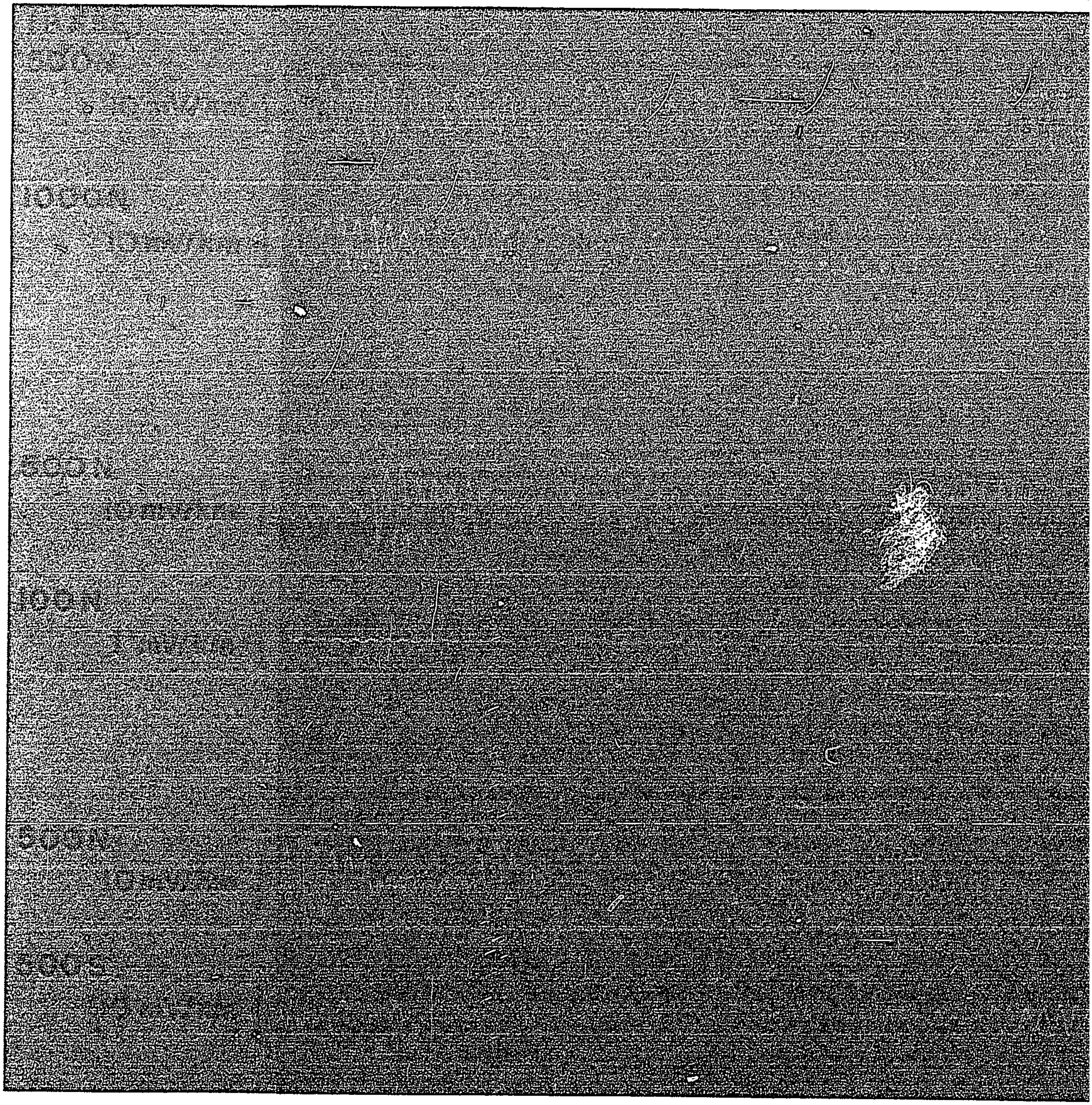

Fig. 3.8 Correlation of telluric signals (Test Site I,

(a)

(b)

(c)

ls (Test Site I, Line A-A' (Section 4.1)).

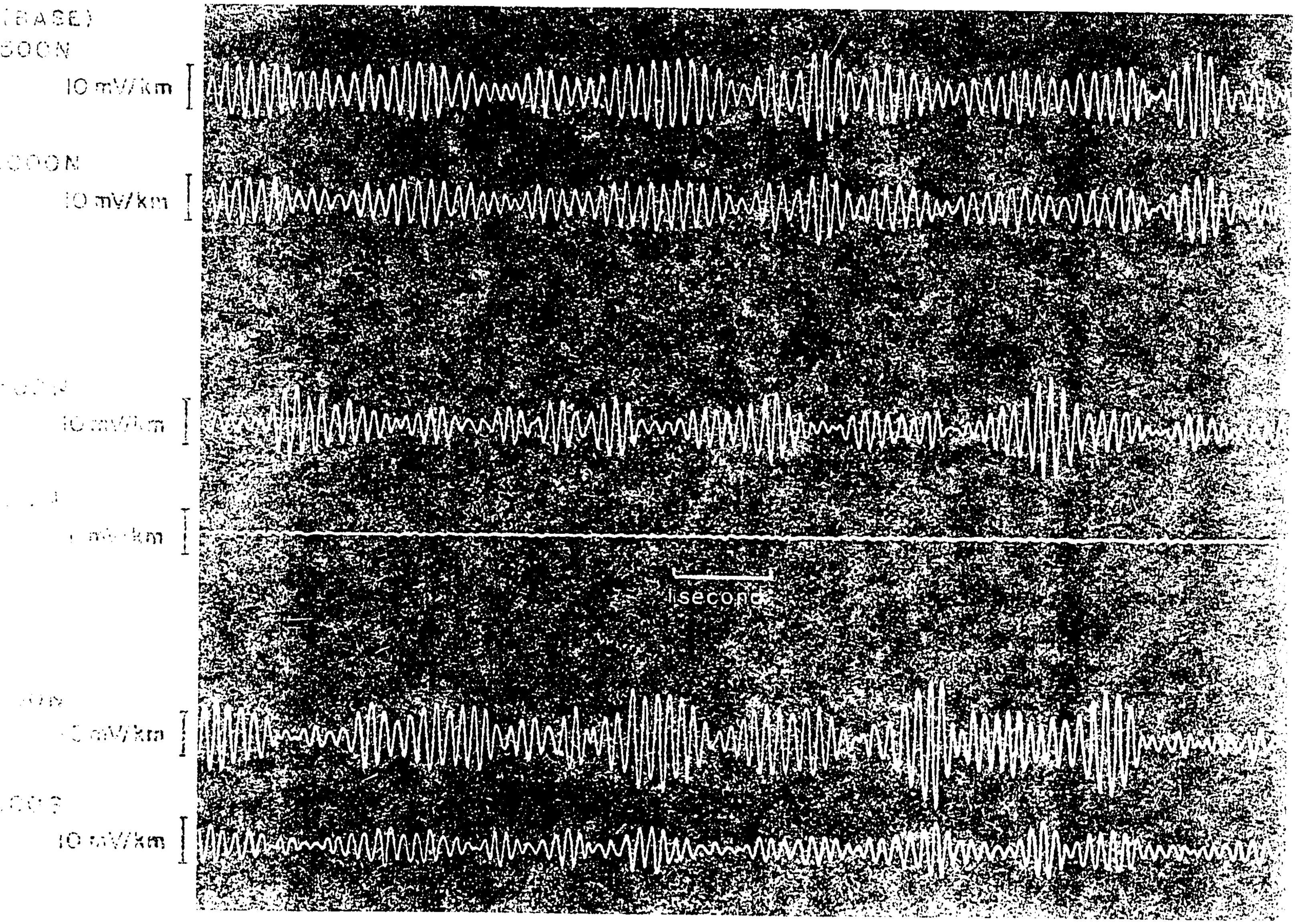
(BASE)
10 mV/km
10 mV/km
10 mV/km
10 mV/km
10 mV/km
1 second

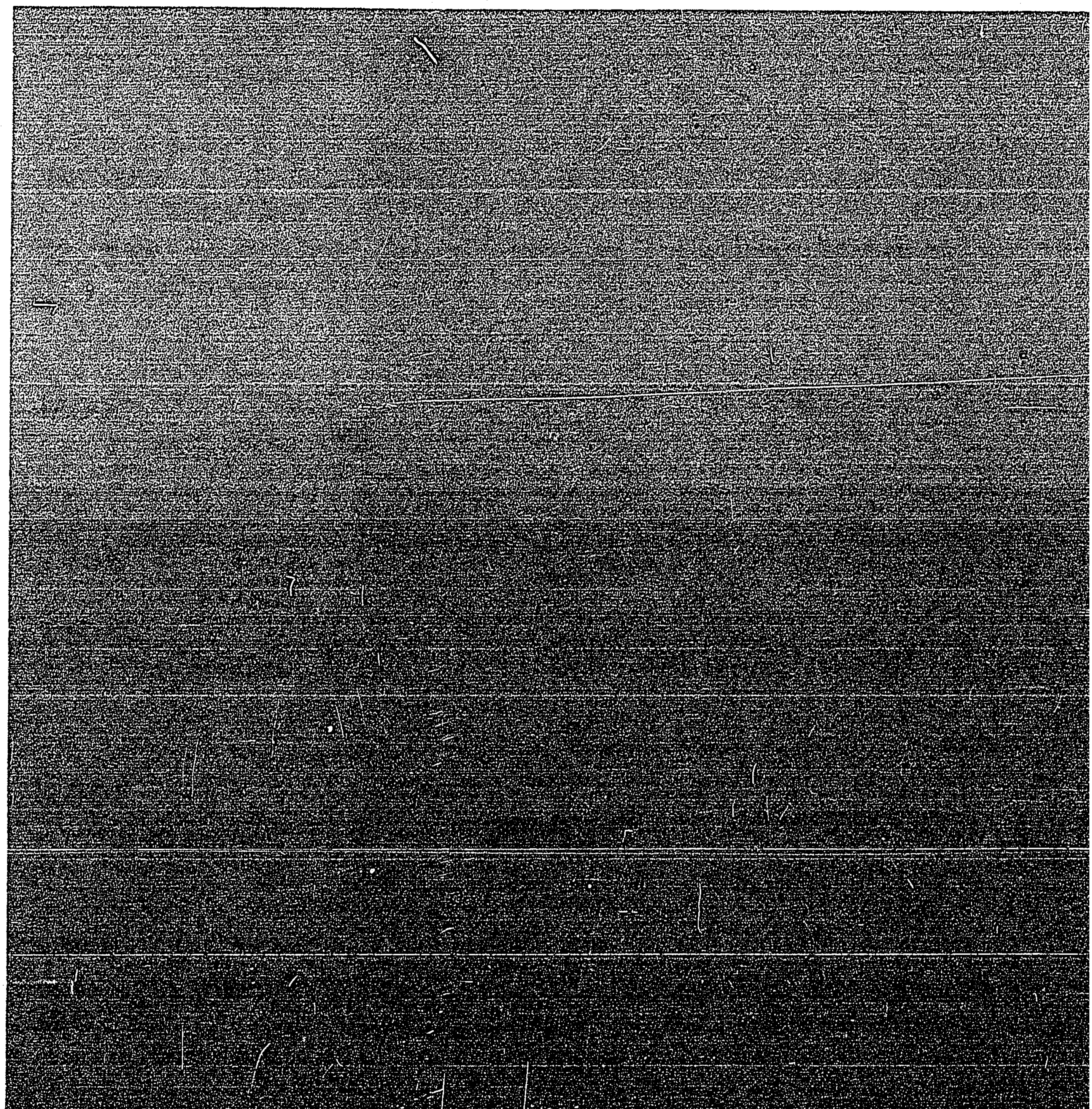

Fig. 3.9 Correlation of telluric signals (Test Site

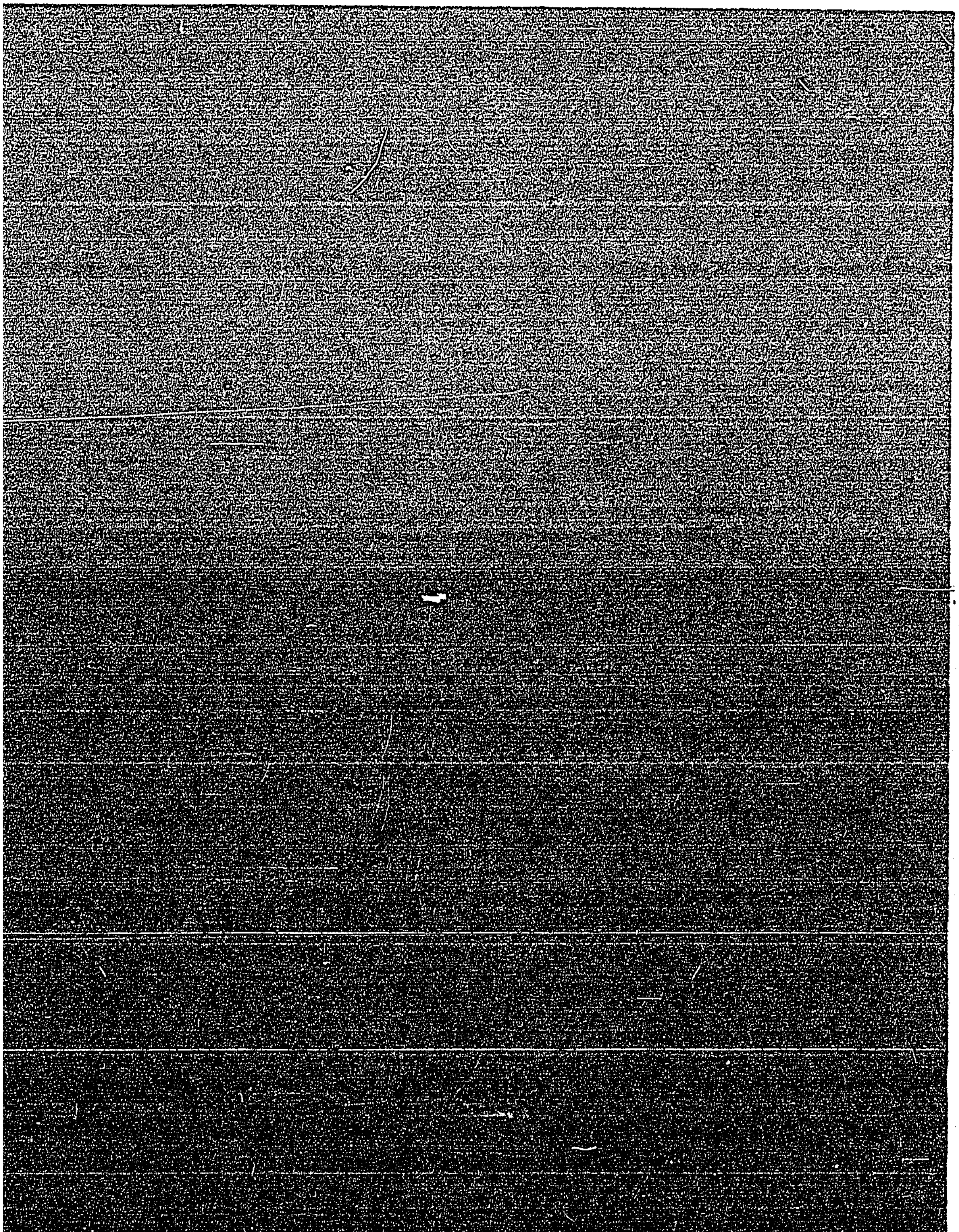

(a)

(b)

(c)

gnals (Test Site 5, Line 3600S (Section 4.5)).

Magnetotelluric Signals

The correlation between the space orthogonal magnetic and telluric fields was found to be variable, ranging from good (Fig. 3.6(a)) to nonexistent (Fig. 3.6(c)). Excepting a few locations, where the signals correlated to some extent for all orientations of the telluric spread, the degree of correlation depended on the direction of measurement. However, in all cases it was possible to find one direction where the electric and magnetic signals correlated well. Near conductive zones the best correlation was observed when the electric field normal and the magnetic field parallel to the strike were measured.

The phase relationship between the magnetic and telluric fields was variable. The accuracy of phase determinations was limited by the recording equipment but Figure 3.6(b) shows that the phase of the electric field leads the magnetic by approximately 45°. However, even in this instance, the relative phase at the beginning and end of each signal burst is not the same.

3.6 Field Data Processing

When the field signals were integrated the integrator readings could be used to determine both the average intensity and the amplitude ratio of the fields. The simple calculations necessary to determine either the relative telluric field strength or the apparent resistivity were made during the actual survey. Of course, this technique provided no information on either the phase or correlation of the field signals.

When the signals were recorded, the relative signal amplitudes could be determined quantitatively but only qualitative treatment of the phase and correlation data proved possible. In cases of good correlation between the base and field signals in a telluric survey (or the electric and magnetic signals in a magnetotelluric survey) the relative field strength was calculated by measuring the amplitudes of corresponding signal bursts. Because the amplitude ratios were found to vary as much as 20%, the values for 3 to 10 signal bursts were averaged to obtain either the relative telluric field strength or the apparent resistivity. When the two signals did not correlate the relative telluric field strength or the apparent resistivity were estimated by taking the ratio of the average amplitudes of the signals.

The correlation between the two signals was estimated on an arbitrary scale ranging from 0 for no correlation to 5 for excellent correlation. Similarly, the phase angle was estimated to lie within a range of values. Although no use was made of either the phase or correlation in plotting field results, the variations observed in both parameters were found to be highly significant in the theoretical modelling of actual geologic structures.

CHAPTER IV

FIELD RESULTS AND INTERPRETATION

The field results presented are from the 1967 and 1968 field seasons only. The results obtained in 1966 are of questionable value because field measurements showed a consistent lack of repeatability due to the thermal instability and wide pass band of the amplifiers.

The field results are presented in chronological order based on the first visit to the site. Initial field tests were designed to determine the optimum survey methods and to establish the reliability and repeatability of measurements. Massive near-surface sulphide zones, which could be expected to show well-defined anomalies, were chosen for the first field tests. From these trials it was clear that measurements of the telluric field strength normal to the strike of the target zone, combined with magnetotelluric determinations of the background apparent resistivity, provided maximum information in relation to the work involved. Subsequent test sites were selected to examine the usefulness of the methods in a variety of geologic situations. Figure 4.1 shows the general location of the test sites.

Only in cases where the mineral rights are not privately owned are the specific locations given in the text. Also, the original

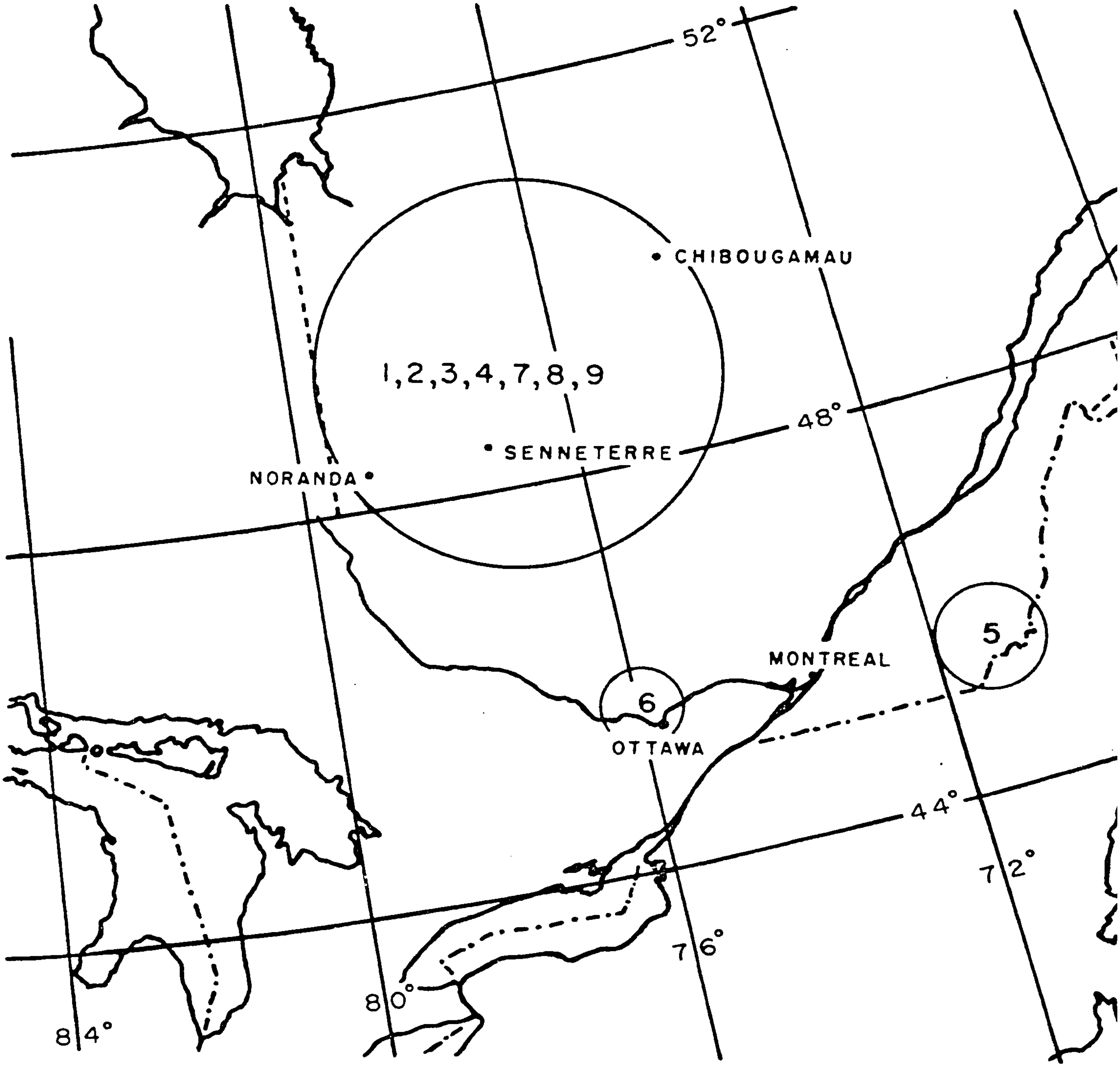

Fig. 4.1 General location of t

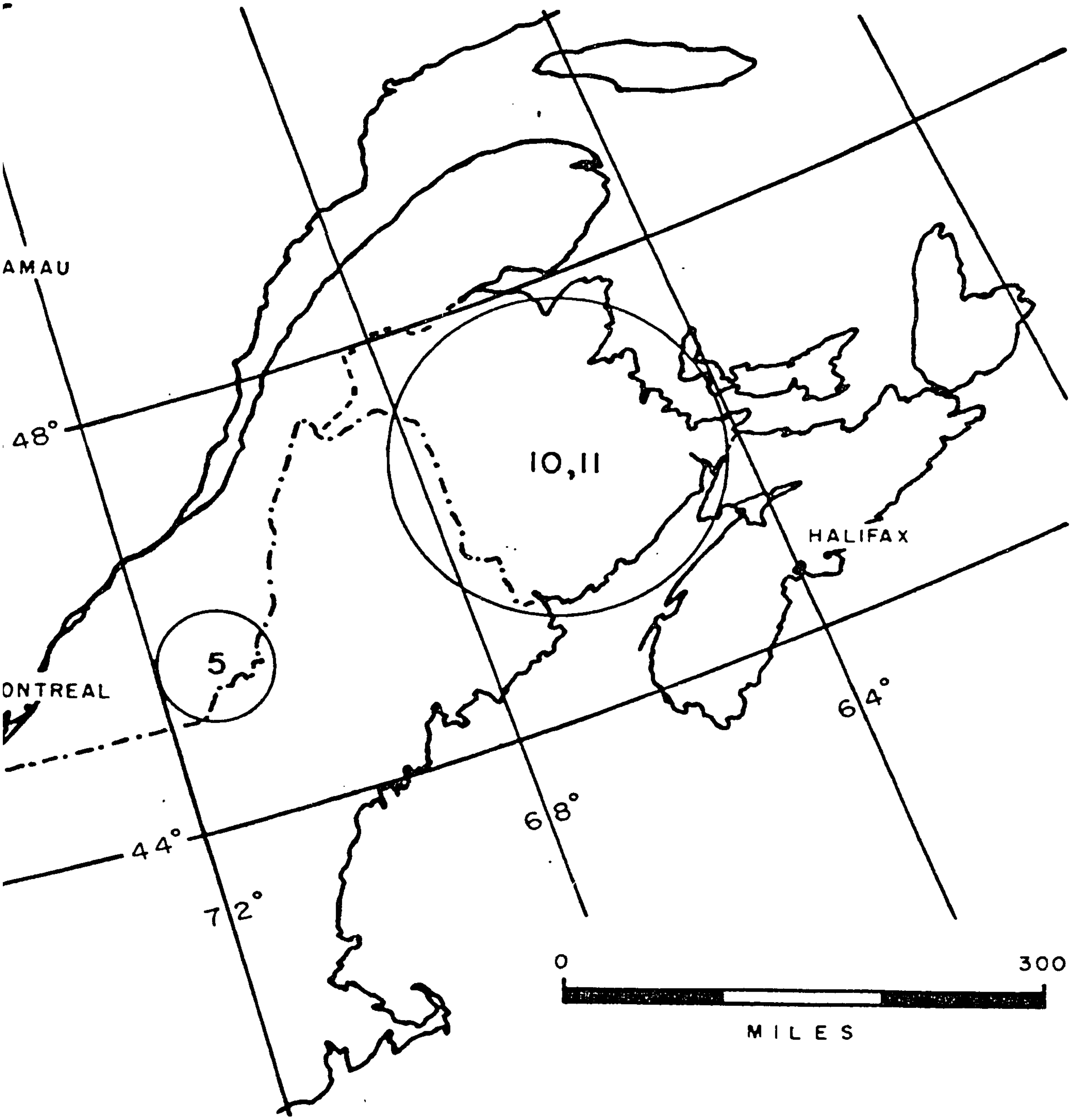

neral location of test sites.

requests for information and access included the provision that any information beyond the general outline of the mineralization and the total sulphide content would remain confidential.

The conductivity models used to compute the theoretical profiles that accompany the field results are based on diamond drill logs. In most cases there was sufficient information to model the geology with relatively good accuracy.

The resistivity of the host rocks assumed for the models was the background apparent resistivity obtained from magnetotelluric measurements. The overburden resistivity was taken to be 500 ohm-meters if the test site was well-drained, and 100 ohm-meters if the ground was swampy. The resistivity of the sulphide zones ranges from 0.1 ohm-meters for very massive sulphides to 20 ohm-meters for disseminated zones.

For simplicity, the theoretical models used assume structures with well-defined boundaries where the resistivity changes abruptly. This approach ignores gradual resistivity changes that may be caused by thin sulphide veins and haloes of disseminated mineralization that exist around most sulphide zones. However, in cases involving closely spaced parallel or sub-parallel sulphide bodies, this sporadic mineralization may form an electrical connection between the main zones. This situation was approximated in the theoretical models by means of a thin conductive layer joining the bottoms of the zones at a sufficient depth so that by itself it does not produce a significant anomaly.

4.1 Test Site 1

This test site is in Bartouille Twp., on Hwy. 58 from Senneterre to Chibougamau. The mineralization consists of pyrite and pyrrhotite. Some graphite is also present. The host rocks are meta-sedimentary breccias and tuffs interbedded with lava flows. Twenty-five diamond drill holes and an SP survey have outlined the sulphide zone in some detail (Fig. 4.2). In the more heavily mineralized parts the total sulphide content ranges from 40% to 70% with an average of approximately 30% for the entire zone. The overburden is generally less than 10 feet thick.

The following are approximate RMS values for the amplitudes of the 8 Hz field components at 1000N on traverse A-A':

$$E_{\perp} = 3 \text{ mV/km}$$

$$E_{\parallel} = 1 \text{ mV/km}$$

$$H_z = 0.2 \text{ m}\gamma$$

$$H_{\perp} = 1.25 \text{ m}\gamma$$

$$H_{\parallel} = 1.25 \text{ m}\gamma$$

Consequently, the apparent resistivities for the $E_{\perp}$ and $E_{\parallel}$ polarizations are 70000 and 8000 ohm-meters respectively.

The results of surveys along traverse A-A' are summarized in Figure 4.3. All the surveys indicate the presence of the known mineralization. The most intense and best defined anomaly is shown in the $E_{\perp}$ results, the $E_{\parallel}$ and H_z anomalies are broader and give less indication of the multiple conductive zones.

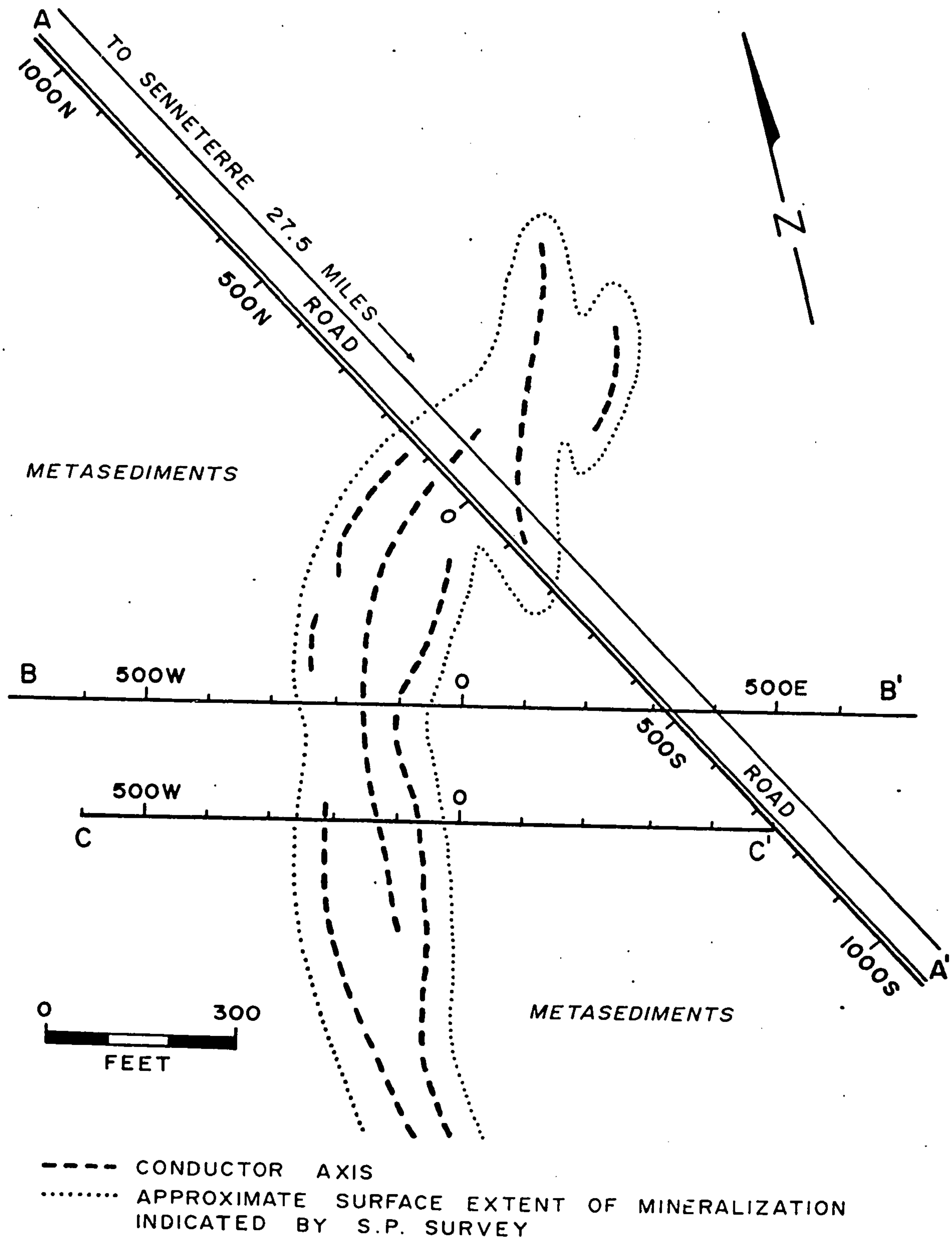

Fig. 4.2 Plan of Bartouille Twp. sulphide zone (Test Site 1).

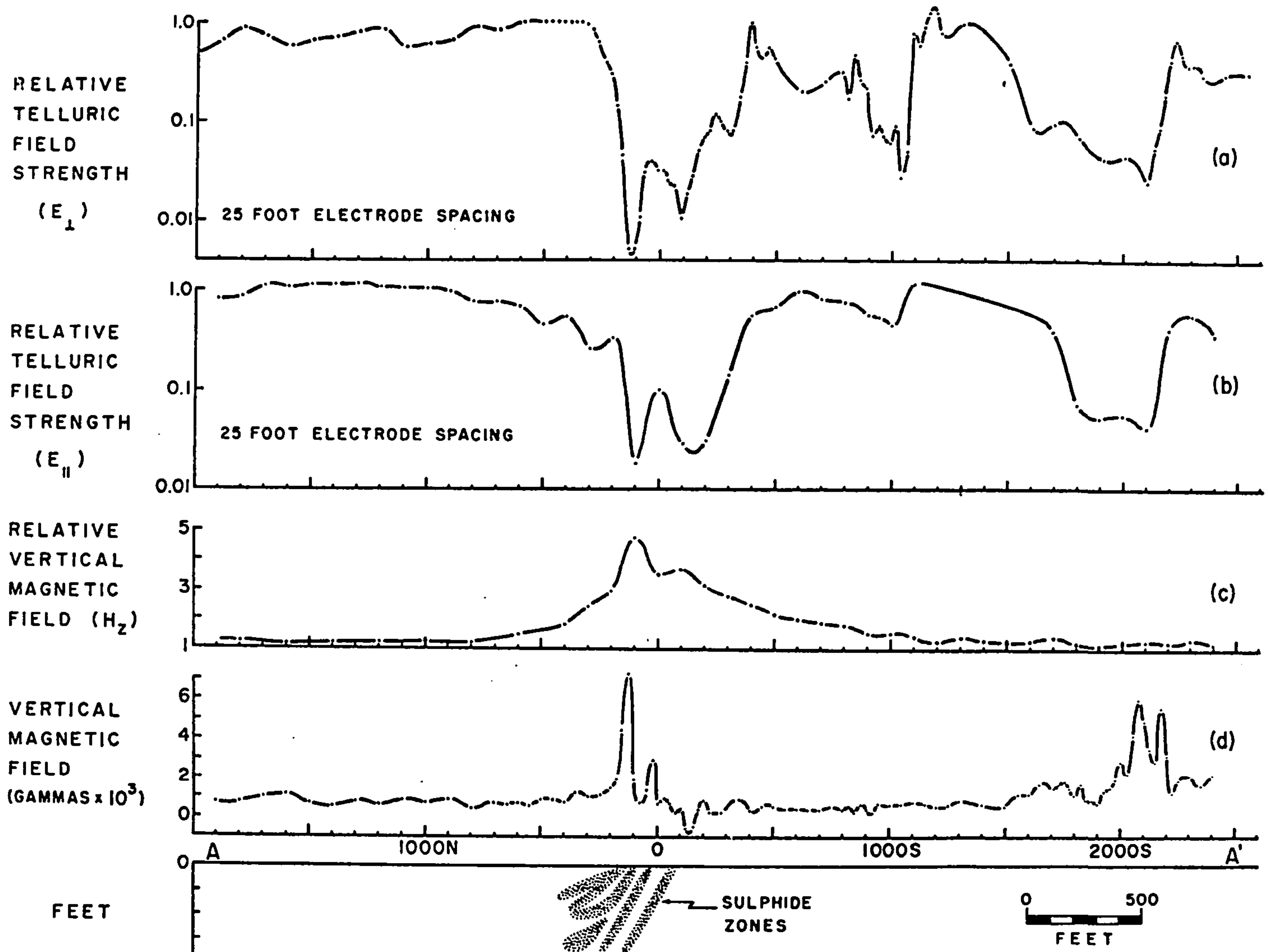

Fig. 4.3 Test Site 1. Survey results along traverse A-A'.

The H_z results show an anomaly only over the known sulphide zone whereas both telluric profiles indicate the presence of additional conductive zones around 1000S and 2000S. Although both these anomalies coincide with swampy areas it is doubtful that they are caused by highly conductive overburden as there is no anomaly over a similar swamp between 600N and 800N. Also, the magnetometer profile shows a magnetic high between 1500S and 2200S that corresponds very closely to the telluric anomaly at 2000S.

The $E_{\parallel}$ signals correlate well and are in phase along the entire traverse. The $E_{\perp}$ signals show poor correlation and are approximately 180° out of phase on opposite sides of both the known sulphide zone (Fig. 3.8) and the conductive zone at 2000S. Also, in the interval between 925S and 1050S the signal is approximately 180° out of phase but correlates well with the signals on both sides. A possible cause of such phase shifts is discussed in Section 5.1 .

Measurements of the directional variations in the telluric field strength can provide some indication of the strike of a nearby conductive zone (Fig. 4.4). The direction of the minimum telluric field at 1000N, 500N and 400S reflects the strike direction of the known mineralized zone. This might be expected in view of the telluric survey results which show that $E_{\parallel}$ starts to decrease much farther from the sulphide zone than does $E_{\perp}$. However, excepting these stations, the results do not show a clear pattern. At 1350N and 1825N there should be no effect due to the sulphide zone yet the ratio of maximum to minimum field strength is greater than 3. This might be partly due to

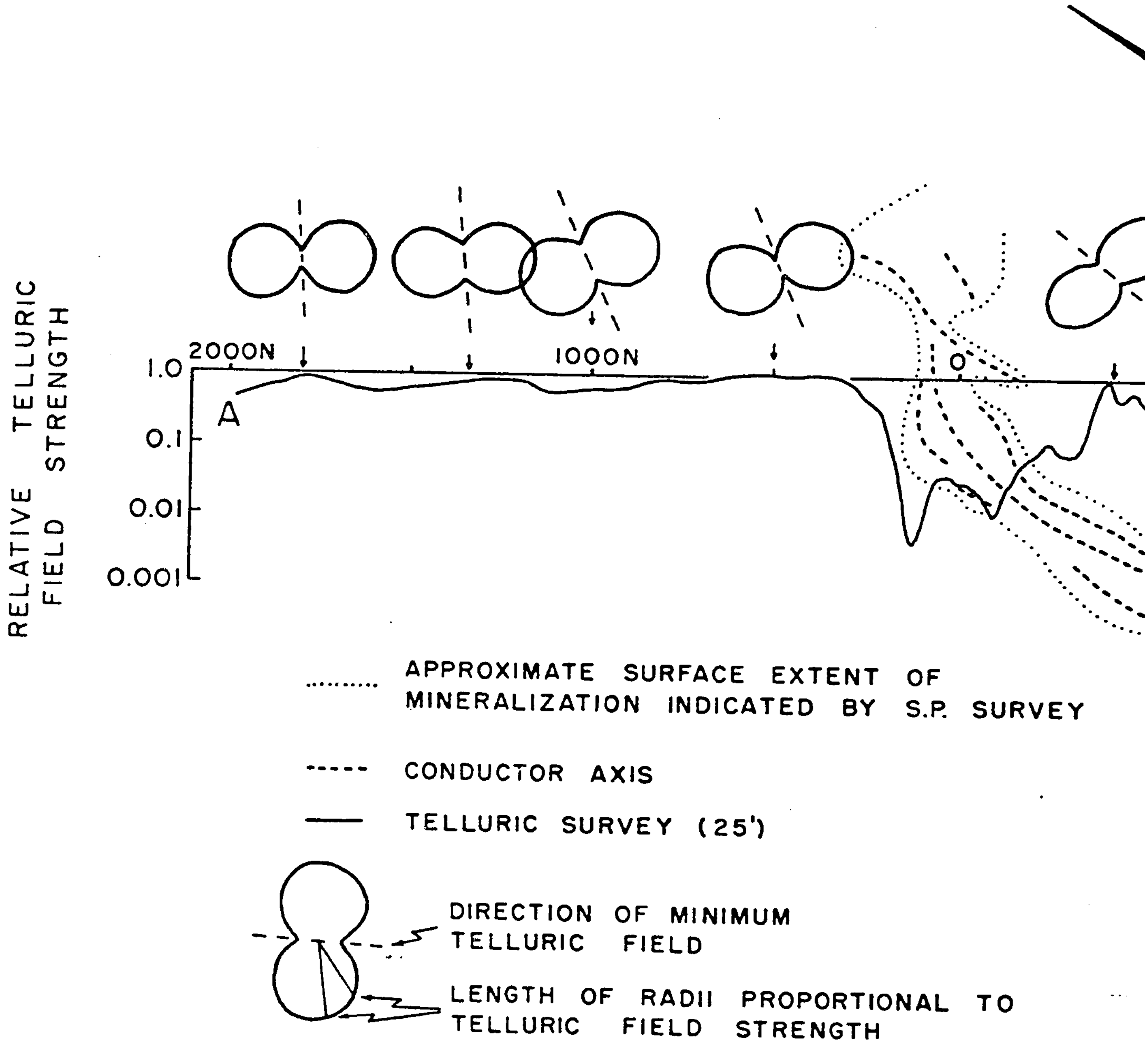

Fig. 4.4 Test Site 1, Line A-A'. Directional v

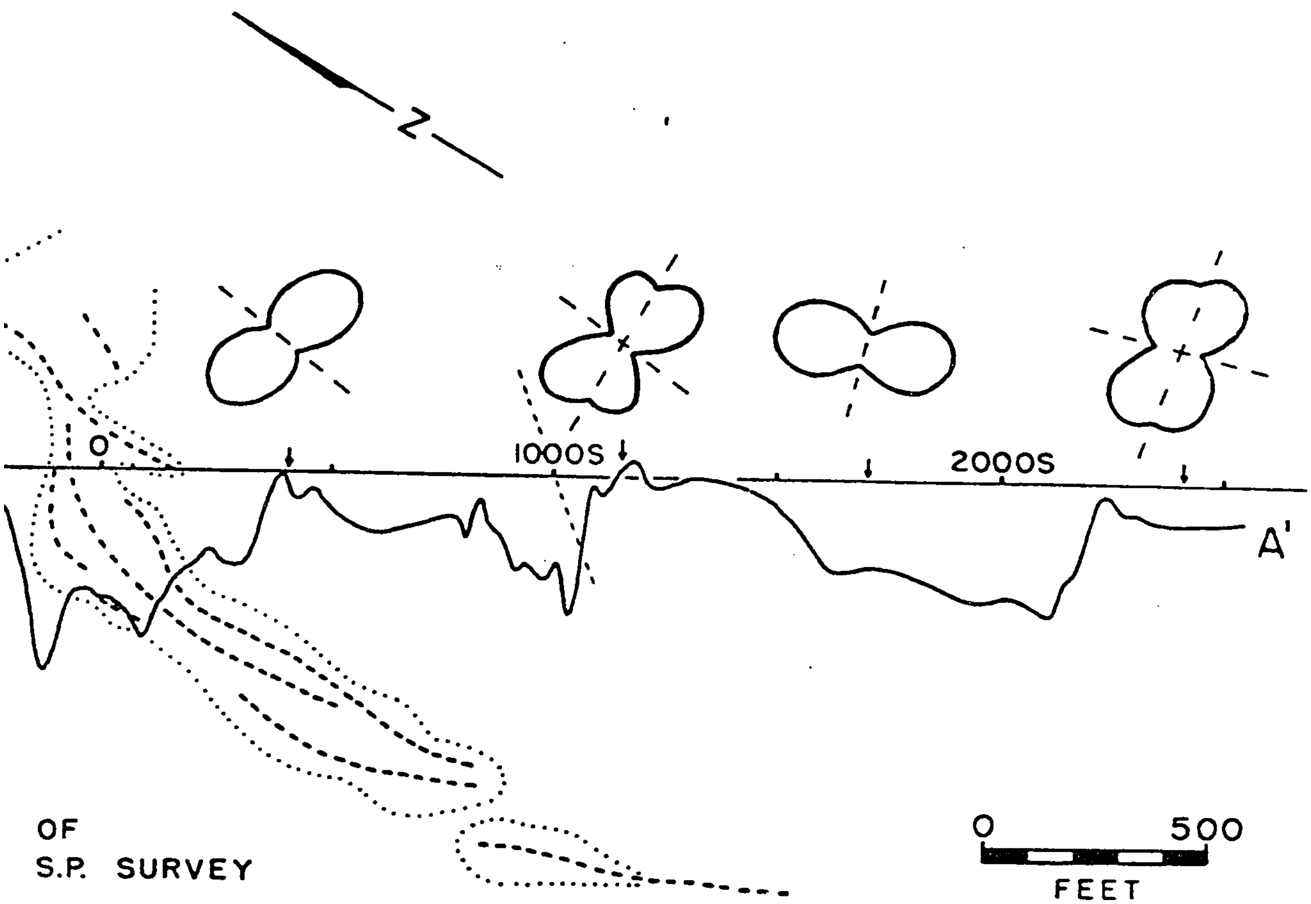

ONAL TO

Directional variations in telluric field strength.

anisotropic country rock which has a minimum resistivity parallel to the approximately north-south strike of the geology in the area. The results at 1125S, 1700S and 2400S suggest that the conductive zone between 1600S and 2200S strikes east-west. This appears doubtful in view of the strike of the regional geology.

The results of repeated traverses using 100 foot electrode spacing agree well (Fig. 4.5(a)). Discrepancies occur mainly where the field and base stations are on opposite sides of the sulphide zone when the signals do not correlate and amplitude ratios have to be estimated. Directly over the conductive zones the telluric signal is too small to measure accurately on the records (Fig. 3.8(b)).

Except for better detail over the anomalous zones the profile obtained using a 25 foot electrode spacing (Fig. 4.5(b)) is very similar to that from the 100 foot survey. This demonstrates that, because telluric measurements sample an existing electric field strength pattern, the length of the electrode spacing does not affect the penetration of the method. The use of long spreads does, however, reduce the resolution, as anomalies are smoothed out; for still larger spreads they may disappear completely.

The only major difference, caused by variable electrode separation, is at 1000S where the 100 foot results show a much more intense anomaly. The reason for this lies in the observed phase changes at 925S and 1050S. The 100 foot electrode spreads, between 900S and 1000S and between 1000S and 1100S, measured fields of both normal

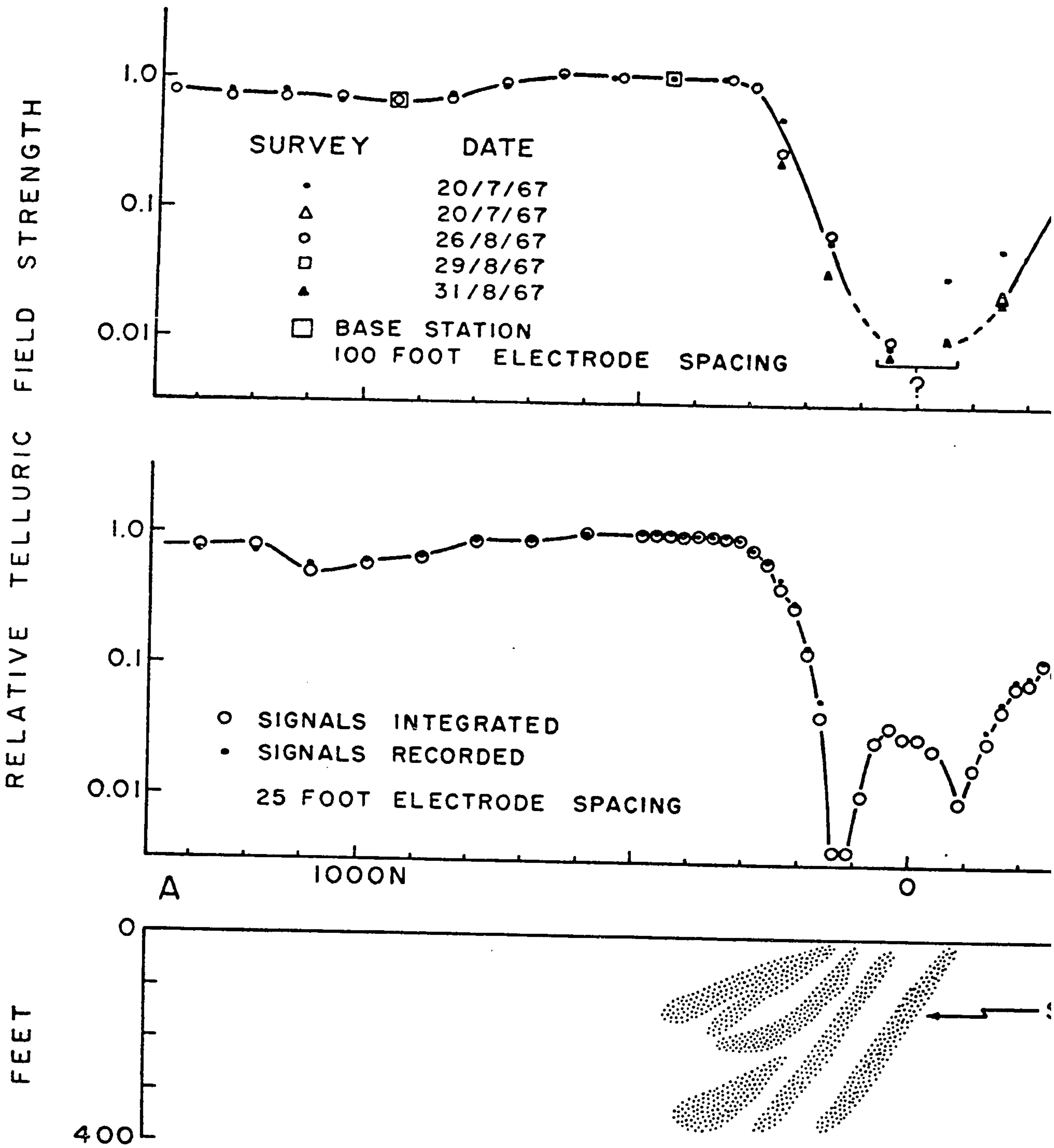

Fig. 4.5 Test Site 1, Line A-A'. Results of telluric

spacings ($E_\perp$ polarization).

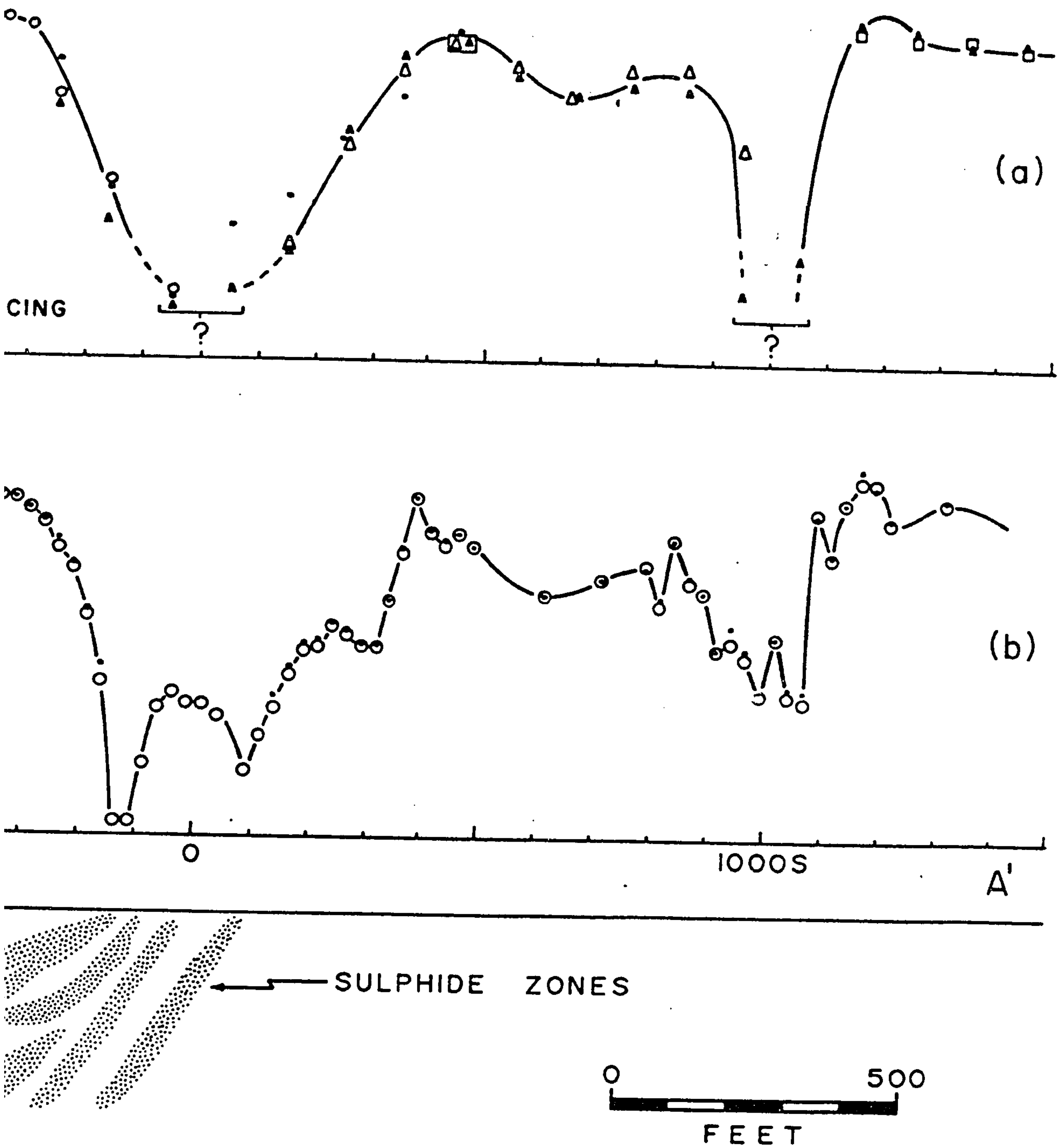

:esults of telluric traverses using 100 and 25 foot electrode and reversed phase which cancelled to produce a small resultant signal.

There is generally good agreement between the integrated signals and the results obtained by calculating amplitude ratios from records. However, while the signal over the sulphide zone is too small to measure on the records, integration gives apparently reliable results.

The relative telluric field strength and apparent resistivity profiles are similar (Fig. 4.6(a)) but the scatter in the measured apparent resistivity values is considerably greater than in the telluric field strength ratios. The telluric field strength ratios obtained by integrating the signals show negligible scatter except where the signal level is very low (Fig. 4.6(b)). This suggests that a single integration for each field station would have given results very similar to those obtained by averaging the values from several integrations.

The theoretical profile for the $E_{\perp}$ polarization is very similar to that observed over the proven mineralized zones (Fig. 4.7), except for a major difference south of the zones, where the field results suggest the presence of additional conductive material. This agrees with diamond drill data that show sporadic mineralization, averaging 5% total sulphides, south of the main zones. Unfortunately the drill logs are not sufficiently specific to use for theoretical modelling.

Figure 4.8 compares observed and theoretical results over the mineralized zone for the $E_{\parallel}$ polarization. The decrease in the

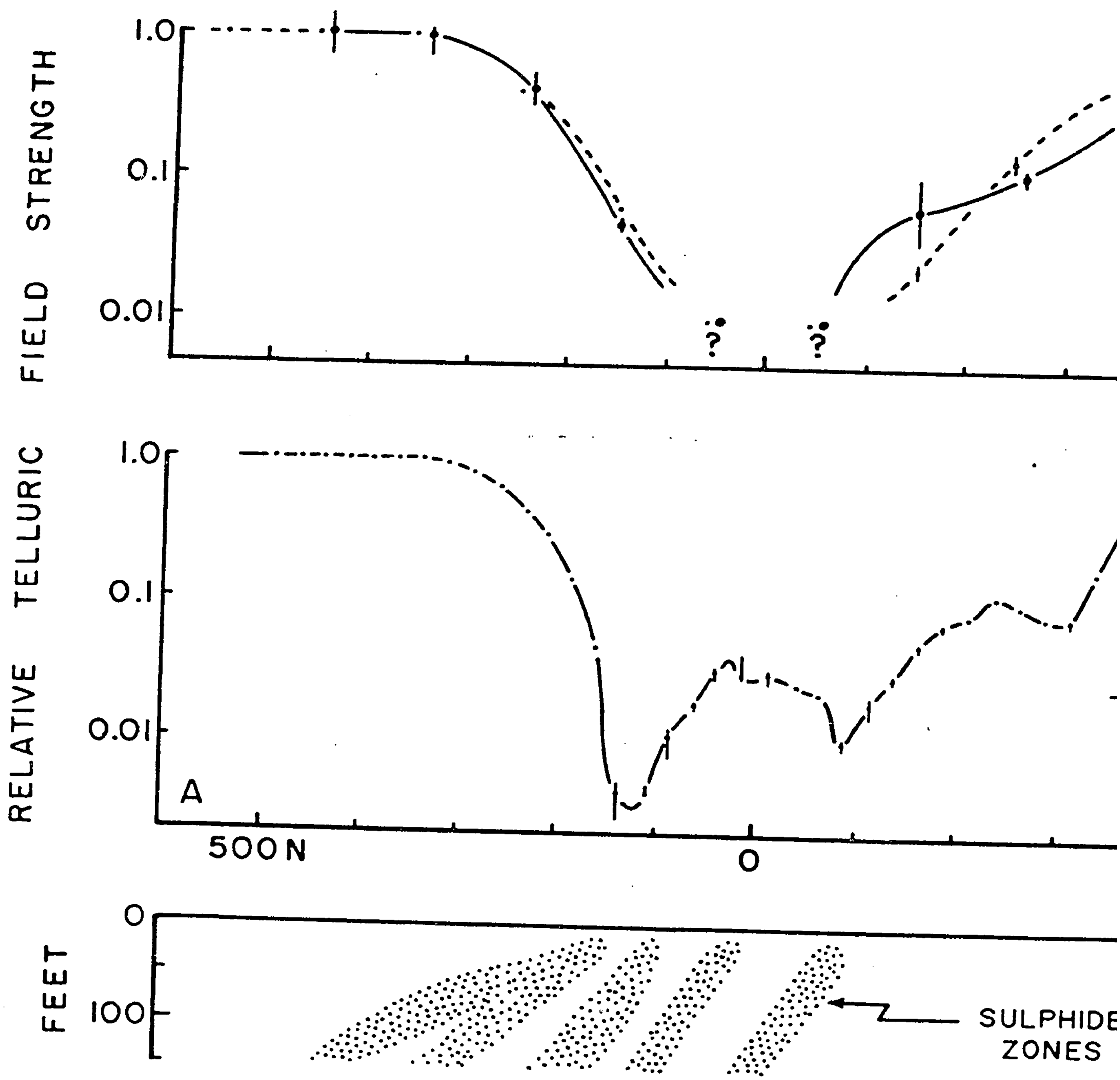

Fig. 4.6 Test Site 1, Line A-A'. (a) Comparison of telluric an

(b) Scatter in measured value

($E_{\perp}$ polarization).

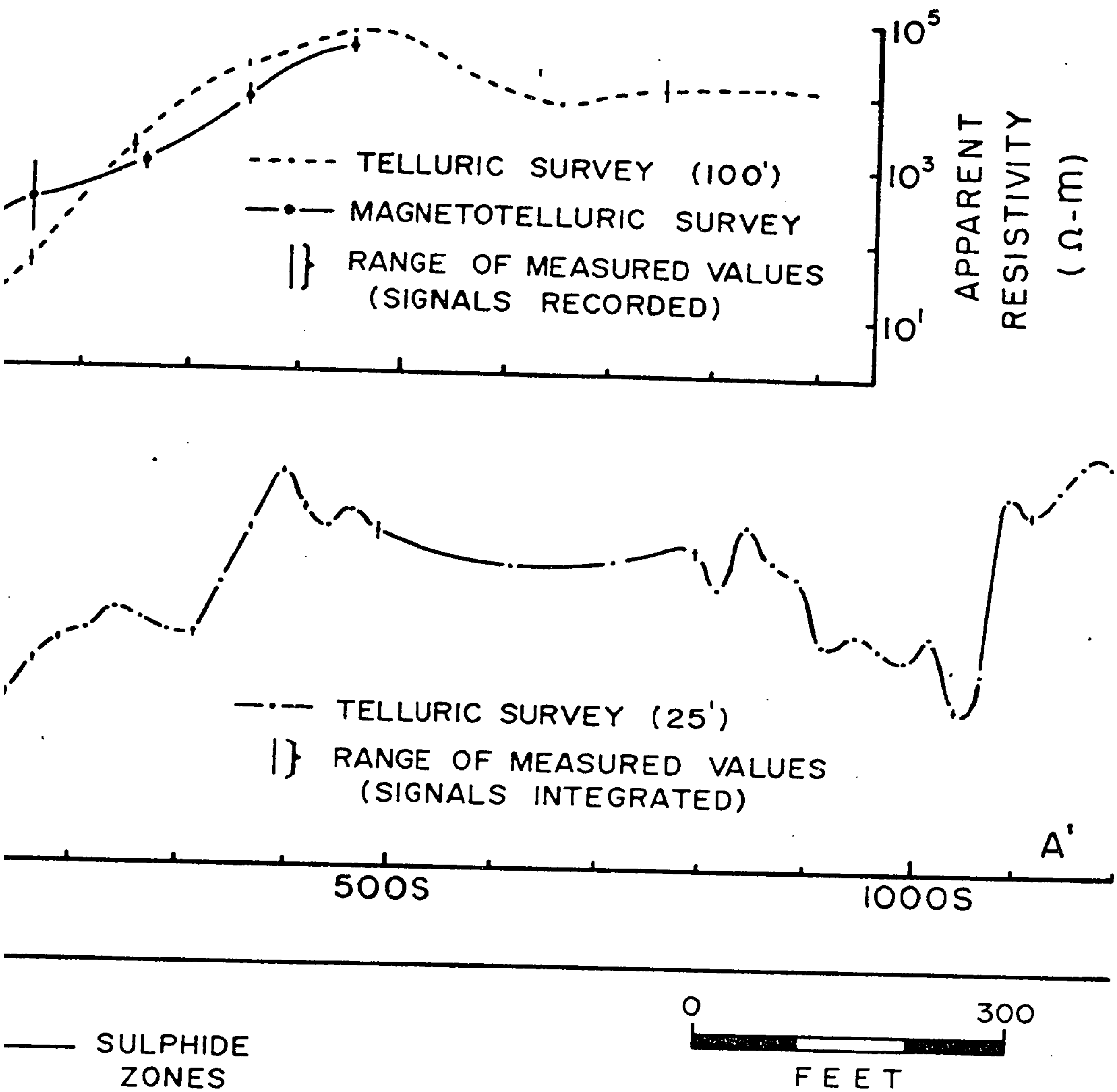

f telluric and magnetotelluric survey results ($E_\perp$ polarization).
easured values of the relative telluric field strength
tion).

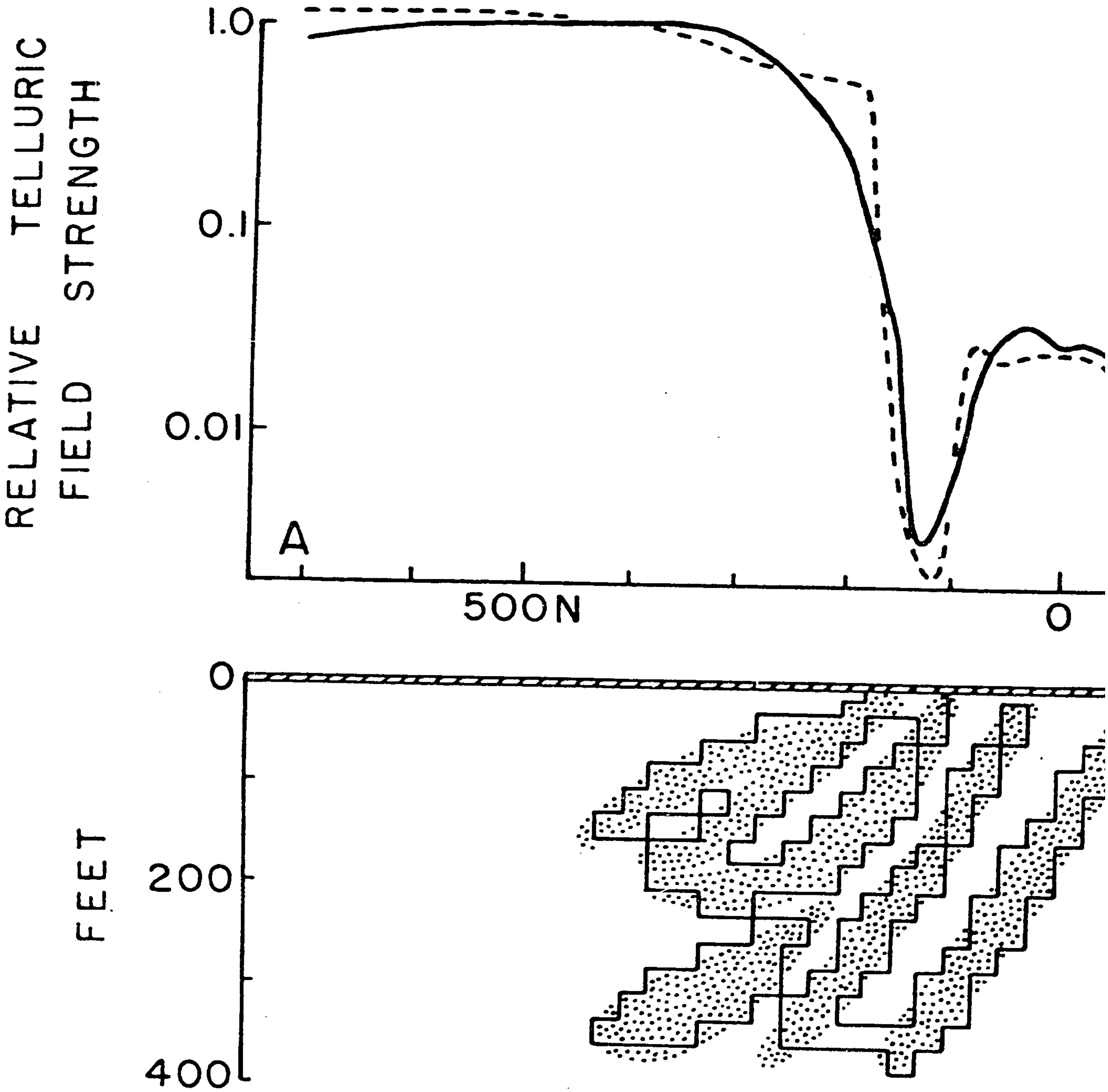

Fig. 4.7 Test Site 1, Line A-A'. Observed and theor

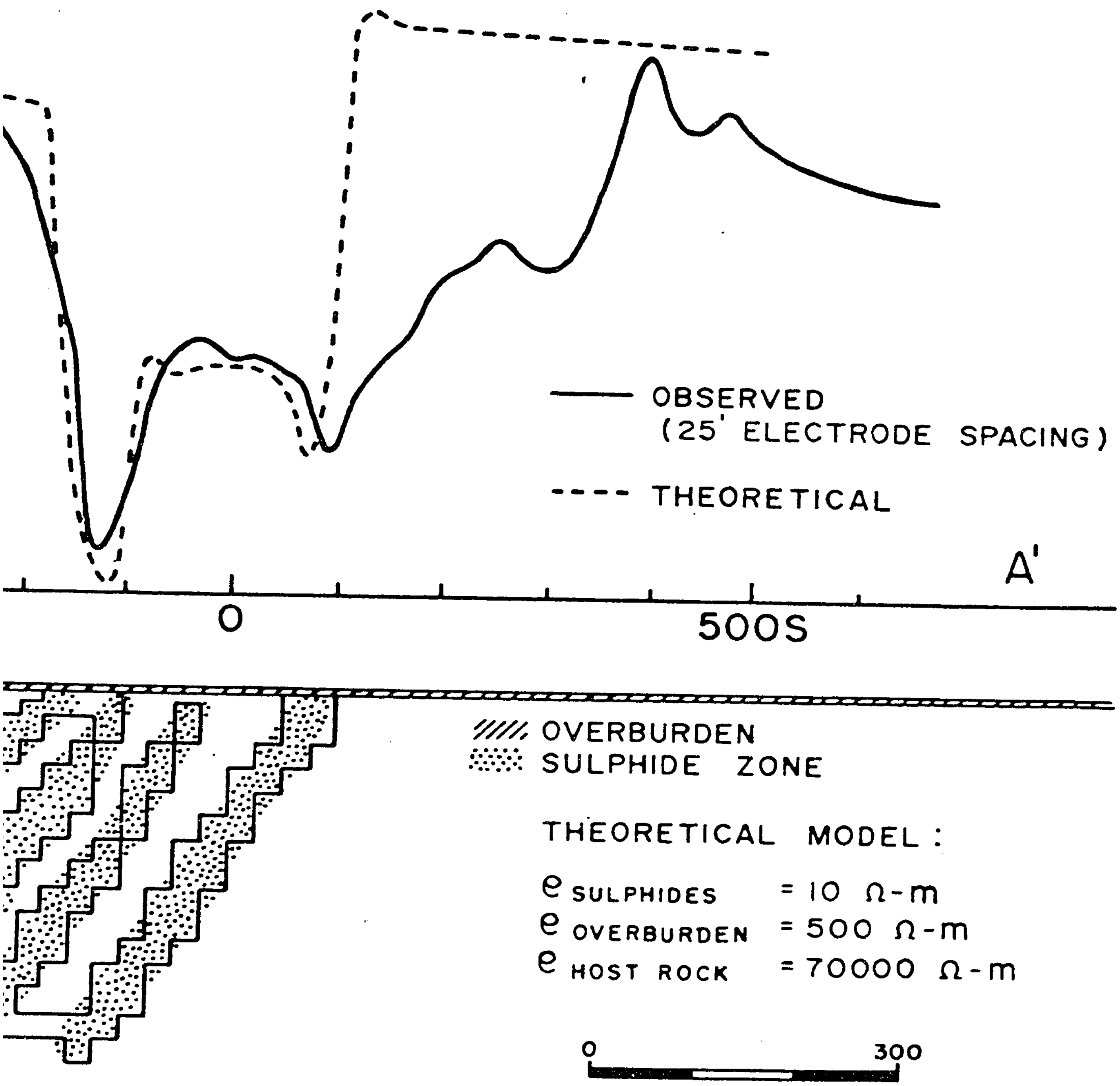

served and theoretical telluric profiles ($E_{\perp}$ polarization).

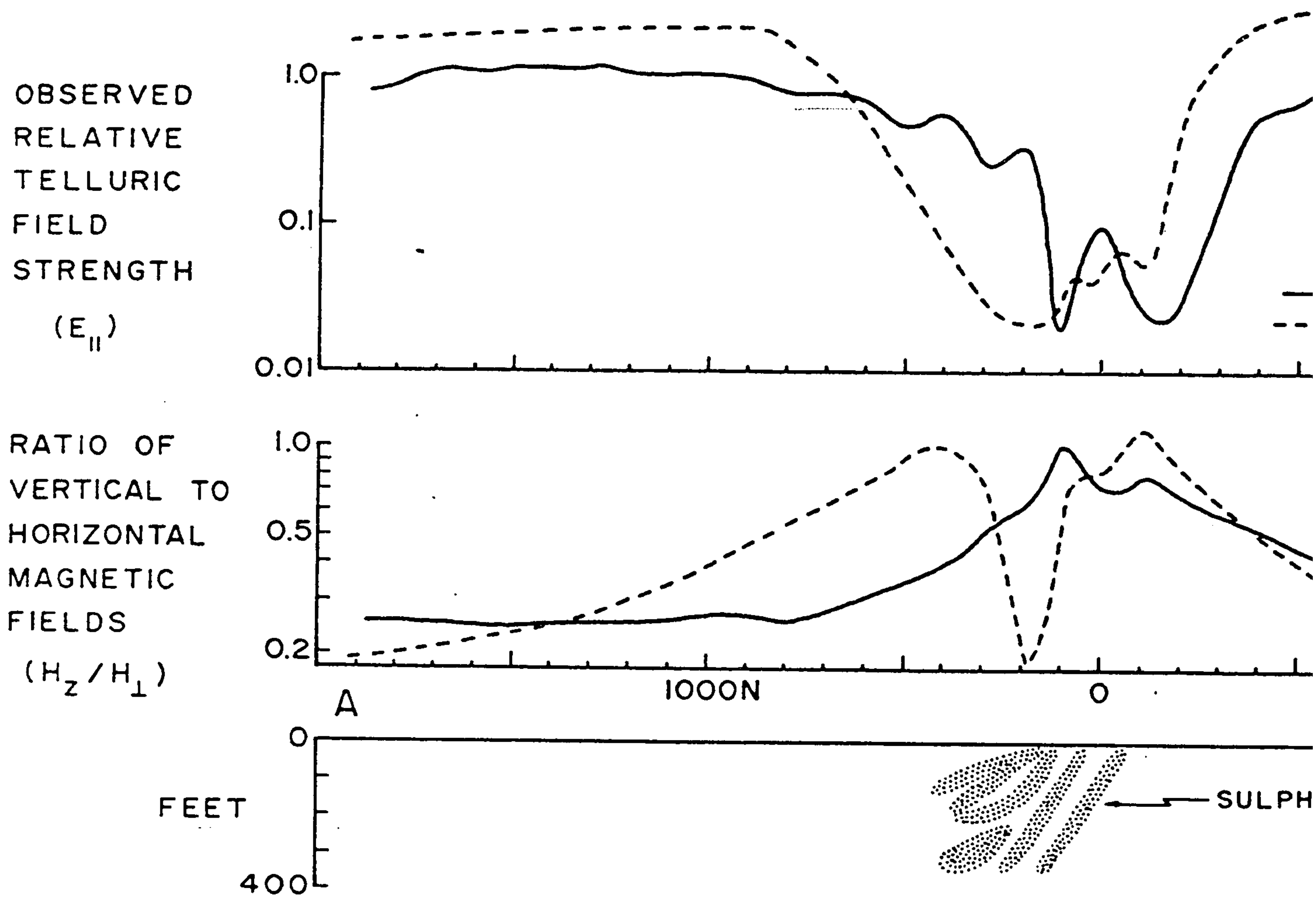

Fig. 4.8 Test Site 1, Line A-A'. Observed and theo:

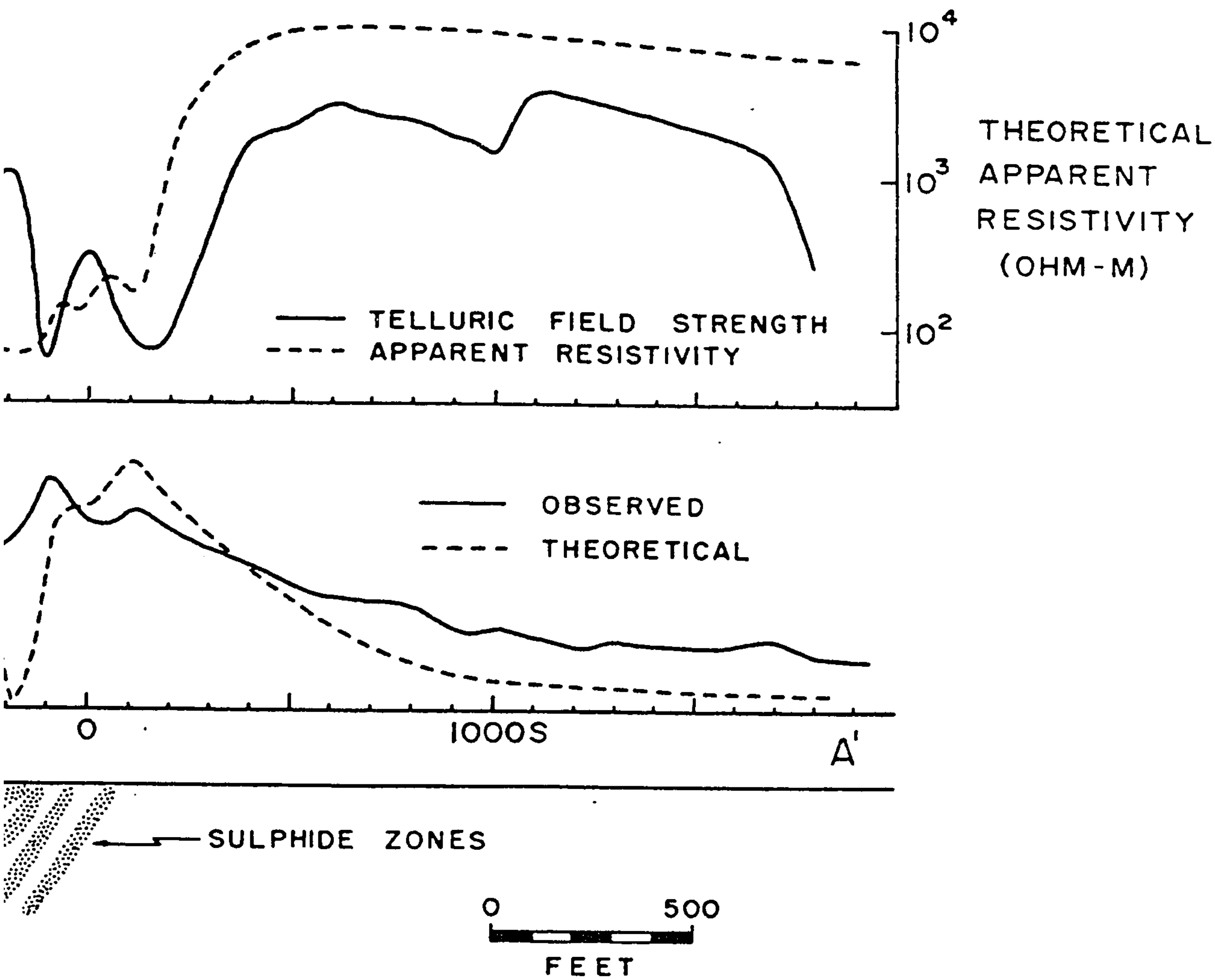

erved and theoretical results ($E_{\parallel}$ polarization).

theoretical apparent resistivity is due entirely to an increase in the magnitude of the horizontal magnetic field ($H_{\perp}$); the theoretical electric field remains constant across the conductive zone. This supports the argument (Section 2.2) that, for the $E_{\parallel}$ polarization, two-dimensional models are not applicable to three-dimensional field situations. The theoretical and observed profiles of the vertical magnetic field show relatively little correlation except that in both cases the maximum vertical field is approximately equal in amplitude to the undisturbed horizontal magnetic field.

The results of telluric and magnetotelluric surveys along traverse B-B' are summarized in Figure 4.9 . They are similar to those along A-A' in the agreement between telluric and magnetotelluric profiles, the better definition obtained by using 25 foot electrode spreads, and the similarity of recorded and integrated results. As in the case of A-A' the field results suggest that there is additional mineralization on the updip side of the main zones.

The intensities of the theoretical and observed telluric anomalies are comparable (Fig. 4.10). On the basis of the two profiles it is probable that the top of the smallest sulphide zone is actually closer to bedrock surface than illustrated.

The observed and theoretical results along traverse C-C' are shown in Figure 4.11 .

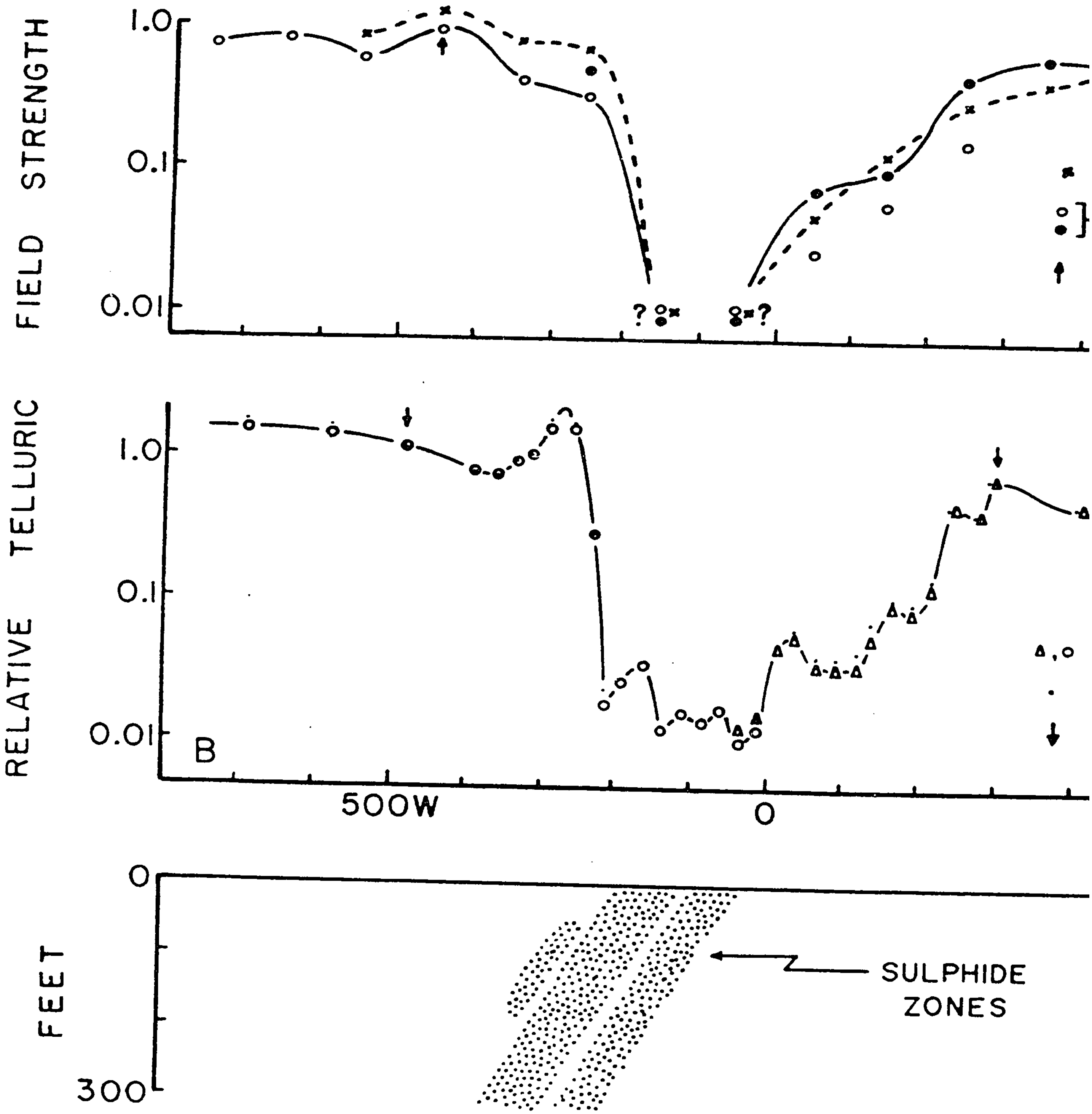

Fig. 4.9 Test Site 1, Line B-B'. Telluric and magnetotel

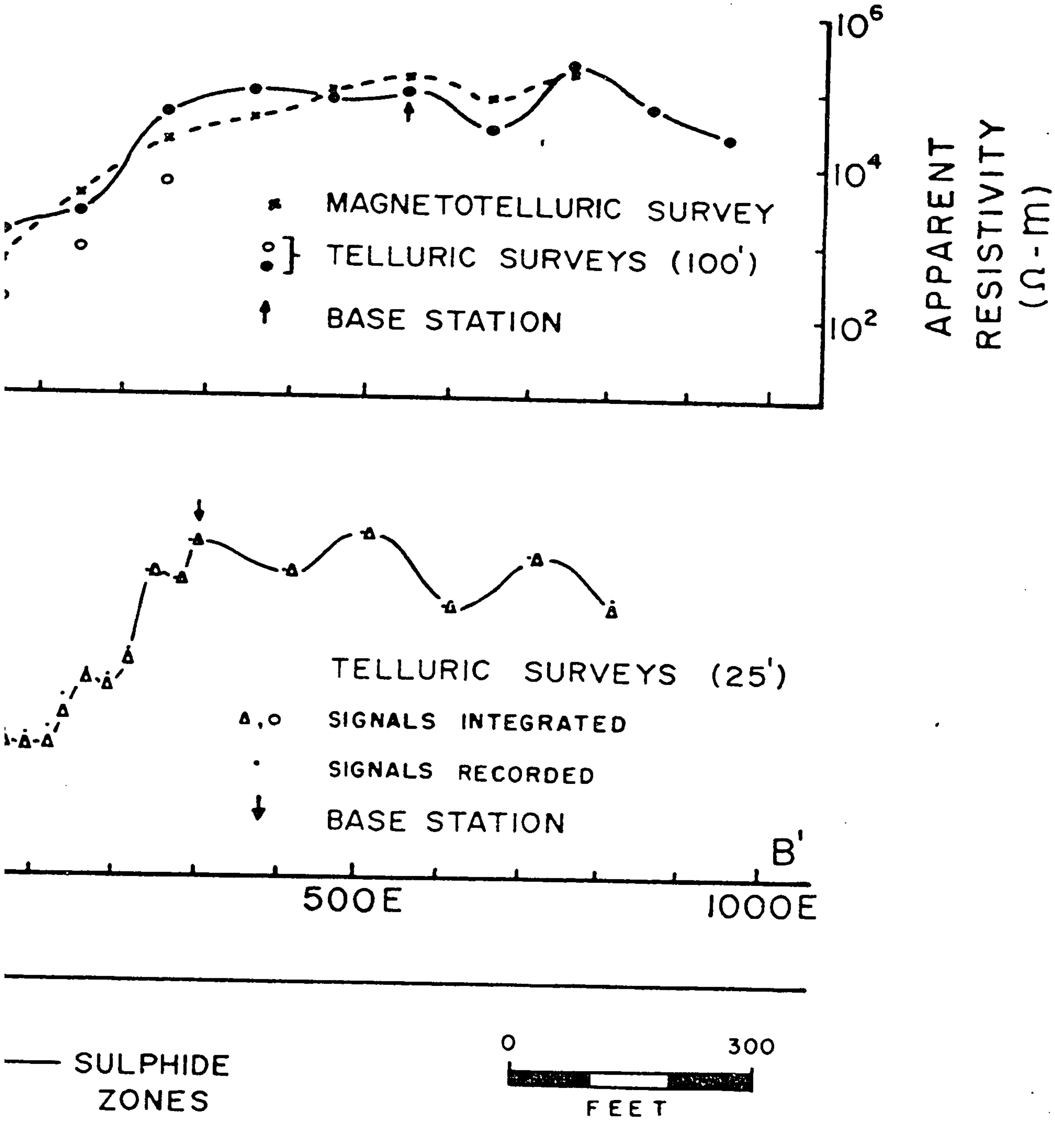

c and magnetotelluric survey results ($E_\perp$ polarization).

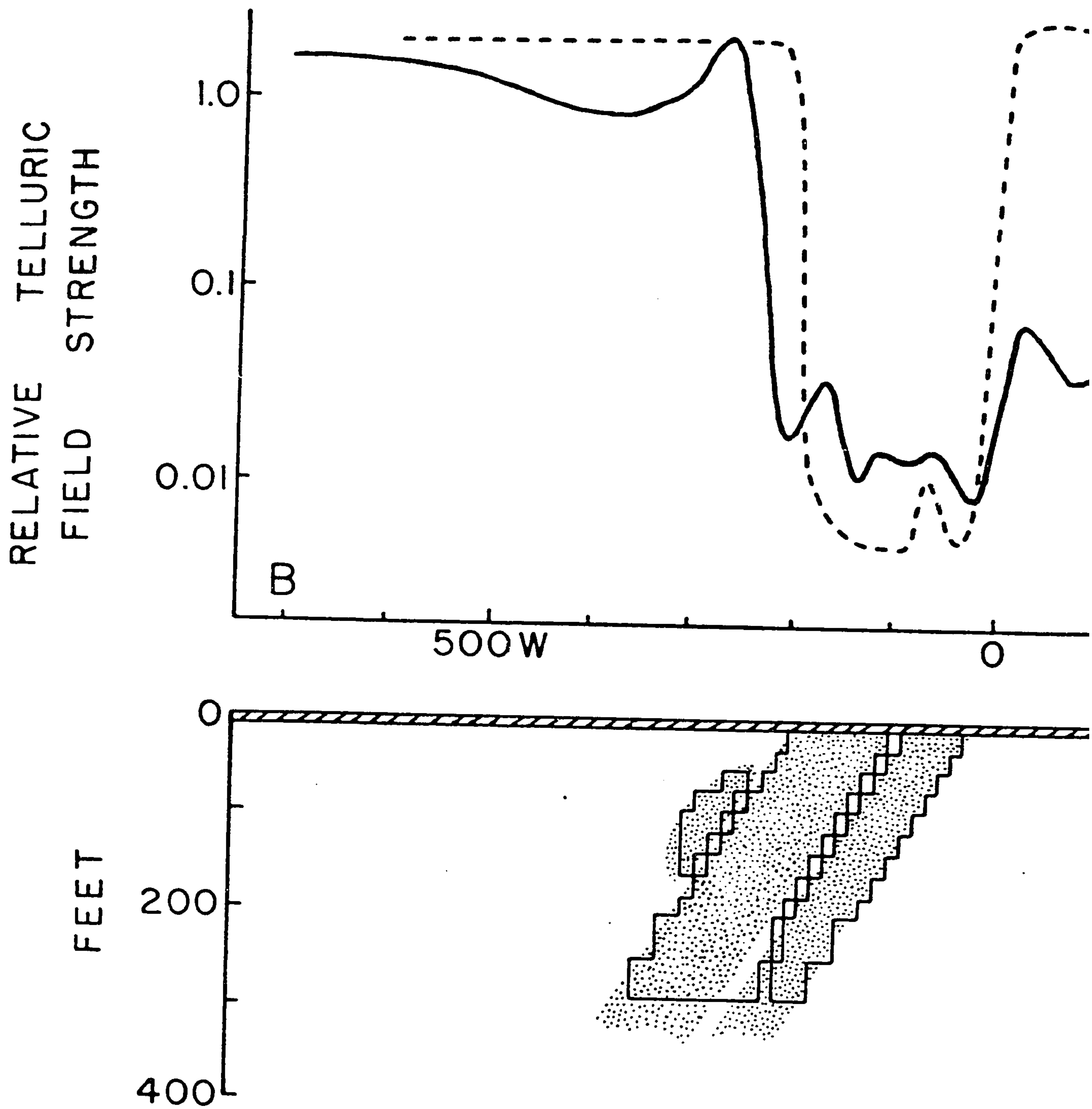

Fig. 4.10 Test Site 1, Line B-B'. Observed and theor

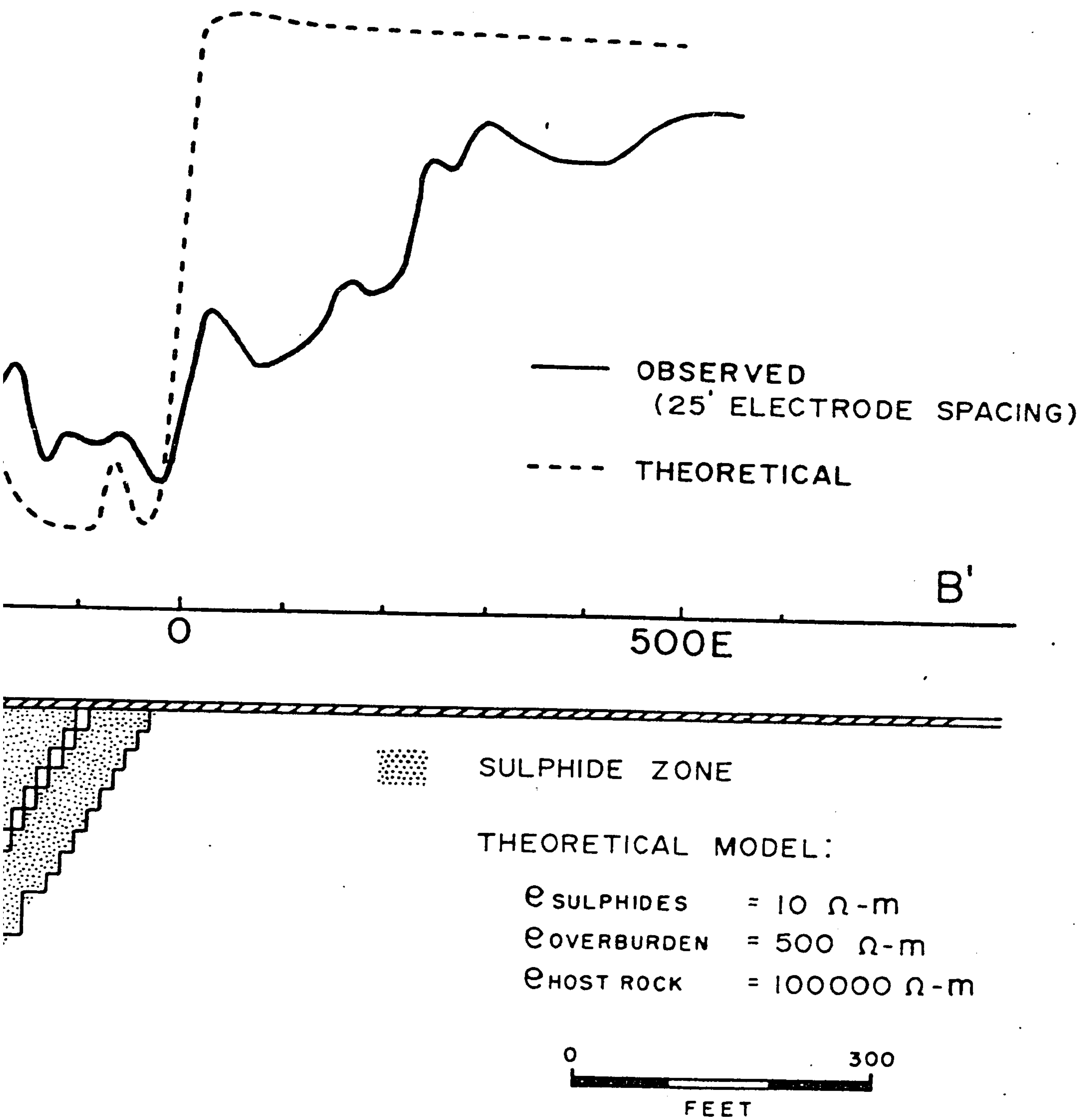

served and theoretical telluric profiles ($E_\perp$ polarization).

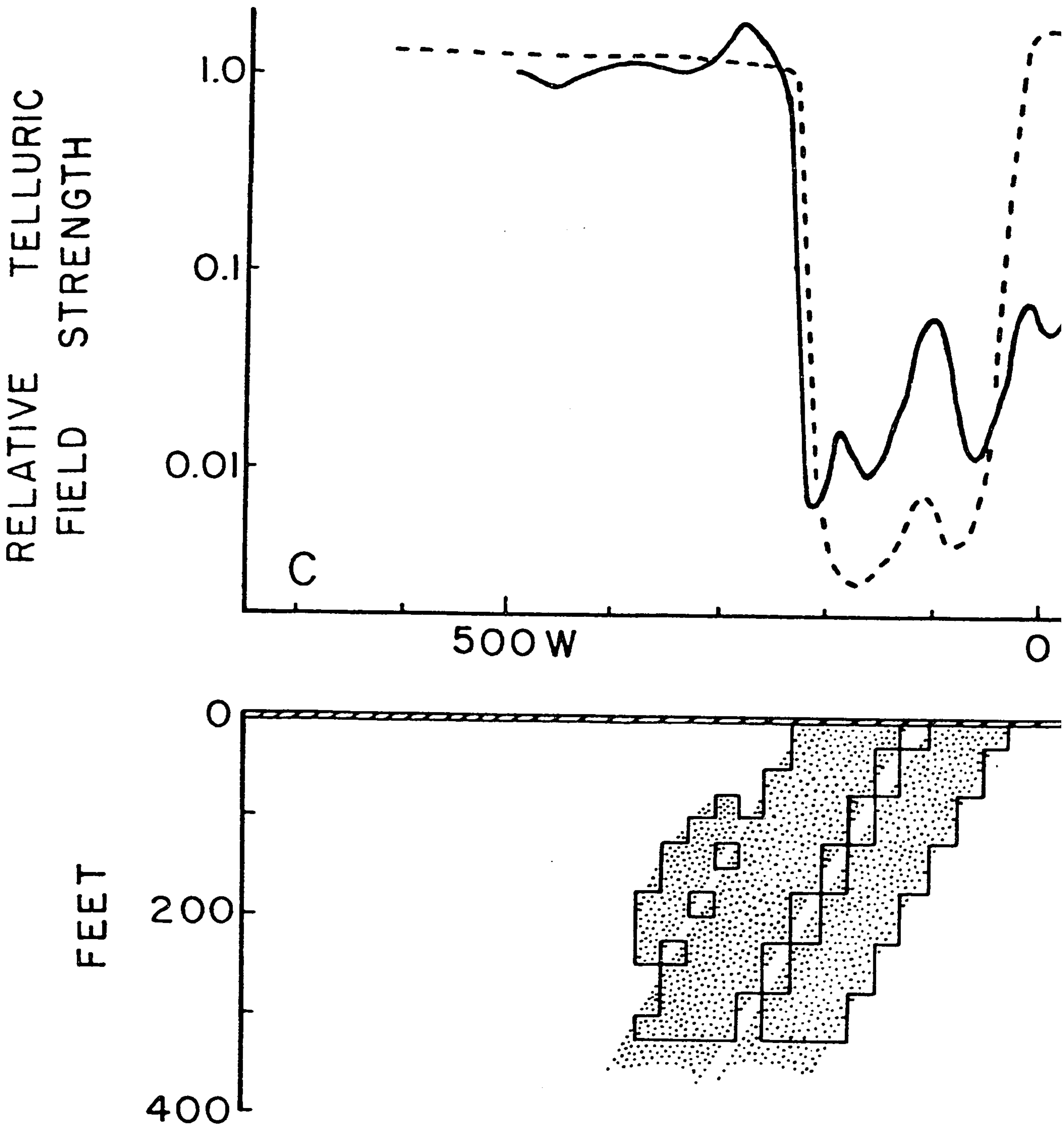

Fig. 4.11 Test Site 1, Line C-C'. Observed and the

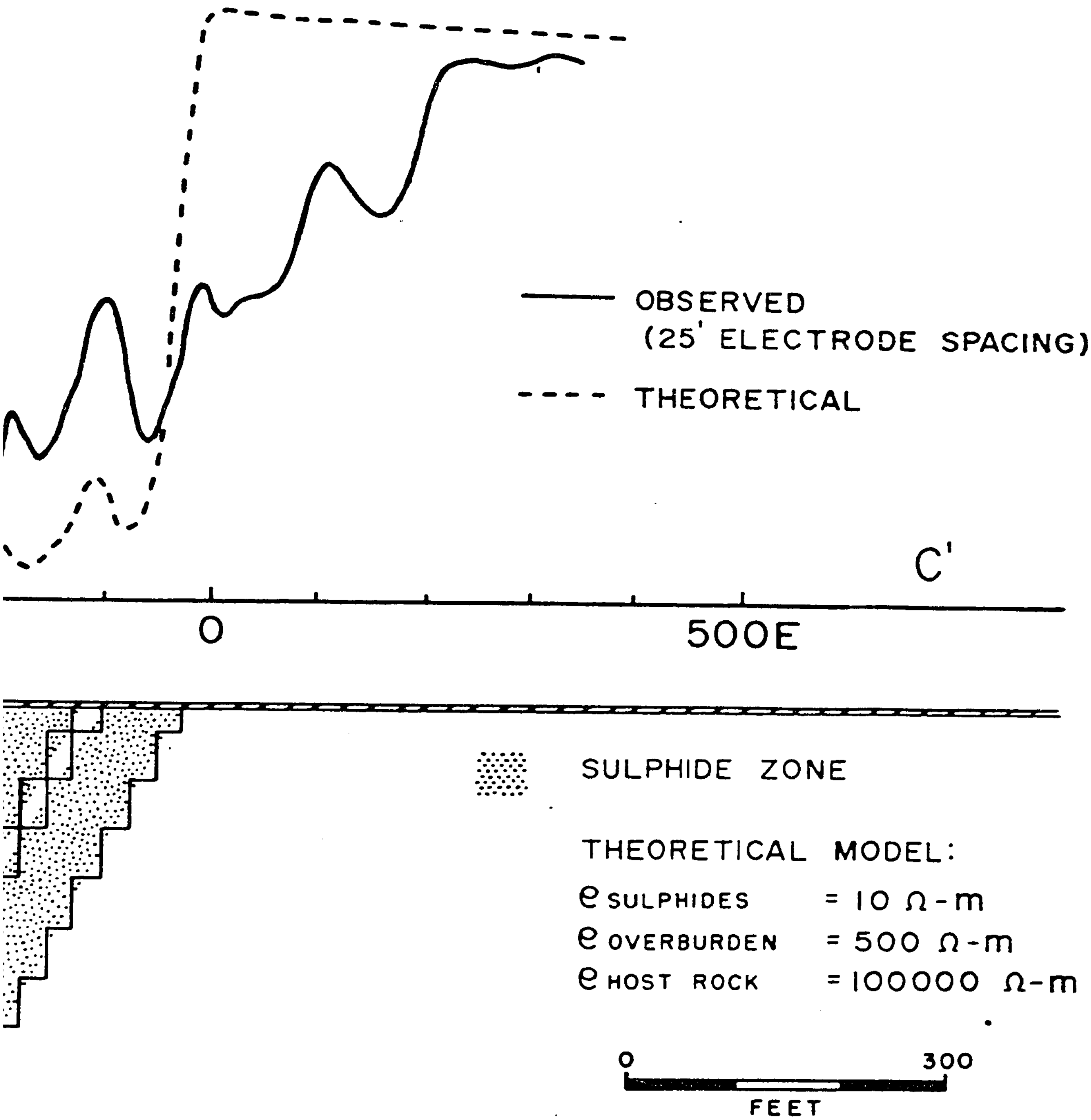

erved and theoretical telluric profiles ($E_\perp$ polarization).

4.2 Test Area 2

This survey consisted of magnetotelluric determinations of apparent resistivity every 3-5 miles along Highway 58 from Senneterre to Chapais with a total of 45 stations located along 170 miles of highway. Initially the apparent resistivity was measured in one arbitrary direction but later, when it became evident that the resistivity is anisotropic, measurements were taken in two orthogonal directions and the vertical magnetic field was also measured. At a few stations the apparent resistivity was measured in 30° increments through 180°.

The observations may be summarized as follows:

1. There is little change in the amplitude of the horizontal magnetic field from location to location.
2. The amplitude of the horizontal magnetic field does not vary appreciably with direction. The highly anisotropic apparent resistivity is caused by directional variations in the telluric field intensity.
3. The correlation and phase relationship between space orthogonal telluric and magnetic fields is variable and exhibits no clear pattern except that the correlation appears to be poorest when the telluric field is small.
4. The vertical magnetic field is small except in a few instances where its amplitude approaches that of the horizontal field. In these cases the apparent resistivity was often highly anisotropic.

It was concluded that random magnetotelluric measurements are of little use in areas of complex Precambrian geology as the measured apparent resistivities cannot be related to the underlying rocks. In some cases the resistivity anisotropy appears to reflect a nearby feature shown on geologic maps or suggested by aeromagnetic surveys but, again, the results cannot be interpreted. The problems encountered are similar to those illustrated by the directional telluric measurements at Test Site 1 (Fig. 4.4) where the direction of minimum telluric field strength appears to be related to the geology in some cases but not in others.

The only positive results were obtained when one magnetotelluric station was fortuitously located directly over a conductive zone. The telluric survey that followed outlined a wide, highly conductive body. Information supplied by the Quebec Department of Natural Resources shows that the anomaly is caused by a known pyrite zone. However, it should be pointed out that, had the magnetotelluric station been located 500 feet either way, the zone would not have been detected.

4.3 Test Site 3

These field surveys were carried out over a series of steeply dipping massive sulphide zones. Only the main zones are outlined by diamond drilling: many drill holes show additional narrow sulphide intersections but the information available is not sufficient to delineate them. The total sulphide content averages 50-60% for most zones. There are high tension power lines and shallowly buried water pipes along the base line. Figures 4.12 and 4.13 show a plan of the geology and summarize the field results over the northern and southern parts of the test area.

The telluric and magnetotelluric profiles show intense and similar anomalies over the sulphide zones (Fig. 4.12). The telluric field decreases by more than a factor of 30 and the minimum apparent resistivity is less than 300 ohm-meters compared to a background value of 10000 to 20000 ohm-meters. On both traverses the telluric signals on opposite sides of the series of mineralized zones were in phase and showed some correlation. Over the zones, no correlation and highly variable phase were observed between 200W and 400W on line 1200N and between 100W and 300W on line 1500N. The direction of minimum telluric field is indicative of the approximate strike of the mineralization.

The power lines did not affect the telluric surveys when the field was measured normal to them. However, close to the lines, the parallel telluric field was very large and its appearance did not resemble that of the usual 8 Hz signal.

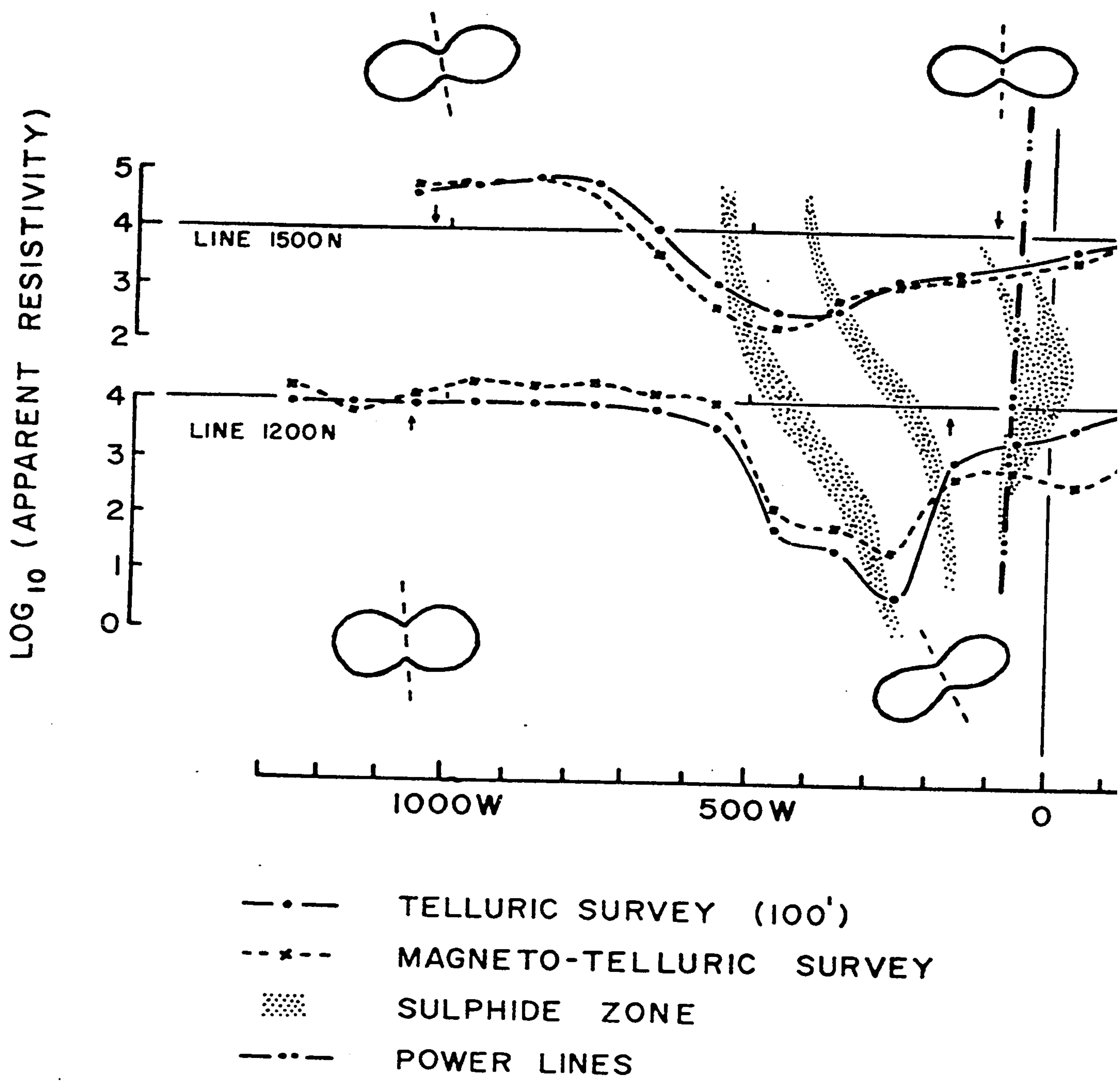

Fig. 4.12 Test Site 3. Telluric and magnetotelluric test site ($E_{\perp}$ polarization).

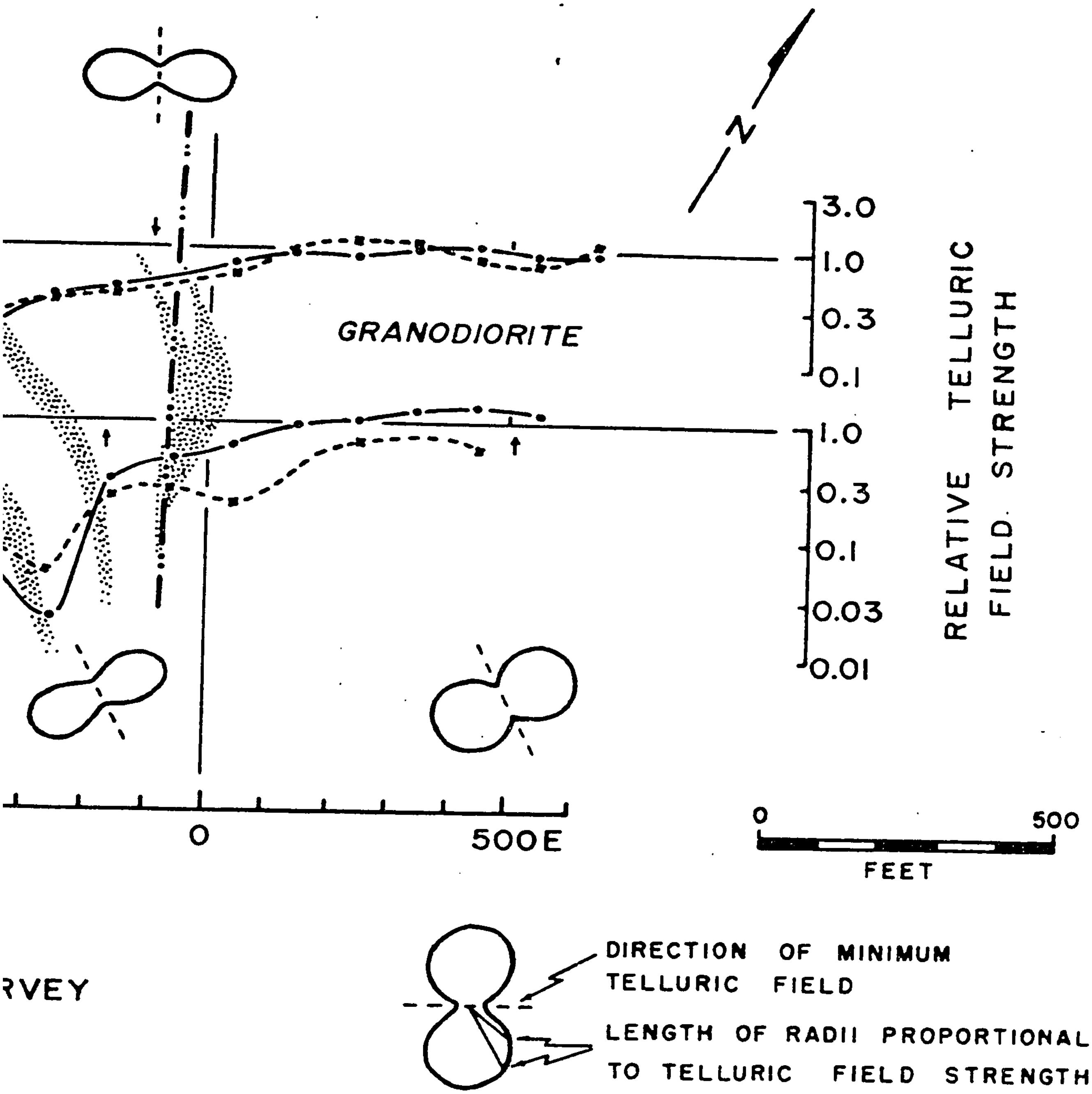

nagnetotelluric survey results over northern part of the
polarization).

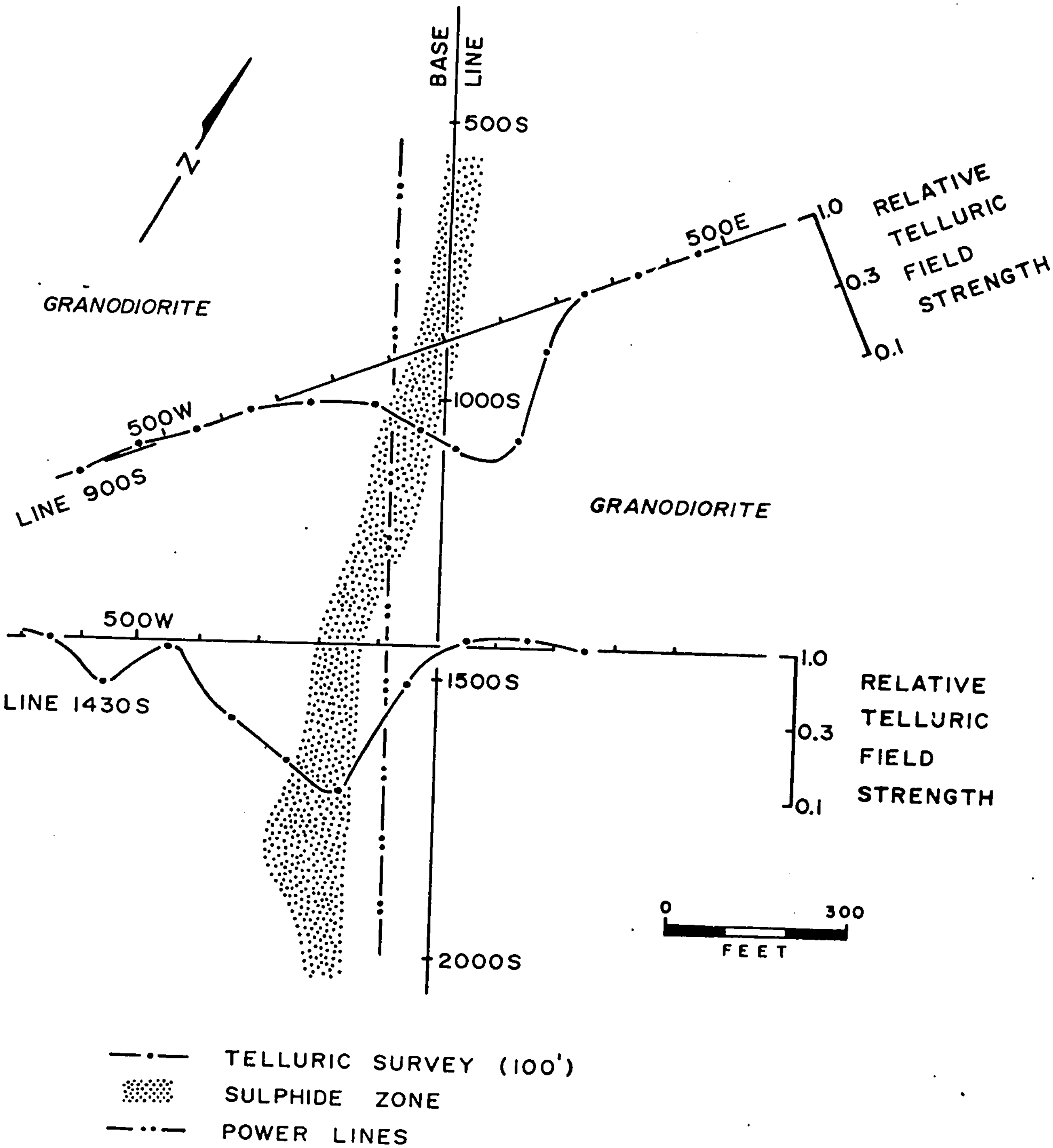

Fig. 4.13 Test Site 3. Results of telluric surveys in southern part of the test site ($E_\perp$ polarization).

The theoretical telluric field strength profile for line 1200N shows some similarity to the observed (Fig. 4.14). The greater width of the observed anomaly probably results from the fact that the traverse crosses two of the sulphide zones at an oblique angle. In order to obtain an anomaly of approximately the same intensity as the observed, the theoretical model assumes that two of the zones are electrically connected. As a consequence the theoretical results show that between 200W and 400W the electric field leads the magnetic by a phase angle of 160° compared to the background value of 45°. This means that, if the theoretical base station electrode spread were located between 900W and 1000W and the field spread between 300W and 400W, the telluric signals would differ in phase by 115°. Furthermore, as the theoretical phase changes gradually over a distance, the signal detected between the field electrodes will be distorted by destructive and/or constructive interference. This would explain the loss of correlation that accompanies phase changes on the field records.

On line 900S the agreement between the theoretical and observed profiles is poor. Unfortunately only one drill hole exists in the area of this traverse so that the geologic section presented may be incomplete. The field results suggest the presence of a much wider conductive zone than outlined by the drilling or, as on line 1200N, the observed anomaly may be affected by the fact that the field was not measured normal to the strike.

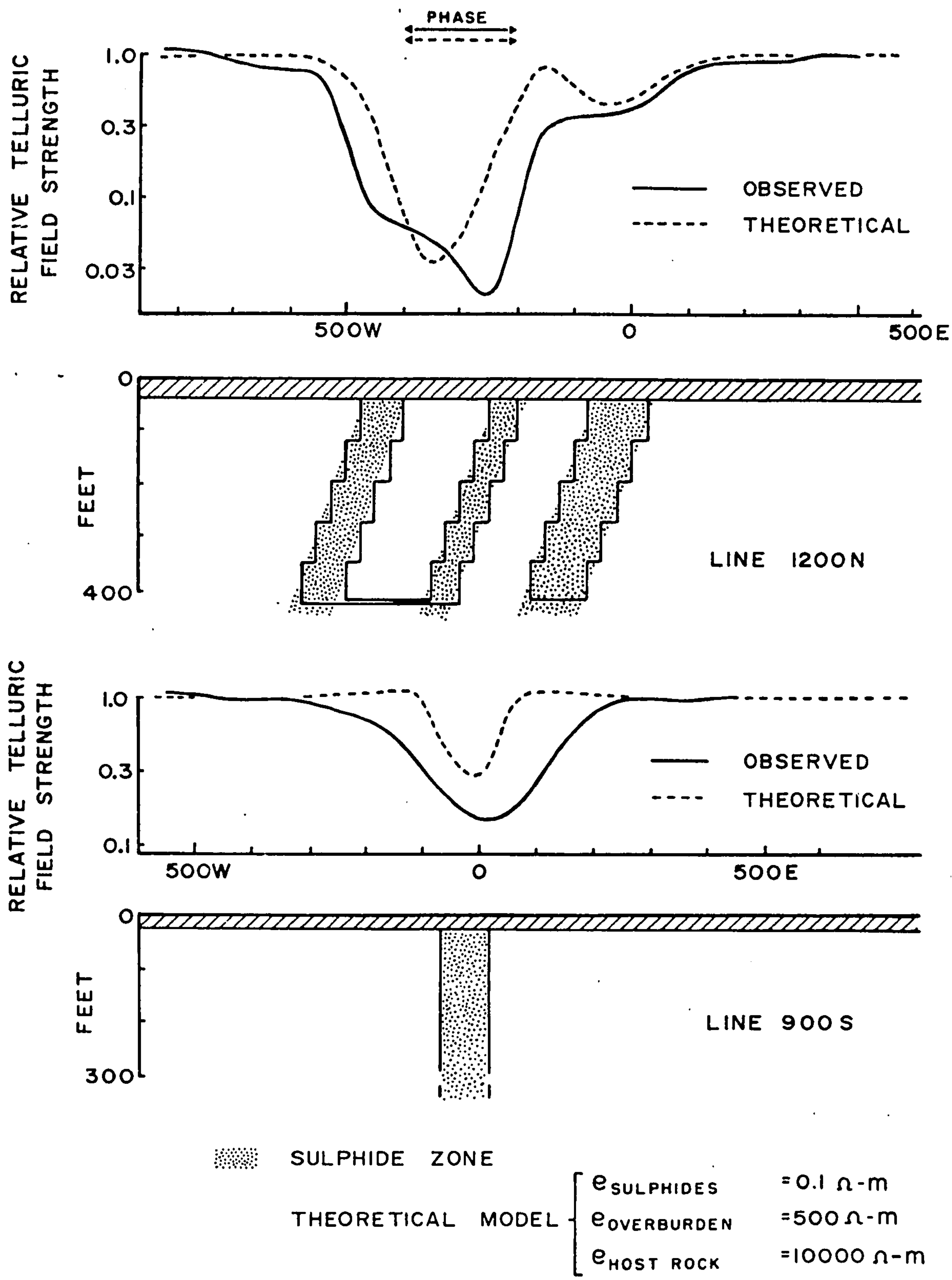

Fig. 4.14 Test Site 3. Observed and theoretical telluric profiles ($E_{\perp}$ polarization).

4.4 Test Site 4

The mineralization at this test site consists of a body of massive sulphides located at the contact between rhyolite and basic volcanic rocks (Fig. 4.15). There are farm buildings in the immediate area and both power and telephone lines cross the zone. Sporadic man-made noise was observed on the telluric records and in some instances obscured the natural 8 Hz signals.

The field results obtained were disappointing in view of the weak anomaly over the sulphides compared to those at Test Sites 1 and 3. Also, although the change in the telluric field strength between 300N and 700N appeared to reflect different resistivities in the rhyolite and the basic volcanics, the location of the indicated contact was 500 feet from its actual position.

The theoretical results (Fig. 4.16) seem to explain some of the field observations. In this case the resistivities of the host rocks and the overburden used in the theoretical model are based on measured values (Seigel et al., 1957). The change in the telluric field strength north of the sulphide zone appears to be caused by a change in the overburden thickness from 30 feet over the sulphide zone to 90 feet at 1000N.

This is an indication that, although uniformly thick conductive overburden does not greatly affect results (Fig. 2.12), major variations in its thickness can produce anomalies similar to those caused by lateral resistivity changes. The theoretical results also suggest

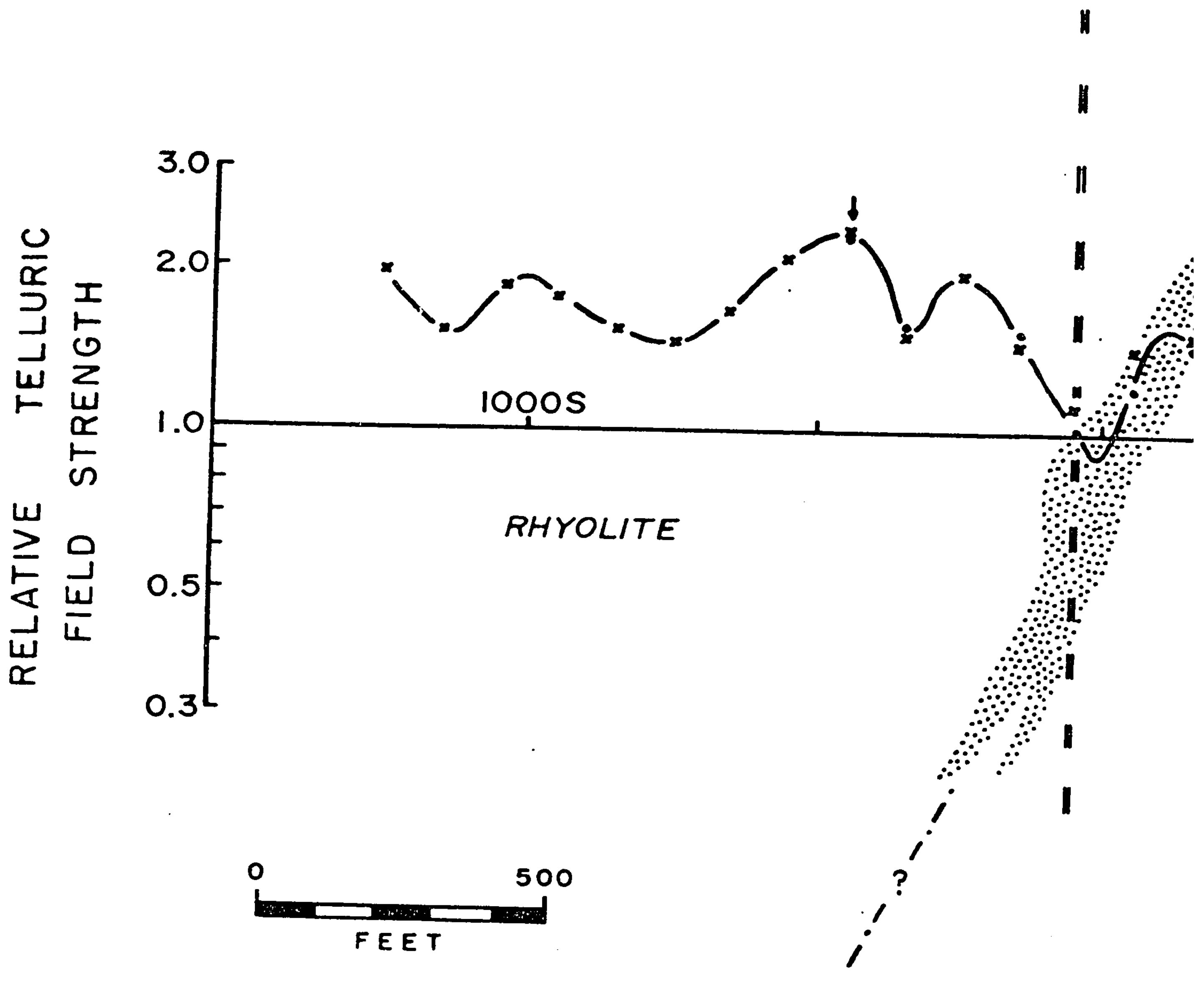

Fig. 4.15 Test Site 4. Plan of sulphide zone and result

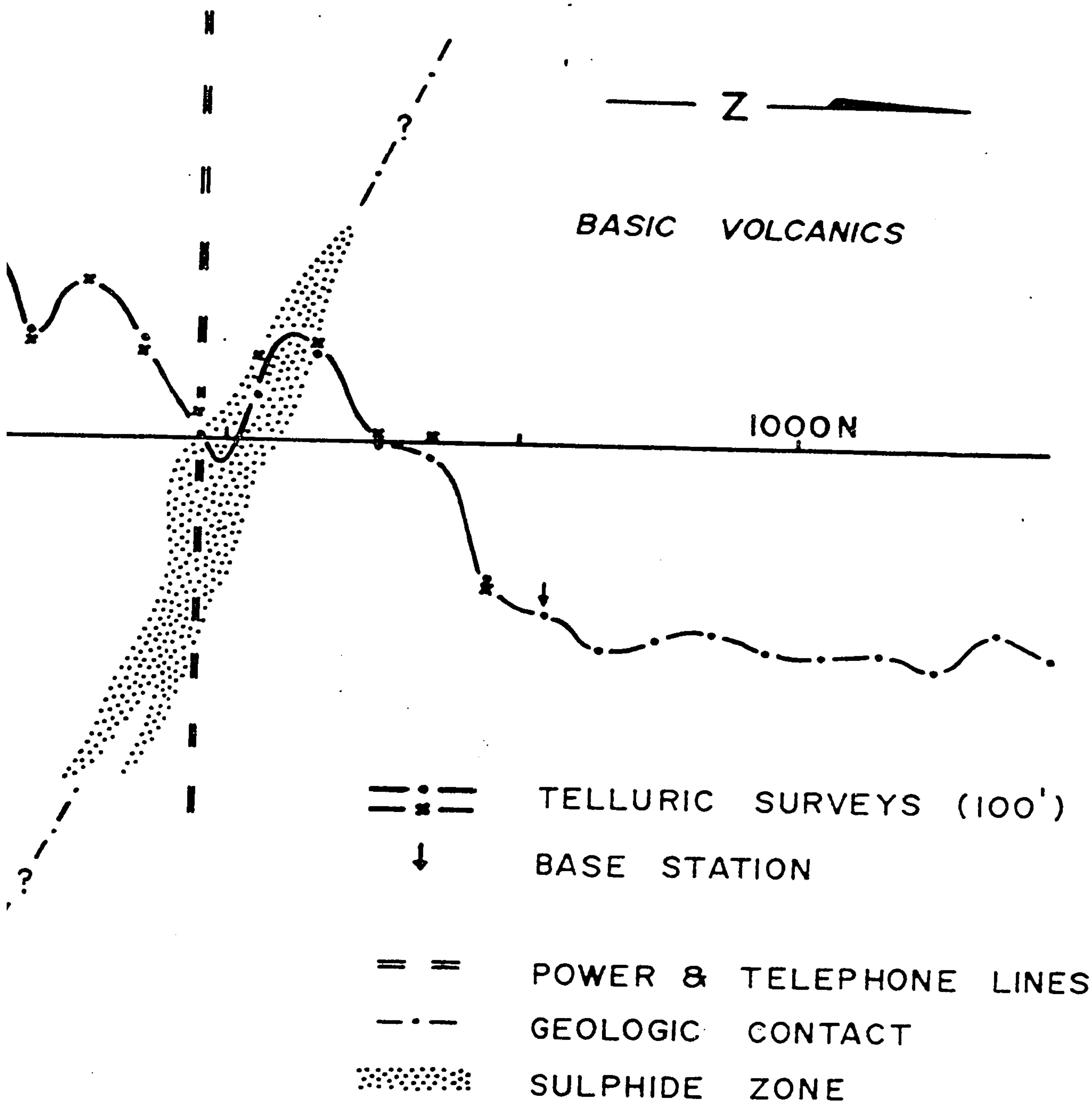

e zone and results of telluric traverse ($E_\perp$ polarization).

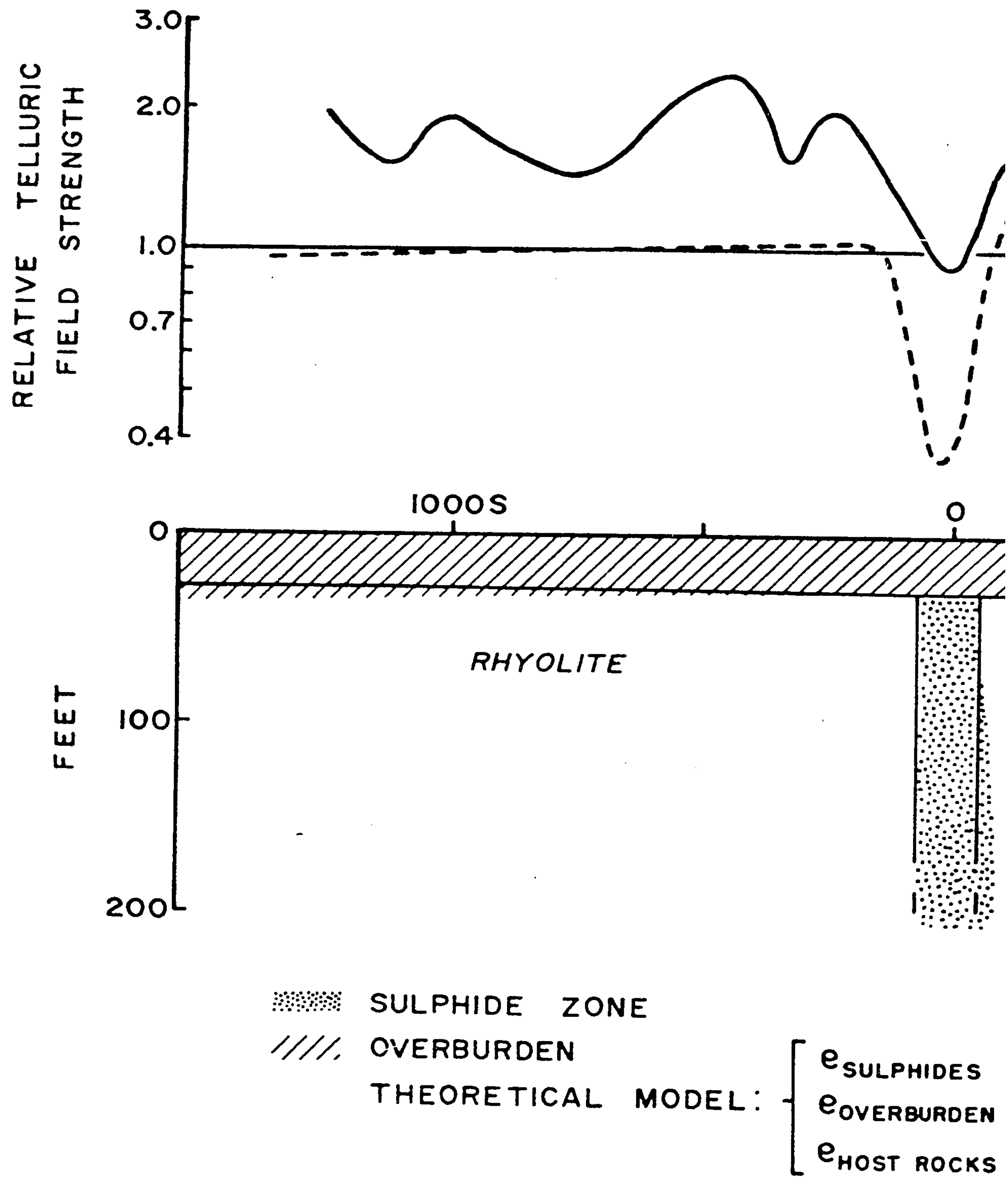

Fig. 4.16 Test Site 4. Observed and theoretical

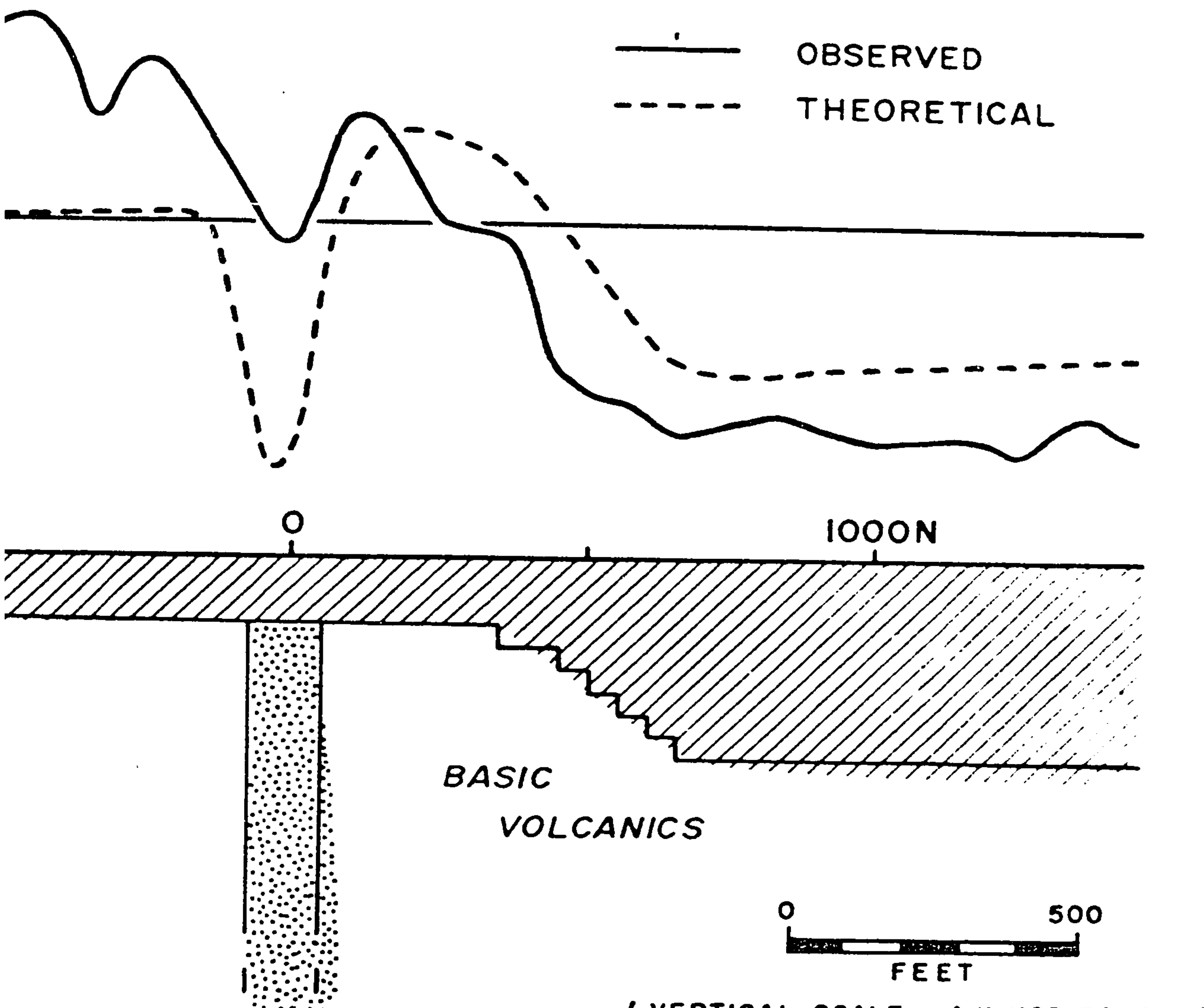

EL: $\rho_{SULPHIDES} = 1\ \Omega\text{-m}$
$\rho_{OVERBURDEN} = 70\ \Omega\text{-m}$
$\rho_{HOST\ ROCKS} = 7000\ \Omega\text{-m}$

d and theoretical telluric profiles ($E_{\perp}$ polarization).

that either the overburden depth decreases south of the sulphide zone or that the rhyolites may actually be somewhat more resistive than the basic rocks.

4.5 Test Site 5

The mineralization at this test site consists of several parallel sulphide lenses located in a shear zone near a contact between volcanic and sedimentary rocks (Fig. 4.17). The location of the sulphide zones is based on diamond drill data and that of the electromagnetic conductors on a horizontal loop survey. The sulphide content ranges from massive to disseminated and there is considerable mineralization between the main zones.

Both the 100 and 25 foot telluric surveys show an anomaly over the known sulphide zones but only the 25 foot survey suggests that multiple conductors may be present. West of the mineralized zones the telluric field is relatively constant and there is no indication of the geologic contact. To the east the variations in the field strength suggest the presence of additional conductive zones.

The telluric signals on opposite sides of the sulphide zones were in phase and correlated fairly well (Fig. 3.9(c), p.56). Over the zones, the phase relationship was variable and little correlation was observed (Fig. 3.9(b)).

The results of horizontal loop surveys (Fig. 4.18) clearly show the presence of the massive sulphide zone but give little indication of the disseminated zones which contain 5-35% sulphides.

Figure 4.19 shows telluric field strength profiles for the $E_{\parallel}$ polarization. The presence of the conductive zones is indicated, but the anomalies are not as definitive as in the $E_{\perp}$ surveys.

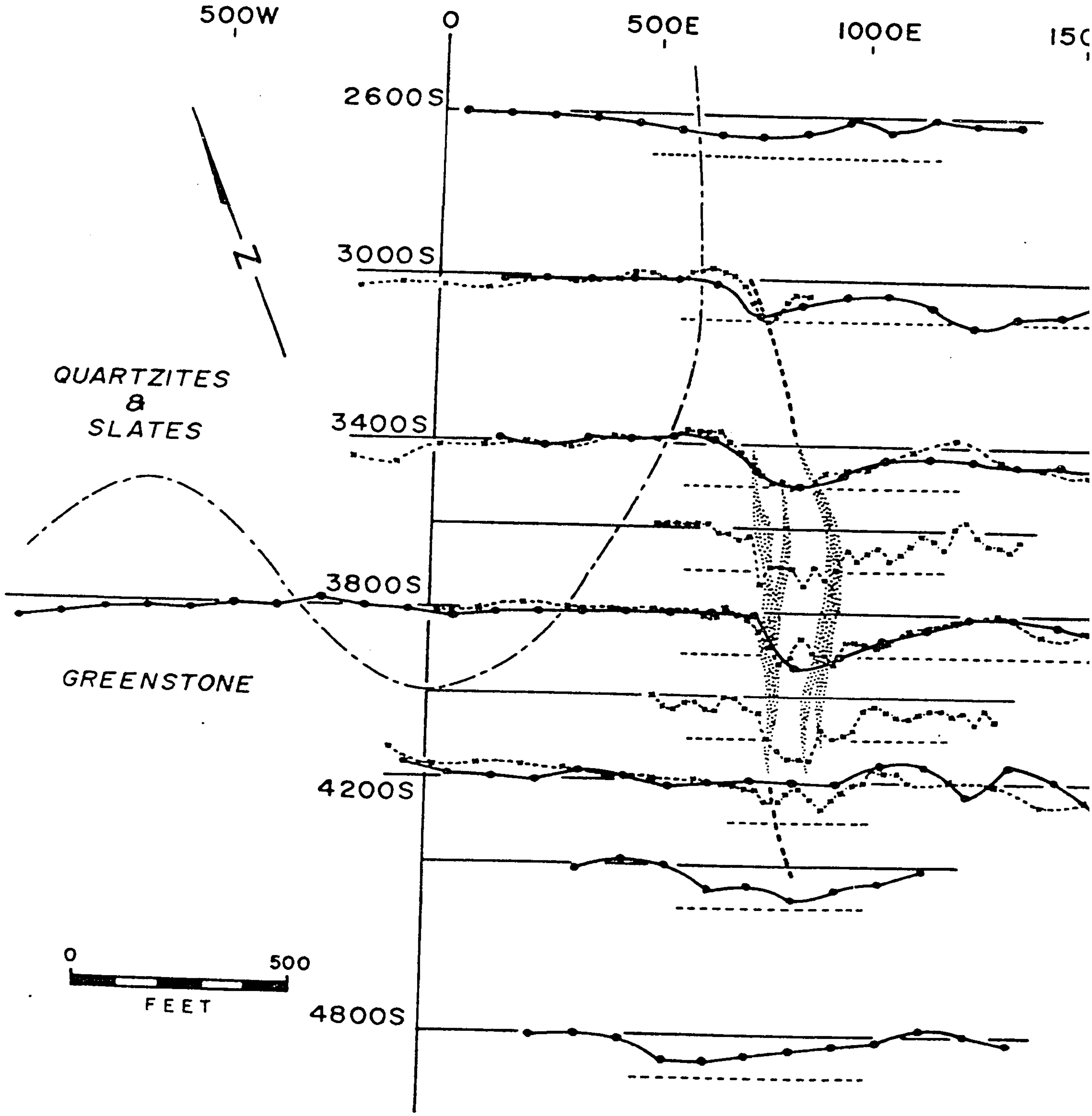

Fig. 4.17 Test Site 5. Results of telluric su

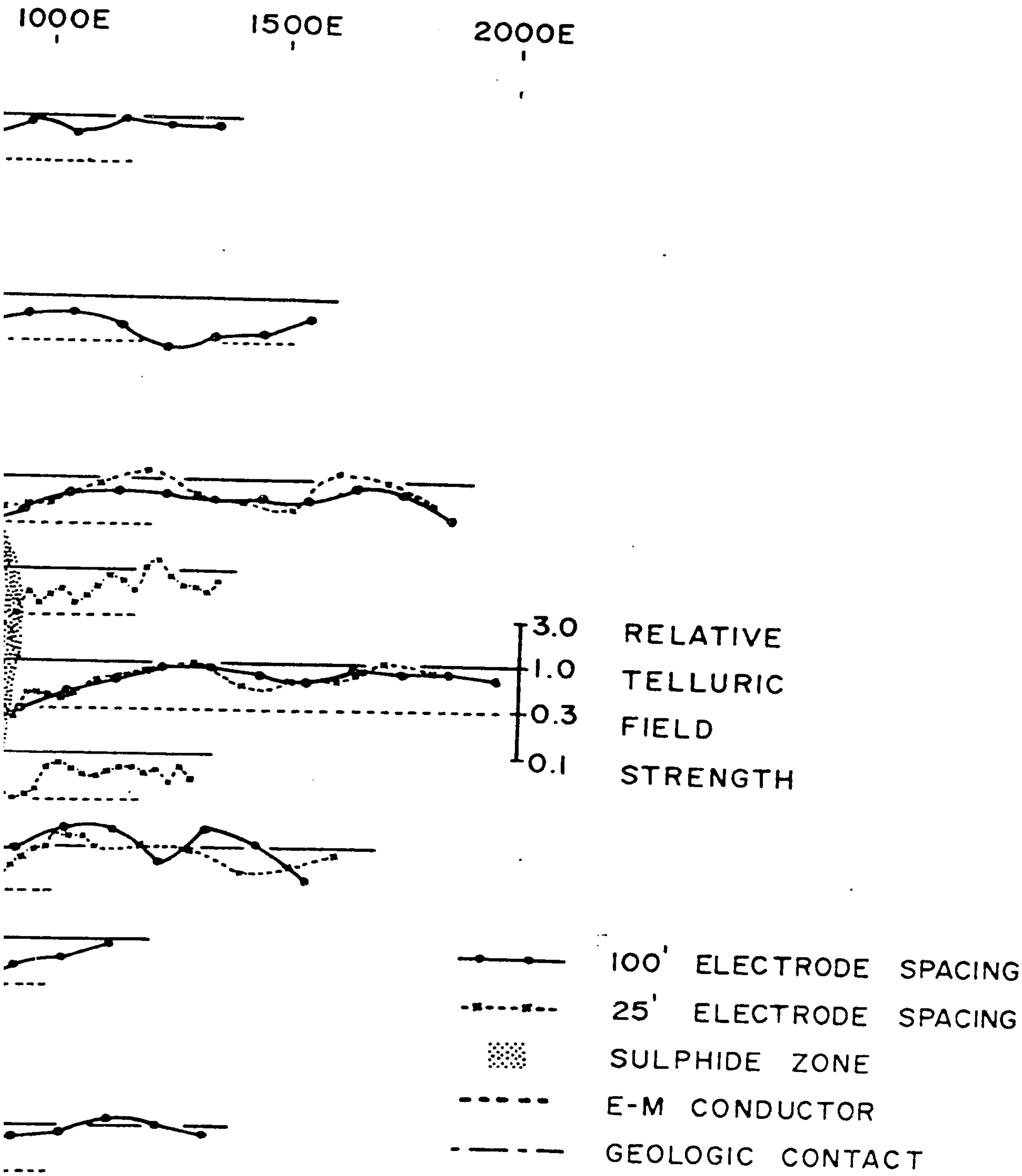

of telluric surveys ($E_\perp$ polarization).

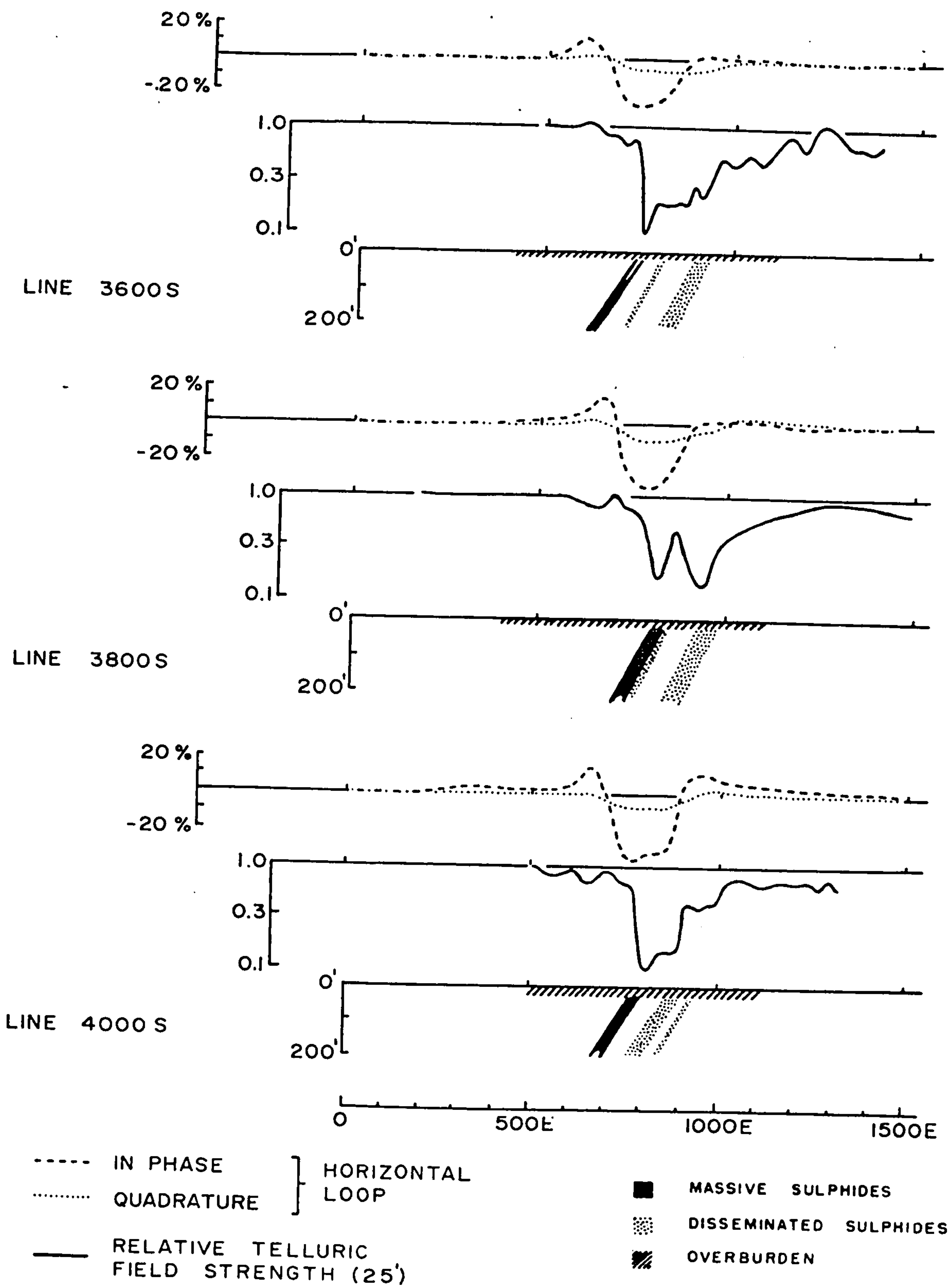

Fig. 4.18 Test Site 5. Comparison of horizontal loop and telluric ($E_{\perp}$) survey results.

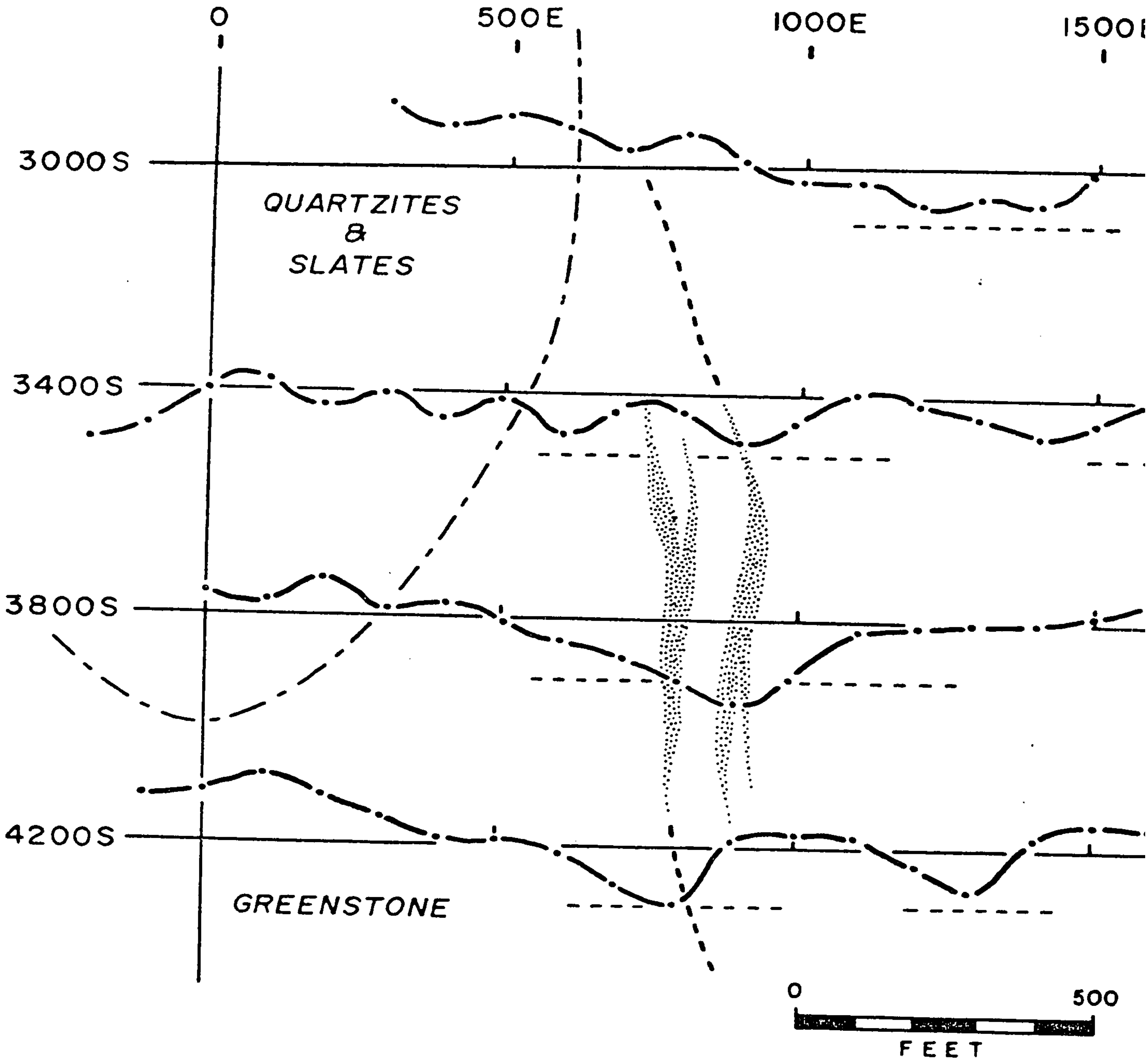

Fig. 4.19 Test Site 5. Results of telluric s

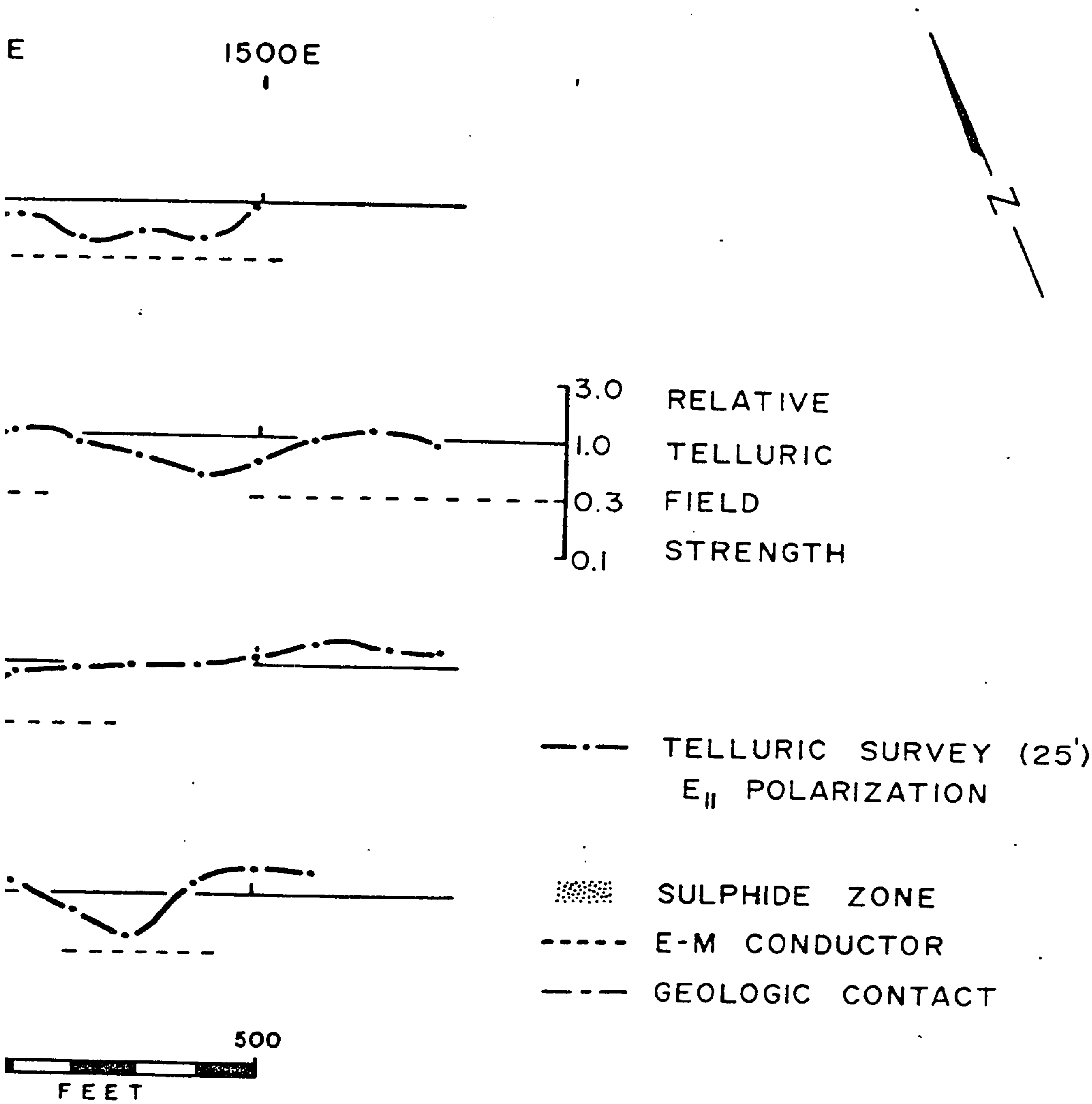

lts of telluric surveys ($E_{\parallel}$ polarization).

The intensity of the background $E_{\parallel}$ field is about 0.25 of the background $E_{\perp}$ field.

Figures 4.20, 4.21 and 4.22 compare theoretical and observed telluric profiles along three lines where the geology is relatively well known. On line 3800S the drill holes do not reach the sulphide zones between 925E and 980E: their location is based on drill results on lines 3600S and 4000S.

The theoretical and observed results are comparable both in the intensity of the anomalies and in the areas where phase shifs occur. The theoretical results show the limits where the phase differs by more than 10° from the background value. The maximum theoretical phase difference between the background telluric field and that over the conductive zones ranges from 70° on line 4000S to 130° on line 3800S.

The theoretical results for the $E_{\parallel}$ polarization are similar to those obtained at Test Site 1 (Section 4.1). The apparent resistivity profiles show a low over the sulphide zones but the telluric field strength remains constant.

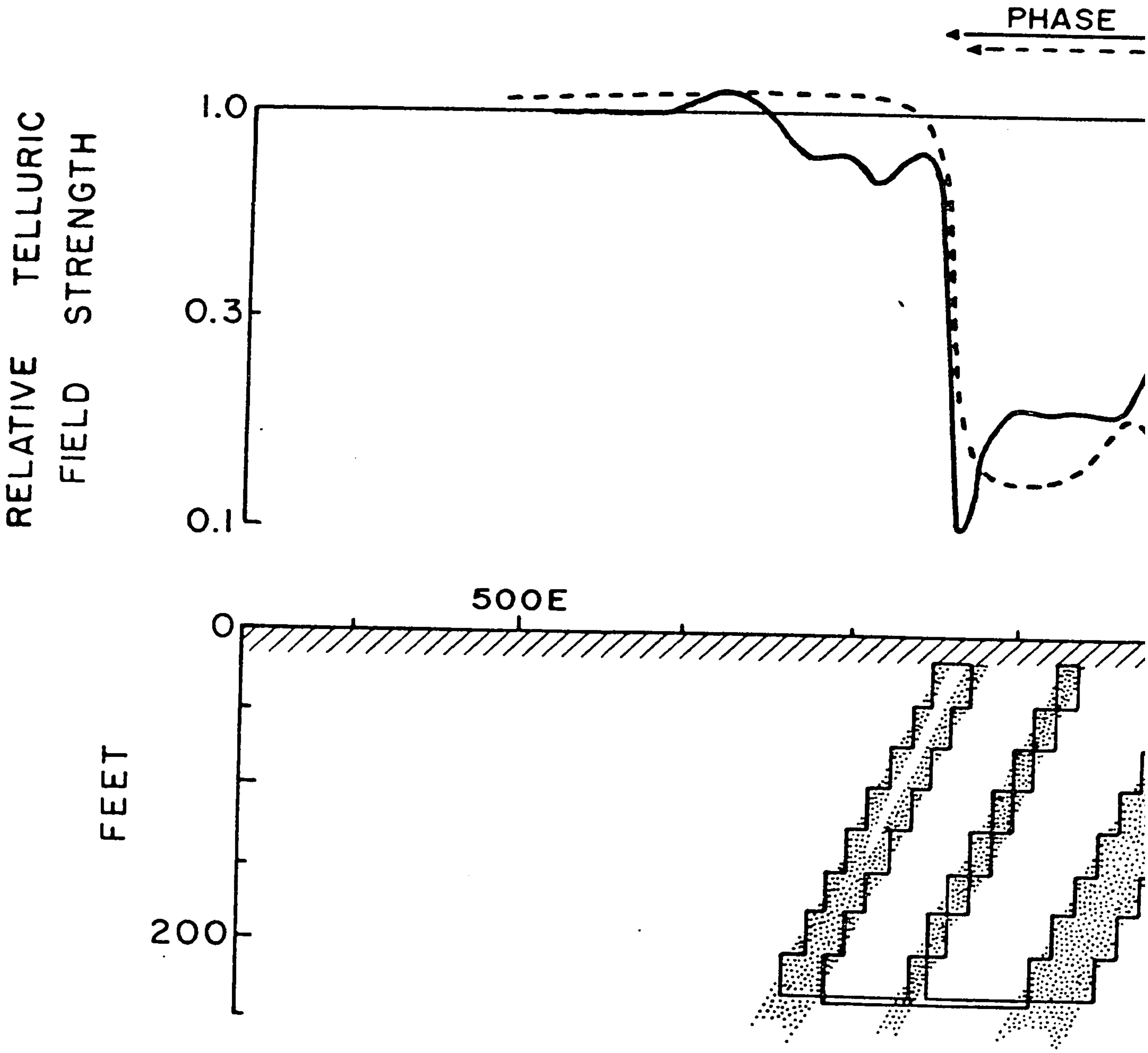

Fig. 4.20 Test Site 5, Line 3600S. Observed and theo

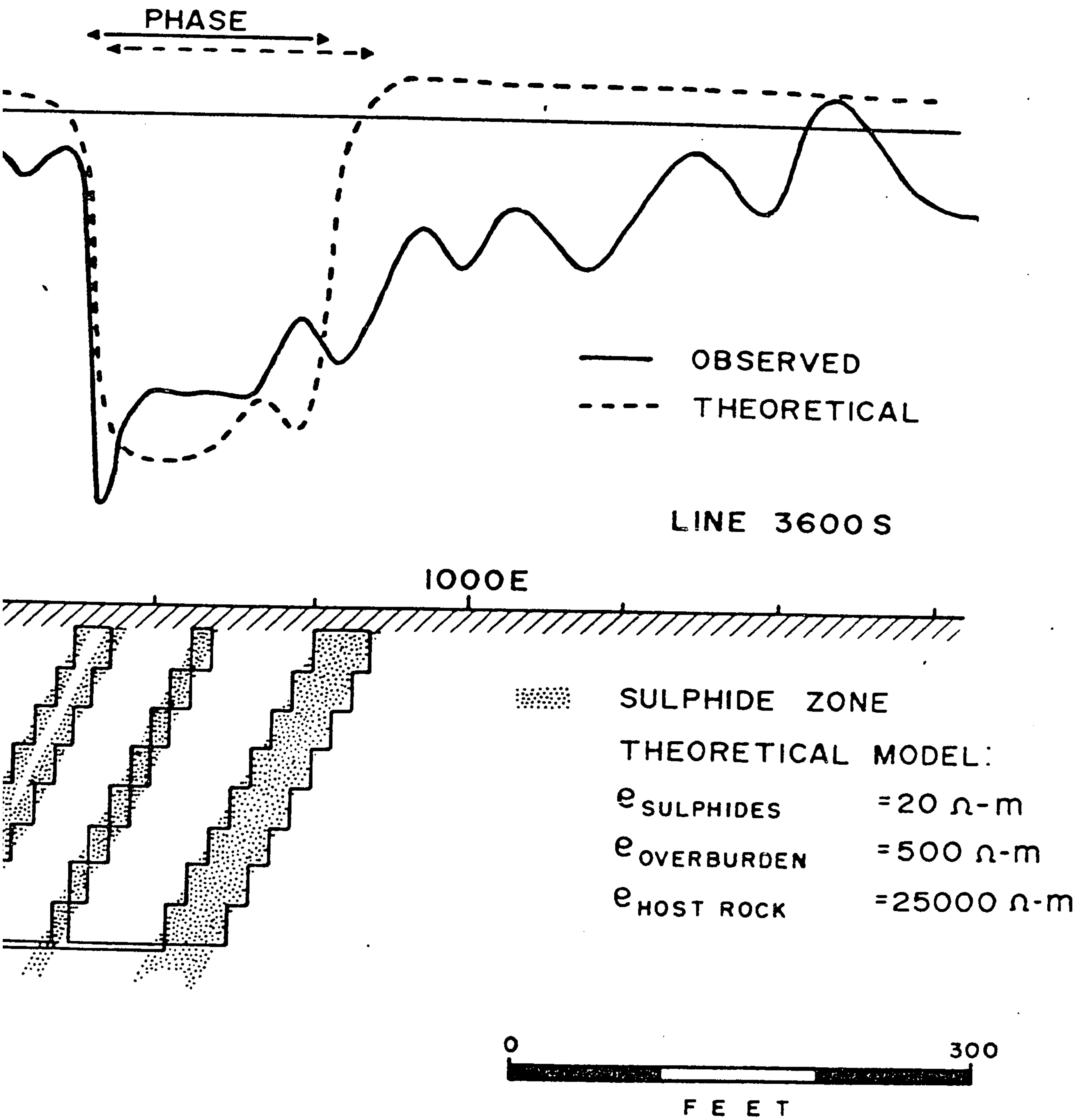

›served and theoretical telluric profiles ($E_{\perp}$ polarization).

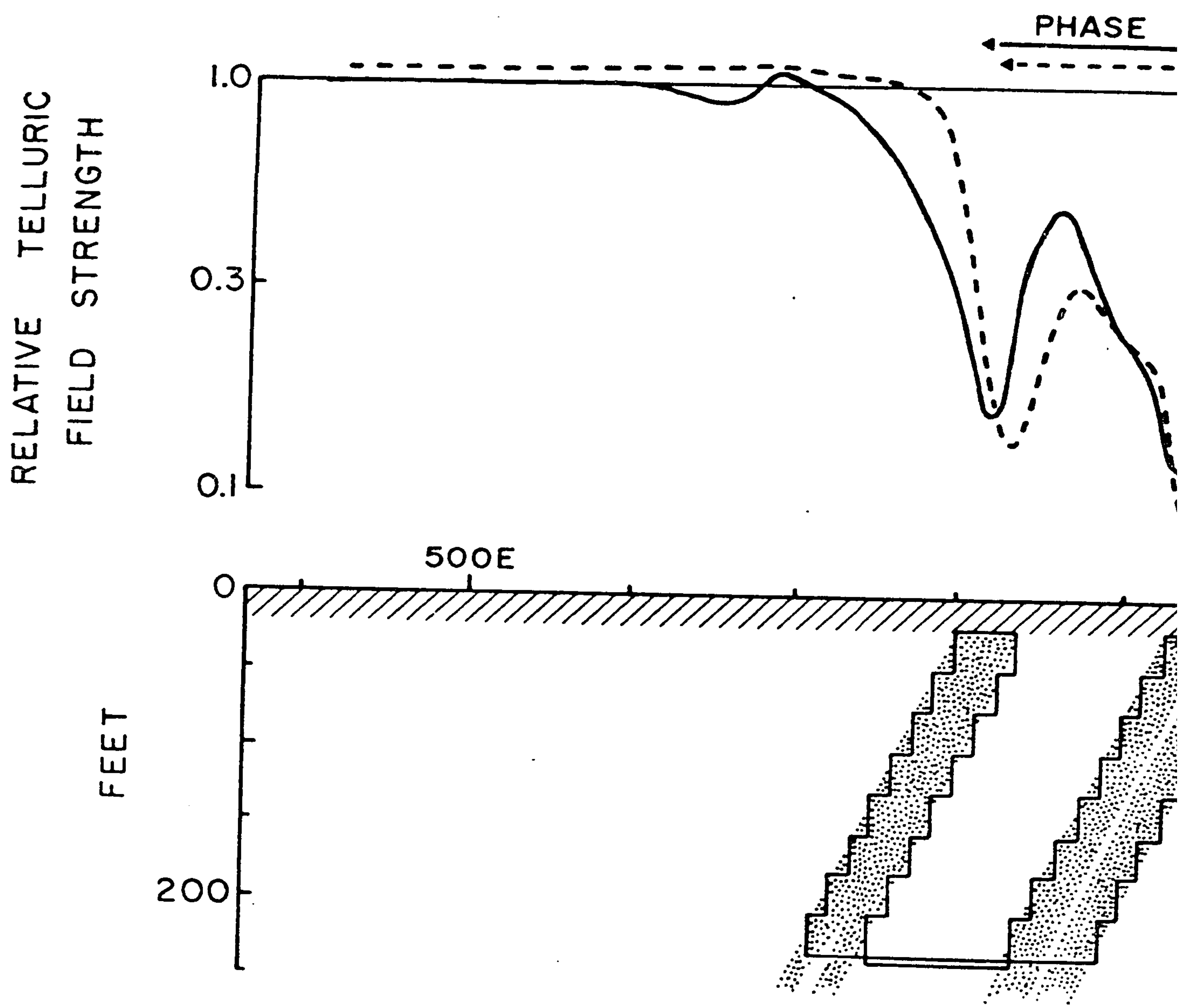

Fig. 4.21 Test Site 5, Line 3800S. Observed and theoretic

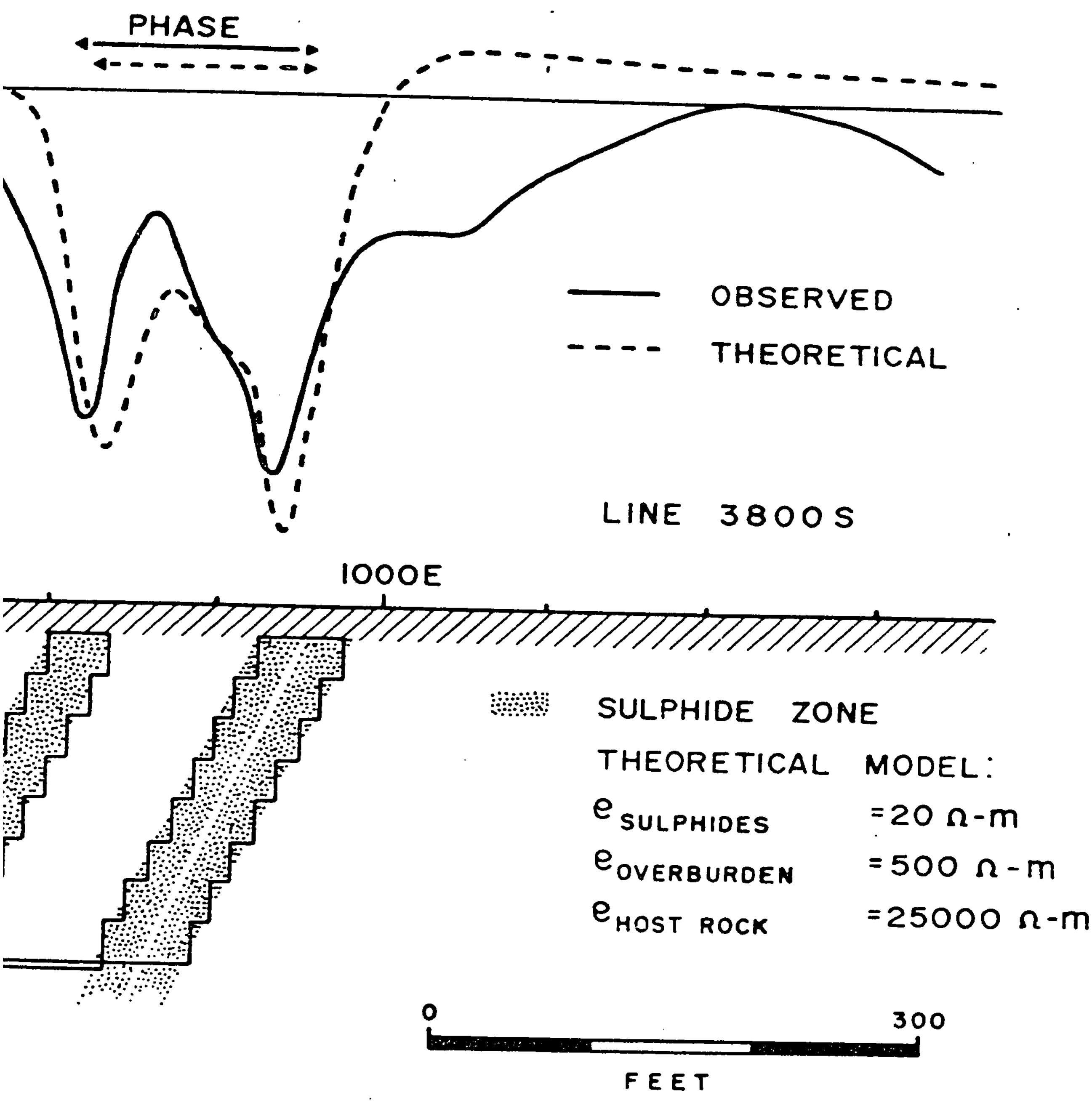

l and theoretical telluric profiles ($E_{\perp}$ polarization).

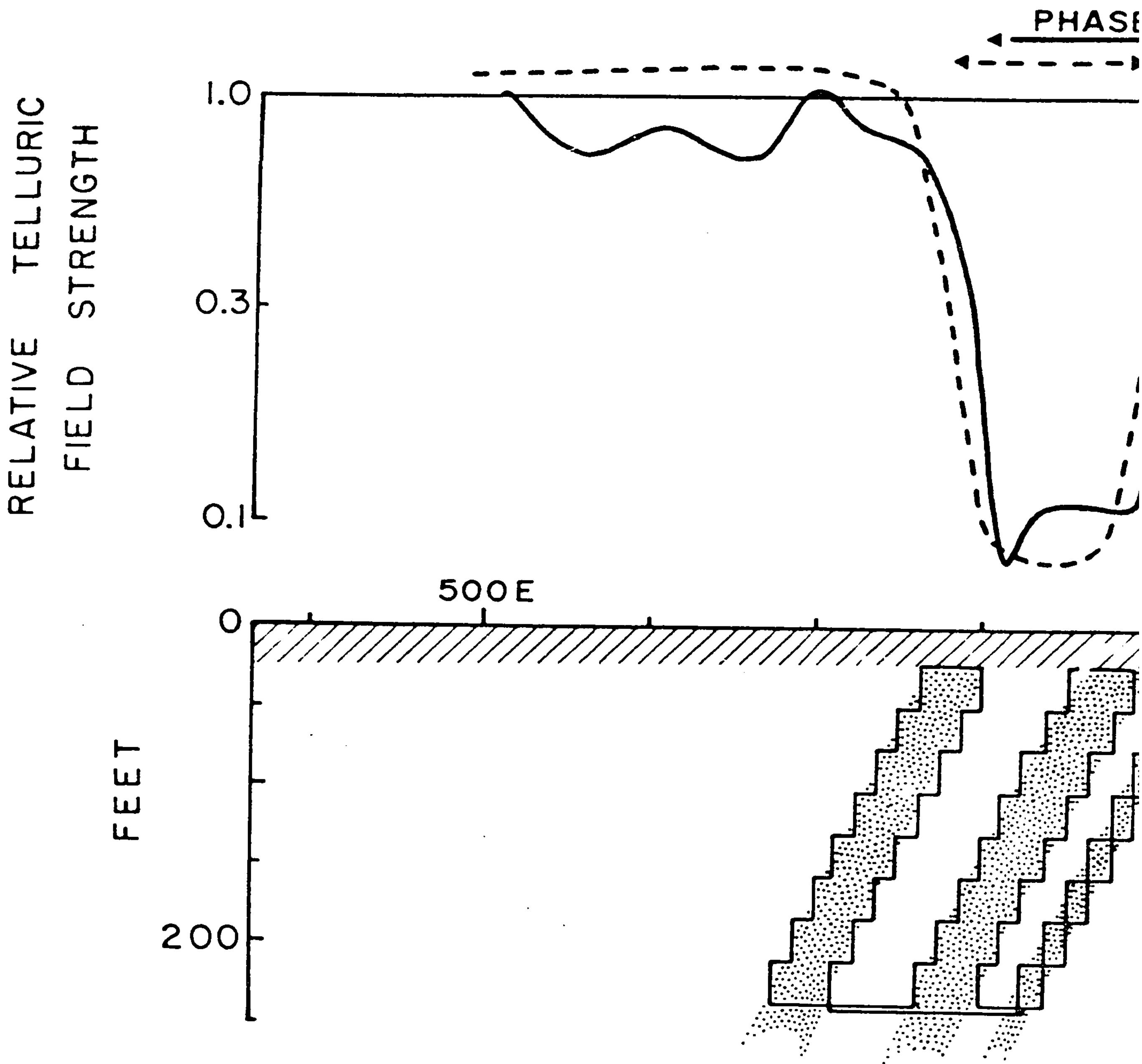

Fig. 4.22 Test Site 5, Line 4000S. Observed and theor

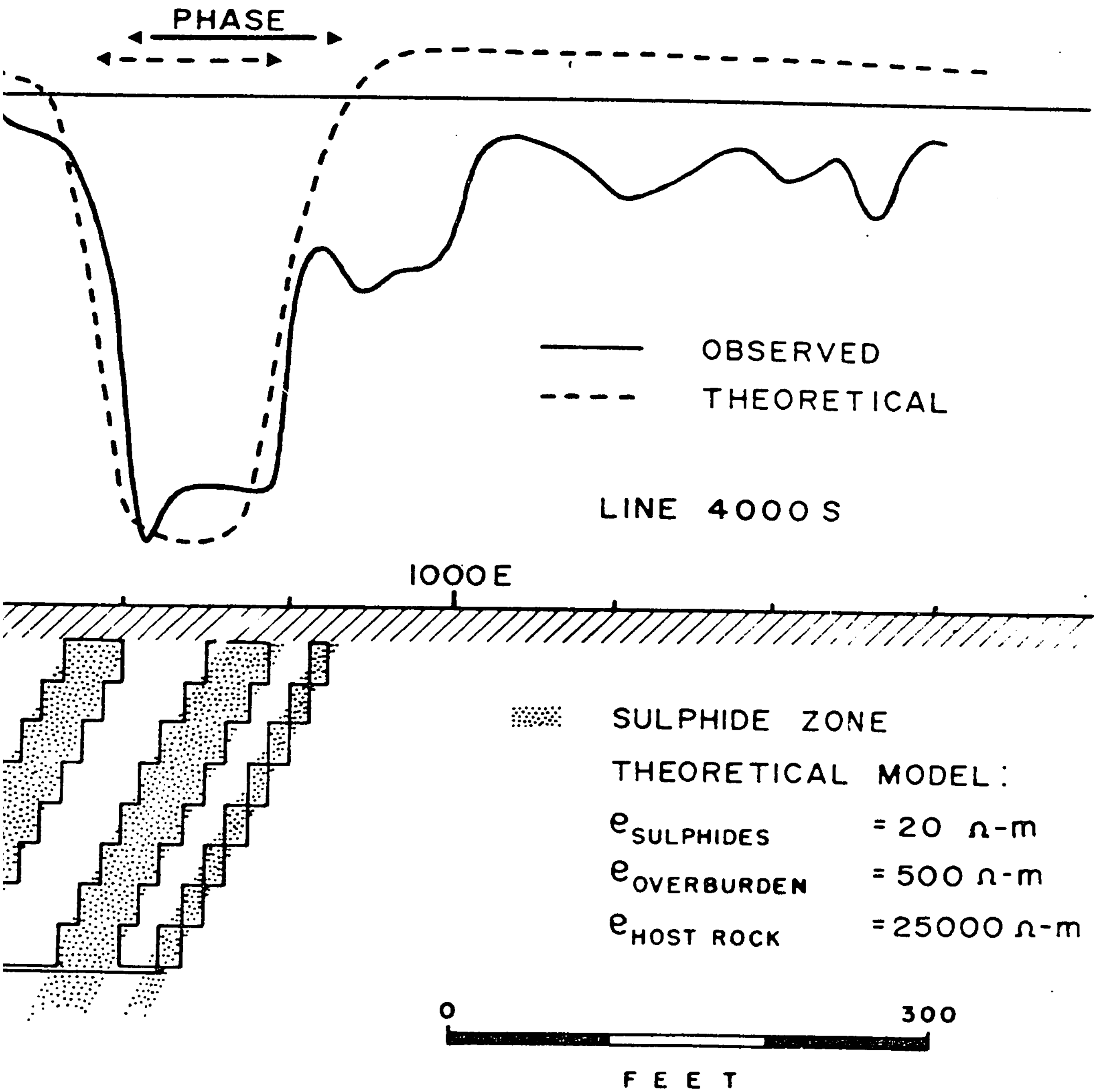

erved and theoretical telluric profiles ($E_{\perp}$ polarization).

4.6 Test Site 6

This site is located in Eardley Twp., Quebec, about 20 miles west of Ottawa. Several telluric and magnetotelluric surveys were carried out over a contact between Precambrian syenites and diorites and Paleozoic shales, sandstones, limestones and dolomites (Sabourin, 1954). Figure 4.23 shows the geology of the area and the location of the survey stations. Because the stations were not located along a straight line, the results have been projected on line X-X' perpendicular to the strike of the contact.

The initial survey measured the directional variations in apparent resistivity at 14 stations. In subsequent traverses, where the behaviour of specific magnetic and telluric field components was examined, intermediate stations were added. The survey results are summarized in Figures 4.24, 4.25 and 4.26 . The last figure also shows theoretical results for a very simple model of the geologic section.

The results from eight representative stations show that the apparent resistivity becomes progressively more anisotropic as the Precambrian-Paleozoic contact is approached from the north (Fig. 4.24) and the direction of minimum apparent resistivity closely approximates the direction of the strike of the contact. This suggests that the telluric field on the resistive side is polarized perpendicular to the strike of the contact a considerable distance away.

Figure 4.25 illustrates the equivalent results obtained from telluric and magnetotelluric measurements for the $E_\perp$ polarization.

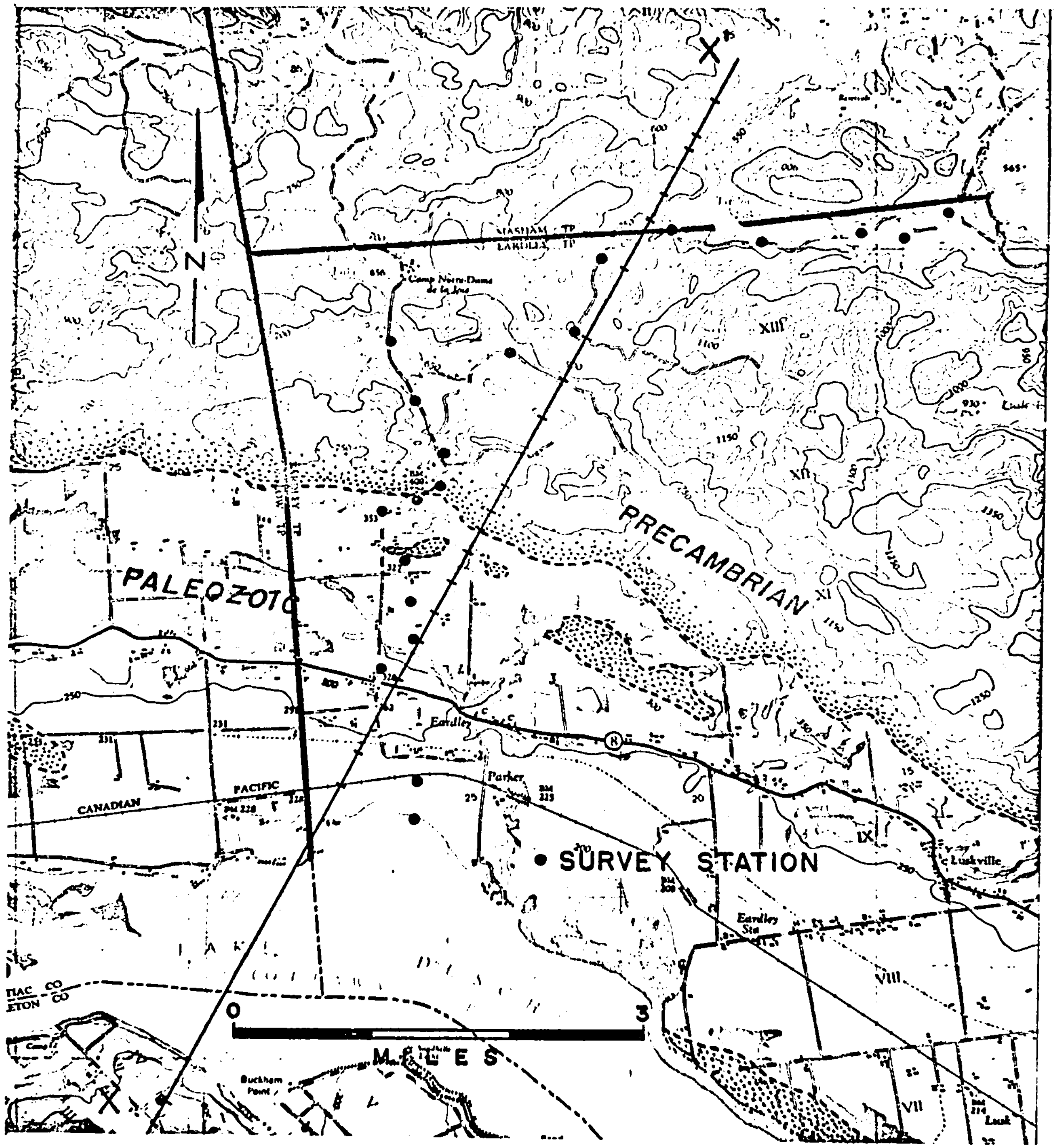

Fig. 4.23 Test Site 6. Location of survey stations.

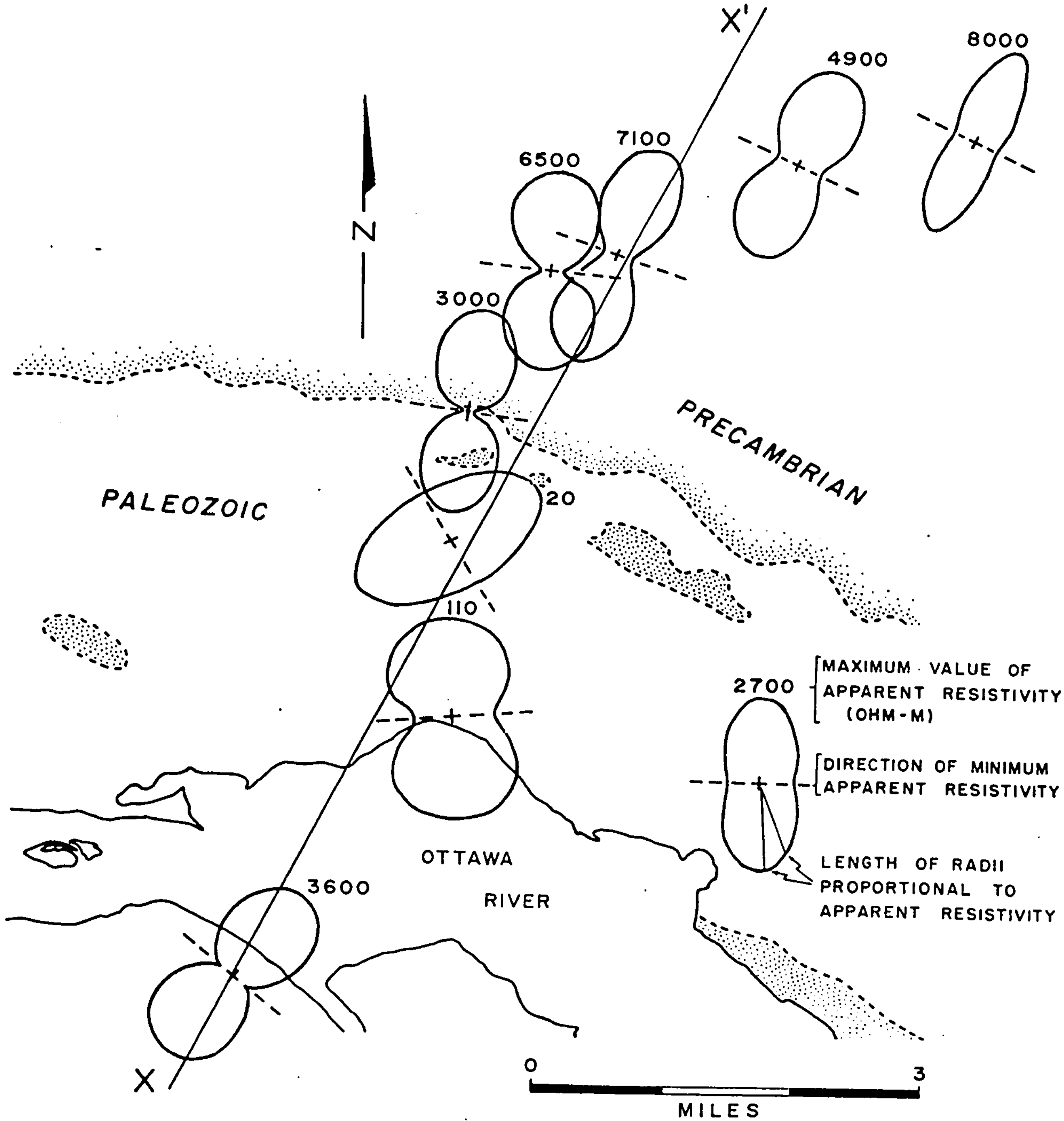

Fig. 4.24 Test Site 6. Directional variations in apparent resistivity.

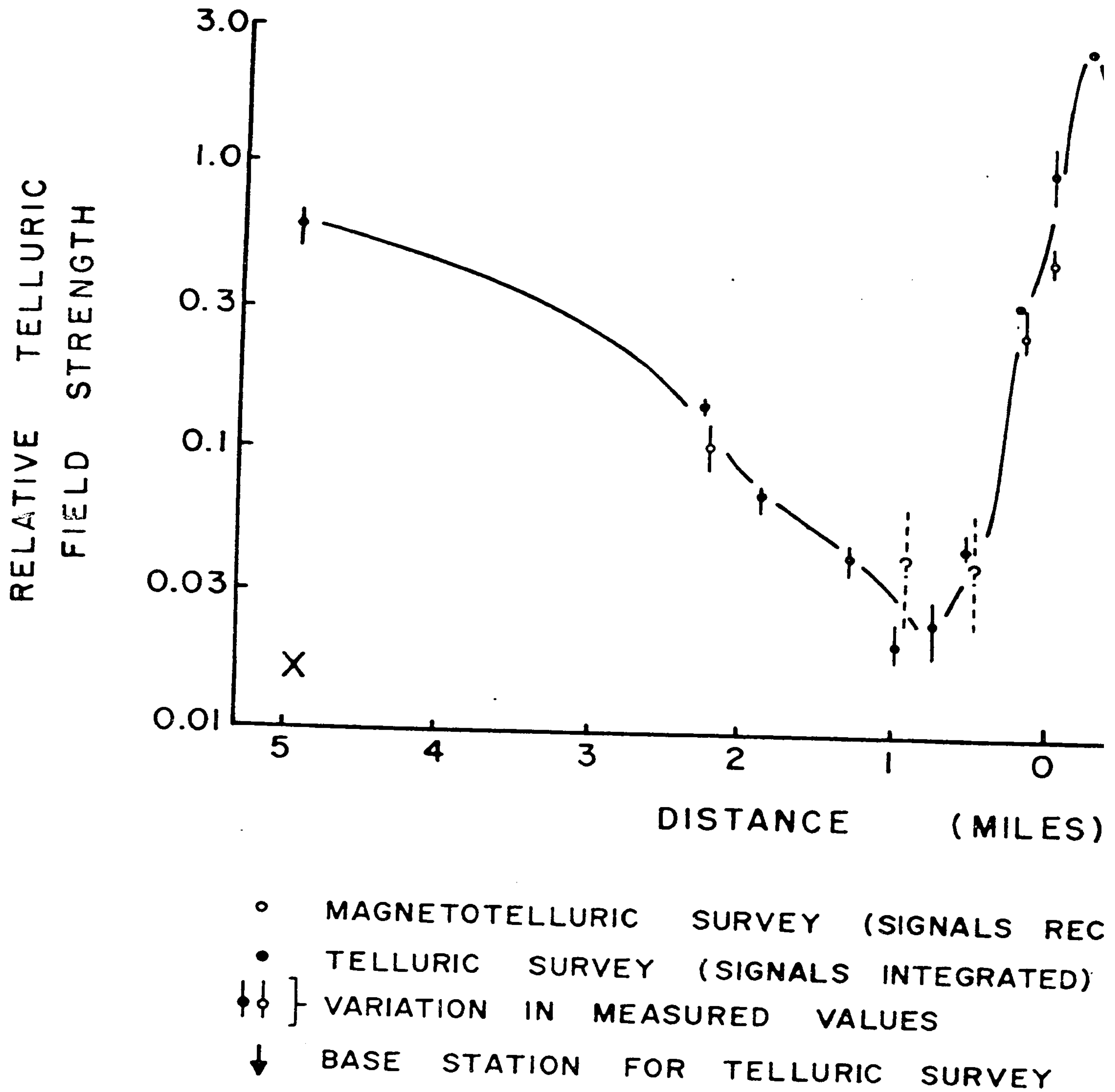

Fig. 4.25 Test Site 6. Comparison of telluric and magnetote

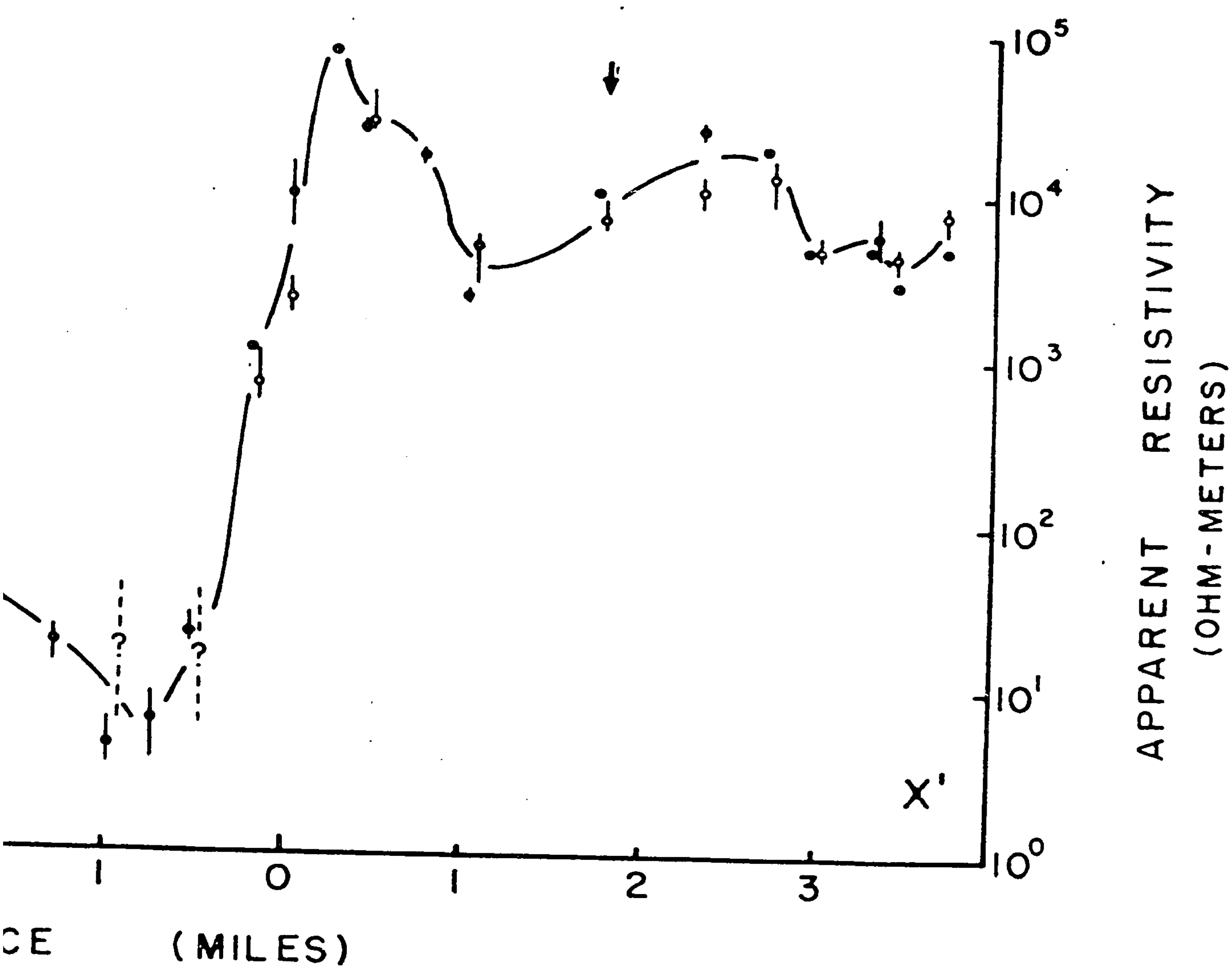

ᑕE (MILES)

Y (SIGNALS RECORDED)

LS INTEGRATED)

VALUES

.URIC SURVEY

ıric and magnetotelluric survey results ($E_\perp$ polarization).

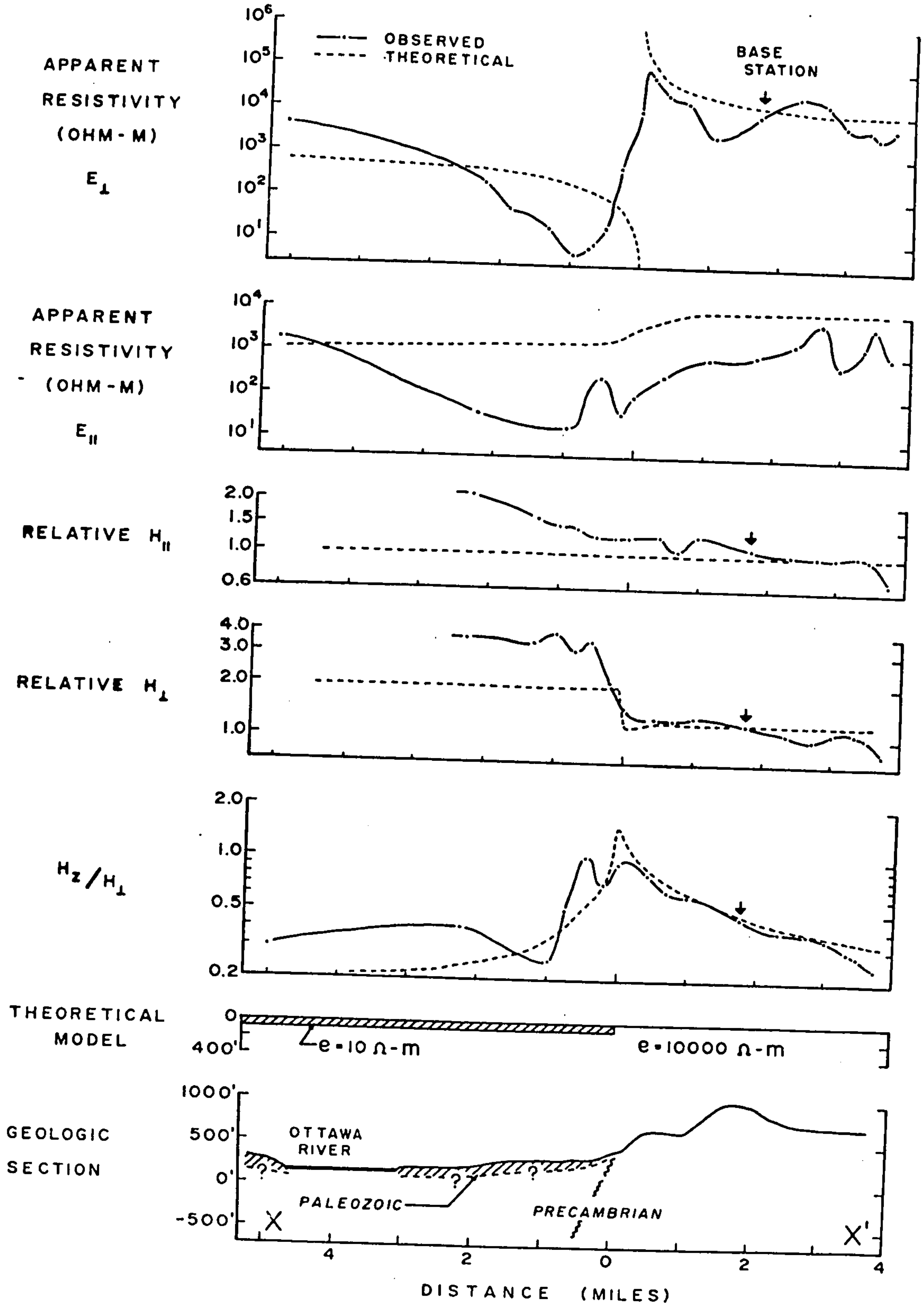

Fig. 4.26 Test Site 6. Observed and theoretical results.

There is considerable variation in the measured values of apparent resistivity, despite the fact that only signal bursts - where the amplitude ratio of the two signals appeared representative of the average over the whole record - were used in the computations. Random sampling would have at least doubled the scatter. However, in several tests where the magnetic and telluric signals were integrated, the variation in the apparent resistivity values obtained from repeated integrations was usually less than ±10%.

Excepting the $E_{\parallel}$ profile, which is derived from the measured directional variations in apparent resistivity, the field results shown in Figure 4.26 are based on surveys that measured specific components of the 8 Hz electromagnetic field. The amplitudes of the field components were measured with respect to the telluric field strength at the base station. The $E_{\parallel}$ field was used for the $H_{\perp}$ and H_z surveys and the $E_{\perp}$ field for the $E_{\perp}$ and $H_{\parallel}$ surveys. The signals were integrated.

It had been hoped that at this location the geologic structure would be a good approximation of a contact between two media of different resistivities. The field results suggest that the situation is, as usual, more complex. The theoretical results support this; although the changes in the field components show trends similar to the observed, the general agreement is not particularly good.

The Precambrian-Paleozoic contact is indicated on all the surveys except for the $H_{\parallel}$ field which theoretically should remain invariant. The field components change gradually across the contact, suggesting that there is a zone of variable resistivity between the resistive igneous and conductive sedimentary rocks. Actually, there is an outcrop of Precambrian rocks about 0.5 miles south of the main contact.

The existence of a large vertical 8 Hz magnetic field near the contact at this location and also over the mineralized zone at Test Site 1 suggest that Afmag surveys at 8 Hz may be possible.

4.7 Test Site 7

This location and Test Site 8 (Section 4.8) were selected because of the availability of results from Turam, induced polarization, horizontal loop and magnetic surveys (Lavoie, 1968).

The mineralization consists of two parallel sulphide bodies, containing 10-40% total sulphides, located at the contact between acidic flows and rhyolite porphyry. The area is covered by muskeg.

Telluric surveys (Fig. 4.27) show no anomaly over the sulphides but seem to indicate the geologic contact. Of the other geophysical methods, only the magnetic survey shows an anomaly over the sulphide zones (Fig. 4.28).

The theoretical results (Fig. 4.29) suggest that the observed telluric profile mainly reflects variations in the overburden thickness rather than different resistivities on opposite sides of the contact. The thickness and resistivity of the overburden in the model are based on seismic refraction (Scott, 1970) and induced polarization (Lavoie, 1968) results.

As at Test Site 4, the above results illustrate potential limitations of both telluric and magnetotelluric measurements for geological mapping. In both cases anomalies, similar to those observed over contacts between rocks of different resistivities, are actually caused by major changes in overburden thickness. Furthermore, on the basis of these theoretical results, it seems there is little difference

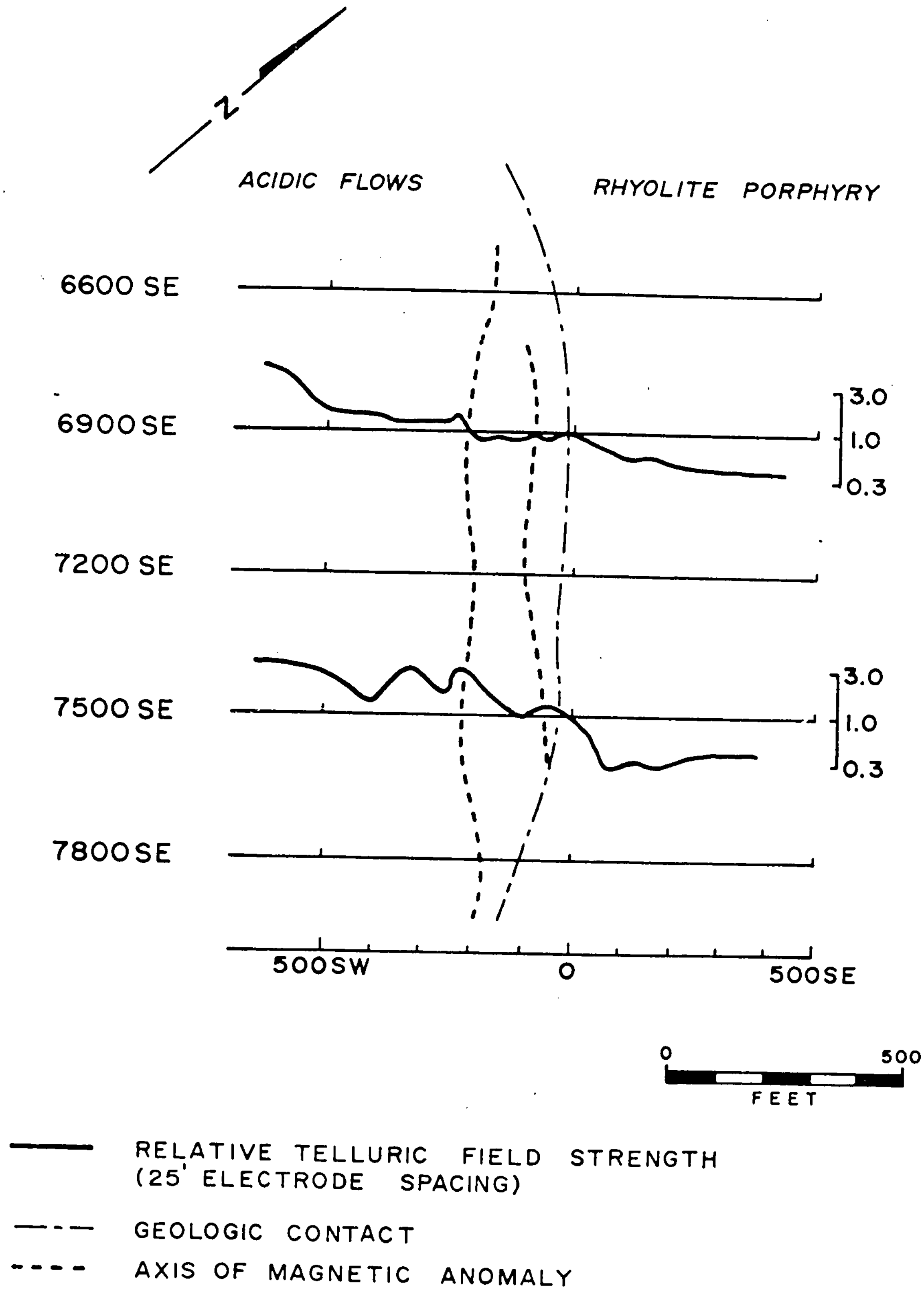

Fig. 4.27 Test Site 7. Results of telluric surveys ($E_\perp$ polarization).

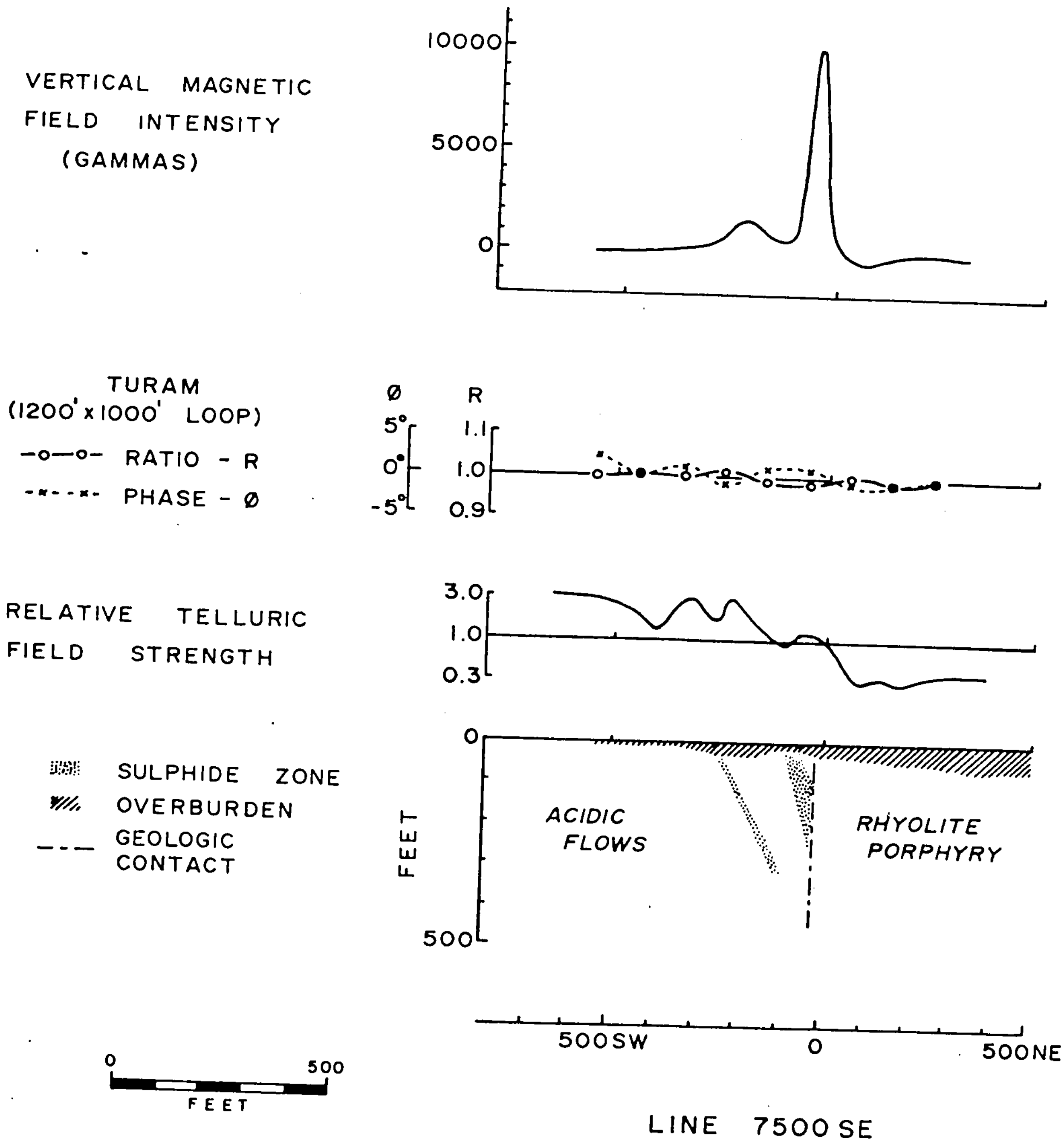

Fig. 4.28 Test Site 7, Line 7500SE. Comparison of vertical magnetic field, Turam and telluric ($E_{\perp}$) survey results.

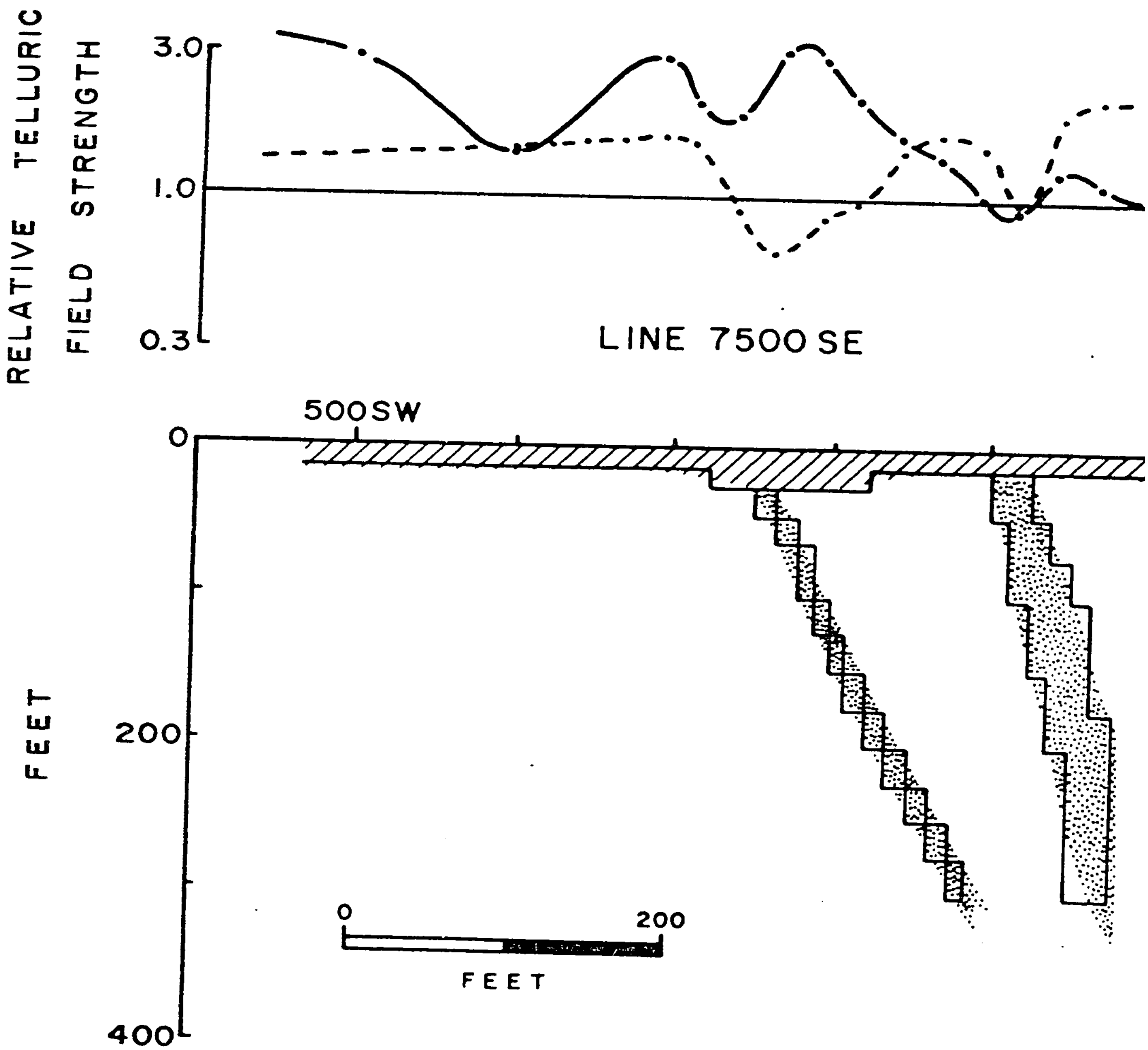

Fig. 4.29 Test Site 7, Line 7500SE. Observe

profiles ($E_{\perp}$ polarization).

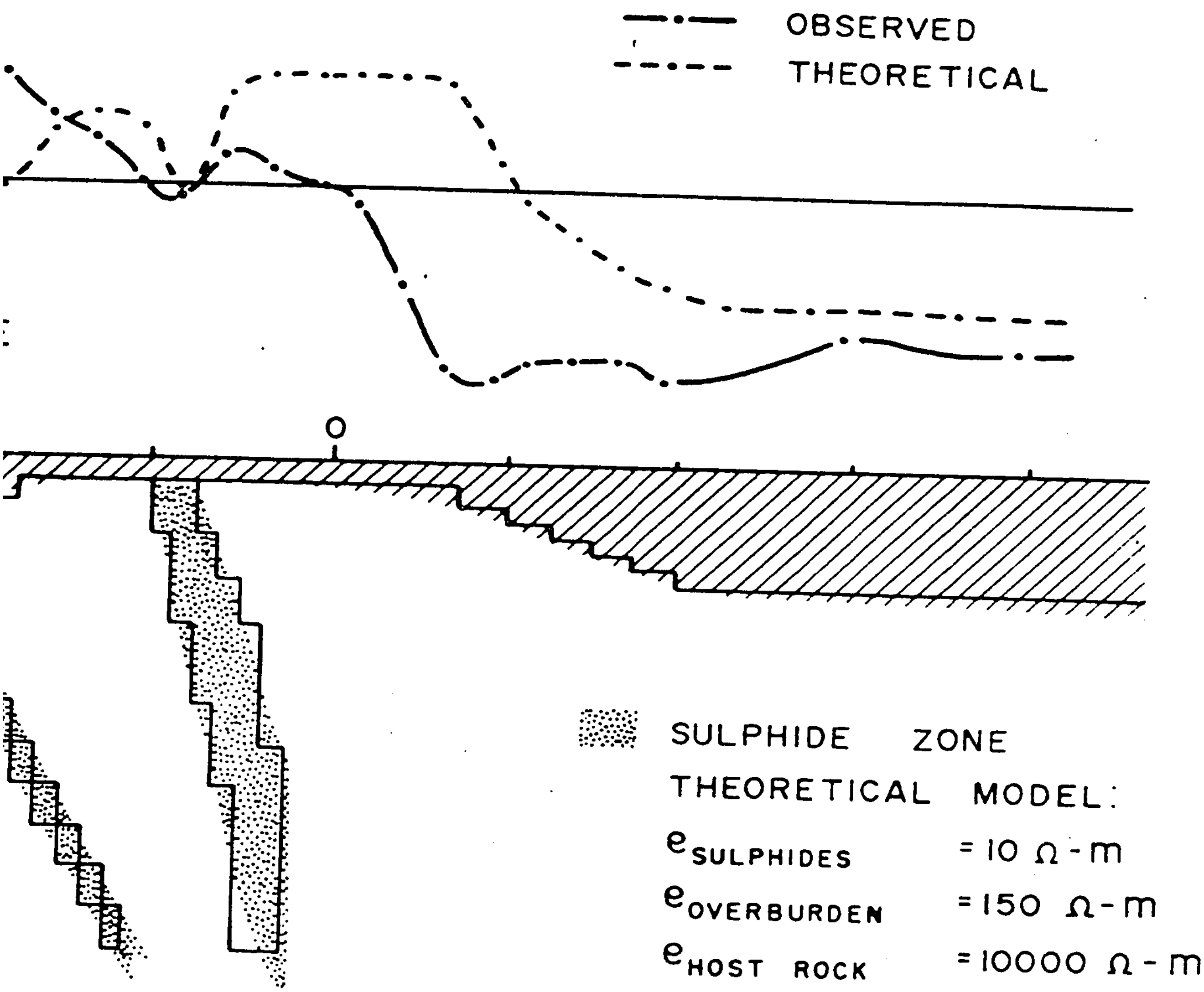

;00SE. Observed and theoretical telluric

;ation).

in the resistivities of the rock types on opposite sides of the contacts. This is not necessarily typical of Precambrian geology but, on the other hand, most of the apparent resistivities measured during the regional survey (Section 4.2) were in the range of 2000 to 20000 ohm-meters.

4.8 Test Site 8

There are two areas of geophysical interest in this vicinity, the provén sulphide zone at 100S on line 400W and the magnetic anomaly at 400N on line 100W (Fig. 4.30). As at the previous test site, none of the electrical or electromagnetic surveys detected either the known sulphide zone or a possible conductor associated with the magnetic anomaly (Lavoie, 1968). Similarly, the telluric surveys for both the $E_{\perp}$ and $E_{\parallel}$ polarizations show no response. The apparent reason is that the overburden, which is nearly 100 feet thick and highly conductive (100 ohm-meters), limits the penetration of all electrical and electromagnetic methods.

A theoretical telluric profile over the known sulphide body does show that the field strength over the zone is 0.9 of the background value. However, in view of the inherent variations in the background telluric field strength as well as the accuracy of field measurements (generally ±5%), an observed anomaly of this magnitude would not be considered significant.

This points up one of the problems encountered in the telluric work: because variations in the field strength by factors of 2 or 3 are common, there is good reason to ignore anomalies where the telluric field does not decrease by at least a factor of 5. Thus, unless the background field is very uniform, the telluric method can detect only very large or near surface conductive zones.

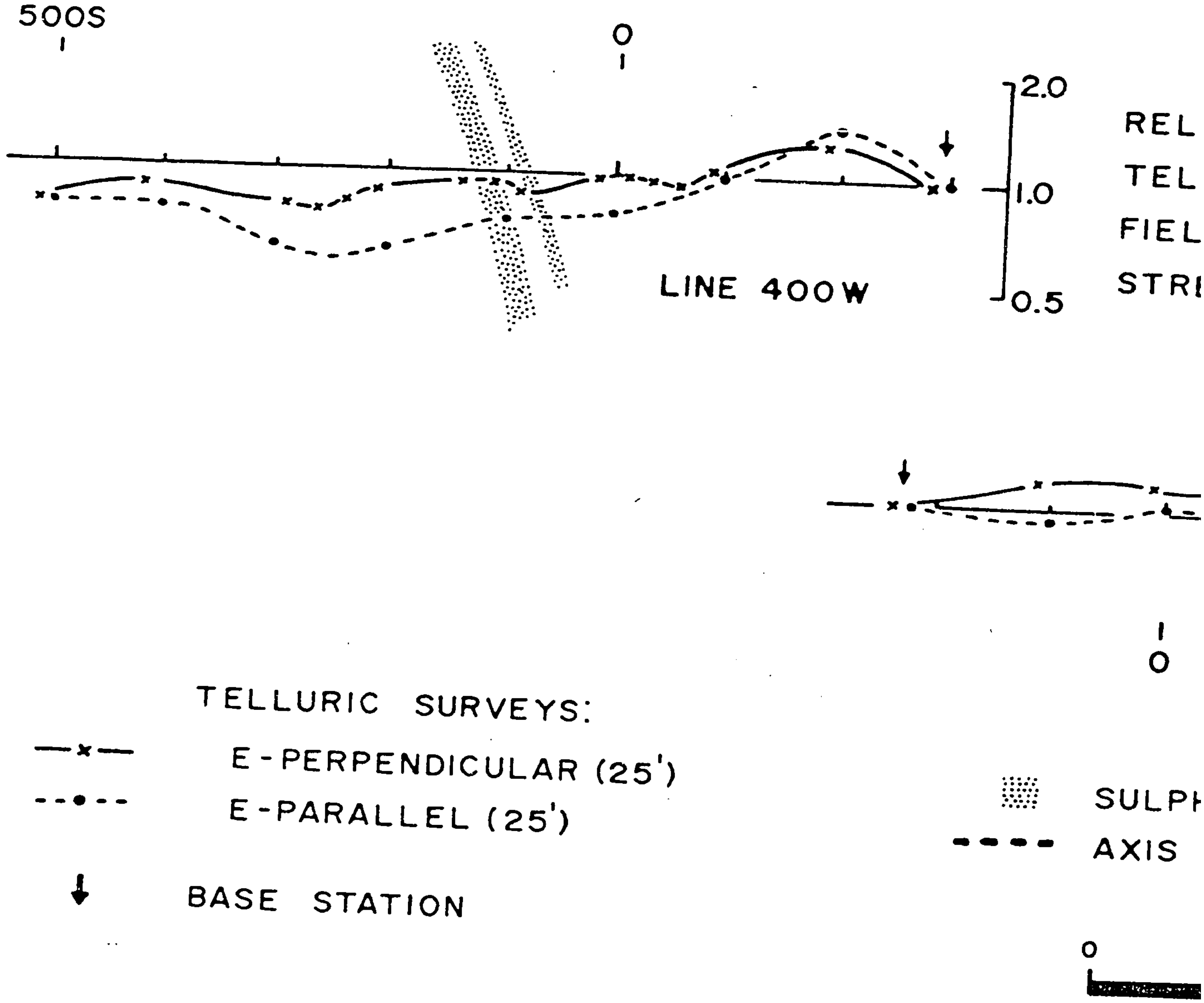

Fig. 4.30 Test Site 8. Telluric survey result

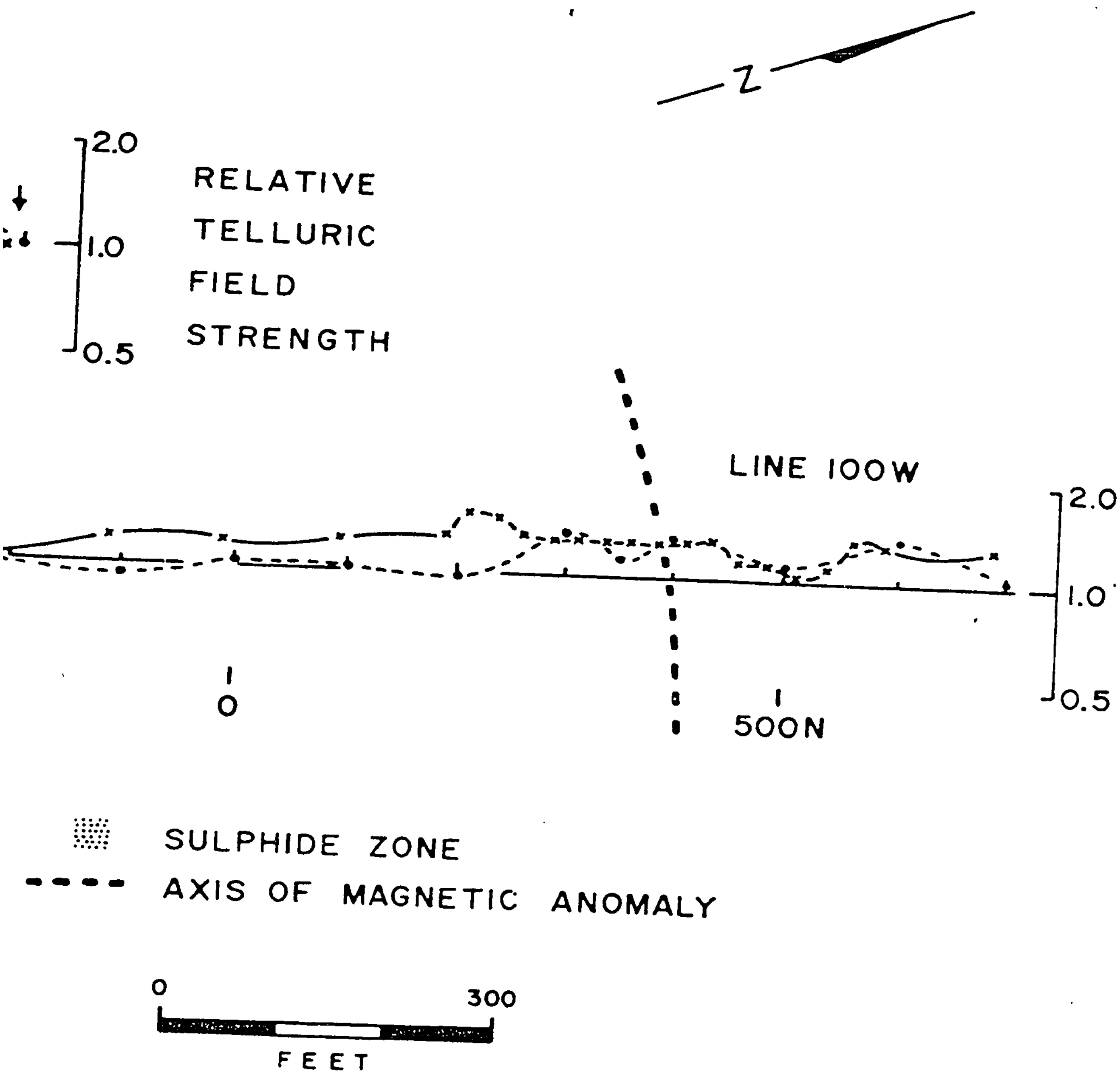

: survey results for $E_{\perp}$ and $E_{\parallel}$ polarizations.

4.9 Test Site 9

The mineralization consists of several zones of disseminated sphalerite (Fig. 4.31) and very minor amounts of other sulphides. The ground is swampy and the bedrock depth ranges from 20 to 40 feet.

Since sphalerite is generally a poor conductor it is not surprising that the telluric results show at best vague indications of the mineralization. In practice these would certainly be ignored in view of the much greater variations in the field strength, such as the low between 500N and 900N on line 000, caused by changes in the overburden thickness.

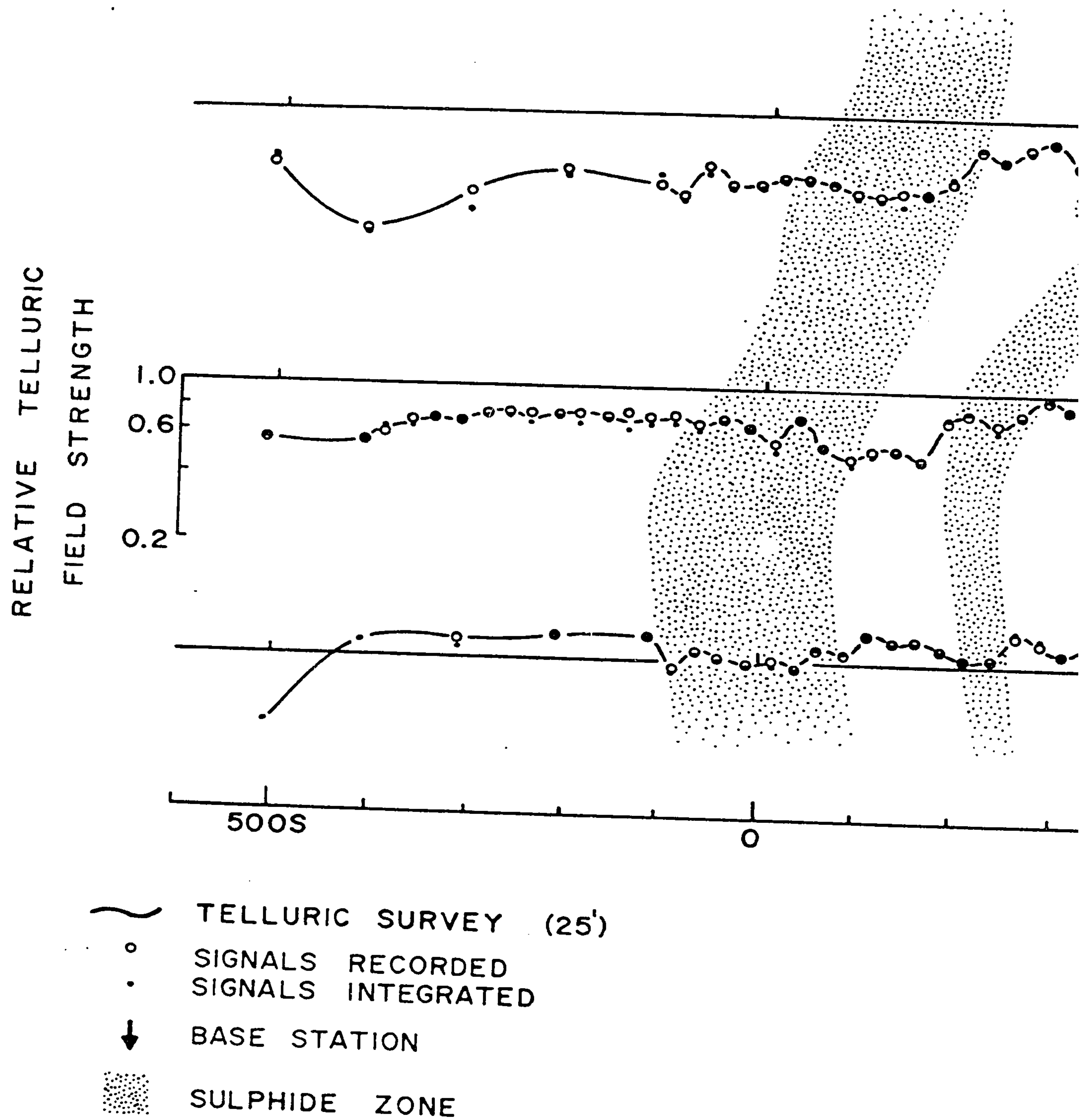

Fig. 4.31 Test Site 9. Results of telluric

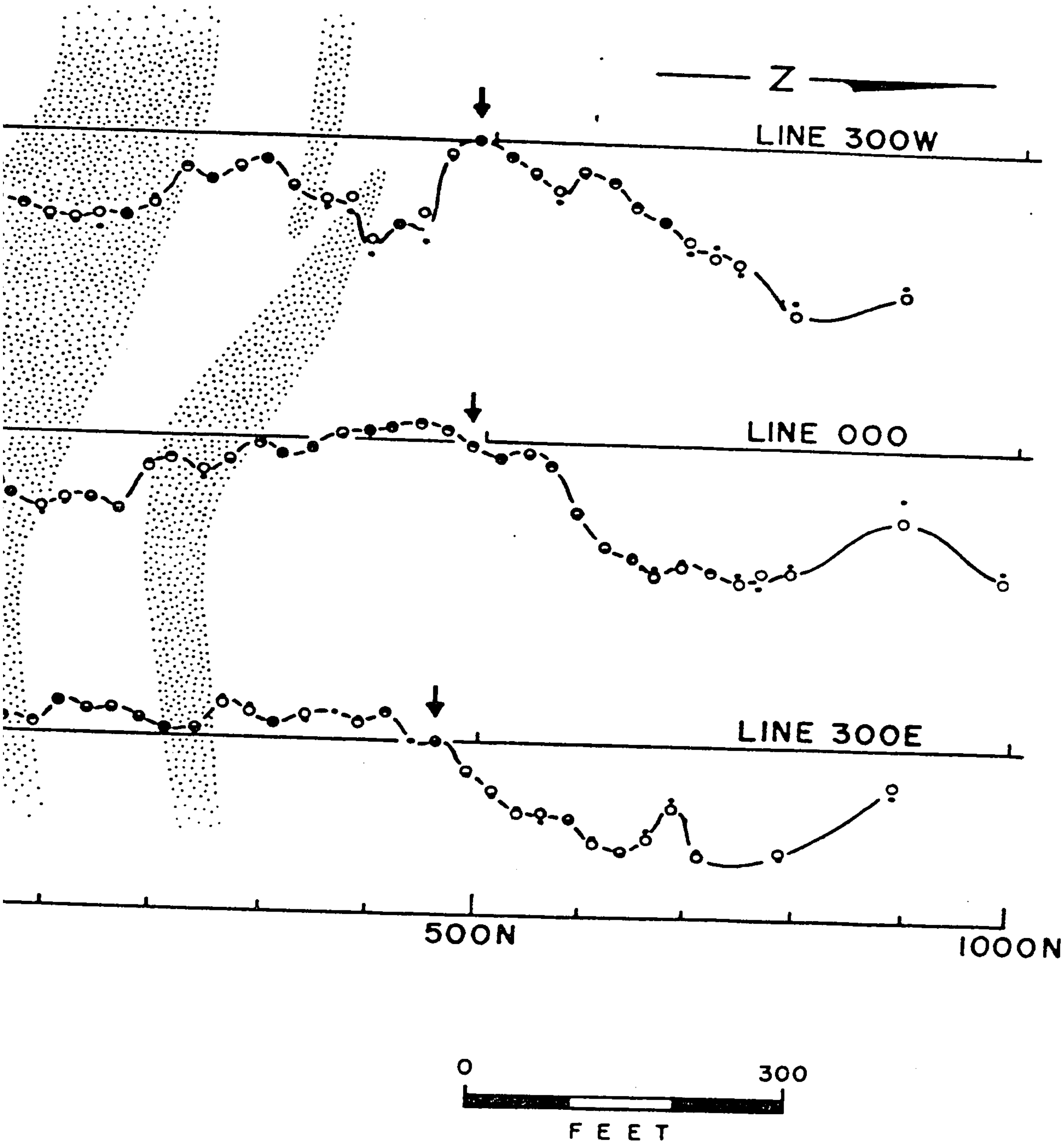

ts of telluric surveys ($E_\perp$ polarization).

4.10 Test Site 10

The mineralization at this test site consists of a large body of massive sulphides located in diorite-rhyolite host rock (Fig. 4.32). Nearly 100 diamond drill holes have outlined the sulphide zone in detail. The zone subcrops below thin overburden in the south and plunges gently to a depth of 400 feet at the north end.

Because the telluric fields within 200 to 300 feet of the sulphide zone showed a complete lack of correlation the telluric surveys were carried out by integrating the signals. The low signal level necessitated the use of 100 foot electrode spreads.

The survey results, summarized in the form of an apparent resistivity map (Fig. 4.32) clearly indicate the presence of the sulphide zone. The apparent resistivity is lowest in the south end where the zone is near-surface and the results suggest that the sulphides may extend farther south than shown by the map. In fact, two drill holes located on the base line between traverses T3 and T4 show short intersections of mineralization at a depth of less than 100 feet.

To the north, the last definite indication of the sulphide zone is on line 1930S where it is more than 200 feet deep.

Figures 4.33, 4.34 and 4.35 compare theoretical and observed telluric profiles along lines 2630S, 2330S and 1930S, respectively. There is fair agreement between the two profiles on lines 2330S and 2630S but on line 1930S the field results suggest that the middle of the sulphide zone is deeper than the sides.

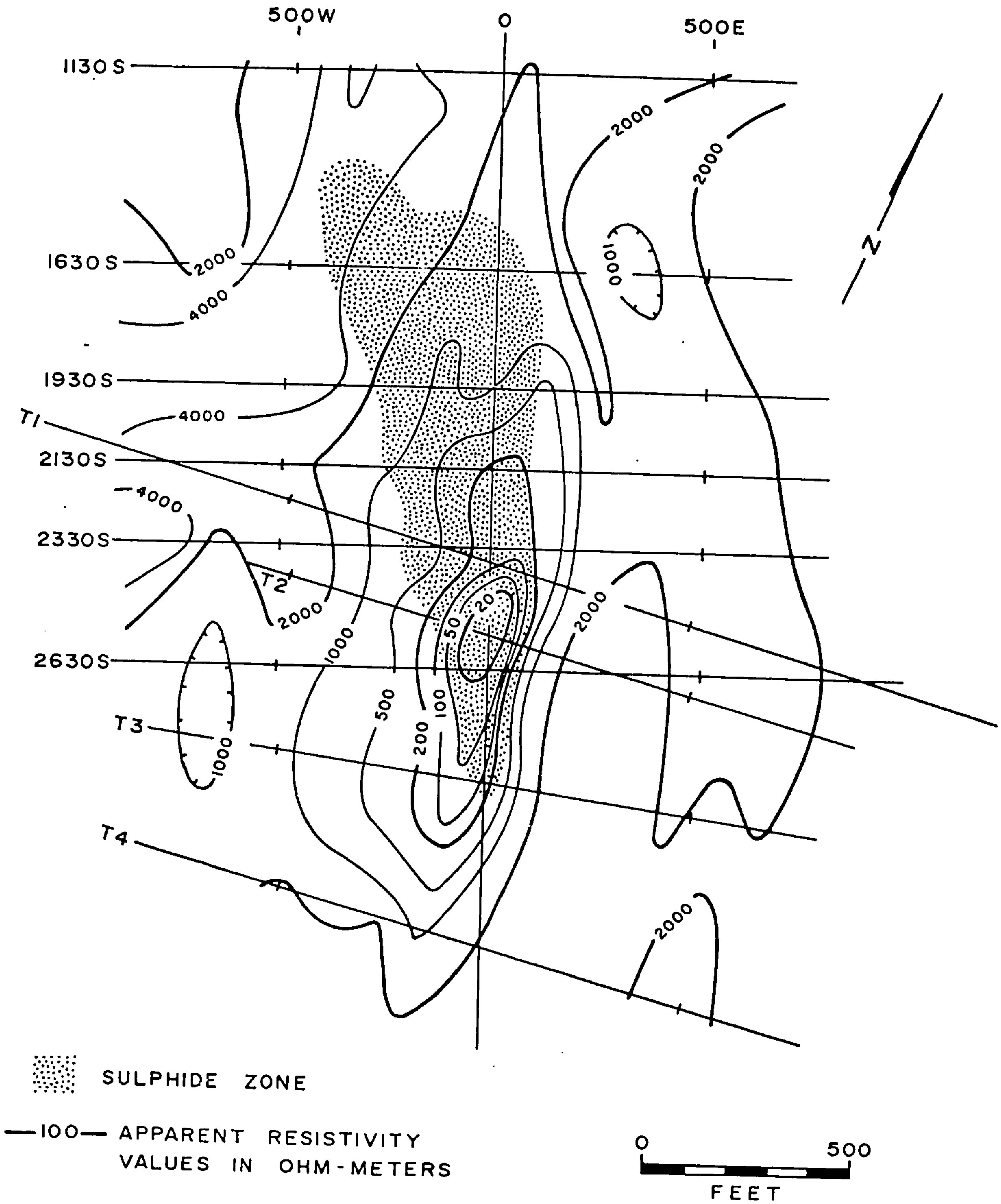

Fig. 4.32 Test Site 10. Apparent resistivity map based on results of relative telluric field strength measurements ($E_\perp$ polarization).

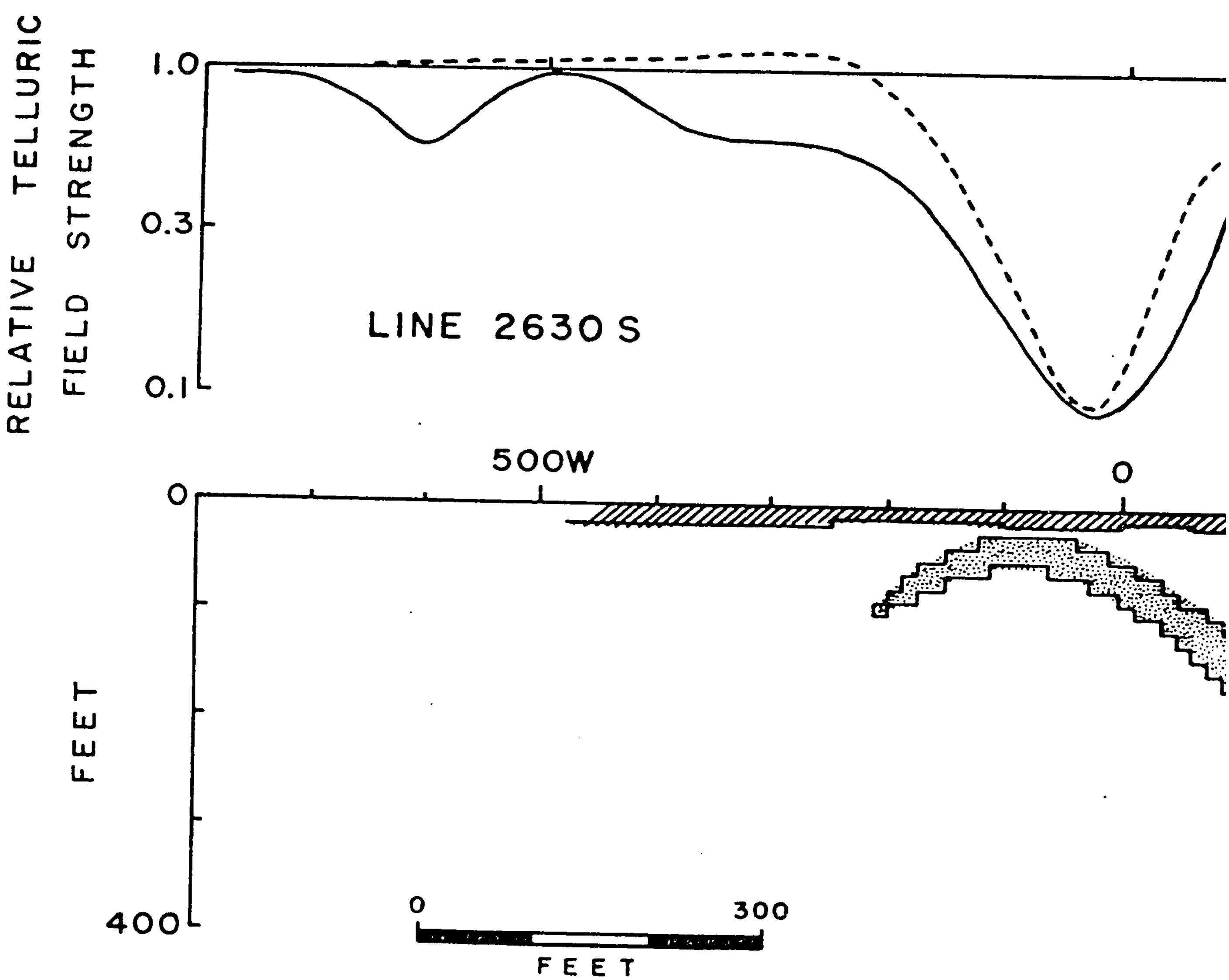

Fig. 4.33 Test Site 10, Line 2630S. Observed and theoret

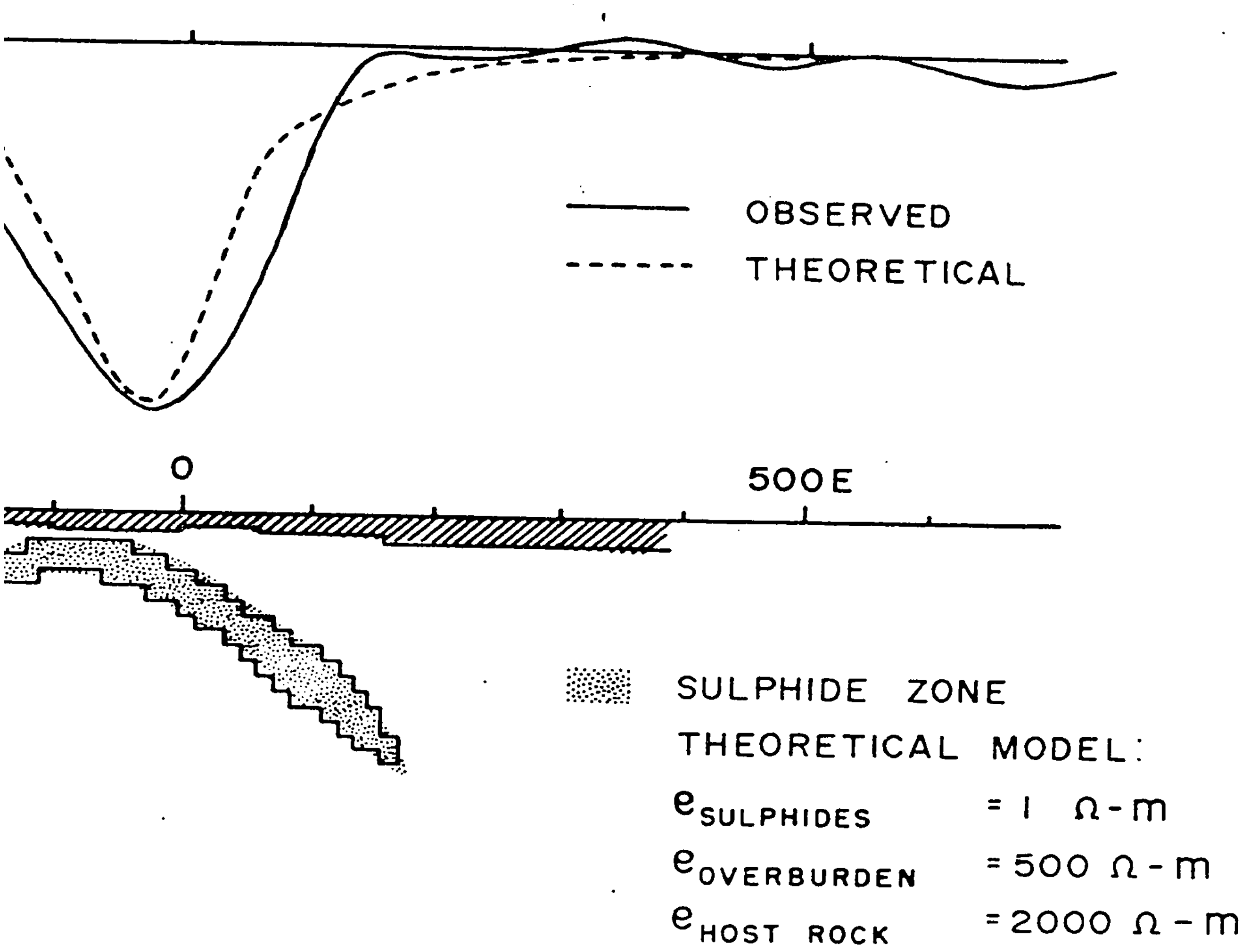

ed and theoretical telluric profiles ($E_{\perp}$ polarization).

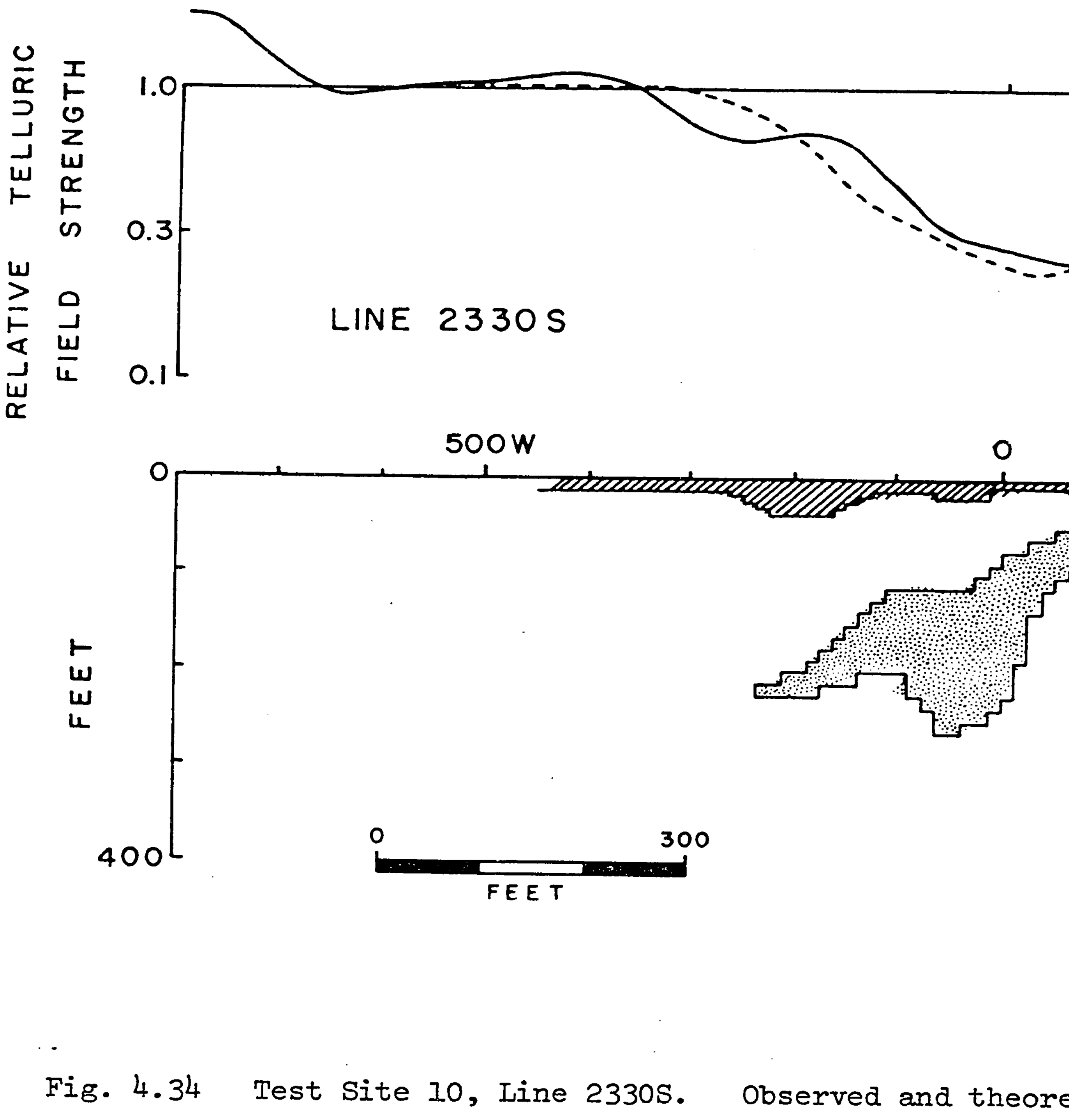

Fig. 4.34 Test Site 10, Line 2330S. Observed and theore

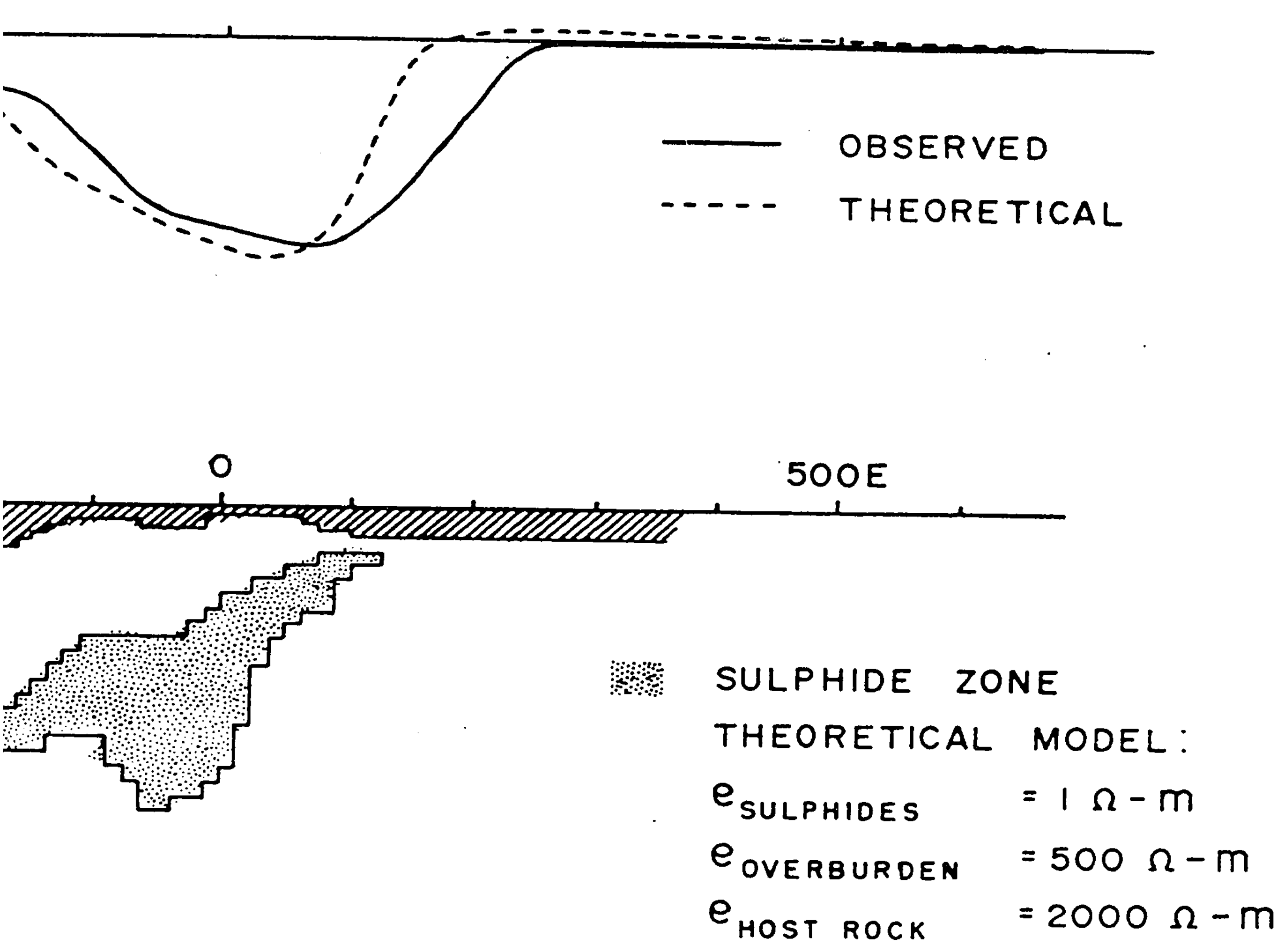

:ved and theoretical telluric profiles ($E_\perp$ polarization).

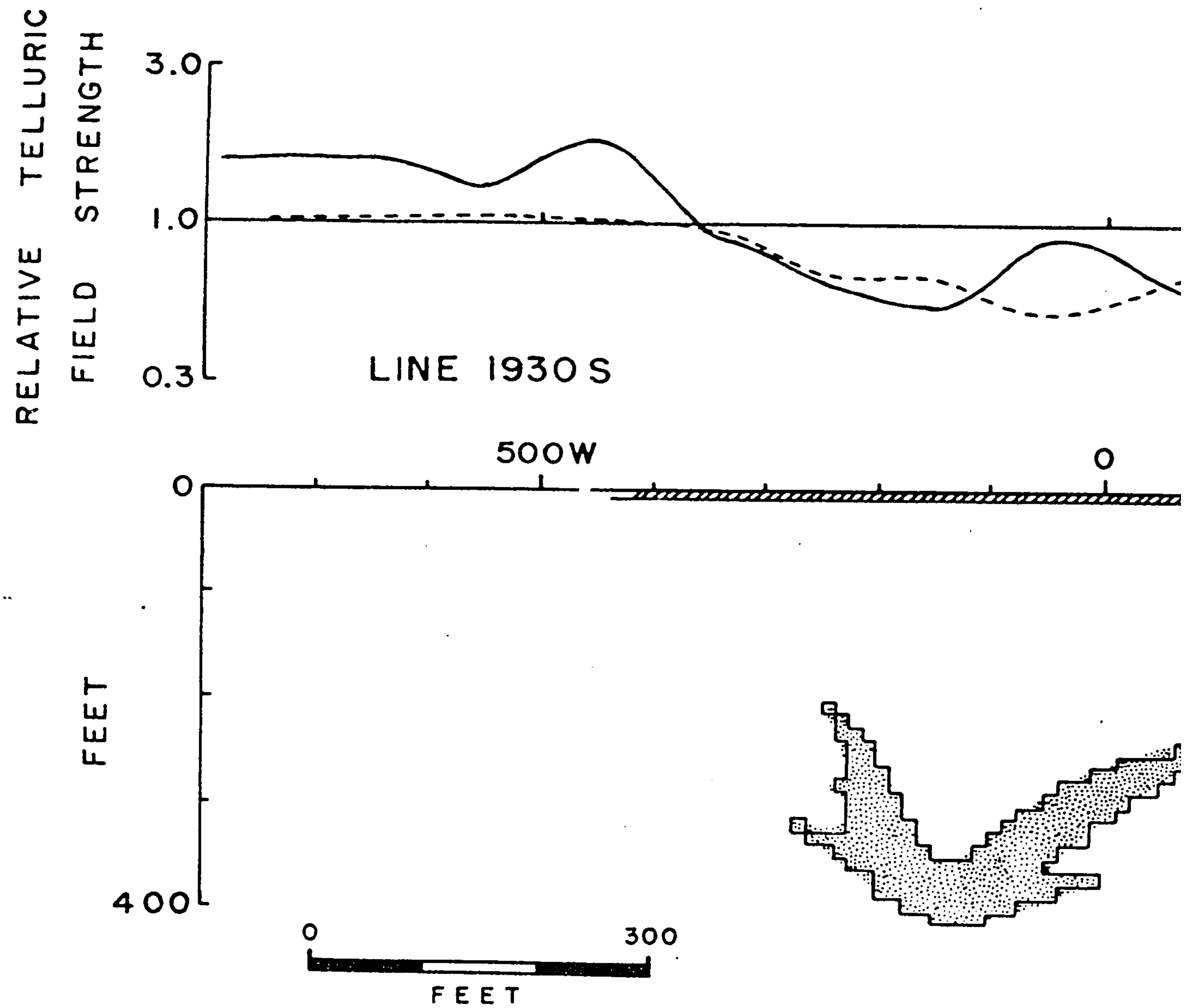

Fig. 4.35 Test Site 10, Line 1930S. Observed and theore

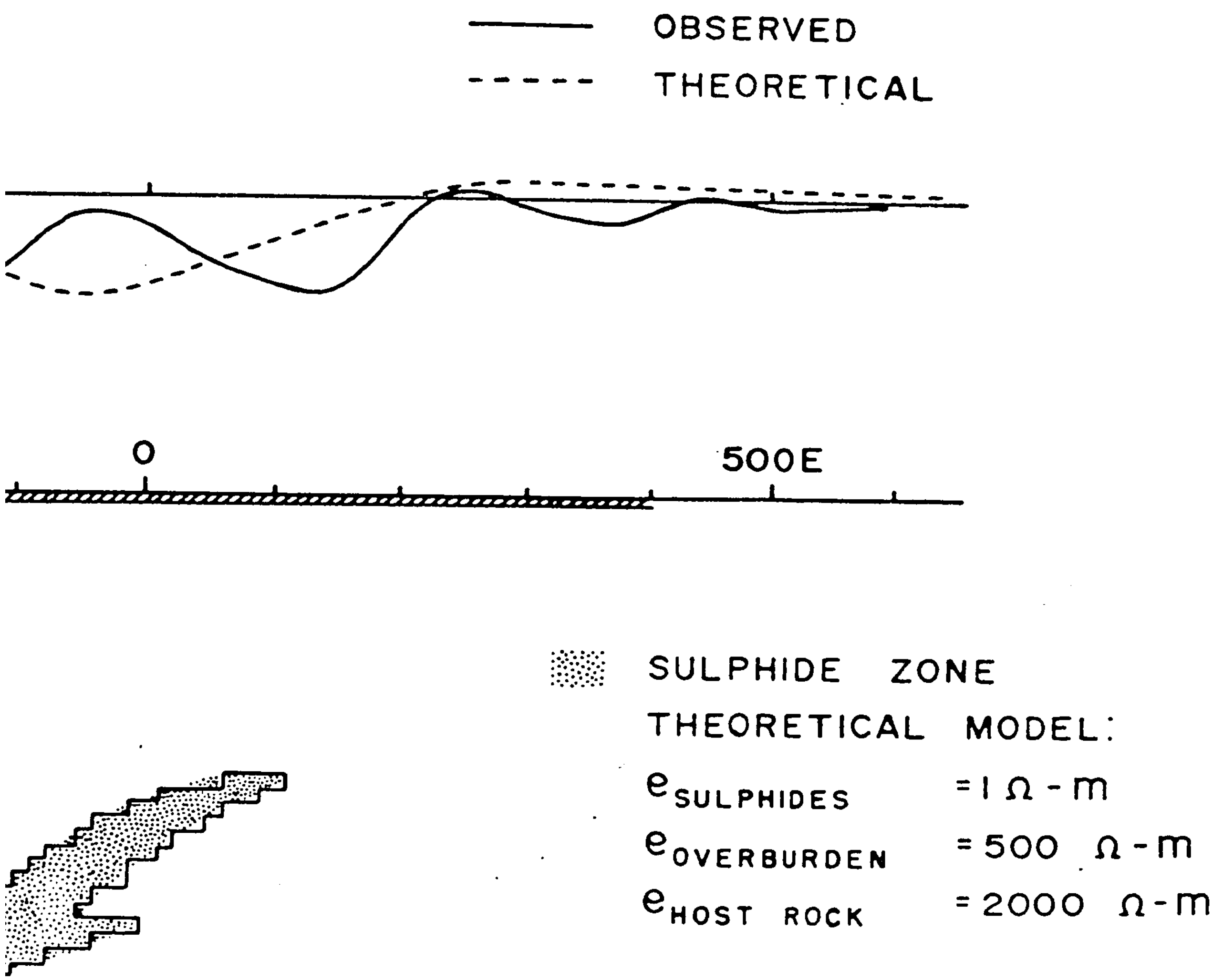

and theoretical telluric profiles ($E_{\perp}$ polarization).

4.11 Test Site 11

The target zones for the telluric surveys at this test location included a body of massive sulphides as well as several electromagnetic conductors outlined by a horizontal loop survey. These zones are located in a large gabbro stock that has been intruded into sedimentary quartzites and argillites.

During the telluric surveys the correlation between signals at the field and base stations was generally poor. Irregular man-made electrical noise from nearby sources was present at most times.

The apparent resistivity maps based on telluric and induced polarization measurements (Fig. 4.36) show no definite indication of either the mineralized zone or the electromagnetic conductors. There is no agreement between the results of the two surveys except for some similarity in the east-west pattern of resistivity highs and lows across the survey area.

Some of the telluric anomalies may be caused by rapid changes in overburden thickness but otherwise there is no apparent explanation for the results.

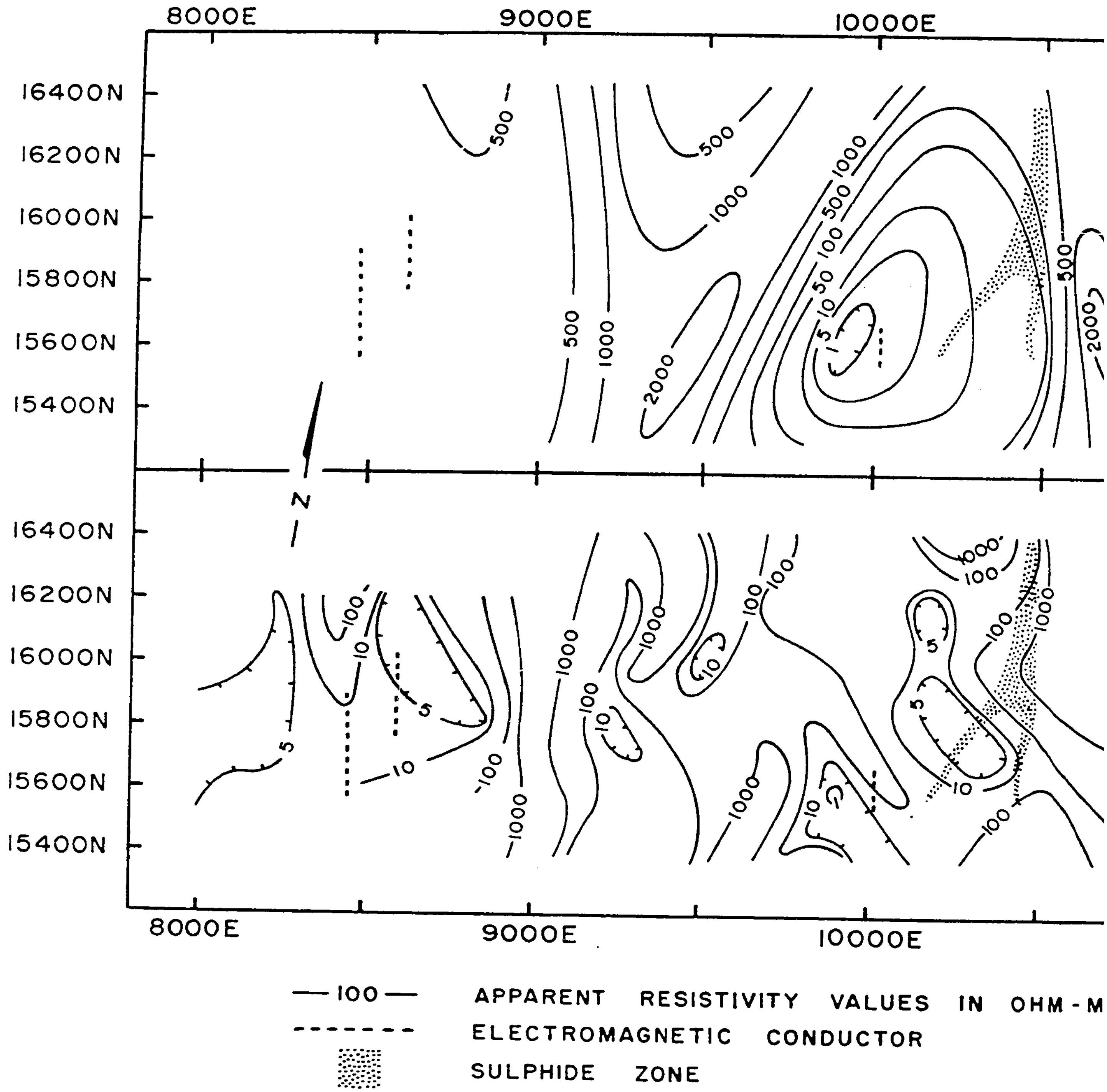

Fig. 4.36 Test Site 11. Comparison of apparent resistivity and telluric surveys.

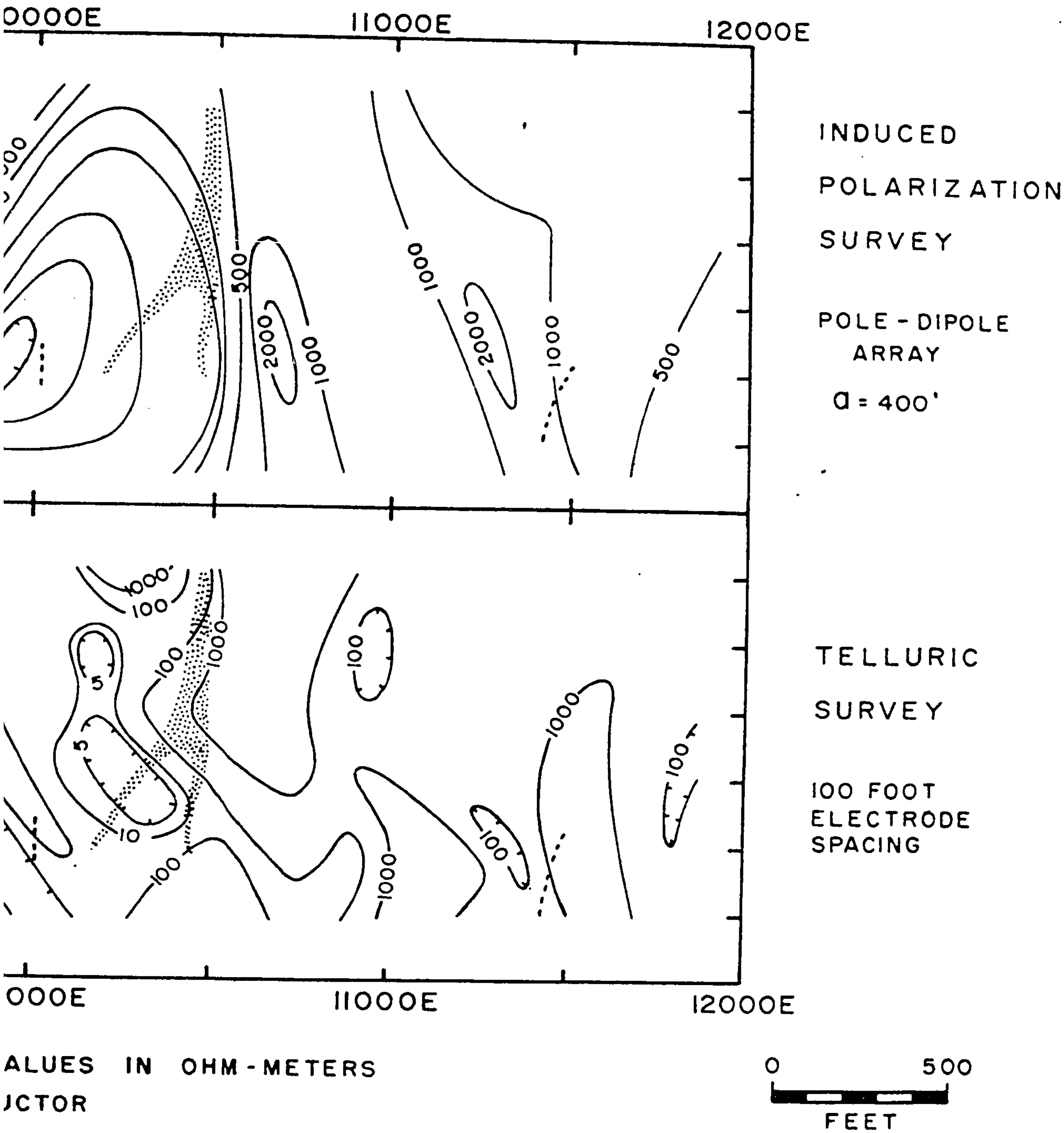

nt resistivity maps based on induced polarization

.

CHAPTER V

DISCUSSION AND CONCLUSIONS

5.1 Phase Changes in the Telluric Fields

The most puzzling phenomenon noted during the field surveys was the lack of correlation and/or variable phase relationship between the background $E_{\perp}$ signal and the signal near, over, or on the opposite side of a conductive zone. This was observed in all cases where a sulphide body or other highly conductive zone was detected. There seems to be no mention of similar observations in the literature.

The first suggestion of a possible theoretical explanation was found in the numerical solutions for geologic situations involving several conductive zones. In some cases these showed unexpectedly large variations in the phase angle between the electric and magnetic fields. Further investigation indicated that, under certain conditions, significant changes in the theoretical $E_{\perp}/H_{\parallel}$ phase are observed over the conductivity model shown in Figure 5.1 .

The amount of phase change depends both on the resistivities and the dimensions of the model. In general, the resistivities must be such that $\rho_2 < \rho_3 \leq \rho_1$. Also, for a given set of resistivities, there is no phase shift if the ratio D/W is either very small or very large or if B is too large. The thickness (T) of the most conductive medium does not affect the results. Thus, the phase changes appear to be caused by

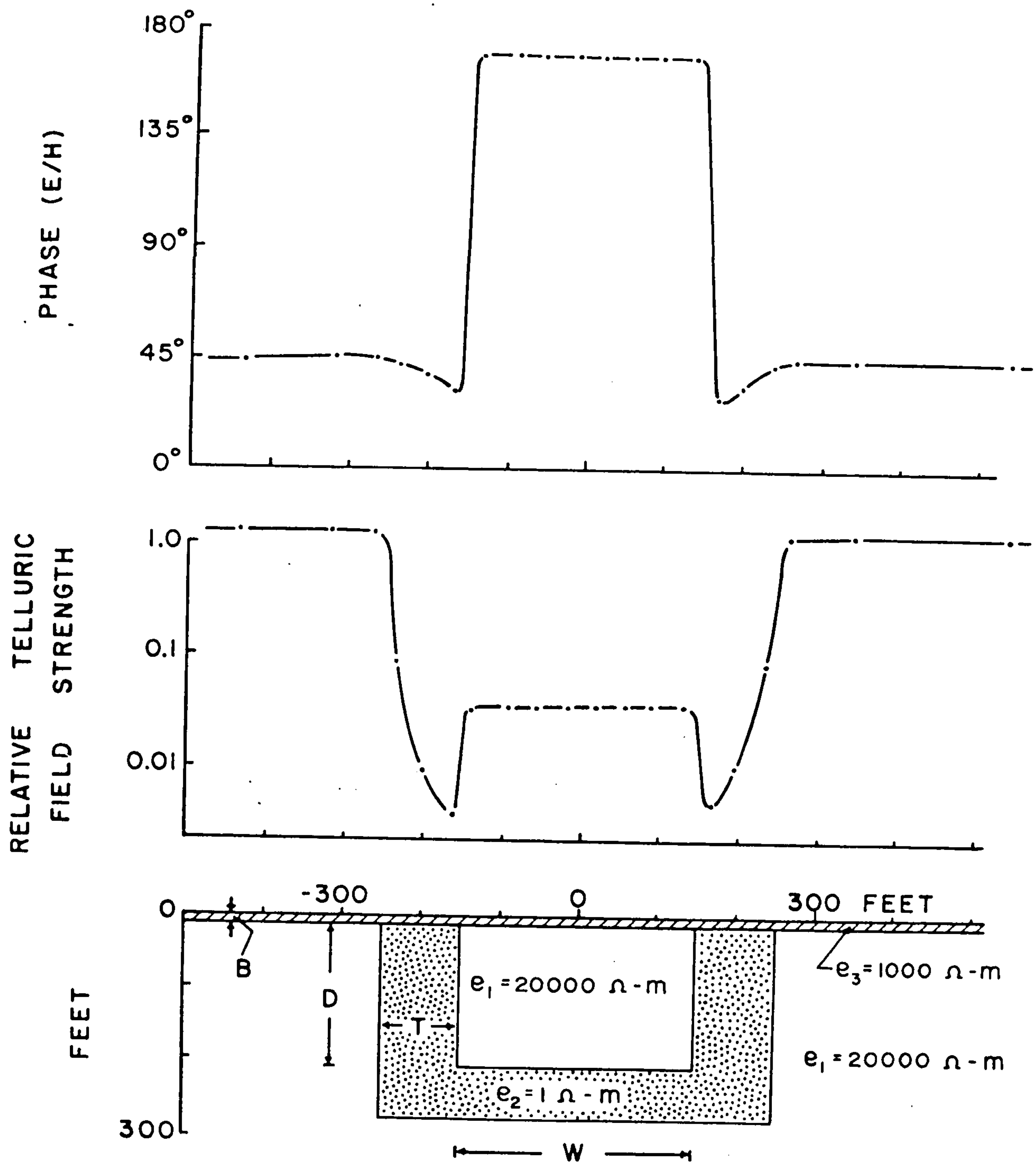

Fig. 5.1 Theoretical results over basic conductivity model required to produce large changes in E/H phase angle ($E_\perp$ polarization).

a resonant cavity effect but further study is needed to determine more exactly the parameters involved.

More realistic (i.e. complex) conductivity cross sections that show large phase changes can be devised provided that the topology of the basic model is retained. Figure 5.2 shows the theoretical results over a model approximating a system of conductive shear zones. The most interesting observation in this case is that the phases of the telluric fields on opposite sides of the vertical conductive zone differ by approximately 150°. This situation is very similar to the actual results obtained over the known mineralized zone at Test Site 1 (Section 4.1).

These theoretical results also provide a possible explanation for the observed lack of correlation in the telluric signals. If the phase of the telluric field changes over a distance similar to the spacing between two electrodes, then the measured signal will be distorted by the constructive and destructive interference of fields of various phases.

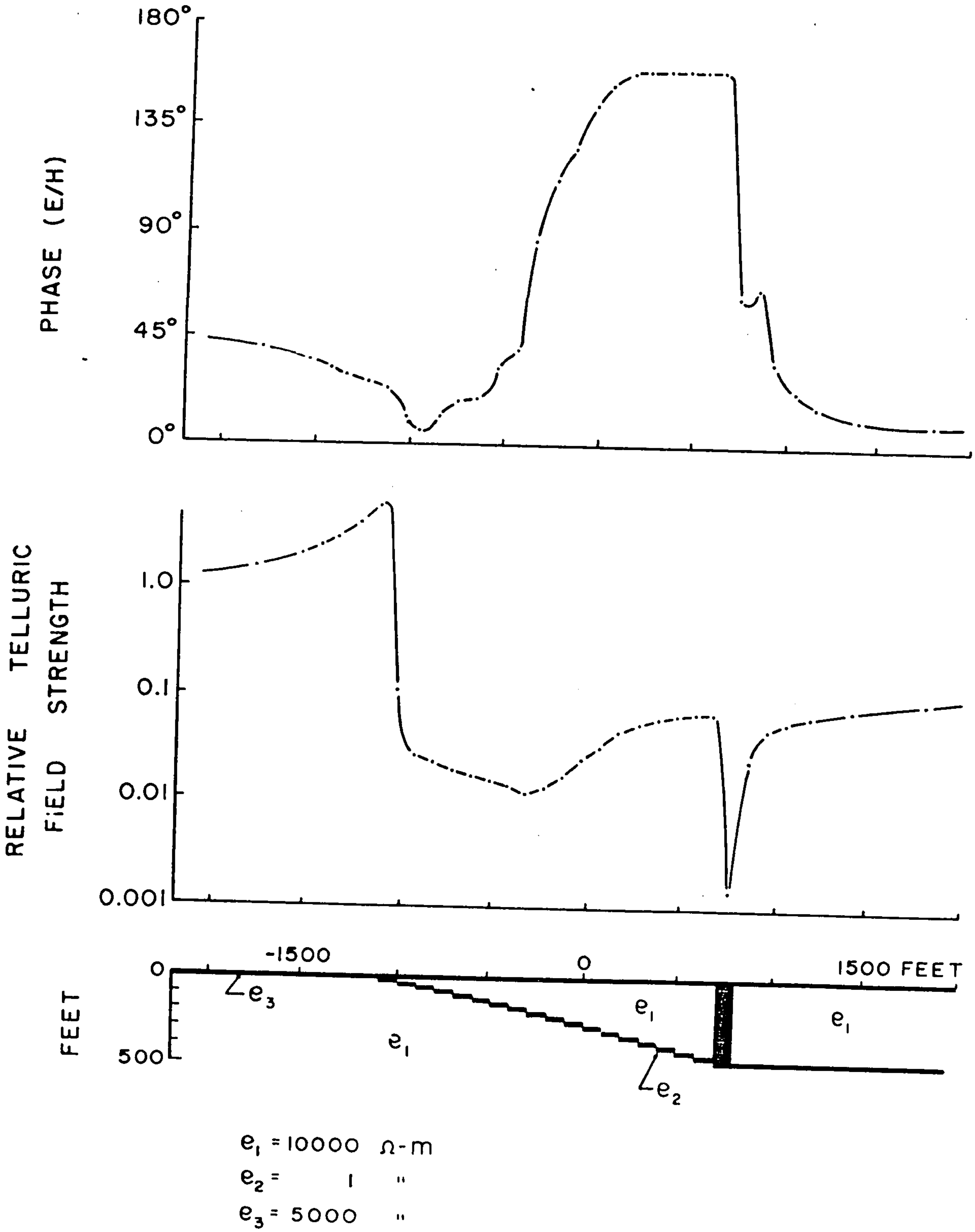

Fig. 5.2 Theoretical results over model of two intersecting conductive zones ($E_{\perp}$ polarization).

5.2 Telluric Surveys Without a Base Station

The field tests showed that the scatter in the measured telluric field strength ratios is generally small and that the 8 Hz signal intensity does not show large diurnal variations. Thus it may be possible to carry out telluric surveys without the base station. Obviously this would be a great advantage, because of the reduction in equipment, personnel and time. Although no field surveys were performed in this manner, from the integrator readings it is possible to reconstruct the results that would have been obtained by this method.

Figure 5.3 compares the observed and hypothetical telluric profiles for three surveys at Test Sites 5, 7 and 10. The hypothetical profiles are based on the assumption that if the first two readings at a survey station agreed to within 30%, the amplifier would have been moved to the next station. Otherwise one additional reading would have been taken.

In all cases the two profiles are so similar that, at least for reconnaissance surveys, a base station does not appear necessary. However, an important prerequisite for this method is the absence of local lightning and irregular man-made noise.

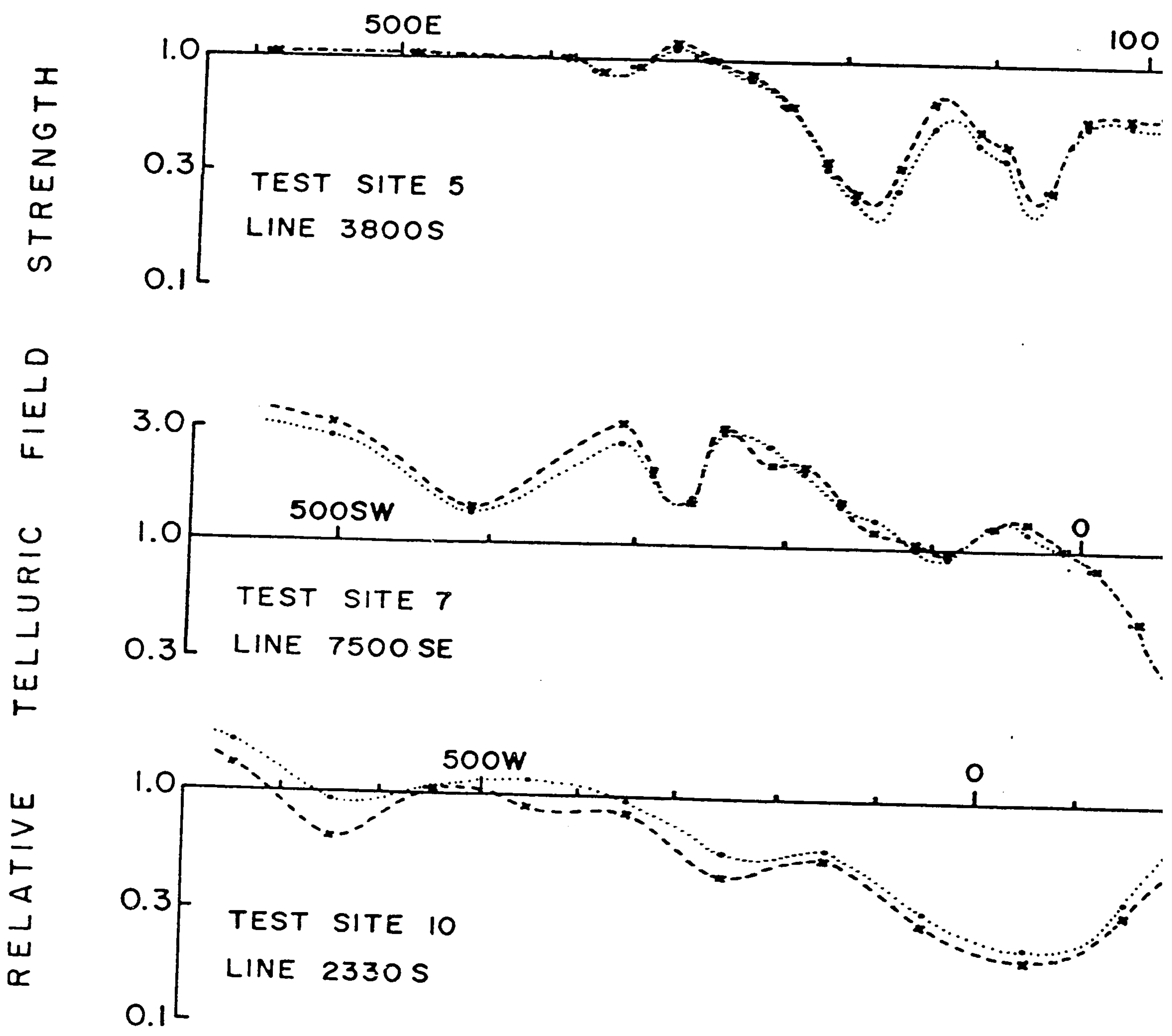

Fig. 5.3 Comparison of actual telluric survey results with without a base station.

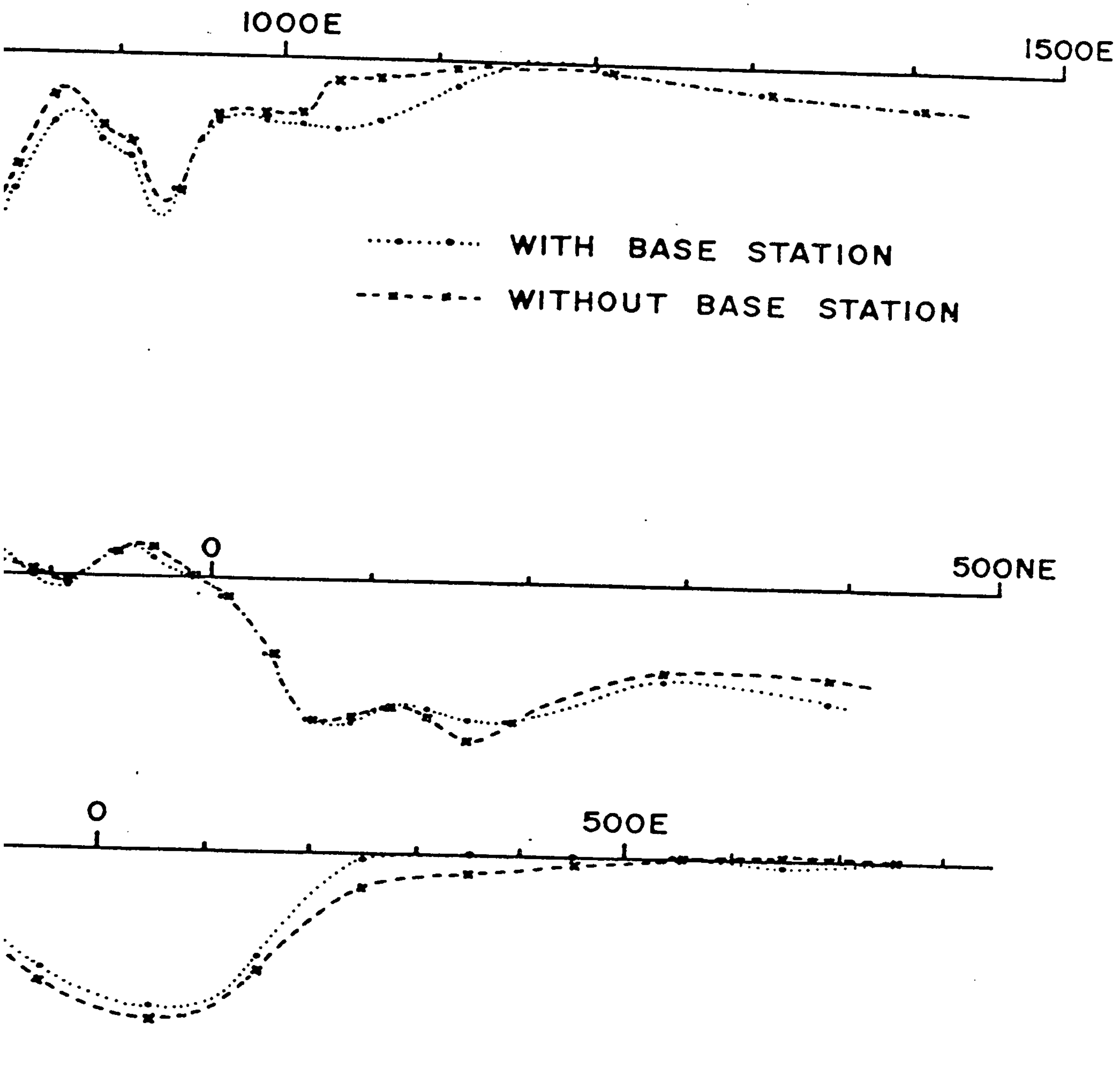

vey results with results that would have been obtained

5.3 Summary of Conclusions

Field Operations

1. The 8 Hz thunderstorm signal is highly suitable for both telluric and magnetotelluric measurements. During the field tests the signal strength was at all times sufficient for survey purposes and the diurnal variations rarely exceeded a factor of 3.

2. The sensitivity of the telluric amplifiers (1 μV) was adequate at all test locations provided that 100 foot electrode spreads were used. Over relatively conductive ground ($\rho_{apparent} < 2000$ ohm-m), 0.5 μV sensitivity is required in order to use 25 foot electrode spacings.

3. Equivalent results are obtained by measuring relative signal amplitudes from records and by integrating the signals. For field surveys integration is obviously preferable because data processing is much simpler.

4. Survey results are not adversely affected by signals originating from local lightning except for the risk of overloading the amplifiers. Similarly, strong but uniform 60 Hz noise does not pose a problem if adequate filtering is employed. However, the presence of random man-made electrical signals makes it impossible to carry out meaningful measurements.

Telluric Surveys

1. Telluric surveys will detect conductivity anomalies associated with some metallic sulphide deposits and geologic features.

2. The best results are obtained by measuring the telluric field perpendicular to the strike of a conductivity discontinuity. The anomalies observed are more intense and more diagnostic than those for the parallel telluric field. However, the parallel field will detect the presence of a conductive zone at a greater distance.

3. Survey results are repeatable.

4. In all cases where the results from other methods are available for comparison, the penetration and resolution of telluric surveys are comparable to those of standard electrical and electromagnetic geophysical techniques. The penetration of the telluric method is not affected by electrode spacing but the resolution is improved when short spreads are used.

5. In simple geologic situations the direction of the minimum telluric field near a conductive zone is approximately parallel to the strike of the conductor.

6. In the absence of major conductivity discontinuities the telluric fields are in phase and correlate well over distances of several thousand feet. The telluric signal over a good conductor does not correlate with the background signal and the phase relationship between the two signals is highly variable.

7. It appears that one operator can carry out satisfactory telluric surveys by measuring the average signal level at each survey station.

Magnetotelluric Surveys

1. Magnetotelluric measurements show that in Precambrian areas the apparent resistivity is anisotropic. This anisotropy is caused by directional variations in the telluric field strength: the horizontal magnetic field intensity does not vary appreciably with direction.

2. Magnetotelluric surveys can detect conductivity anomalies associated with some geologic features and mineralized zones. Near a conductive zone the apparent resistivity becomes more anisotropic and the direction of minimum apparent resistivity is in most cases parallel to the strike of the conductor.

3. For the $E_{\perp}$ polarization, magnetotelluric determinations of apparent resistivity and relative telluric field strength measurements give equivalent results.

4. Near some conductivity discontinuities the magnitude of the vertical magnetic field approaches that of the horizontal field. Thus, Afmag surveys using the 8 Hz magnetic fields may be possible and, in fact, because of the uniform signal level, may have certain advantages over the 140 Hz and 510 Hz frequencies now in use.

5. The results of non-systematic regional magnetotelluric measurements of apparent resistivity cannot be interpreted.

Theoretical Results

1. Theoretical solutions that assume infinite strike extent are applicable to actual situations where strike lengths are finite only for the $E_{\perp}$ polarization.

2. For the $E_{\perp}$ polarization, conductivity cross sections based on drill logs may be selected to produce theoretical anomalies which match the field profiles very closely. The theoretical results also explain the variations in phase and correlation that were observed in the field.

5.4 Suggestions for Further Work

1. Telluric surveys without a base station should be tested in the field.

2. Afmag measurements at 8 Hz appear to be possible. For ground surveys the weight and bulk of the present magnetic sensing system would need to be reduced drastically. Some form of AC magnetometer would be most attractive in this application.

3. Theoretical results indicate that there is a large and anomalous vertical electric field around conductivity discontinuities. Thus, measurements of the vertical electric field in existing drill holes should be investigated as a method for mineral exploration at depth.

4. Telluric surveys at several frequencies should be attempted. Theoretical results over some of the sulphide zones investigated in this work suggest that such measurements may provide information on the depth of burial of the target zone. There is also the possibility that induced polarization effects may be observed. The best frequencies for this appear to be either of the two highest Schumann resonance modes (32 and 40 Hz) and the signals used for Afmag (140 and 510 Hz).

5. Further theoretical study and field investigation into the nature and causes of the loss of correlation and variable phase relationship of telluric fields is warranted. These phenomena appear to be characteristic of conductivity discontinuities and, thus, may provide additional geologic information.

6. It would be useful to extend existing numerical methods to three-dimensional geometries, particularly for the $E_{\parallel}$ polarization. This problem, however, is far from trivial, both in the mathematical formulation of the physical situation and in the complexity of the numerical method required for its solution.

CHAPTER VI

CONTRIBUTIONS TO KNOWLEDGE

1. The feasibility of using telluric surveys at 8 Hz for mineral exploration in Precambrian areas has been demonstrated and optimum measurement techniques have been developed.

2. Magnetotelluric surveys have been shown to be impractical for regional geologic mapping and inferior to telluric measurements for detailed investigations.

3. The possibility of making Afmag measurements using the 8 Hz magnetic fields and of performing telluric surveys without a base station has been demonstrated.

4. The first reports of phase changes in the telluric fields ($E_\perp$), caused by conductivity discontinuities, are included in this work. Theoretical conductivity models that show phase changes similar to the observed have been developed.

5. It has been established that only for the $E_\perp$ polarization are two-dimensional theoretical solutions applicable to geologic structures of finite strike length.

REFERENCES

Becker, A., 1967, Design formulas for electromagnetic sensing coils: Geoexploration, v. 5, p. 81-88.

Becker, A., and T.R. Flint, 1967, A portable microvoltmeter for the measurement of 8 cps telluric currents: Proc. of EEMTIC, Bonanza Press, Ottawa.

Berdichevskii, M.N., 1960, Electrical surveying by means of telluric currents: Moscow, Gostoptekhizdat. Eng. trans., Keller, G.V., 1965, Quarterly of the Colorado School of Mines, v. 60, no. 1.

Blake, J.R., and D. Swift, 1967, The magnetotelluric coast effect near a dyke or long promontory: Report of the Geophysical Institute, University of Alaska, UAG R-203.

Bleil, D.F., ed., 1964, Natural Electromagnetic Phenomena Below 30 Kc/s, Plenum Press, New York.

Boissonas, E., and E.G. Leonardon, 1948, Geophysical exploration by telluric currents, with special reference to a survey of the Haynesville salt dome, Wood County, Texas: Geophysics, v. 13, no. 3, p. 387-403.

Cagniard, L., 1953, Basic theory of the magneto-telluric method of geophysical prospecting: Geophysics, v. 18, no. 3, p. 605-635.

Chari, M.V.K., 1970, Finite element solution of non-linear magnetic field problems in electrical machines: Ph.D. Thesis, Dept. of Electrical Engineering, McGill University, Montreal.

Dahlberg, R.S., Jr., 1945, An investigation of natural earth currents: Geophysics, v. 10, no. 4, p. 494-506.

d'Erceville, I., and G. Kunetz, 1962, The effect of a fault on the earth's natural electromagnetic field: Geophysics, v. 27, no. 5, p. 651-665.

Forsythe, G.E., and W.R. Wasow, 1960, Finite Difference Methods for Partial Differential Equations, John Wiley and Sons, Inc., New York.

Galejs, J., 1964, Terrestrial extremely low frequency propagation: in Natural Electromagnetic Phenomena Below 30 Kc/s, D.F. Bleil ed., Plenum Press, New York.

Lavoie, C., 1968, Etude géophysique de trois gisements de sulfures sous des morts-terrains épais et conducteurs: M.Sc. Thesis, Département de Génie Géologique, Ecole Polytechnique de Montréal, Montreal.

Leonardon, E.G., 1928, Some observations upon telluric currents and their applications to electrical prospecting: Terr. Mag., v. 33, p. 91-94.

Madden, T.R., and P. Nelson, 1964, A defense of Cagniard's magneto-telluric method: ONR Project NR-371-401, Geophysics Lab., M.I.T., Cambridge, Mass.

Madden, T.R., and C.M. Swift, Jr., 1969, Magnetotelluric studies of the electrical conductivity structure of the crust and upper mantle: in The Earth's Crust and Upper Mantle, P.J. Hart ed., A.G.U., Washington, D.C.

Madden, T.R., and W. Thompson, 1965, Low frequency electromagnetic oscillations of the earth-ionosphere cavity: Reviews of Geophysics, v. 3, p. 211-254.

Neunschwander, E.F., and D.F. Metcalf, 1942, A study of electrical earth noise: Geophysics, v. 7, no. 1, p. 67-77.

Neves, A.S., 1957, The magneto-telluric method in two-dimensional structures: Ph.D. Thesis, Department of Geology and Geophysics, M.I.T., Cambridge, Mass.

Patrick, F.W., and F.X. Bostick, Jr., 1969, Magnetotelluric modeling techniques: Tech. Rept. No. 59, Electrical Geophysics Research Lab., University of Texas at Austin, Austin, Texas.

Price, A.T., 1962, The theory of magnetotelluric methods when the source field is considered: J.G.R., v. 67, no. 5, p. 1907-1918.

Rankin, D., 1962, The magneto telluric effect on a dike: Geophysics, v. 27, no. 5, p. 666-676.

Sabourin, R.J.E., 1954, Geology of the Onslow-Masham area, Quebec Dept. of Mines, P.R. 293.

Schlumberger, M., 1939, The application of telluric currents to surface prospecting: A.G.U. Trans., Pt. III, p. 271-277.

Scott, W.J., 1970, Private communication.

Seigel, H.O., H.A. Winkler, and J.B. Boniwell, 1957, Discovery of the Mobrun Copper Ltd. sulphide deposit Noranda mining district, Quebec: in Methods and Case Histories in Mining Geophysics, Mercury Press, Montreal.

Shand, J.A., 1966, Some quantitation characteristics of the Schumann-ELF natural electromagnetic background: Can. Jour. Phys., v. 44, no. 3, p. 449-459.

Sheldon, J.W., 1958, Algebra approximations for Laplace's equation in the neighbourhood of interfaces: Math. Tables, Aids Comput., v. 12, no. 63, p. 174-186.

Slankis, J.A., and A. Becker, 1969, Telluric and magneto-telluric measurements at 8 Hz: AIME Trans., v. 244, p. 237-244.

Slater, J.C., 1942, Microwave Transmission, Dover, New York.

Srivastava, S.P., J.L. Douglass, and S.H. Ward, 1963, The application of the magnetotelluric and telluric methods in central Alberta: Geophysics, v. 28, no. 3, p. 426-446.

Strangway, D.S., and K. Vozoff, 1970, Mining exploration with natural electromagnetic fields: Mining and Groundwater Geophysics 1967, Queen's Printer for Canada, Ottawa.

Swift, C.M., Jr., 1967, A magnetotelluric investigation of an electrical conductivity anomaly in the southwestern United States: Ph.D. Thesis, Department of Geology and Geophysics, M.I.T., Cambridge, Mass.

Tikhonov, A.N., 1950, Determination of the electrical characteristics of the deep strata of the earth's crust: Dok. Akad. Nauk., U.S.S.R., v. 73, no. 2, p. 295-301.

Vine. J., 1966, Impedance Networks: in Field Analysis, D. Vitkovitch ed., D. van Nostrand Co., Ltd., London.

Vitkovitch, D., ed., 1966, Field Analysis, D. van Nostrand Co., Ltd., London.

Wachspress, E.L., 1966, Iterative Solution of Elliptic Systems, Prentice-Hall, Inc., Englewood Cliffs, New Jersey.

Wait, J.R., 1954, On the relation between telluric currents and the earth's magnetic field: Geophysics, v. 19, no. 2, p. 281-289.

Ward, S.H., 1967, Electromagnetic theory for geophysical applications: in Mining Geophysics, S.E.G., Tulsa, Oklahoma.

Weaver, J.T., 1963, The electromagnetic field within a discontinuous conductor with reference to geomagnetic micropulsations near a coastline: Can. Jour. of Physics, v. 41, p. 484-495.

Westlake, J.R., 1968, A Handbook of Numerical Matrix Inversion and Solution of Linear Equations, John Wiley and Sons, Inc., New York.